NASA CR- 66379

A STUDY OF DATA REQUIREMENTS, SYSTEM CONSTRAINTS, OPERATIONAL METHODOLOGY, AND DATA ANALYSIS TECHNIQUES FOR A 15-MICRON HORIZON RADIANCE MEASUREMENT EXPERIMENT

Horizon Definition Study

Distribution of this report is provided in the interest of information exchange. Responsibility for the contents resides in the author or organization that prepared it.

N67-32521
(ACCESSION NUMBER)
319
(PAGES)
CR-66379
(NASA CR OR TMX OR AD NUMBER)
(THRU)
1
(CODE)
31
(CATEGORY)
FACILITY FORM 602

May 1967

Prepared under Contract No. NAS 1-6010 by

HONEYWELL INC.
Systems & Research Division
Minneapolis, Minn.

for

NATIONAL AERONAUTICS AND SPACE ADMINISTRATION

N67-32521

ERRATA

NASA CR-66379

A STUDY OF DATA REQUIREMENTS, SYSTEM CONSTRAINTS, OPERATIONAL METHODOLOGY, AND DATA ANALYSIS TECHNIQUES FOR A 15-MICRON HORIZON RADIANCE MEASUREMENT EXPERIMENT

Page 70: This page should be numbered page 71.

Page 71: This page should be numbered page 70.

Issue date: 2 October 1967

May 1967

NASA CR-66379

A STUDY OF DATA REQUIREMENTS, SYSTEM CONSTRAINTS, OPERATIONAL METHODOLOGY, AND DATA ANALYSIS TECHNIQUES FOR A 15-MICRON HORIZON RADIANCE MEASUREMENT EXPERIMENT

By Roy E. Peterson
John R. Thomas
William F. Vogelzang
Bruce F. Watson

ABSTRACT

The conceptual design for a satellite experiment was based on a comprehensive analysis of the required number of radiance profile samples for a global, one-year measurement program. These requirements are defined in terms of the numbers of space/time cells and profile samples/cell necessary for analyzing latitudinal, longitudinal, seasonal, and synoptic variations in horizon radiance. A total of approximately 360 000 profiles/year are required, covering a global set of 588 space cells and 13 time cells (each 28 days long). A variable data acquisition rate of 0.43-1.00 profiles/min was selected to afford requisite levels of data coverage within different latitude intervals. In addition, requirements were established for diurnal data sampling; these requirements led to the choice of a 3 o'clock (nodal crossing) sun-synchronous orbit.

An extensive analysis of radiometer calibration, drift, and noise errors established tradeoffs between the radiometer design specifications and the experiment design requirements. Other design interfaces include those with the data handling, power, and attitude control subsystems. The effect of various operational alternatives, options, and contingencies was considered. In addition, definition was made of requirements and methodology involved in data reduction, analysis, and application.

NASA CR-66379

A STUDY OF DATA REQUIREMENTS, SYSTEM CONSTRAINTS, OPERATIONAL METHODOLOGY AND DATA ANALYSIS TECHNIQUES FOR A 15-MICRON HORIZON RADIANCE MEASUREMENT EXPERIMENT

By Roy E. Peterson
John R. Thomas
William F. Vogelzang
Bruce F. Watson

HORIZON DEFINITION STUDY

Distribution of this report is provided in the interest of information exchange. Responsibility for the contents resides in the author or organization that prepared it.

May 1967

Prepared under Contract No. NAS 1-6010 by
Honeywell Inc.
Systems and Research Division
Minneapolis, Minnesota

for

NATIONAL AERONAUTICS AND SPACE ADMINISTRATION

FOREWORD

This report documents Phase A, Part II of An Analytical and Conceptual Design Study for an Earth Coverage Infrared Horizon Definition Study performed under National Aeronautics and Space Administration Contract NAS 1-6010 for Langley Research Center.

The study was performed in two parts. Part I, which was previously documented, provided for the initial delineation of the experimental data required to define the earth's infrared horizon on a global basis for all time and space scales of interest. The capabilities of a number of flight techniques to collect the experimental data were then evaluated; a rolling wheel spacecraft in a nominal 500 km polar orbit was selected as the baseline technique.

The Part II portion of the study, which this report documents, provides a more extensive analysis of the sampling requirements and operational methodology for the measurement program, including the evaluation of various system constraints. In addition, design requirements and conceptual designs are established for the overall system and its associated subsystems, including radiometer, attitude determination, data handling, communications, attitude control, electric power, structures and integration, flight vehicle operations and launch support.

Honeywell Inc., Systems and Research Division performed this study program under the technical direction of Mr. L. G. Larson. The program was conducted from 28 March 1966 to 10 October 1966 (Part I) and from 10 October 1966 to 29 May 1967 (Part II).

Gratitude is extended to NASA/Langley Research Center for their technical guidance, under the program technical direction of Messrs. L. S. Keafer and J. A. Dodgen with direct assistance from Messrs. W. C. Dixon, Jr., E. C. Foudriat, H. J. Curfman, Jr., R. E. Davis, and T. B. McKee, as well as the many people within their organization.

CONTENTS

	Page
FOREWORD	iii
SUMMARY	1
INTRODUCTION	3
EXPERIMENT DEFINITION AND OBJECTIVES	5
Horizon Sensor Application Objective	5
Scientific Objectives	9
RADIOMETER AND DATA SAMPLING REQUIREMENTS	9
Radiometric Requirements	9
Refinement of Additional Data Sampling Requirements	12
EFFECTS OF SYSTEM CONSTRAINTS	38
The Effect of Random Radiometer Errors Upon Sample Size Requirements for Horizon Locators	38
EFFECTS OF SYSTEM CONSTRAINTS	44
Radiometer Errors	44
Data Collection Effects	61
Attitude Control Effects	68
Sampling Azimuth Effects	69
Definition of Experiment Sampling Methodology	72
Conclusions	82
DATA REDUCTION, ANALYSIS, AND APPLICATIONS	84
Data Reduction	84
Data Analysis and Utilization	86
CONCLUSIONS AND RECOMMENDATIONS	97
APPENDICES	
APPENDIX A - THE EFFECTS OF TEMPERATURE ERRORS UPON SYNTHESIZED RADIANCE PROFILES	
APPENDIX B - DETERMINATION OF DIURNAL DATA SAMPLING REQUIREMENTS	
APPENDIX C - EFFECTS OF ERRORS AND UNCERTAINTIES ON DATA REQUIREMENTS	

CONTENTS (Continued)

APPENDIX D - EFFECT OF INSTRUMENT ERROR ON DATA REQUIREMENTS - STATISTICAL ANALYSIS

APPENDIX E - PROFILES, ERRORS, LOCATORS, AND COMPUTATIONS

APPENDIX F - PARAMETRIC ERROR ANALYSIS - PLOTTED RESULTS

APPENDIX G - PARAMETRIC ERROR ANALYSIS - TABULAR RESULTS

REFERENCES

ILLUSTRATIONS

Figure		Page
1	Examples of Horizon Sensor Operation	6
2	Calculated Radiance as a Function of Wavelength for Various Cloud Conditions	8
3	Estimate of Uncertainty, $\hat{\sigma}$, Versus Latitude L1 (0.2).	16
4	Required Sample Size, N, Versus Estimate of Uncertainty, $\hat{\sigma}$	18
5	Variation of Diurnal Temperature Amplitude with Altitude as a Function of Latitude and Time of Year	31
6	Typical Curve of Diurnal Temperature Variation	33
7	Illustrative Example of Diurnal Data Coverage in a Time/Space Cell	36
8	Distribution of Minimum, Mean, and Maximum Radiance Profiles in 0-3.0 W/m^2 -sr Interval	39
9	Effects of Random Radiance Errors, Mean Profile Case, All Locators	41
10	Locations of Synoptic Data Points	49
11	Location of the 15 Pairs of Profile Locations	50
12	Mean Located Horizons for Selected Locators	53
13	Confidence Level for Obtaining 0.5 km Confidence Interval on Horizon Standard Deviation Versus Instrument Error Confidence Interval	57
14	Telemetry Data Gap	62
15	Experimenter Data Reduction Function	85
16	Data Analysis and Utilization	88
17	Model Verification	89
18	Data Analysis	90

TABLES

Table		Page
1	Outline of Three Sets of Data Sampling Requirements	11
2	Recommended Locators for Determining Experimental Data Requirements	14
3	Estimate of Uncertainty, $\hat{\sigma}$, (km), Based Upon Extrapolation Procedure	17
4	Cell Sample Size, N, for Various Locators	19
5	Number of Space Cells per 10° Latitude Interval for Recommended Locators	21
6	Data Sampling Requirements per 10° Latitude Interval for Recommended Locators[a]	22
7	Total Additional Samples Required for Random Error Compensation	23
8	Tangent Height and Tangent Height Error Statistics for Various Locators	28
9	Diurnal Range of Locator Tangent Height, km, Attributable to Diurnal Temperature Variation	34
10	Tangent Height Error Standard Deviation and Additional Cell Samples Required for an Assumed Radiance Error Standard Deviation of 0.0033 W/m^2-sr	42
11	Profile Pairs With 40 Great Circle Degrees Separation	47
12	Locators Listed by Mean, σ, and Spread of Located Horizon	54
13	Mean, σ, and Spread Listed by Locator	55
14	Sensitivity Coefficients	59
15	Allowable Instrument Caused Horizon Error, Standard Deviation and Mean[a]	60
16	Longitudinal Dimensions of Space Cells Affected by the Telemetry Gap	61
17	Results of Miser F Analysis of Data Coverage from a 270 N.MI. Sun-Synchronous Orbit	66
18	Data Sampling Requirements for Recommended Locators Compensated for Errors and Losses[a]	67
19	Azimuthal Sampling Effects Upon Determination of Diurnal (Day/Night) Differences	70
20	Profile Acquisition Rates, Profile/Min, Needed to Satisfy Compensated Data Sampling Requirements	73
21	Possible Combinations of Profile Acquisition Rates Needed to Satisfy Cumulative Data Sampling Requirements, Error and Loss Compensated	75
22	Number of Data Samples Obtainable With Recommended Variable Rate Sampling Methodology	78
23	Level of Confidence in Data Samples Obtained With Recommended Sampling Methodology, Percent	79
24	Level of Percent Confidence in Data Samples Based Upon Minimum Methodology for Basic Data Requirements	81

A STUDY OF DATA REQUIREMENTS, SYSTEM CONSTRAINTS, OPERATIONAL METHODOLOGY, AND DATA ANALYSIS TECHNIQUES FOR A 15-MICRON HORIZON RADIANCE MEASUREMENT EXPERIMENT

By Roy E. Peterson
John R. Thomas
William F. Vogelzang
Bruce F. Watson

SUMMARY

The conceptual design for a satellite experiment to measure the earth's infrared horizon radiance characteristics in the 15 micron CO_2 absorption band has been developed.

Comprehensive analysis was made of the required number of radiance profile samples for a global, one-year measurement program. These requirements are defined in terms of the numbers of space/time cells and profile samples/cell necessary for analyzing latitudinal, longitudinal, seasonal,and synoptic variations in horizon radiance. A total of approximately 360 000 profiles/year are required, covering a global set of 588 space cells and 13 time cells (each 28 days long). A variable data acquisition rate of 0.43-1.00 profiles/min was selected to afford requisite levels of data coverage within different latitude intervals. In addition, requirements were established for diurnal data sampling to provide the basis for analyzing day/night radiance variations. These requirements led to the choice of a 3 o'clock (nodal crossing) sun-synchronous orbit to provide the basic sampling mode for diurnal data.

The above studies produced a body of data which achieved a consistently high confidence level in the final results. Subsequently, an extensive analysis of radiometer calibration, drift, and noise errors was performed to establish tradeoffs between the radiometer design specifications and the experiment design requirements. Other design interfaces include those with the data handling, power, and attitude control subsystems. The effect of various operational alternatives, options, and contingencies was considered, e.g., data coverage from different types of orbit, data losses resulting from gaps in the STADAN telemetry network, and suspension of data collection during periods of spacecraft attitude and spin rate correction.

Definition has also been made of requirements and methodology involved in data reduction, analysis, and application. Of special importance are 1) the basic reduction of radiometric, spacecraft attitude, and tracking data into radiance profiles, 2) error analysis, 3) analysis of radiance variability in terms of the space/time cells, 4) analysis of diurnal radiance variations, and 5) applications of the profile data to accomplish various engineering and scientific objectives.

INTRODUCTION

The experiment design studies documented herein are a portion of the Horizon Definition Study (HDS) conducted for NASA Langley Research Center, Contract NAS 1-6010, Phase A, Part II. The purpose of the HDS is to develop a complete horizon radiance profile measurement program to provide data which can be used to determine the earth's atmospheric state, especially at high altitudes. These data can then be effectively used in the many atmospheric sciences studies and in the design of instruments and measurement systems which use the earth's horizon as a reference. Part I of the HDS resulted in the following significant contributions to the definition of the earth's radiance in the infrared spectrum:

- The accumulation of a significant body of meteorological data covering a major portion of the Northern Hemisphere.
- A large body of synthesized horizon radiance profiles computed from actual temperature profiles obtained by rocket soundings.
- A very accurate analytical model and computer program for converting the temperature profiles to infrared horizon profiles (as a function of altitude).
- An initial definition of the quantity, quality, and sampling methodology required to define the earth's infrared horizon in the CO_2 absorption band for all temporal and spatial conditions.
- An evaluation of the cost and mission success probabilities of a series of flight techniques which could be used to gather the radiance data. A rolling-wheel spacecraft was selected in a nominal 500-km polar orbit.

The Part II study effort was directed toward the development of a conceptually feasible measurement system, which includes a spacecraft, to accomplish the measurement program developed in Part I. In the Part II HDS, a number of scientific and engineering disciplines were exercised simultaneously to conceptually design the required system:

- The scientific experimenter refined the sampling methodology that must be accomplished by the measurement system. This portion of the study recommends the accumulation of approximately 380 000 radiance profiles taken with a sampling rate that varies with the spacecraft's latitudinal position.
- A conceptual design was defined for a radiometer capable of resolving the earth's radiance in the 15-micron spectrum to

0.01 watt/meter^2-steradian with an upper level of response of 7.0 watt/meter^2-steradian.

- A starmapper and attitude determination techniques were defined capable of determining the pointing direction of the spacecraft radiometer to an accuracy of 0.25 km in tangent height at the earth's horizon.

- The combination of the radiometer and starmapper instruments is defined as the mission experiment package.

- A solar cell-battery electrical power subsystem conceptual design was defined which is completely compatible with the orbital and experimental constraints. This system is capable of delivering 70 watts of continuous electrical power for one year in the sun-synchronous, 3 o'clock nodal crossing, 500-km orbit.

- A data handling subsystem conceptual design was defined which is capable of processing in digital form all the scientific and status data from the spacecraft. The subsystem is completely solid state and is designed to store the 515 455 bits of digital information obtained in one orbit of the earth. This subsystem also includes command verification and execute logic.

- A communications subsystem conceptual design was developed to interface between the data handling system of the spacecraft and the STADAN network. The 136 MHz band is used for primary data transmission and S band is used for the range and range-rate transponder.

- A spacecraft structural concept was evolved to contain, align, and control the thermal environment for the spaceborne subsystems. The spacecraft is compatible with the Thor-Delta launch vehicle.

- An open-loop, ground-commanded attitude control subsystem conceptual design was defined utilizing primarily magnetic torquing which interacts with the earth's field as the force for correcting attitude and spin rates.

- A selection of the Thor-Delta as booster was made from the 1972 NASA "stable" which provides low cost and adequate capability.

- Western Test Range was selected as the launch site due to polar orbit requirements. This site has adequate facilities except for minor modifications to handle the program and is compatible with the polar orbital requirements.

This report documents the areas of study directly related to the conceptual design of the satellite experiment. The final conclusions of the Part I study are noted to indicate the starting point for the Part II studies. The quantity of data was established at approximately 110 000 profiles collected uniformly over a period of one year and distributed according to a model containing 408 latitude/longitude cells. This data quantity was designed to yield horizon profile resolution to ±0.5 km in elevation at the 95 percent confidence level. In addition, upper and lower data limits were established.

These three sets of data requirements represent the baseline values for the experiment conceptual design study conducted during Part II. These data requirements were preliminary, establishing only the basic sampling methodology, tangent height error, and data quantities. Further considerations during Part II involved the analysis of a full range of locators (horizon sensor mechanization concepts), diurnal content of the data, error effects (temperature and instrument), and various system and operational constraints.

EXPERIMENT DEFINITION AND OBJECTIVES

HORIZON SENSOR APPLICATION OBJECTIVE

Since the initiation of the United States' space program, the earth's infrared horizon has been used to determine attitude of many satellites. In some cases, horizon sensors have been used as the primary or backup sensors for attitude control and stabilization; in other cases, the sensors have been used merely to determine attitude for purposes of controlling scientific packages or analyzing the scientific data.

Satellites, such as Nimbus and OGO, use horizon sensors as primary attitude sensing elements for stabilization of the vehicle to local vertical. The Discoverer series, Mercury, and Gemini used horizon sensors as backup to inertial attitude systems and to establish local vertical references. Tiros spin-stabilized weather satellites were provided with horizon sensors to determine when the line of sight was crossing the earth for operating the cameras.

Various configurations of horizon sensors have been designed: for example, fixed point sensors which view the horizon at several fixed points relative to the spacecraft; the conical scanner which sweeps out a conical segment intercepting both the earth and space; and the dithering sensor which oscillates between space and earth as it scans in azimuth. These examples are illustrated in Figure 1.

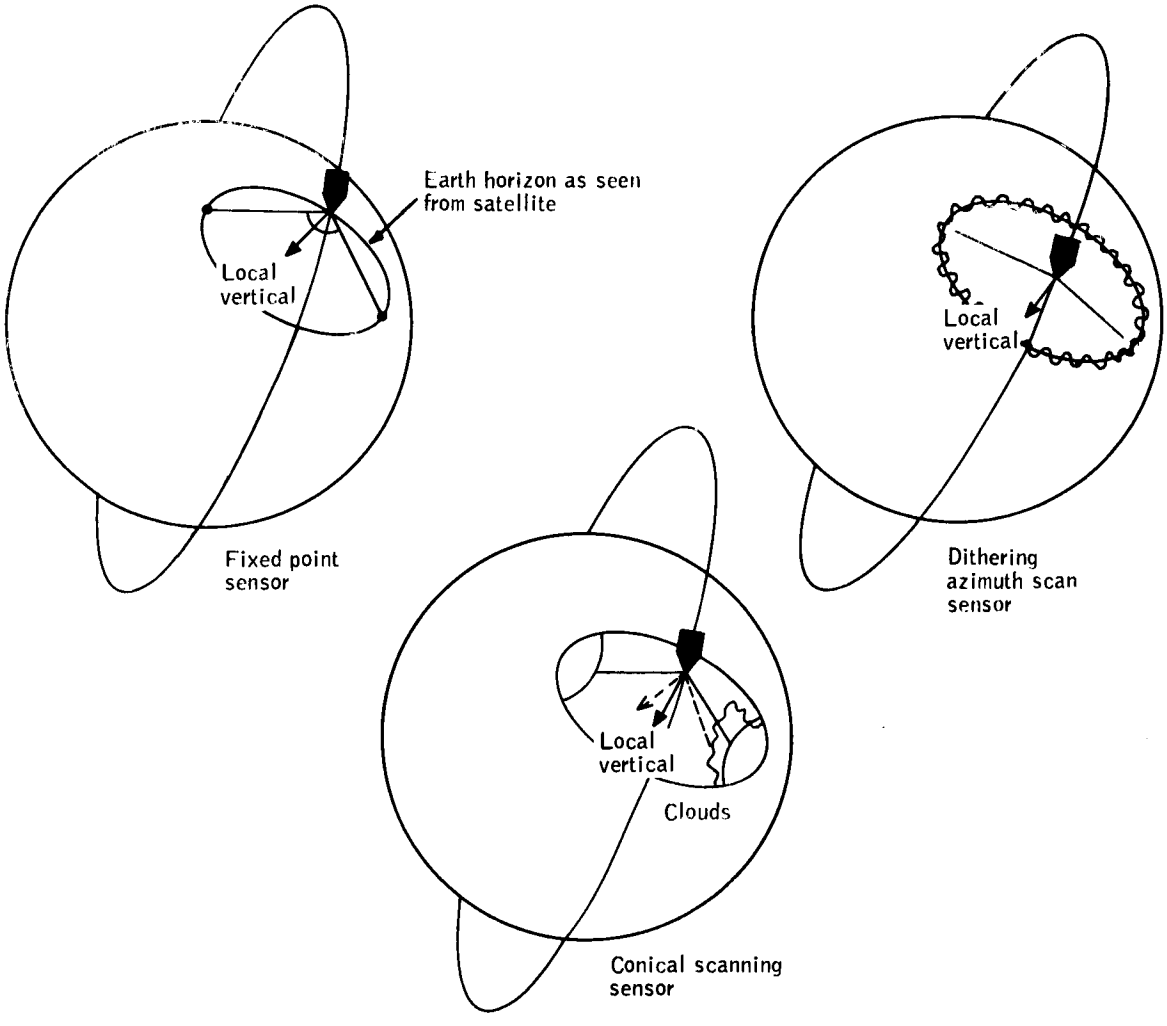

Figure 1. Examples of Horizon Sensor Operation

The first horizon sensors, developed as early as 1957, operated on radiation within the atmospheric window, nominally 2-to 18-μ wavelengths or wider. This broad band was selected for its high energy level to maximize signal-to-noise ratio based on considerations of detectors, optics, and electronics state of the art. A further consideration by the early horizon sensor designers was a desire to sense the actual "hard" earth horizon which is made visible by the transparency of the atmosphere to radiation in this spectral band.

It was determined from early flights that erratic behavior resulted in erroneous vertical reference, often having steady-state error of 5° and transients considerably greater. These flight results provided the impetus for further detailed examinations of the horizon phenomena. It appeared from theoretical work that the earth's horizon was not a well-defined discontinuity between the cold of space and the warm planet; furthermore, the effects of clouds became increasingly apparent. Experiments conducted by the U. S. Air Force on U-2 flights confirmed the existence of "cold cloud" effects on horizon sensors. It was concluded that these clouds absorb infrared radiation within this spectral region and re-emit at their nominal temperature, thereby appearing as a colder body than the earth. As can be seen in Figure 2, the cloud condition within the atmosphere has a significant effect on the energy emitted by the earth. Another important aspect of this problem is also shown in this figure; little, if any, cloud effect is apparent in the spectral interval of approximately 14 to 16 μ. Interest in this spectral range developed rapidly.

Results of recent theoretical and experimental efforts, notably those conducted with the X-15 and the suborbital Scanner, have shown that the 15-μ CO_2 absorption band may be the most stable region in the infrared; however, the true spectral shape of the optimum band and its attendant stability have not been demonstrated. It becomes necessary, therefore, to experimentally establish the variations in the horizon profile in the 14- to 16-μ region. With this information, the horizon sensor designer can improve the instrument design by calibrating out the systematic variations of the horizon profile.

The results of previous analyses have indicated that horizon sensor error improvement is predicated on assimilating a more complete body of data from which the horizon anomalies may be statistically defined. Horizon anomalies which have been considered include:

- Earth oblateness
- Season
- Diurnal
- Atmospheric effects
- Latitude, longitude
- Topographical features
- High-altitude clouds

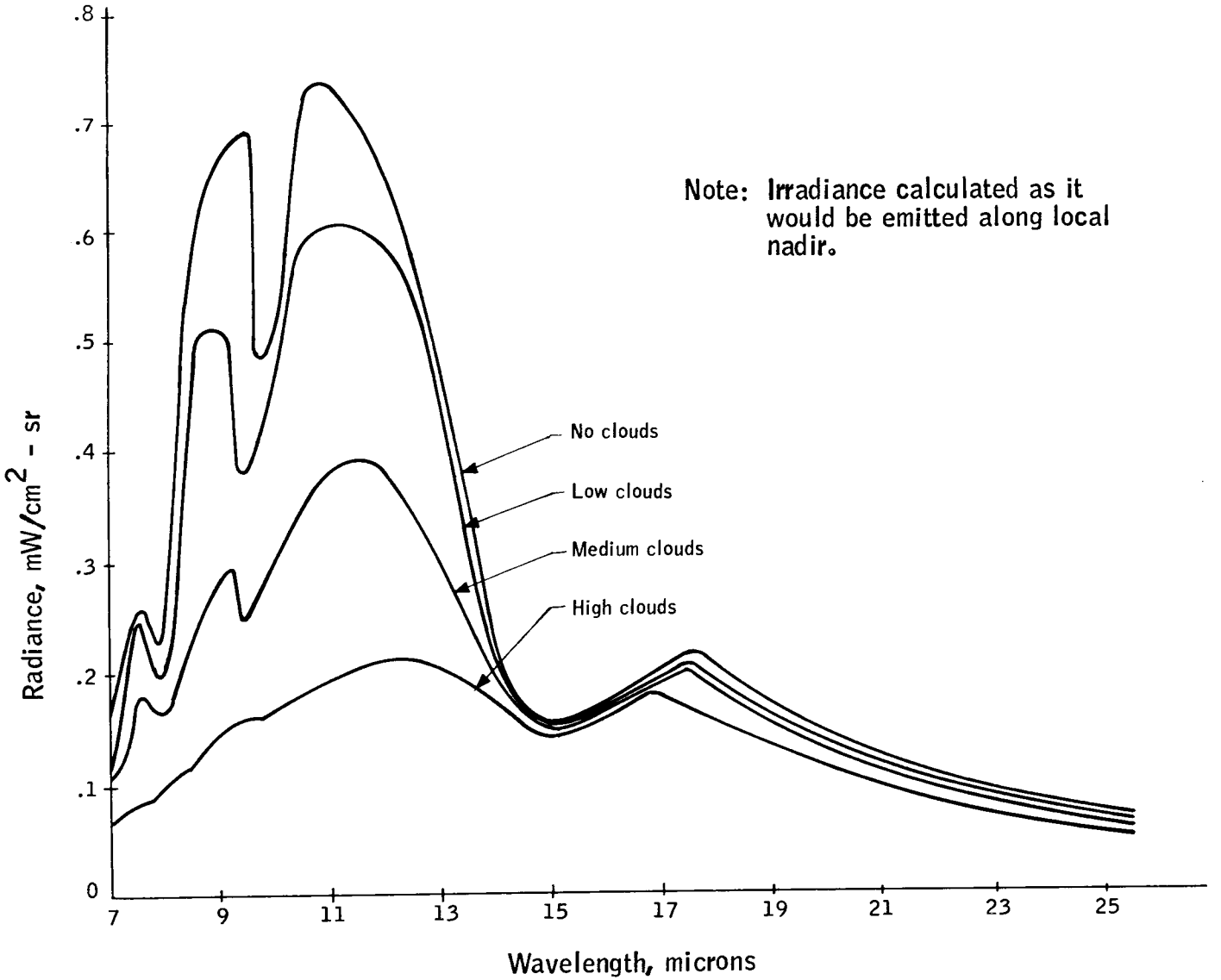

Figure 2. Calculated Radiance as a Function of Wavelength for Various Cloud Conditions

These anomalies, with the exception of earth oblateness (ref. 1), are caused by atmospheric effects and it is an objective of the measurement program to determine the manner in which these anomalies introduce errors in the determination of local vertical by horizon sensors.

The studies and analyses conducted during Part I of this study indicate that compensations for seasonal, diurnal, and geographical effects to produce accuracies to within 0.01° are feasible. The 0.01° represents the residual error in the horizon after compensating for the above mentioned deterministic variations. Thus, the quantitative goal of the measurement program is to measure the horizon variations with sufficient accuracies that horizon sensors intended to produce local vertical accuracies in the 0.01° range can be confidently designed.

SCIENTIFIC OBJECTIVES

The scientific objectives are linked to the unique capability which the HDS satellite has for high resolution horizon measurements on a global scale with sufficient spatial resolution to allow statistical, parametric investigations. These data will provide unique measurements in some cases and in others will provide a sound base upon which other satellite programs can build.

The capability to estimate the mesosphere and the upper stratosphere temperatures represents a unique feature. The HDS stratospheric data base will augment the specific investigations performed by the Satellite Infrared Spectrometer (SIRS) used.

RADIOMETER AND DATA SAMPLING REQUIREMENTS

The radiometric and data sampling requirements serve to define the goals of the measurement program. The conclusions reached as a result of the Phase A, Part I study, which evaluated the profile characteristics, their accuracies, and global distribution made up the initial requirements set. Amendments to this initial set were the result of additional data application, mission profile, and radiometer instrument specification requirements analysis.

This section establishes the initial set of radiometric and data sampling requirements for which a feasible system design was required as a product of the Part II study, the analyses conducted, and the recommended set of requirements for the program.

RADIOMETRIC REQUIREMENTS

The radiometric requirements define the exact nature of the earth's phenomenon which is to be observed. The accuracy of each observation and the quantity and global distribution is established. These requirements are subdivided into the spectral interval, provile accuracy, and data requirements.

Spectral Interval

The spectral interval is selected as the 615 cm^{-1} to 715 cm^{-1} (14.0 to 16.28μ) carbon dioxide absorption band. This band has been established as being capable of providing the most stable horizon profiles. Part I profile synthesis and numerous programs have contributed to the establishment of this requirement. This requirement has remained firm throughout the Part II studies.

The accuracy of the radiance profile refers to the variation of the measured radiation from the absolute radiation. Measurement instruments must be designed to accommodate all these requirements expressed in terms of radiance characteristics and resolution. The radiance profile characteristics and accuracy requirements are as follows:

• Peak radiance:	Maximum	= $7 W/m^2$ - sr
	Minimum	= $3 W/m^2$ - sr
• Minimum radiance		= $0.01 W/m^2$ - sr
• Slope resolution:	Maximum	= $0.6 W/m^2$ - sr-km
	Minimum	= $0.02 W/m^2$ - sr-km
	Maximum change	= $0.15 W/m^2$ - sr-km^2
• Radiance magnitude resolution		= $0.01 W/m^2$ - sr

The basic requirements for horizon profile positional accuracy relates to both the horizontal position and the altitude at which radiometric readings are taken. The basic requirement for horizontal resolution is ≤ 25 km with the altitude or tangent height resolution requirement being ±0.25 km over the complete altitude interval of + 80 to - 30 km.

Basic Data Sampling Requirements

The basic data requirements are defined as the data sampling conclusions from the Part I study. These data specifications are noted in Table 1. One select locator (i.e. horizon sensor mechanization) was shown to provide a confidence level of 95 percent with respect to a tangent height confidence interval of 0.5 km The scientific set of requirements (Table 1) was similarly evolved from another select locator to provide a 95 percent confidence level and represented an upper limit of useful data quanitty. The minimum set was established as a lower check point below which the effectiveness of the program would be questionable.

The Part II studies were directed toward a refinement of the Part I data requirement specifications, based upon additional knowledge of the experiment, and development in the areas of hardware and operational constraints.

TABLE 1. - OUTLINE OF THREE SETS OF DATA SAMPLING REQUIREMENTS

Latitude, deg	Minimum				Basic				Scientific			
	No. of space cells	No. of time cells	Samples per time/ space cell	Total per lat intervals	No. of space cells	No. of time cells	Samples per time/ space cell	Total per lat intervals	No. of space cells	No. of time cells	Samples per time/ space cell	Total per lat intervals
0 - 5	6	9	34	1836	17	13	16	3536	17	13	40	8840
5 - 10					17	13	16	3536	17	13	40	8840
10 - 15	6	9	34	1836	9	13	16	1872	21	13	40	10 920
15 - 20					9	13	16	1872	21	13	40	10 920
20 - 25	6	9	34	1836	18	13	16	3744	21	13	40	10 920
25 - 30					18	13	16	3744	21	13	40	10 920
30 - 35	9	9	34	2754	18	13	16	3744	30	13	160[a]	62 400
35 - 40	(6)			(1836)	18	13	16	3744	30	13	160[a]	62 400
40 - 45	9	9	34	2754	18	13	16	3744	30	13	160[a]	62 400
45 - 50	(6)			(1836)	18	13	16	3744	30	13	160[a]	62 400
50 - 55	9	9	34	2754	18	13	38	8892	30	13	160[a]	62 400
55 - 60	(6)			(1836)	18	13	38	8892	30	13	160[a]	62 400
60 - 65	9	9	34	2754	18	13	38	8892	30	13	160[a]	62 400
65 - 70	(6)			(1836)	18	13	38	8892	30	13	160[a]	62 400
70 - 75	1	9	34	306	8	13	38	3952	18	13	160[a]	37 440
75 - 80									8	13	80[a]	8320
80 - 85												
85 - 90												
Total, northern hemisphere	46			14 076	204			55 016	384			606 320
Total, southern hemisphere	37			11 322	204			55 016	384			606 320
Total, globe	83			25 398	408			110 032	768			1 212 640

[a]40 samples per azimuth sampling direction

REFINEMENT OF ADDITIONAL DATA SAMPLING REQUIREMENTS

Determination of Data Sampling Requirements for Additional Locators

In the Part I study, the locator concept was employed to facilitate the statistical analyses. The locator is some characteristic of the horizon which produces a consistent definition of a sharp reference horizon.

Table 2 presents a select list 12 horizon locators, which were recommended as providing the primary basis for determining the experimental data requirements.

Attention was focused upon the L4 (2.5) and L1 (3.0) horizon locators in defining data requirements for the basic and scientific measurement programs. respectively.

In the Part II study, the data requirement problem was examined within a larger context, encompassing all recommended locators.

The specific data requirements for the additional locators were readily determinable by applying essentially the same methods as were developed for the L1 (3.0) and L4 (2.5) locators (ref. 2) to establish the space cell dimensions and sample sizes.

Estimation of sample size requirements. -- The estimation of sample size is based upon the following expression (ref. 3):

$$Ic \cong \frac{3\hat{\sigma}}{\sqrt{N-1}} \tag{1}$$

where Ic is the 95 percent confidence interval (km), $\hat{\sigma}$ is the estimate of uncertainty associated with temporal variations in the sample (km), and N is the number of samples required per space/time cell (a 28-day time cell, or map period, is assumed). In the Part I study, a value of 0.5 km was determined as a reasonable upper bound of the confidence interval, Ic. The calculation of N thus essentially depends upon the estimated value of $\hat{\sigma}$

As pointed out in reference 3, the $\hat{\sigma}$ estimate was made from the large body of the synthesized radiance profiles that was obtained from the Cape Kennedy one-year data series. In order to determine $\hat{\sigma}$ as a function of latitude for the L1 (3.0) and L4 (2.5) locators, an extrapolation procedure was used in the Part I study, whereby the $\hat{\sigma}$ value at Cape Kennedy (based upon the 6th harmonic residual) was extrapolated to the entire range of latitudes along the 90th meridian by using the 3rd harmonic residual statistic of the synoptic/time

curve fits as a guide. The same kind of extrapolation procedure was used in this study, with some minor modification. The required statistical data for determining $\hat{\sigma}$ for all 12 locators was already available from the comprehensive computer runs performed during the Part I study.

TABLE 2. - RECOMMENDED LOCATORS FOR DETERMINING EXPERIMENTAL DATA REQUIREMENTS

Locator	Value	Mean altitude, km	Applicable to		
			(1)Atmospheric Physics	(2) Present horizon sensors	(3) Future horizon sensors
L1, radiance	0.2	60.15	X		X
	1.0	48.56	X	X	
	2.0	41.40	X	X	
	3.0	35.91	X	X	
L2, normalized radiance	0.06	57.32	X		X
	0.3	44.10	X	X	
	0.5	37.93	X	X	
	0.95	23.26	X		
L4, integral normalized radiance	0.50	55.27			X
	2.50	44.01		X	
L7, slope extrapolation	0.75 1.50	57.51		X	
L17, inflection point	----	34.82		X	

Figure 3 exemplifies the extrapolation procedure as it was applied to locator L1 (0.2). First, the curve of latitudinal variation in the 3rd harmonic residual statistic was plotted. Then, a step-function fit was made to the highest value of this statistic within each of the L4 (2.5) space cell latitude intervals (i.e., 10° intervals between 0-20° and 60-90°; 5° intervals elsewhere). Next, the difference was measured between the values of the 6th harmonic residual at Cape Kennedy (28.5° N) and the 3rd harmonic residual from the synoptic curve fit at the same latitude. The step-function fit was then adjusted upward by this differential value (0.48 km, in this case). The same procedure was also applied to the corresponding sets of statistics for the other 11 locators. This procedure differed somewhat from that used in the Part I study for determining $\hat{\sigma}$ for locators L1 (3.0) and L4 (2.5); in that instance, only two extrapolated values of $\hat{\sigma}$ were determined for each of the two locators. In this study, a finer scale fit was made so as to provide a more detailed basis for comparing the data requirements for the 12 different locators.

Table 3 lists the $\hat{\sigma}$ values which were obtained for the 12 locators, as a function of latitude interval. For comparison purposes, the $\hat{\sigma}$ values determined for L4 (2.5) and L1 (3.0) in the Part I study have also been included. The values for these locators as originally determined in the Part I study are indicated by the use of "prime" notation. It may be noted that there is a general increase in $\hat{\sigma}$ at latitudes above 60°, that the $\hat{\sigma}$ values for locator L17 are relatively large at all latitudes, that the two sets of $\hat{\sigma}$ values for L4′(2.5) and L4 (2.5) are in very close agreement, and that the two sets of $\hat{\sigma}$ values for L1′ (3.0) and L1 (3.0) show some pronounced differences, reflecting the generally conservative approach which was taken to estimating $\hat{\sigma}$ for L1′ (3.0) in the Part I study, as well as the differences in the distribution of time/space cells used in both sets of calculations.

The next step in the analysis was to calculate the required sample size, N, as a function of the estimate of uncertainty, $\hat{\sigma}$. Figure 4 was developed to facilitate this calculation, based upon equation (1). Table 4 presents the results of this calculation, in terms of the sample size per time/space cell within each latitude interval for the 12 different locators. The results in this table show 1) that the cell sample size requirements for locators L4 (0.5) and L2 (0.95) are completely subsumed by those for locator L4 (2.5), 2) that the sample sizes required for the other locators are, in varying degrees, considerably larger than for L4 (2.5), and 3) that the data requirement for locator L17 stands out by itself as extremely large. In view of this last result, locator L17 was eliminated from any further consideration.

Determination of space cell requirements. -- The interpolation of space cell requirements was based upon the numbers determined for locators L4 (2.5) and L1 (3.0) in the Part I study; these numbers essentially represent the opposite extremes for the 11 locators being considered. The interpolation of the required number of space cells for a particular locator was based upon its value of $\hat{\sigma}$ (estimated uncertainty) relative

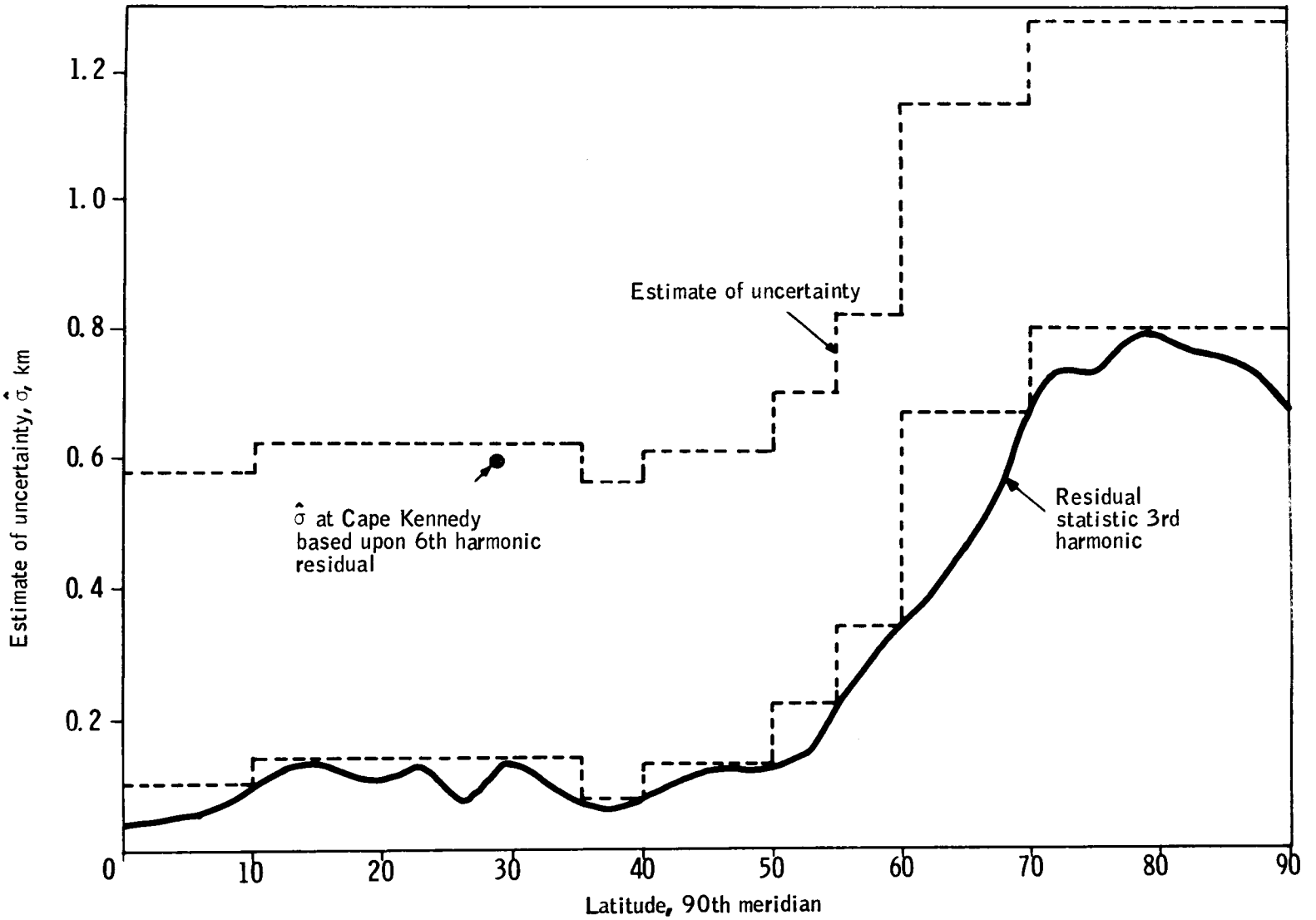

Figure 3. Estimate of Uncertainty, $\hat{\sigma}$, Versus Latitude L1(0.2).

TABLE 3. - ESTIMATE OF UNCERTAINTY, $\hat{\sigma}$ (km), BASED UPON EXTRAPOLATION PROCEDURE

Latitude, deg	Locator													
	L1 (0.2)	L1 (1.0)	L1 (2.0)	L1 (3.0)	L2 (0.06)	L2 (0.3)	L2 (0.5) (a)	L2 (0.95)	L4 (0.5)	L4 (2.5)	L7	L17	L4(2.5) Part 1 study	L1'(3.0) Part 1 study
0-10	0.58	0.70	0.43	0.60	0.50	0.41	0.48	0.45	0.35	0.44	0.92	2.06	0.50	1.00
10-20	0.62	0.70	0.56	0.66	0.54	0.50	0.60	0.42	0.39	0.46	0.91	2.13	0.50	1.00
20-25	0.62	0.65	0.70	0.80	0.55	0.56	0.86	0.43	0.41	0.47	0.73	3.10	0.50	1.00
25-30	0.62	0.68	0.84	0.89	0.56	0.64	0.99	0.52	0.43	0.50	0.70	2.73	0.50	1.00
30-35	0.62	0.68	0.85	0.89	0.56	0.68	0.99	0.53	0.43	0.50	0.80	2.65	0.50	1.00
35-40	0.56	0.68	0.81	0.73	0.51	0.70	0.94	0.53	0.41	0.52	0.79	2.15	0.50	1.00
40-45	0.61	0.91	0.83	0.94	0.51	0.71	0.91	0.52	0.40	0.55	0.86	2.58	0.50	2.00
45-50	0.61	0.91	0.83	0.98	0.51	0.71	0.84	0.48	0.35	0.55	0.93	2.60	0.50	2.00
50-55	0.70	0.94	0.90	1.21	0.51	0.61	0.73	0.46	0.34	0.49	0.93	3.23	0.50	2.00
55-60	0.82	1.18	1.10	1.45	0.53	0.63	0.71	0.54	0.38	0.52	0.85	3.49	0.50	2.00
60-70	1.15	1.82	1.62	1.90	0.83	1.05	0.90	0.79	0.63	0.83	1.36	3.45	1.00	2.00
70-80	1.28	1.90	1.82	1.94	1.08	1.25	1.17	0.92	0.83	1.00	1.57	3.65	1.00	2.00
80-90	1.28	1.80	1.78	1.59	1.13	1.27	1.19	0.92	0.89	1.06	1.88	3.53	1.00	2.00

(a) Based upon estimated value of $\hat{\sigma}$ at Cape Kennedy for the 6th harmonic residual.

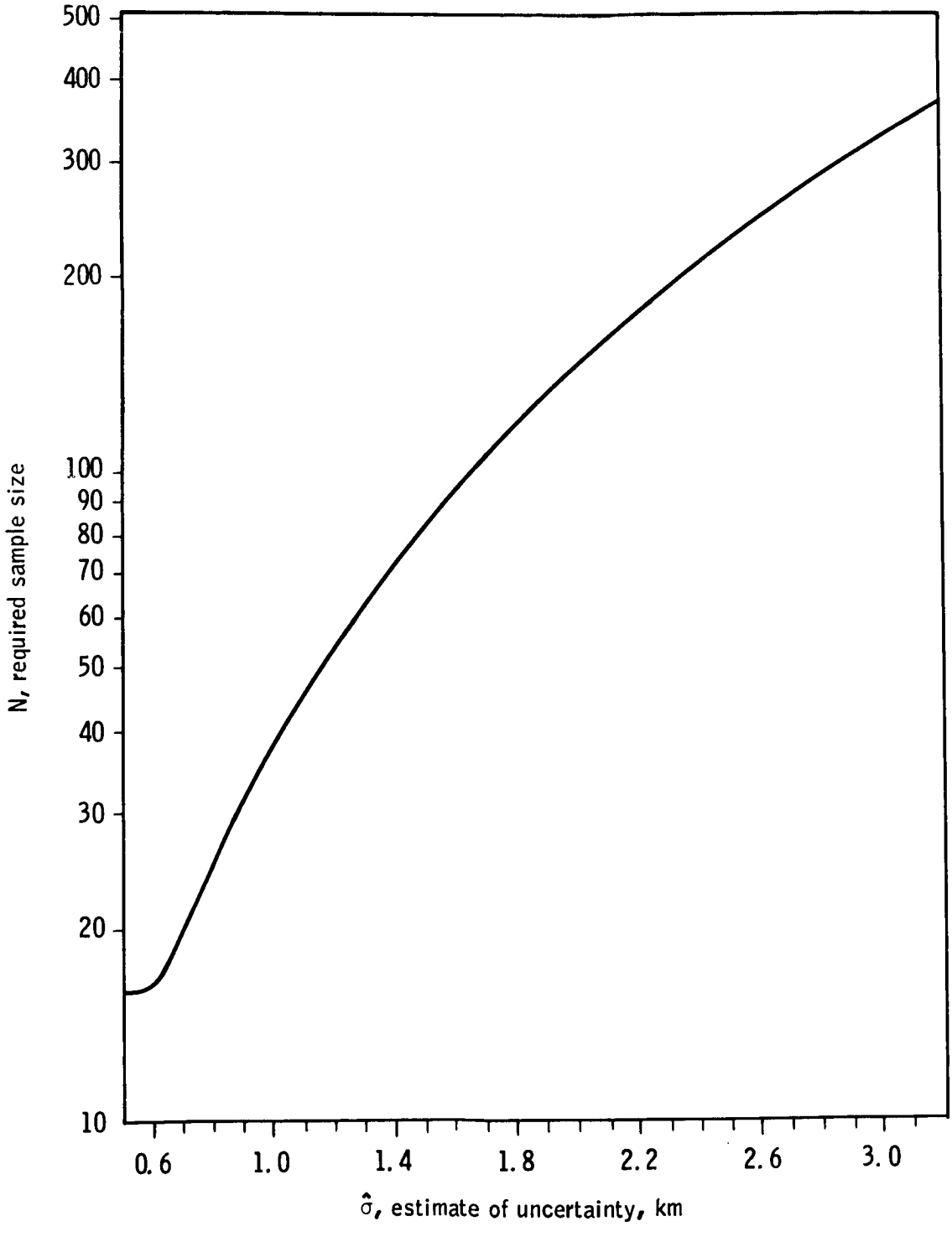

Figure 4. Required Sample Size, N, Versus Estimate of Uncertainty, $\hat{\sigma}$

TABLE 4. - CELL SAMPLE SIZE, N, FOR VARIOUS LOCATORS

Latitude, deg	Locator											
	L1 (0.2)	L1 (1.0)	L1 (2.0)	L1 (3.0)	L3 (0.06)	L2 (0.3)	L3 (0.5)	L2 (0.95)	L4 (0.5)	L4 (2.5)	L7	L17
0-10	16	20	16	17	16	16	16	16	16	16	32	156
10-20	17	20	16	18	16	16	19	16	16	16	32	163
20-25	17	18	20	25	16	16	29	16	16	16	31	346
25-30	17	19	28	31	16	18	37	16	16	16	20	270
30-35	17	19	28	31	16	19	37	16	16	16	25	252
35-40	16	19	25	21	16	20	34	16	16	16	25	168
40-45	17	32	27	34	16	20	32	16	16	16	29	240
45-50	17	32	27	37	16	20	27	16	16	16	33	261
50-55	20	34	31	54	16	17	21	16	16	16	33	377
55-60	26	52	45	77	16	18	20	16	16	16	28	440
60-70	49	121	96	131	27	41	31	24	17	27	67	431
70-80	60	131	121	137	44	57	51	33	27	38	90	485
80-90	60	118	116	93	48	59	52	33	31	42	129	453

to the $\hat{\sigma}$ values of locators L4 (2.5) and L1 (3.0). This approach was adopted because the ratio of the overall number of space cells for L4 (2.5) and L1 (3.0), 0.53 (408/768), is approximately the same as the ratio of their $\hat{\sigma}$ values, 0.55 (0.486/0.885). This appeared to reflect a basic relationship between the quantization interval between adjacent cells (which essentially determines the number of space cells required for a given locator) and the estimated uncertainty of samples collected within an individual space cell (which serves to establish the required sample size for each space cell). Because of the general nature of the interpolation method, no specific assignment of cell dimensions was made for the nine additional locators; instead, the numbers of the required space cells were determined on an aggregate basis for each 10° latitude interval. Table 5 presents the space cell distributions as determined for the various locators. It should be noted that there is an increase in the number of space cells (and a reduction in their latitudinal and longitudinal dimensions) extending from Locator L4 (2.5) to L1 (3.01).

The required sample sizes per space cell for the eleven locators have been defined previously. The total data sampling requirements can now be established for each locator over 10° latitude intervals, using the newly defined space cell distributions. These requirements, shown in Table 6, provide a baseline from which the effects of random radiometer errors and data telemetry losses can be evaluated prior to establishment of an overall sampling methodology.

The next step in the analysis was to determine, for the various locators, the increases in cell sample size, ΔN, needed to compensate for the effects of random radiometer errors in order to maintain a given level of confidence in the Fourier time series analysis of HDS data. For this purpose, the material contained in the analysis of additional data requirements subsection of this report was used. This provides a series of graphs for the various locators relating a given size radiance error to an equivalent tangent height error, which in turn can be used to compute ΔN. In this analysis, a value of 0.003 W/m^2-sr was adopted for the error standard deviation in radiance, σN. This value reflects the 3σ value of 0.01 W/m^2-sr which was established as a working estimate of the basic radiometer design requirement.

The computation of ΔN's was based primarily upon the σ_N versus σ_e (equivalent error standard deviation in tangent height) graph for the mean profile case. However, a detailed analysis was also made for a minimum profile case as discussed later to determine the additional cell samples which would be required for special error compensation at high latitudes (i.e., 50-90°) in the winter season (i.e., the four 28-day time cells spanning the months December - February). It was shown that relatively small additional samples were required, in the case of all locators, to compensate for random radiometer error effects in low radiance profiles at higher latitudes in winter.

Table 7 summarizes the results of the sample error compensation analysis. It should be noted that the error compensation, viewed in terms of the percentage of additional samples required, is very significant for locators L2 (0.95) and L2 (0.06), far less important for locators L2 (0.3), L1 (0.2) and L2 (0.5), and almost negligible for the other six locators.

TABLE 5. - NUMBER OF SPACE CELLS PER 10° LATITUDE INTERVAL FOR RECOMMENDED LOCATORS

Latitude interval, deg	Locator								
	L4 (0.5) L2 (0.95) L4 (2.5)	L2 (0.06)	L1 (0.2)	L2 (0.3)	L2 (0.5)	L1 (1.0)	L7	L1 (2.0)	L1 (3.0)
0-10	17	17	17	17	17	17	17	17	17
10-20	17	17	17	17	17	17	17	17	17
20-30	18	22	24	24	26	28	30	34	42
30-40	36	38	38	38	38	38	38	40	42
40-50	36	38	42	42	44	46	48	50	60
50-60	36	38	42	42	44	46	48	50	60
60-70	18	23	29	30	32	35	39	45	60
70-80	18	23	29	30	32	35	39	45	60
80-82.6	8	10	13	14	15	15	18	22	26
Totals:									
Northern hemisphere - 1 time cell	204	226	251	254	265	277	294	320	384
Globe - 1 time cell	408	452	502	508	530	554	588	640	768
Globe - 13 time cells	5304	5876	6526	6604	6890	7202	7644	8320	9984

TABLE 6. - DATA SAMPLING REQUIREMENTS PER 10° LATITUDE INTERVAL FOR RECOMMENDED LOCATORS[a]

Latitude interval, deg	Locator										
	L4 (0.5)	L2 (0.95)	L4 (2.5)	L2 (0.06)	L2 (0.3)	L1 (0.2)	L2 (0.5)	L7	L1 (1.0)	L1 (2.0)	L1 (3.0)
0-10	272	272	272	272	272	282	282	544	340	272	289
10-20	272	272	272	272	272	289	323	544	340	272	306
20-30	288	288	288	352	408	408	858	615	518	816	1 176
30-40	576	576	576	608	741	627	1 349	950	722	1 060	1 092
40-50	576	576	576	608	840	714	1 298	1 388	1 472	1 350	2 130
50-60	576	576	576	608	735	966	902	1 464	1 978	1 900	3 930
60-70	306	432	486	621	1 230	1 421	992	2 613	4 235	4 320	7 860
70-80	486	594	684	1 012	1 710	1 740	1 632	3 510	4 585	5 445	8 220
80-82.6	248	264	336	480	826	780	780	2 322	1 770	2 552	2 418
Totals: Northern hemisphere 1 time cell	3 600	3 850	4 066	4 833	7 034	7 217	8 406	14 050	15 960	17 987	27 421
Globe - 1 time cell	7 200	7 700	8 132	9 666	14 068	14 434	16 812	28 100	31 920	35 974	54 842
Globe - 13 time cells	93 600	100 100	105 716	125 658	182 884	187 642	218 556	365 300	414 960	467 662	712 946

[a]Based upon a 95 percent confidence level

TABLE 7. - TOTAL ADDITIONAL SAMPLES REQUIRED FOR RANDOM ERROR COMPENSATION

	Δ N Additional samples required			
Locator	Mean profile	Minimum profile	Total	Percent of total sampling requirement
L4 (0.5)	318	6	324	0.35
L2 (0.95)	14 056	333	14 389	14.37
L4 (2.5)	0	3	3	0.003
L2 (0.06)	48 301	782	49 083	39.06
L2 (0.3)	7 529	157	7 686	4.20
L1 (0.2)	3 198	326	3 524	1.80
L2 (0.5)	4 272	49	4 321	1.83
L7	1 529	346	1 875	0.49
L1 (1.0)	216	37	253	0.05
L1 (2.0)	83	32	115	0.02
L1 (3.0)	100	50	150	0.02

The Effects of Temperature Errors Upon Synthesized Radiance Profiles

Summarized below are the highlights of the study made to evaluate the effects of temperzture errors upon synthesized radiance profiles. Appendix A presents a more detailed discussion of the study methods and results.

Study objectives. -- There are two basic reasons for studying the effects of temperature sounding and extrapolation errors upon synthesized radiance profiles. First, the overall data sampling requirements for the HDS experiment are based upon an extensive set of 1039 synthesized profiles which were derived from Meteorological Rocketsonde Network (MRN) and radiosonde observational data and from extrapolated temperatures above the level of effective MRN data coverage. It is important, therefore, to assess the effects of temperature errors upon these synthesized profiles since they were used to determine statistical properties of horizon locators (i. e., L4 (2. 5) and L1 (3. 0) in the Part I study and several additional locators in the Part II study) which were used as the basis for determining the required global distribution of space and time cells, as well as the sample sizes required within each cell.

The second basic reason for examining the temperature error effects problem is to help determine a realistic methodology for comparing samples of radiance profiles measured by the HDS experiment with synthesized profiles calculated from meteorological sounding data at coincident times and locations. This comparison of measured and synthesized profiles is a necessary part of the experiment data analysis in order to check the validity and representativeness of the HDS radiance profiles and to check the adequacy of the analytical model. Obviously, only a relatively small number of profiles can be subjected to this type of comparative analysis. It is important, therefore, that the temperature error effect in synthesized profiles be clearly established so that the radiance (and tangent height) deviations resulting from such comparisons can be reasonably analyzed and interpreted.

Study approach. -- The altitude range over which meteorological data are used to calculate synthesized radiance profiles extends from 0 to 90 km. This range can be divided into three altitude intervals where distinctly different types of temperature data are available: 1) 0 to 30 km, covered by relatively accurate radiosonde data from a global network of upper-air reporting stations; 2) 30 to 60 km, covered by less accurate rocketsonde data mostly concentrated over North America, but also including some European stations and a few other widely scattered locations; and 3) 60 to 90 km, covered by infrequent mesopheric soundings made at widely diverse times and places. During the Part I study (ref. 4), some attention was directed toward estimating the likely temperature errors within these three altitude intervals.

From 0 to 30 km, an error standard deviation, $\hat{\sigma}_T$, of ±2°C provides a representative estimate.

Temperature error estimation for MRN observations is considerably more difficult and uncertain (ref. 5). A σ_T value of ±4°C was adopted as a working

estimate of MRN temperature error between 30-60 Km. Since $3\sigma_T$ values of ±12°C were also used, the analysis of temperature error effects can be generalized over a wide range.

From 60 to 90 km, the temperature errors are considerably larger than those which apply to the two lower altitude intervals. In the Part I study, the temperatures were estimated above 60 km by an extrapolation technique. The estimated σ_T between 60 to 90 km is ±7°C in summer and ±10°C in winter.

For the purposes of this preliminary study, it was decided to apply the $+\sigma_T$ and $\pm 3\sigma_T$ temperature errors separately to each of the three altitude intervals for one selected profile, Profile 943 (July, 20°N, 90°W). By assuming a particular size temperature error in one altitude interval and no error in the other two intervals, the error effects could then be separately examined. Thus, values of σ_T = 2.0°C and $3\sigma_T$ = ±6°C were applied from 0 to 30 km; σ_T = 4.0°C and $3\sigma_T$ = ±12.0°C applied from 30 to 60 km and σ_T = 7.0°C and $3\sigma_T$ = ±21.0°C applied from 60 to 90 km. Profile 943 represented a convenient choice since this summer, low-latitude profile was also used in the study of diurnal temperature variability effects, discussed elsewhere in this report. In order to provide a winter, high-latitude comparison for 60 to 90 km temperature error effects, Profile 883 (Jan., 75°N, 90°W) was selected as the baseline case for evaluating σ_T = 10.0°C and $3\sigma_T$ = ±30.0°C

The 12 error-perturbed profiles, as defined above, were calculated by applying the various plus of minus temperature deviations to the basic sets of temperature values determined for Profiles 943 and 883 in the Part I study.

The effects of temperature errors were analyzed in terms of 1) absolute and percentage deviations in radiance for perturbed versus baseline profiles and 2) tangent height deviations in select horizon locators derived from the perturbed and baseline profiles. The latter portion of the study was designed to reveal whether or not the data sampling requirements, based as they were upon the analysis of the variability of specific locators, were unduly sensitive to the effects of temperature errors.

Discussion of Results. -- The overall results of this study have shown that the effect of temperature errors upon locator tangene heights can vary over wide limits. Temperature errors between 0 to 30 km have the greatest impact upon locators L 2(0.95) and L2 (0.50); for three σ temperature errors of ±6°C, the absolute values of the tangent height deviations for these locators lie within the range 0.6 to 1.7 km. Temperature errors between 30 to 60 km mostly affect locators L1 (3.0), L1 (2.0) and L2 (0.95); for 3 σ errors of ±12°C, the deviations in tangent height for these locators fall within an absolute value range of 1.4 to 4.2 km. Temperature errors between 60 to 90 km produce the largest tangent height deviations in locators L1 (0.2), and L3 (4.5), and L4 (0.5); for 3 σ errors of ±21°C, the absolute values of these deviations lie within a range of 1.0 to 2.3 km. Overall, temperature errors between 30 to 60 km appear to have the greatest effect upon the

locators included in this study. This result is entirely reasonable since, with the exception of L2 (0.95), all locators operate within the tangent height range of 30 to 60 km.

In addition, this study has revealed a remarkable consistency, in terms of the tangent height deviations per °C temperature error which are produced upon a given horizon locator by errors of different signs and magnitudes. Locator L2 (0.95) is the only one to exhibit any real inconsistencies in the normalized deviations; these occur in the (2, 6: 0-30) and (4, 12: 30-60) error cases. The overall results suggest that a nomogram could be developed, for each class of locators, which would permit rapid, accurate estimation of tangent height deviations as a function of 1) basic temperature error combinations within the 0 to 90 km altitude interval, and 2) some general profile descriptor such as peak radiance which would sufficiently identify the radiance profile slope characteristics in order to take into account the functional relationship between the tangent height deviation and the radiance deviation caused by temperature errors. The development of such a series of nomograms could proceed on the basis of 1) selecting a representative number of radiance profiles which cover a range of different latitudes and seasons, 2) defining a greater number of plus and minus error combinations, and 3) establishing firmer estimates of σ_T, the error standard deviation in temperature, over the 0 to 90 km interval.

Effects of temperature errors upon experiment design. -- The results of the analysis of tangent height deviations for various locators provide a basis for estimating possible effects which temperature errors in synthesized profiles may have produced upon the experiment design. Of specific interest are: 1) The data requirements which were established in the Part I study for the "scientific" and "engineering" measurement program, based upon the time series analysis of locators L1 (3.0) and L4 (2.5), respectively, and 2) the data requirements defined in the Part II study for other additional locators.

The tangent height deviations which were determined for the 12 different locators can be identified as error standard deviations in tangent height, σ_{h_T}, which correspond to the assigned values of error standard deviation in temperature, σ_T. Thus, the following three types of tangent height error can be defined: 1) σ_{h_T} (0-30), associated with a constant value of σ_T = 2°C between 0 to 30 km; 2) σ_{h_T} (30-60), which correspond to σ_T = 4°C between 30 to 60 km; and 3) σ_{h_T} (60-90), which is associated with σ_T = 7°C between 60 to 90 km. Estimates of σ_{h_T} are provided by the recent study results (even though the analysis only included positive $1\sigma_T$ errors, the values for negative $1\sigma_T$ errors are expected to be approximately the same over this small a total error interval).

The ideal basis for examining the relative influence of the three σ_{h_T} values would be a set of σ_h values which denote the standard deviation in tangent height for the various locators within specific space/time cells. This type of information is not available, however, because of basic data limitations. It is necessary, therefore, to draw inferences from the locator tangent height statistics which were generated during the Part I study. Values of standard deviation σ_h for the locators of interest were determined: 1) over an extensive North American grid area for eight synoptic cases; 2) at specific stations (i. e., Cape Kennedy, Ft. Churchill and White Sands Missile Range) over various time periods extending from two days to one year; and 3) at specific times along a space cross section extending from White Sands Missile Range to Antigua. For purposes of illustration, σ_h values were selected for the June and January synoptic cases, the May time series case for Cape Kennedy, and the October cross-section case. These values, together with σ_{h_T} values for each interval and for the entire 0 to 90 km altitude range, are presented in Table 8.

There are some notable features in the distribution of σ_h and σ_{h_T} values shown in this table. Of the 12 locators considered, the σ_{h_T} (0-90) values exceed the June synoptic case σ_h values in seven instances, exceed the May Cape Kennedy σ_h values in eight instances, and exceed the October WSMR-Antigua σ_h values in six instances. This result has some interesting implications, since these three sets of σ_h values represent either periods of the year or locations when σ_h is at a near minimum. It would normally be expected that these σ_h values would be larger than the σ_{h_T} (0-90) values, so as to reflect the combined influence of natural variability as well as temperature error effects upon the synthesized radiance profiles. The σ_h value for the January synoptic case (where the natural variability is at a near maximum) does indeed exceed the σ_{h_T} (0-90) values by a considerable margin, with but one exception, the L4 (0.5) locator. In this January case, the error component in σ_h which can be attributed to the assumed temperature error distribution is relatively small; for example, if we subtract out the effect of σ_{h_T} = 0.87 km, for the L1 (3.0) locator, from σ_h = 4.79 km, we obtain a value of 4.71 km, representing only a very minor correction.

In the three cases where the σ_{h_T} (0-90) values frequently exceed the σ_h

TABLE 8. - TANGENT HEIGHT AND TANGENT HEIGHT ERROR STATISTICS FOR VARIOUS LOCATORS

Locator	Tangent height standard deviations, km, caused by temperature error				Tangent height standard deviations, km, for Part I study cases			
	σ_{h_T}, 10-30, 2°C	σ_{h_T}, 30-60, 4°C	σ_{h_T}, 60-90, 7°C	σ_{h_T}, 0-90	σ_h, June synoptic case	σ_h, January synoptic case	σ_h, May Cape Kennedy	σ_h, October WSMR-Antigua
L1 (3.0)	--	0.87	0.03	0.87	0.58	4.79	0.75	1.36
L1 (2.0)	--	0.64	0.04	0.64	0.53	3.80	0.59	1.32
L1 (1.0)	--	0.48	0.06	0.48	0.51	2.97	0.40	0.63
L1 (0.2)	--	0.13	0.80	0.81	0.27	1.71	0.29	0.27
L2 (0.95)	0.36	0.75	0	0.83	1.24	2.98	0.42	0.48
L2 (0.50)	0.25	0.38	0.02	0.46	0.60	2.34	0.62	0.78
L2 (0.30)	0.16	0.22	0.03	0.27	0.32	2.35	0.48	0.74
L2 (0.06)	0.12	0.08	0.23	0.27	0.18	1.18	0.23	0.10
L3 (4.5)	--	0.20	0.54	0.58	0.25 (a)	1.41 (a)	0.21 (a)	0.27 (a)
L4 (2.5)	0.15	0.13	0.21	0.29	0.22	1.50	0.29	0.30
L4 (0.5)	0.13	0.08	0.70	0.72	0.13	0.66	0.18	0.07
L7 (0.75, 1.5)	--	0.36	0.13	0.38	0.70	1.86	0.50	0.29

[a] Interpolated from L3 (1.5) and L3 (7.5) values

values, there are some important inferences to be drawn regarding the magnitude of temperature errors which were adopted within the three altitude intervals. Most noteworthy are the results obtained for the L1 (0.2), L3 (4.5), and L4 (0.5) locators; here, the σ_{h_T} (0-90) values typically exceed the three sets of σ_h values by a factor of three. In each instance, the σ_{h_T} (60-90) error is the major contributor. This suggests that the value of 7°C adopted as the temperature error between 60 to 90 km may be too large by a considerable factor, possibly as much as three. A similar analysis of the σ_h values with respect to σ_{h_T} (30-60) suggests that the value of 4°C adopted between 30 to 60 km may also be too large by a factor of 1.5 or possibly more. It may also be inferred that the σ_{h_T} value of 2°C adopted for the 0 to 30 km interval is possibly too large by a factor of 1.5.

There are certain inherent limitations to the inferences which can be made from the available information. The most important question is whether or not the σ_h values derived for the synoptic time series and space cross-section cases can be regarded as representative. The answer to this question, which Appendix A discusses in detail, is that these σ_n values are sufficiently representative to justify the inferences as stated above.

For the 60 to 90 km altitude interval, an extrapolation process of temperature estimation was developed, whereby the observed 50 km temperature and the temperature at the highest point in the sounding were used to estimate the remainder of the temperature profile to 90 km. Since the extrapolation process was based upon a limited number of high-altitude rocket soundings, considerable concern has been expressed that the temperature errors from 60 to 90 km may be very large and therefore adversely affect the accuracy of the synthesized radiance profiles and the derived tangent height statistics. The results presented in Table 18 suggest, however, that the value of 7°C associated with σ_{h_T} (60-90) may be too large by a factor of as much as three. This inference is essentially based upon a comparison of σ_{h_T} (60-90) values observed during periods when the natural atmospheric variability is relatively low. If the σ_h values used for this comparison are too low, then the inference is incorrect. There does not appear to be any reason to doubt the general validity of these values.

Overall, the analysis of temperature error effects has revealed that they do not unduly influence the tangent height statistics derived from the set of synthesized radiance profiles in the Part I study. Temperature errors do not appear to seriously affect the higher values of σ_h which were the major factor in determining the data sampling requirements for the

HDS experiment. As a result, it was not necessary to modify the data sampling requirements to compensate for temperature error effects.

Use of synthesized profiles in comparative studies with observed profiles. -- The results of this preliminary study serve to identify many of the problems involved in the computation and application of synthesized radiance profiles. Further study is recommended to develop improved methods whereby synthesized profiles can be more accurately computed and more definitive error limits established. This would provide a firm basis for using such profiles for comparative studies with profiles observed by the HDS experiment.

Determination of Diurnal Data Sampling Requirements

The HDS experiment has as one of its objectives the collection of radiance profile data on such a basis that diurnal effects can be statistically evaluated. The term diurnal is applied to the daily component of variation in radiance profiles. Daily changes in solar energy input, resulting from the effect of the earth's rotation, serve to generate a 24-hour cycle of temperature variation with the largest magnitude in the tropical zone.

Diurnal temperature variability. -- The first step in determining the diurnal data sampling requirements was to review information sources relating to the diurnal variability of atmospheric parameter between 30 to 70 km, the portion of the stratosphere and mesosphere which exerts the greatest relative influence upon 14-to 16-micron radiance profiles. The general nature of the diurnal temperature component, including amplitude and phase, was established as a function of altitude, latitude, and time of year (i.e., solstices and equinoxes). The results of significant studies which have been made of diurnal temperature variability are summarized in Appendix B

Based upon an evaluation and synthesis of these various theoretical and empirical study results, a set of curves has been derived which depicts the amplitude of the diurnal temperature oscillation as a function of altitude (24 to 90 km), latitude (0, 45, and 75°N) and time of year (soltices and equinoxes). These curves are shown in Figure 5.

Figure 5 shows the following important features: 1)overall, the amplitude of diurnal temperature variation is largest near 55 km; 2) the maximum value of diurnal temperature amplitude is approximately 7°C, occuring throughout the year near 55 km in the equatorial region, 3) mean diurnal temperature amplitude at 45°N is 0.5 to 1.5°C less than that at the equator, with somewhat higher values occuring at the vernal and autumnal equinoxes; 4) diurnal temperature amplitude at 75°N is considerably less than at lower latitudes, with extremely large seasonal changes from relative minima at the solstices to relative maxima at the equinoxes; and 5) the smallest diurnal temperature variation occurs in the polar region at the soltices, where the peak value near 55 km probably does not exceed 1°C.

In addition to the amplitude, the phase of the diurnal temperature variation

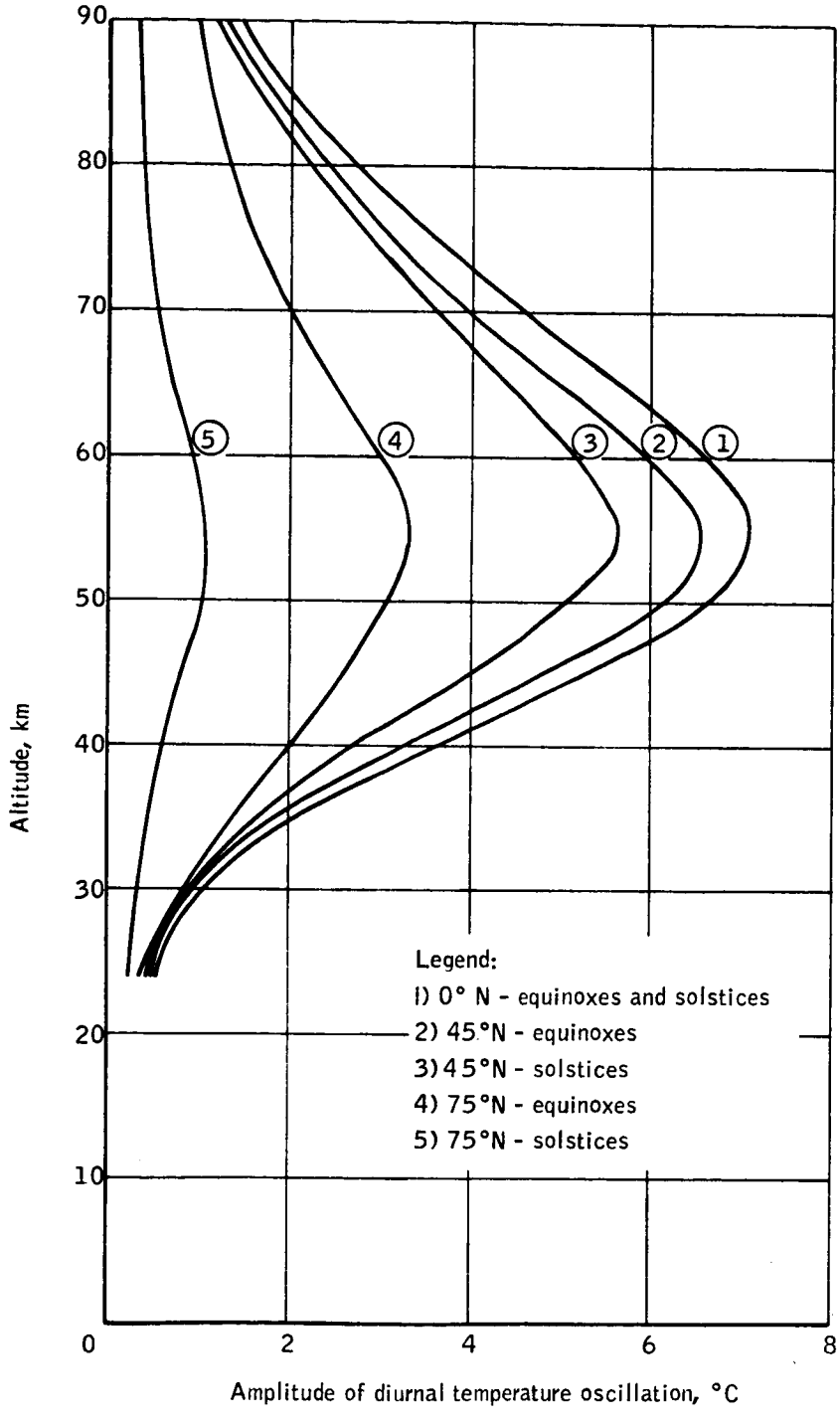

Figure 5. Variation of Diurnal Temperature Amplitude with Altitude as a Function of Latitude and Time of Year

is a significant factor affecting the HDS data sampling requirements. Figure 6 presents a curve showing the phase of diurnal temperature variation as a function of local time, representing an average, representative condition. This curve indicates a broad plateau of maximum temperature occuring early to midafternoon, with a broad minimum occurring near 3:00 a.m. local time. The greatest rates of diurnal temperature increase and decrease are shown to occur within the two to three hour periods following sunrise and sunset, respectively. As noted on Figure 6, the phase is expected to vary within ± one to five hours as a function of latitude, altitude, and time of year.

The effect of diurnal temperature variability upon the determination of horizon locators. -- A representative number of climatological profiles were selected to serve as the basis for evaluating the effect of diurnal temperature variability upon the determination of several recommended horizon locators. (See Appendix B for the detailed description). Since these are significant latitudinal and seasonal changes in the amplitude of diurnal temperature variation, the selection of representative cases for this included latitudes 20°, 45°, and 75°N, and months near the times of the winter solstice, vernal equinox, and summer solstice. The sets of diurnally perturbed radiance profiles were computed with the CORPS program on the basis of the original temperature data as listed in the Part I report compilation, plus and minus a series of temperature deviations equal to one-half the diurnal amplitude at the various altitude levels.

The results of the analysis of locator tangent height deviations attributable to diurnal temperature variability are presented in Table 9. These results indicated that a significant diurnal variability in locator tangent heights will occur in those cases where the maximum amplitude of the diurnal temperature oscillation exceeds a value of 3.3°C.

It would appear from these results that, at low and mid latitudes, the tangent height deviations for most locators, attributable to the diurnal cycle of temperature variation in the stratosphere, lie within the range of 0.50 - 1.00 km throughout most or all of the year. At very high latitude where the maximum amplitude of diurnal temperature variability is relatively small, tangent height derivations of 0.1 - 0.2 km can be normally expected. The higher values of tangent height derivations at low and mid latitudes are especially significant since they are comparable in magnitude to the tangent height standard deviations which occur at locations and during time periods when the synoptic variability of the atmosphere is relatively low. During periods of high synoptic variability, the diurnal component of tangent height variation is relatively small and difficult to isolate, but it should be statistically easier to separate within space/time cells of relatively low synoptic variability.

Orbit Selection. -- On the basis of the study made of diurnal temperature variability, the preliminary recommendation was made that a 3 o'clock sun-synchronous orbit be adopted. This type of orbit provides radiance data samples at local times spaced 12 hours apart.

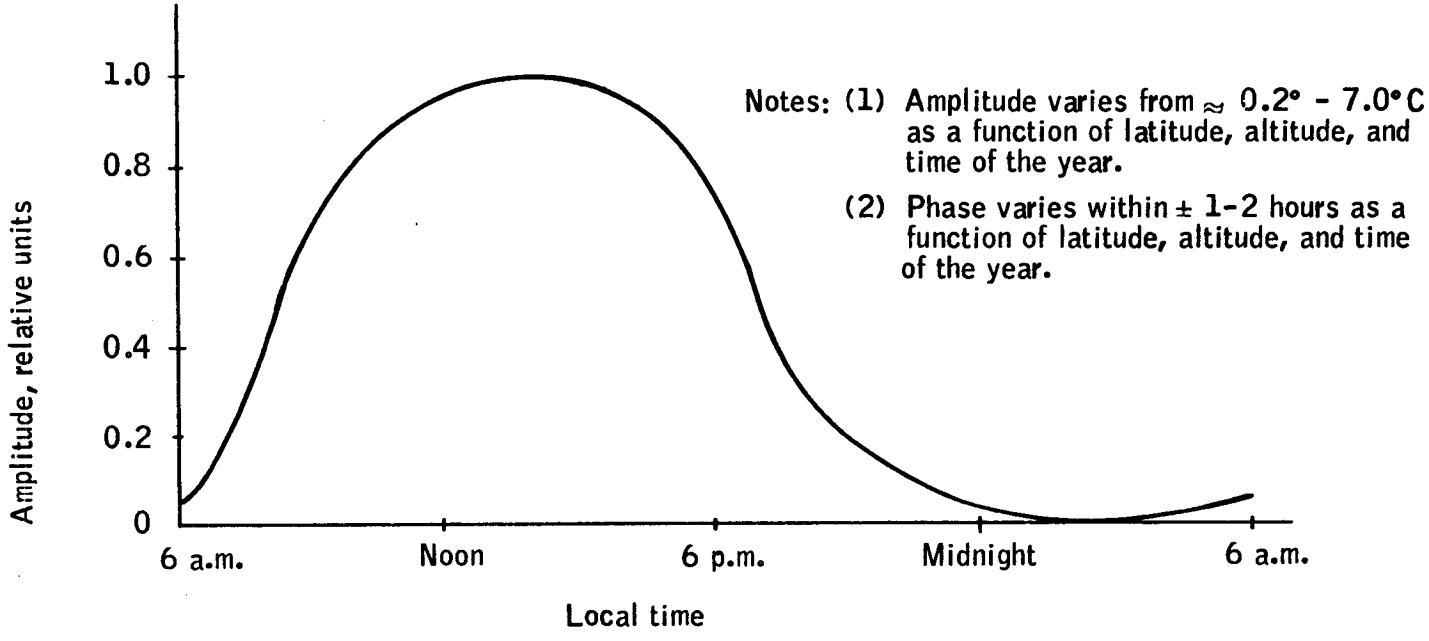

Figure 6. Typical Curve of Diurnal Temperature Variation

TABLE 9. - DIURNAL RANGE OF LOCATOR TANGENT HEIGHT, km, ATTRIBUTABLE TO DIURNAL TEMPERATURE VARIATION

Locator	Locator tangent height parameter, km	Maximum amplitude of diurnal temperature variation, °C								
			1.0		3.3	5.6		6.5	7.0	
		Profile no.	883	983	933	863	963	913	843	943
		Month/latitude	Jan/75	Jul/75	Apr/75	Jan/45	July/45	Apr/45	Jan/20	July/20
		Peak radiance W/m^2-sr	4.3041	7.0477	5.6357	5.1366	6.0699	5.7634	5.3696	5.6445
L1 (0.0)	Diurnal range		0.19	0.16	0.15	0.67	0.79	0.83	1.50	1.06
	Mean height		29.9	43.4	36.8	34.7	41.3	39.4	39.0	39.4
L1 (1.0)	Diurnal range		0.14	0.13	0.14	0.70	0.62	0.64	0.99	0.97
	Mean height		35.1	47.0	42.2	40.2	45.5	43.8	44.7	44.1
L1 (1.0)	Diurnal range		0.18	0.11	0.16	0.98	0.66	0.70	0.76	0.86
	Mean height		43.1	52.7	49.1	47.7	51.0	50.0	50.3	49.9
L1 (0.2)	Diurnal range		0.11	0.07	0.08	0.55	0.61	0.65	0.58	0.71
	Mean height		57.5	62.7	59.8	59.1	61.2	60.2	59.8	60.1
L2 (0.95)	Diurnal range		0.02	0.06	0.04	0.19	0.34	0.28	0.12	0.48
	Mean height		18.2	23.0	20.3	20.4	24.3	21.8	26.8	26.0
L2 (0.50)	Diurnal range		0.06	0.08	0.07	0.44	0.47	0.49	0.79	0.64
	Mean height		34.3	41.5	37.6	37.0	41.1	40.0	41.0	40.2
L2 (0.30)	Diurnal range		0.05	0.07	0.09	0.37	0.43	0.47	0.57	0.60
	Mean height		40.4	46.6	43.8	42.8	46.2	45.1	46.6	45.6
L2 (0.06)	Diurnal range		0.08	0.04	0.06	0.06	0.34	0.41	0.47	0.41
	Mean height		55.6	58.3	56.7	56.1	57.6	57.0	57.1	57.1
L4 (2.5)	Diurnal range		0.11	0.07	0.08	0.50	0.45	0.50	0.46	0.59
	Mean height (a)		42.1	46.6	44.6	43.8	45.2	44.8	44.2	44.6
L4 (0.5)	Diurnal range		0.07	0.04	0.05	0.35	0.41	0.43	0.49	0.56
	Mean height (a)		54.2	56.7	55.6	55.1	55.9	55.7	55.4	55.6
L7	Diurnal range		0.32	0.11	0.06	0.65	0.57	0.43	0.39	0.69
	Mean height		54.6	59.8	58.0	57.7	58.2	57.5	56.8	57.3

[a] Estimated

However to evaluate whether a 3 o'clock syn-synchronous orbit can provide an adequate sampling approach for analyzing the diurnal component of radiance profile variability, comparison was made with a 70 degree inclined maximum precession orbit. This latter orbit provides a daily shift in the local times at which samples are taken with a given time/space cell, during a 28-day map interval the 70 degree inclined orbit essentially provides two periods of approximately six hours each, wherein the local sampling time gradually changes.

Figure 7 illustrates the diurnal data coverage which would be obtained within a typical time/space cell from a 3 o'clock sun-synchronous orbit and a 70° inclined maximum precession orbit. The total sample of 16 points divides, in both cases, into two equal clusters of daytime and nighttime data. It is assumed that the points, as plotted here, represent values from which the synoptic and seasonal trends have been removed, i.e., the reduced data from which the diurnal component is to be evaluated. The sun-synchronous orbit data sample, it may be noted, is highly concentrated with respect to local time, whereas the 70° inclined orbit data are scattered throughout two 6-hour periods. Because of their highly time-concentrated nature, the synoptic and seasonal components can be more easily and accurately removed from the sun-synchronous profile data. In the case of the 70° inclined orbit data, the local time spread renders the analysis of the diurnal component more difficult and less certain, since there is no reliable "anchor point" for separating the synoptic from the diurnal variance within relatively small samples from individual time/space cells. Thus, the 70° inclined orbit for a given sample size does not provide better determination of the amplitude and phase of the diurnal variation, because of the "time smear" problem.

The sun-synchronous orbit does provide relatively accurate statistics at two points in local time spaced 12 hours apart. These points can be selected at the local times which, on the average, correspond to the diurnal maxima and minima.

Comparison of diurnal coverage obtained from 3 and 4 o' clock sun-synchronous orbits. -- The study of theoretical and empirical evidence relating to the diurnal variability of temperature led to the choice of a 3 o'clock local time as one which would provide daytime near-maxima and nighttime near-minima and which would generally avoid the problem of skirting near relatively sharp sunrise and sunset discontinuities. However, a shift to a later local time could provide spacecraft design advantages. The diurnal sampling problem was re-examined, therefore, to determine the annual latitudinal distribution of night and daytime samples obtained with 3 and 4 o'clock orbits. (See Appendix B for the specific details).

The results of this analysis are as follows. On an annual basis, with the 3 o'clock orbit, 91 percent of the 3: p.m. radiance profiles fall within the daylight period, and some 72 percent of the 3:00 a.m. profiles occur during darkness. With the 4 o'clock orbit, these percentages are reduced to 87 and 60 percent, respectively. Another important aspect of the diurnal sampling problem is to define the latitudinal limits within which both day and night

1) 3 p.m./3 a.m. sun-synchronous orbit

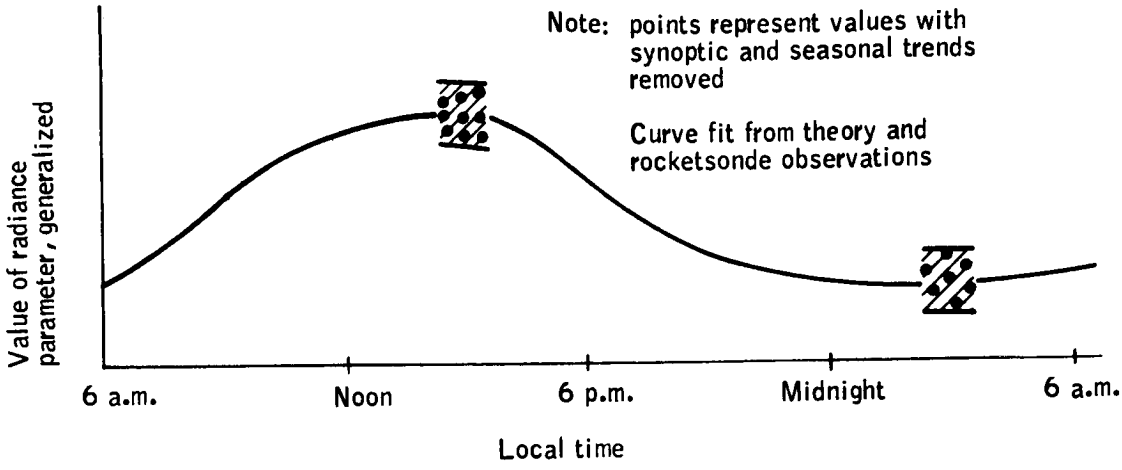

2) 70 deg inclined maximum precession orbit

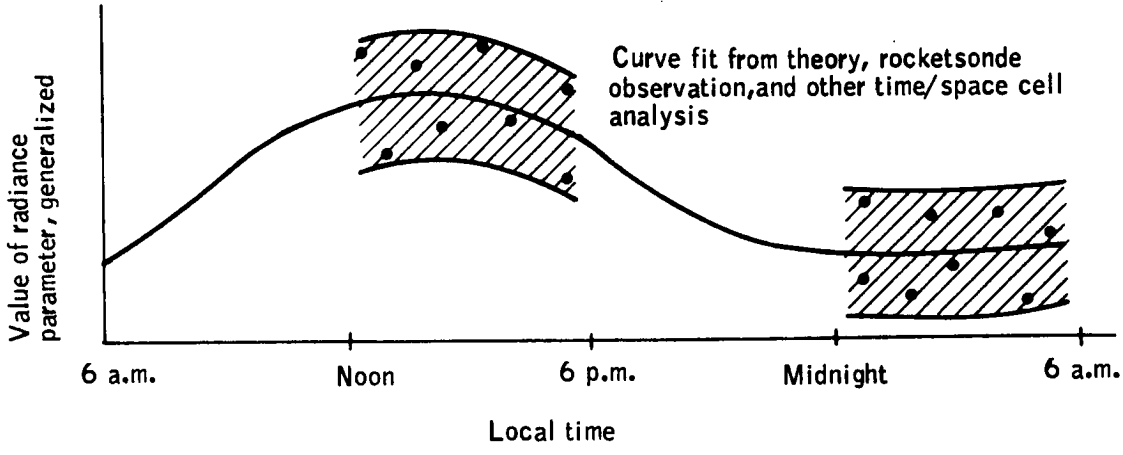

Figure 7. Illustrative Example of Diurnal Data Coverage in a Time/Space Cell

radiance samples can be obtained concurrently. The shift from a 3 o'clock to a 4 o'clock orbit results, throughout the year, in a loss of 5 to 20° latitude within which concurrent diurnal sampling coverage can be obtained; this loss is least in late February and mid-October and greatest during the several-week period centered at the summer solstice.

The basic question is how serious are these relative diurnal data losses incurred in shifting from a 3 o'clock to a 4 o'clock orbit. These losses must be regarded as significant, and should be avoided, if at all possible; they can be reluctantly tolerated, however, if the earlier local time can be shown to impose inordinately heavy design penalties.

EFFECTS OF SYSTEM CONSTRAINTS

THE EFFECT OF RANDOM RADIOMETER ERRORS UPON SAMPLE SIZE REQUIREMENTS FOR HORIZON LOCATORS

Objectives

A preliminary error analysis was made to determine the effect upon the experiment sampling requirements of random errors associated with the operation of the radiometer instrument. This effect was appraised in terms of equivalent tangent height error in 11 recommended horizon locators. This error, in turn, can be expressed in terms of an additional number of profile samples which must be taken within each space/time cell to maintain the same level of confidence as that designated for the no-radiometer-error case.

The results of this preliminary analysis were used to make working estimates of the additional samples required for radiometer error compensation; th also provided a basis for the more extensive study of radiometer error effects, the resuls of which are presented in a subsequent section of this report. The results of this preliminary analysis and those obtained in the subsequent analysis are not directly comparable since, in the latter case, the analysis was aimed at specification of radiometer design requirements an and at predicting horizon sensor performance.

Approach

The approach which was taken in the preliminary analysis was to compute the equivalent tangent height error for three representative cases: the minimum, mean, and maximum profiles which were determined by computer analysis in the Part I study from an extensive series of 839 synoptic profiles. The three radiance profiles, illustrated in Figure 8, are statistical conglomerates. The mean profile consists of mean radiance values determined at one km tangent height intervals between 0 to 50 km and at 2 and 5 km intervals elsewhere. The maximum (minimum) profile consists of a series of maximum (minimum) radiance values selected at each designated tangent height level from the entire set of 839 profiles. It should be pointed out, therefore, that the three select cases are not necessarily representative of real profiles, but represent a convenient synthesis of their average and extreme properties.

Appendix C describes the methods, assumptions and input data involved in the calculation of σ_h, the equivalent error standard derivation (ESD) in tangent height as a function of σ_N, the error standard derivation in radiance The error analysis was conducted on a parametric basis, covering a range of error standard deviation in radiance from 0.0001 to 0.1 W/m^2 - sr.

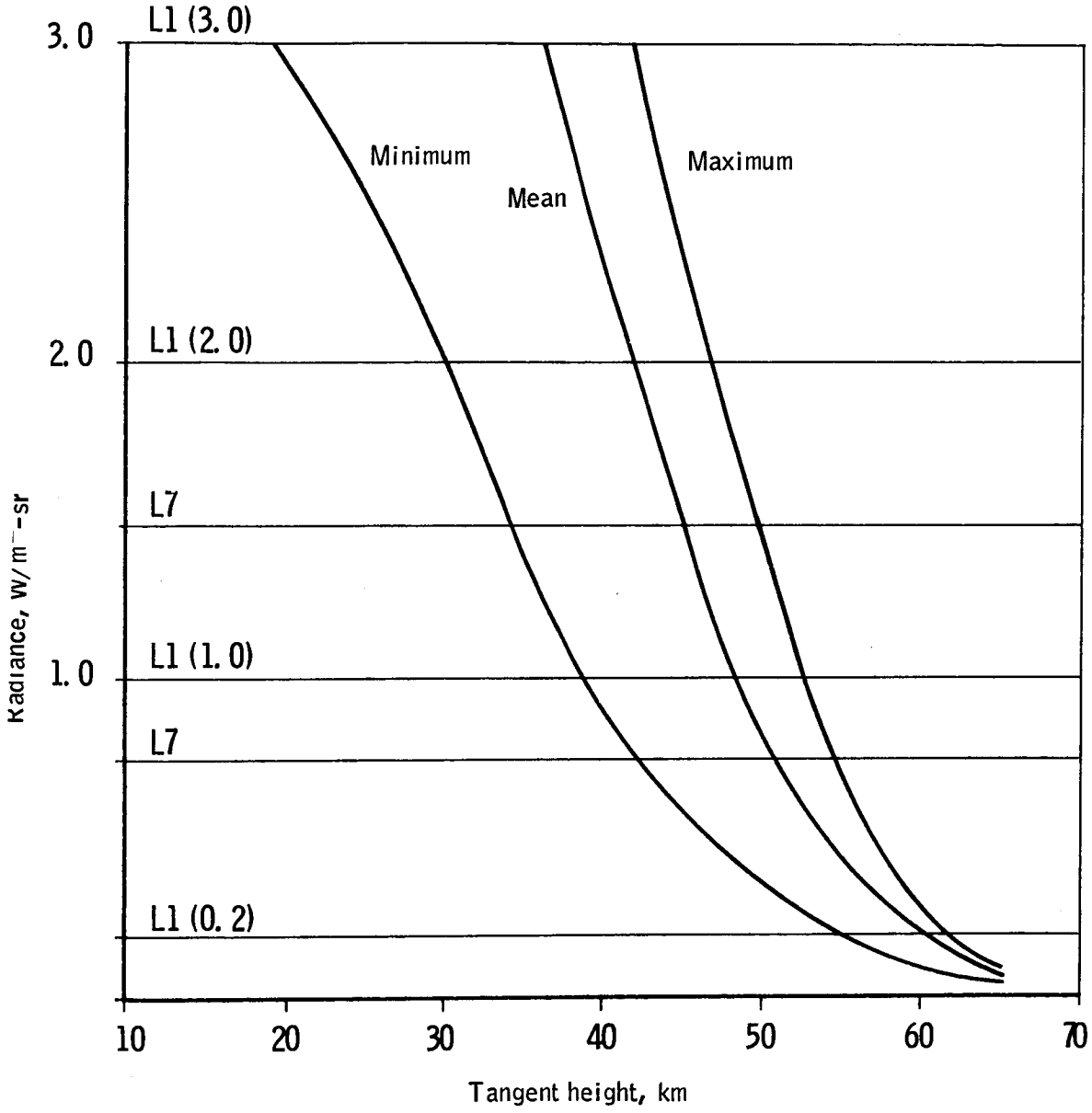

Figurd 8. Distribution of Minimum, Mean, and Maximum Radiance Profiles in 0-3.0 W/m^2-sr Interval

The locators considered in the analysis included: L1 (3.0), L1 (2.0), L1 (1.0), L1 (0.2), L2 (0.95), L2 (0.50), L2 (0.30), L2 (0.06), L4 (2.5), L4 (0.5) and L7 (1.5, 0.75).

Results. -- The results of the error analysis clearly show a wide range of tangent height ESD's for a given value of radiance ESD in the case of the mean profile the results for which are illustrated in Figure 9, the tangent height ESD's vary by a factor of 46 from the least to the most affected locator; and for the maximum and minimum profiles, the comparable factors are 43 and 41. (See Appendix A.) For the mean profile case, the tangent height error sensitivity of the 11 locators follows this ascending order:

L44(2.5), L1 (3.0), L1 (2.0), L1 (1.0), L4 (0.5), L7, L1 (0.2), L2 (0.50), L2 (0.30), L2 (0.95), and L2 (.0.06). Approximately the same order applies to the maximum and minimum profile cases.

Some important implications can be drawn from this parametric analysis regarding design goals for random radiance error. As pointed out in the earlier section of this report, "Determination of Data Sampling Requirements for Additional Locators", the time/space cell sample size can be increased to compensate for random experimental errors, thereby maintaining an estimated uncertainity of $\hat{\sigma}_h$ = 0.5 km at a 95 percent level of confidence. The scale shown in the lower right corner of Figure 9 shows the additional number of profiles, ΔN, required per sampling cell to maintain this level of confidence.

Application to Data Requirements Definition. -- In other project studies a 3° value of 0.01 W/m^2 - sr was established as the radiometer design requirement with respect to random error. Based upon this value, a set of calculations was made to determine the equivalent error standard deviation in tangent height and ΔN, the additional samples required (profiles per cell) to compensate for the error effect. These calculations, which cover 11 recommended locators for the mean, minimum and maximum profile cases, are presented in Table 10. These results, which were used in making the final determination of the total sampling requirements for the various locators (discussed later), indicate that all the L2 locators are most affected by radiometer errors, along with locators L1 (0.2) and L7.

Limitations. -- The mean, maximum, and minimum radiance profiles used as the basis for this error analysis have important limitations with regard to their representativeness. By making appropriate modifications in the analysis (described in Appendix C) it was possible to obtain results, which provided working estimates of the additional data samples required to compensate for random error effects. However, the results clearly indicated the advisability of conducting a more comprehensive analysis of radiometer error effects, one based upon a set of individual radiance profiles. The results of this subsequent analysis are described in Appendix D.

It is important to point out that, although random error effects can be compensated for by increasing the cell samples, it is undesirable to have any

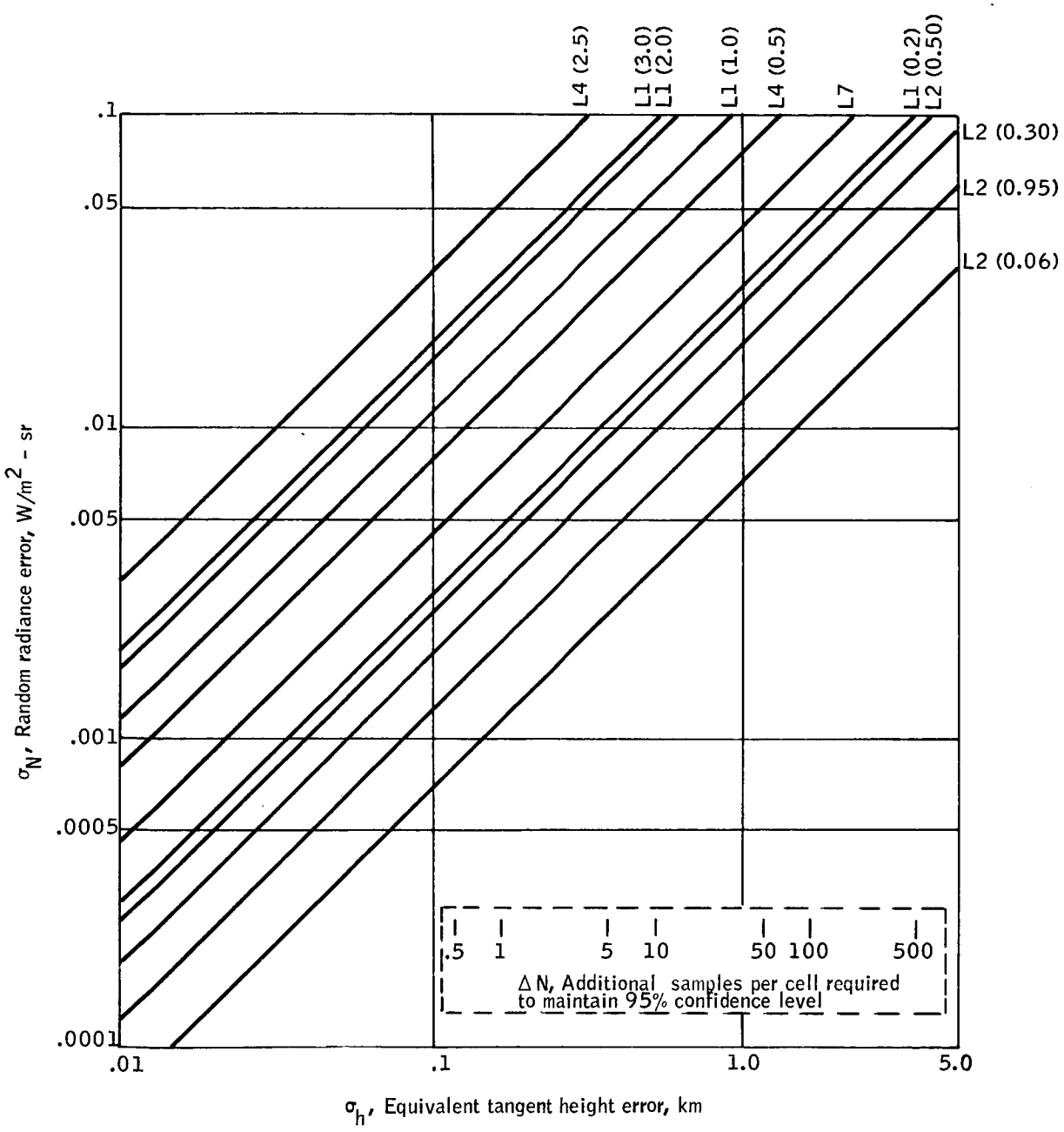

Figure 9. Effects of Random Radiance Errors, Mean Profile Case, All Locators

TABLE 10. - TANGENT HEIGHT ERROR STANDARD DEVIATION AND ADDITIONAL CELL SAMPLES REQUIRED FOR AN ASSUMED RADIANCE ERROR STANDARD DEVIATION OF 0.0033 W/m^2-sr

Locator	Tangent height error standard deviation, km			ΔN, additional samples required, profiles/cell			Total no. of space/time cells, 10^3
	Mean profile	Minimum profile	Maximum profile	Mean profile	Minimum profile	Maximum profile	
L1 (3.0)	0.02	0.04	0.01	0.01	0.06	<0.01	10.0
L1 (2.0)	0.02	0.04	0.01	0.01	0.05	0.01	8.3
L1 (1.0)	0.03	0.05	0.02	0.03	0.11	0.01	7.2
L1 (0.2)	0.12	0.18	0.08	0.48	1.23	0.24	6.5
L2 (0.95)	0.27	0.32	0.25	2.66	3.69	2.18	5.3
L2 (0.50)	0.13	0.14	0.12	0.62	0.71	0.50	6.9
L2 (0.30)	0.18	0.21	0.16	1.14	1.51	0.86	6.6
L2 (0.06)	0.48	0.54	0.42	8.29	10.31	6.35	5.9
L4 (2.5)	0.01	0.01	0.01	<0.01	0.01	<0.01	5.3
L4 (0.5)	0.04	0.05	0.04	0.06	0.09	0.05	5.3
L7	0.07	0.15	0.05	0.19	0.81	0.09	7.6

sizeable error components in the HDS data sample which could be possibly eliminated by more exacting design and calibration of the radiometer. The separation of error variance from the variance of naturally occurring radiance fluctuations, although statistically estimatable, still represents a difficult, time-consuming and often uncertain process. For this reason, random radiance errors should be kept to a minimum.

The data requirements as described previously may be difficult to realize due to system constraints and, therefore, a sampling methodology must be developed for obtaining as much of the data as possible under these constraints. The effects of radiometer errors, data collection, attitude control, and azimuthal sampling will be discussed in the following paragraphs. The recommended sampling methodology is described in the final paragraph.

EFFECTS OF SYSTEM CONSTRAINTS

RADIOMETER ERRORS

Effects of Measurement Errors on Located Horizon Statistics

To obtain estimates of the effects of measurement errors, 120 synthesized radiance profiles were perturbed by two types of errors, scale and bias, applied to the body of data in three different ways to simulate radiometer calibration errors, drift errors, and high frequency (e.g. noise) errors. For each of these six errors (two types applied three ways) four error values were used resulting in 24 sets of 120 perturbed profiles. Each of these 24 sets was operated on by eight combinations of locators and input constants (two input constants for each of locators L1 through L4).

Over each of the 8 x 24 = 192 sets of located horizons, statistics (mean, σ, spread) were calculated and compared with statistics obtained with zero error to determine the change in statistics caused by errors. Local vertical statistics were calculated by the method to be explained below.

Local Vertical Considerations. -- Horizon sensors determine local vertical by finding the center of the horizon circle by one of a varied number of techniques. Single-axis sensors must find two points on the horizon circle which define a chord length or a diameter. The center of this chord length or diameter lies in a plane containing the direction which the horizon sensor indicates is local vertical.

Horizon sensor determine the location of points on the horizon circle by a number of different techniques similar to the various locators used in HDS, (ref. 2). For horizon sensors which bisect a chord or a diameter of the horizon circle, it can be shown that the local vertical direction with respect to the nadir is given by:

$$\theta = 1/2 \frac{\left(h_{\ell_1} - h_{\ell_2}\right)}{\rho}$$

where h_{ℓ_1} and h_{ℓ_2} are located horizon altitudes from the horizon circle and ρ is the distance from the sensor to the horizon, a function of altitude.

If $h_{\ell_1} = h_{\ell_2}$, then local vertical determined by the horizon sensor is aligned to the nadir, or true geometric vertical, which is the desired situation. This statement applies to a spherical earth only; oblateness effects are neglected.

The above expression does not include effects of sensor instrumentation errors and can thus be thought of as being descriptive of local vertical behavior for a particular sensor rather than overall accuracy for that sensor.

Local vertical behavior was determined from measured profiles by calculating located horizons with applicable locators at applicable points on the horizon circle corresponding to the particular sensor being investigated. The accuracy with which local vertical behavior can be predicted is a function of the radiometric errors of measurement. To estimate the effects, local vertical direction with respect to the nadir was calculated from the perturbed synthesized profiles. However, local vertical is dependent on the horizon circle points used and on the orbit altitude.

The orbit altitude used was the HDS orbit altitude of 500 km, for which the horizon diameter is ≈ 40 great circle degrees. The points on the horizon circle which were used are on a diameter since this condition was expected to show the maximum variability in local vertical because of the maximum geographic separation of located horizons. Then

$$\theta = 1/2 \times 0.0225 \frac{\text{degrees}}{\text{km}} \left| h_{\ell_1} - h_{\ell_2} \right|$$

A calculation of the error in local vertical was made according to

$$\Delta\theta = 1/2 \times 0.0225 \frac{\text{degrees}}{\text{km}} \left| \Delta h_{\ell_1} - \Delta h_{\ell_2} \right|$$

where $\Delta\theta$ is the error in local vertical due to errors Δh_{ℓ_1} and Δh_{ℓ_2} in located horizons caused by radiometer errors.

For both θ and $\Delta\theta$, mean, σ, and spread was calculated over each set of locators for each set of perturbed profiles.

Input Profiles. -- Because local vertical statistics were calculated based on located horizons on the diameter of a 40 great circle degree horizon circle, the input profile locations occur in pairs with each profile in a pair separated by 40 great circle degrees. Other than this, the criteria for selecting input profiles were 1) use a large enough sample size such that the resultant statistics would be meaningful, and 2) include at least seasonal and latitudinal effects since these were the largest effects observed in Part I. The synoptic body of profiles was used to provide inputs since these contain the greatest geographic coverage of any of the Part I sets and contain seasonal variability.

All possible pairs of profiles with 40 great circle degree separation were determined by plotting the synoptic locations on a sphere and using a divider. The points were plotted to an accuracy of probably $\pm 1/2$ to $\pm 1°$. Also if two

points were separated by 40 great circle degrees to within about ±2°, they were selected as a pair. Thus, each pair features an actual separation of between 37 and 43 degrees, but this should be close enough for present purposes. The complete listing of pairs is given in Table 11.

From Table 11, 15 pairs were selected using the rather arbitrary procedure of picking every fourth one. The intention was to make a simple selection and see if the resulting geographic coverage was sufficient. With a few minor adjustments, the final selection of locations gives the coverage shown in Figure 10, which illustrates that the complete geographic area of the available data is covered. Figure 11 shows the pairs selected. Note that the pairs selected feature pure latitude variations at upper and lower latitudes, pure longitude variations, and a number of combinations of latitude/longitude variations.

Seasonal effects are included by using the locations of Figure 10 for each of four synoptic dates: 8 April, 12 August, 21 October, and 20 January. Total sample size is 120 profiles. A complete listing of profile locations, dates, and ID numbers is given in Appendix E.

Error Types, Magnitudes, and Application. -- Scale errors are expressed in terms of radiance magnitude, e.g. radiometer noise equivalent radiance of X.XXX W/m^2-sr , rather than percentage. These two kinds of errors affect radiance measurements in three different ways, embodying all previously discussed concepts of accuracy and precision.

The first method of application of error is that the errors are constant in time, such as calibration errors. When a given radiometer is calibrated, all of the actual errors, sometimes called non-linearity, offset, etc., are calibrated out, but a residual calibration uncertainty remains, sometimes referred to in discussions of accuracy.

By analysis, test, or otherwise, the maximum value of the uncertainty is known, but within this ± range the actual value of the uncertainty is unknown. However, the value that existed at the time of calibration remains fixed for a given instrument. That is, if the calibration radiance is known to within ±1 percent, then, for a given calibration the input radiance is somewhere between 0.99 N_o and 1.01 N_o. Assume that it was 0.995 N_o. Then, a fixed calibration error of 0.5 percent did exist which exists for that instrument for all time. These fixed errors would seem to have no effect on local vertical because they affect all profiles in the same direction and subtract out when differences are taken to find local vertical. However, they do affect located horizons since they propagate into located horizon errors as a function of profile shape and magnitude. Then, although the radiometer error is a constant, the resulting located horizon error is not and local vertical is affected.

The magnitudes of this error that were investigated were selected to bracket the expected value of error to be associated with the HDS radiometer calibrati

TABLE 11. - PROFILE PAIRS WITH 40 GREAT CIRCLE DEGREES SEPARATION

Pair no.	Synoptic profile no. (a)	Pair no.	Synoptic profile no. (a)
1	1 20	15	5 28
2	1 33	16	6 22
3	1 54	17	6 18
4	2 15	18	7 55
5	2 31	19	7 39
6	3 14	20	7 16
7	3 20	21	8 40
8	3 35	22	8 30
9	3 49	23	9 38
10	4 21	24	10 50
11	4 36	25	10 56
12	5 16	26	11 38
13	5 22	27	12 40
14	5 33	28	12 51

TABLE 11. - PROFILE PAIRS WITH 40 GREAT CIRCLE DEGREES SEPARATION - Concluded

Pair no.	Synoptic profile no. (a)	Pair no.	Synoptic profile no. (a)
29	13 43	43	20 29
30	13 53	44	23 48
31	13 26	45	31 41
32	14 45	46	31 52
33	14 52	47	33 44
34	14 28	48	34 45
35	15 46	49	36 47
36	15 49	50	38 54
37	16 35	51	40 55
38	17 23	52	42 48
39	18 42	53	43 56
40	19 25	54	44 49
41	20 46	55	46 50
42	20 26	56	24 19

[a]Profile no. refers to the location numbering system used for synoptic data locations, reference 14.

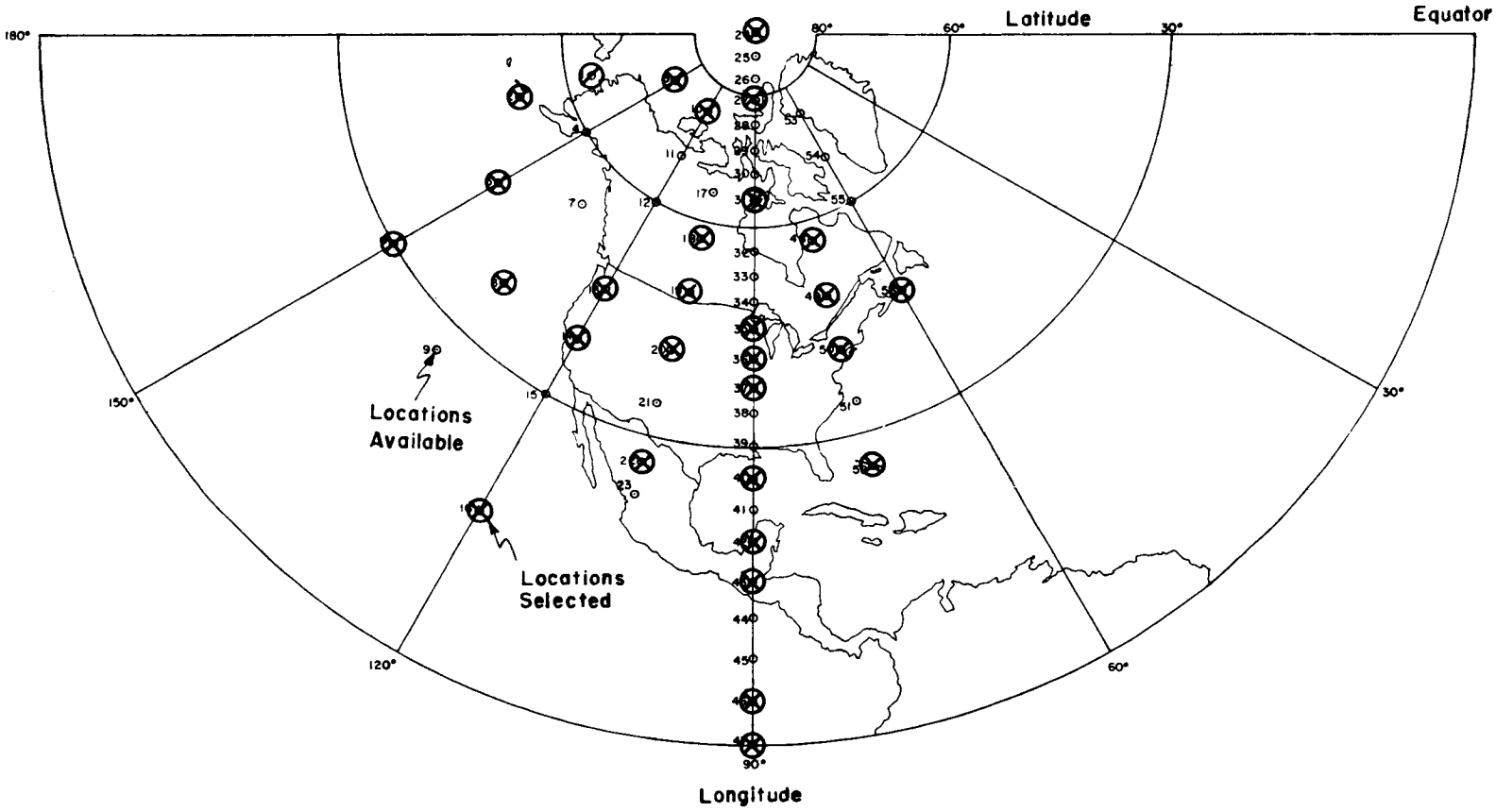

Figure 10. Locations of Synoptic Data Points

Thus, scale errors of 0.4 percent, 1 percent, 2 percent, and 5 percent and bias errors (all W/m^2-sr) of 0.001, 0.004, 0.01, and 0.04 were used.

The kinds of errors that vary over the period of operation of the devices have been referred to in discussions of precision, but since in-flight calibration will be done for the radiometer, this class of errors coming under precision or accuracy could be discussed further. Since repeated calibration is to be done, it is the stability of the calibration which is critical; this stability includes that of the calibration source and that of the radiometer response.

Instabilities are of two kinds, those that fluctuate rapidly like detector or electronics noise, and those that fluctuate slowly like temperature-caused drift. Without discussing the specifics of frequency distributions, it is assumed, for the HDS radiometer application, that a slowly varying error is one which has a constant magnitude over a single profile measurement, but which is different for some other profile measurement. A rapidly varying error is one which changes in ma nitude from point to point on each profile being measured. Both of these are assumed to have gaussian amplitude distributions. The magnitudes chosen are the same as for calibration error, all of which are summarized in Appendix E.

Locator Selection. -- The criteria for selection should be that the locators studies be representative of horizon sensors and that the body of locators studied be representative of the type and magnitude of variations expected in the measured data. For this error study, the located horizon characteristics being considered are limited to mean altitude, standard deviation over the complete sample, and maximum spread, i.e., the difference between minimum and maximum located horizon altitude. Thus, the body of locators to be studied must produce located horizons which cover the range of those characteristics.

From the Part I study, those locators most applicable to horizon sensors are L1 through L4, and only these will be considered. For these locators the range of mean altitude, standard deviation, and spread observed in Part I is:

Mean altitude	25 km - 55 km
Standard deviation	0.9 km - 4.3 km
Spread	5 km - 20 km

The above values are for a range of L1 through L4 input constants, relative to estimates of current instrument state of the art, from a factor of two improvements thereof to a factor of four greater.

The selection process was to determine those locators and input constants which produced uniformly distributed mean located horizon altitudes over the range of 25 to 55 km, and similarly for standard deviation and spread. Those locators which were common to all three sets were chosen to be

studied. This process guarantees that the desired range of characteristics is covered with the minimum number of locators. The values of mean, σ, and spread exhibited by the set of eight locators chosen is

Mean:	=	25, 30, 35, 40, 45, 50, 55 km, Figure 12
Standard Deviation:	=	1.0, 1.5, 2.0, 2.5, 3.0, 3.5, 4.5 km
Spread:	=	5, 10, 15, 20 km

The eight locators are L1(2.0), L1(3.0), L2(0.15), L2(0.90), L3(4.5), L3(20.0), L4(2.5), and L4(10.0).

Tables 12 and 13 show how the locators selected cover the applicable range of characteristics; Table 19 is organized by values of mean, σ, and spread, while Table 13 is organized by locator.

Computations. -- Means, standard deviations and maximum spread were calculated for the following parameters:

h_1: Located horizon altitude

Δh_1: Difference between located horizon altitude with and without error

$|\theta|$: Local vertical direction with respect to nadir, absolute value

$|\Delta\theta|$: Difference between local vertical directions with and without errors applied, absolute value

Absolute values of local vertical direction and error were used to eliminate the dependence of the results on an implied direction of flight or direction of scan. Maximum spread is the difference between the minimum value and maximum value of the applicable parameter. The profiles for which the maximum and minimum values occurred were identified in the output.

Results are summarized in Appendix F (Figures F1 through F12) showing located horizon and local vertical standard deviation, all as functions of instrument error. The complete results are given in Appendix G.

Note that the curves are nearly all linear so that the sensitivity of horizon error to each instrument error can be expressed by a single number, the approximate slope of the curve. Table 14 gives the sensitivity coefficients for mean and standard deviation of horizon error, expressed in km/percent or km/0.01 W/m^2-sr for scale and bias errors, respectively.

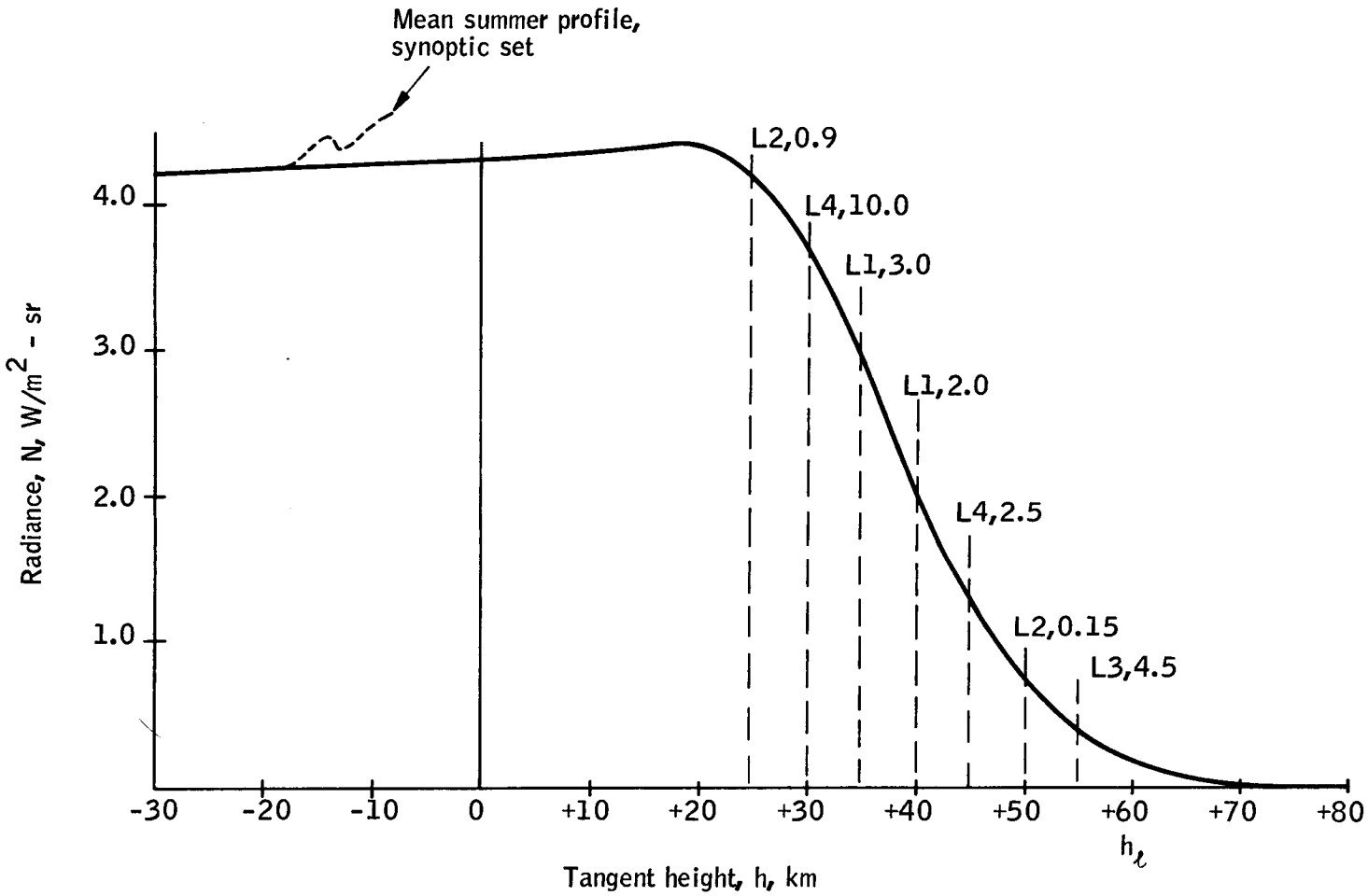

Figure 12. Mean Located Horizons for Selected Locators

TABLE 12. - LOCATORS LISTED BY MEAN, σ , AND SPREAD OF LOCATED HORIZON

Mean		Standard deviation		Spread	
h_1, km	Locator	σ, km	Locator	Spread, km	Locator
25	L2(0.9)	1.0	L4(2.5)	5	L4(2.5) L2(0.15)
30	L4(10.0)	1.5	L3(4.5) L2(0.15)	10	L3(4.5) L2(0.9)
35	L1(3.0)	2.0	L4(10.0)	15	L1(2.0)
40	L1(2.0)	2.5	L3(20)	20	L1(3.0)
45	L4(2.5)	3.0	L2(0.9)		
50	L2(0.15)	3.5	L1(2.0)		
55	L3(4.5)	4.0 4.5	------ L1(3.0)		

TABLE 13. - MEAN, σ , AND SPREAD LISTED BY LOCATOR

Locator	h_1, km	σ_{h_1}, km	Spread, km
L1(2.0)	40	3.5	15
L1(3.0)	35	4.5	20
L2(0.15)	50	1.5	5
L2(0.9)	25	3.0	10
L3(4.5)	55	1.5	6
L3(20)	40	2.5	10
L4(2.5)	45	1.0	5
L4(10.0)	30	2.0	7

These horizon errors caused by instrument errors cause a degradation in the measurement program performance. A measure of program performance is the confidence level in obtaining a given confidence interval on the estimate of horizon noise obtained from the measured profiles. In the Part I study, data sampling requirements were determined which would produce a 95 percent confidence level of estimating the horizon noise to within ±0.5 km. Because of the added effect of instrument-caused horizon noise, this confidence interval must be reduced, or, alternatively, the number of samples must be increased.

The analysis given in Appendix D leads to the following equation relating the parameters of interest.

$$I_c = \frac{\left[2\sigma^2\left(1+\frac{\sigma_1^2}{\sigma_2^2}\right)^2 + m(N-1)\,k^2\frac{\sigma_1^2}{\sigma_2^2}\right]^{1/2}}{m(N-1)\,(1-P/100)}$$

where

I_c = confidence interval on the estimate of natural horizon noise

σ_2 = horizon noise in nature

σ_1 = instrument-caused horizon noise

m = number of time cells

N = number of samples per time-space cell

k = fractional uncertainty in the estimate of σ_1.

The approach taken here is to allow the confidence level to decrease to 90 percent from 95 percent rather than to increase the sample size. The resultant allowable instrument-caused horizon error is determined from Figure 13 which shows the confidence level, P, versus instrument-caused error, σ_1, for various values of horizon noise, σ_2, and k, the fractional uncertainty in σ_1. At the 90 percent confidence level, the following instrument-caused errors are allowable:

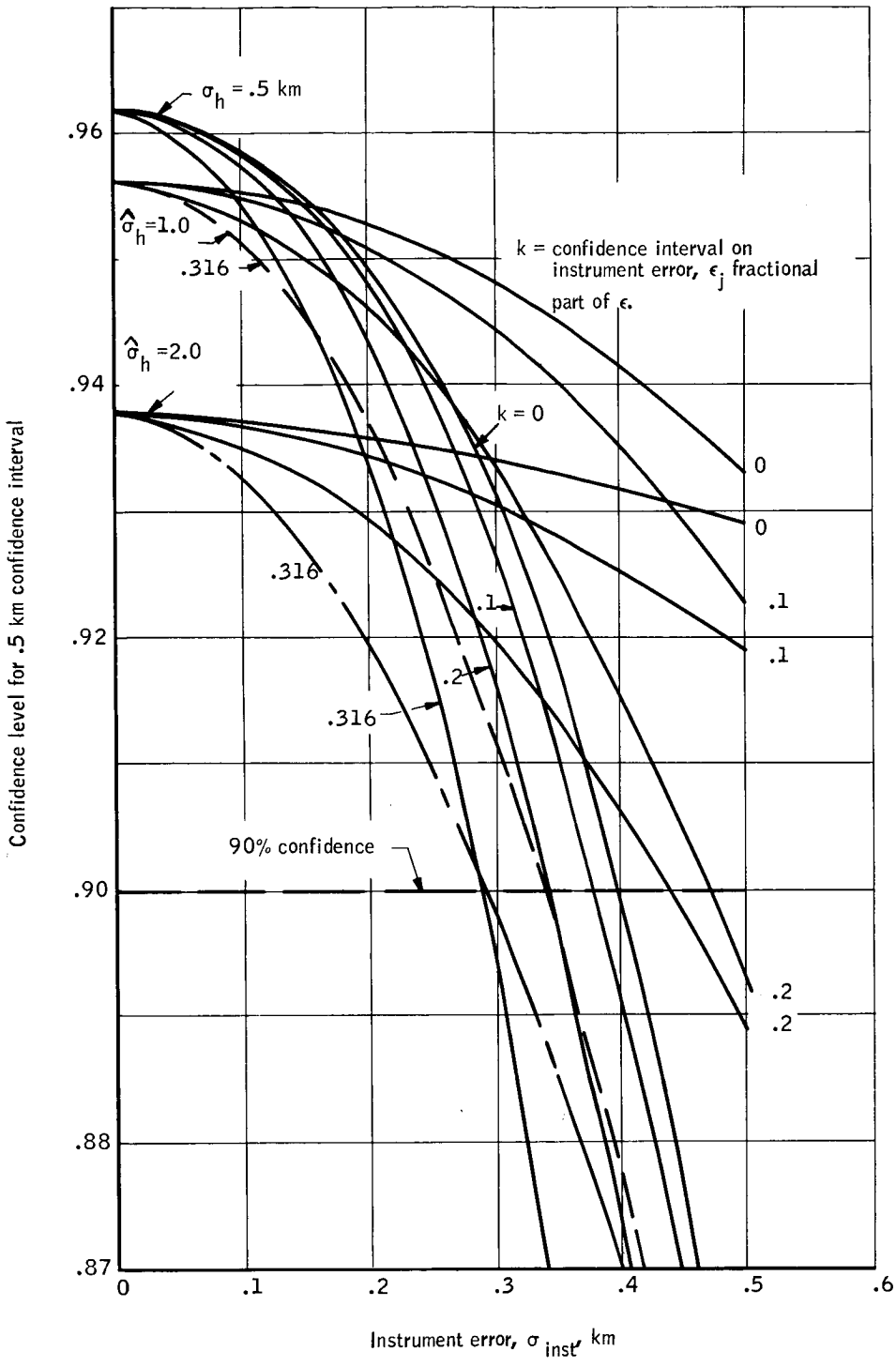

Figure 13. Confidence Level for Obtaining 0.5 km Confidence Interval on Horizon Standard Deviation Versus Instrument Error Confidence Interval

$$\sigma_1 = 0.3 \text{ km } \pm 31.6 \text{ percent; } 0.34 \text{ km } \pm 20 \text{ percent; } 0.38 \text{ km } \pm 10 \text{ percent; } 4 \text{ km } \pm 0 \text{ percent}$$

To simplify the radiometer design problem, both the allowable error and its uncertainty should be made as large as possible. However, as the allowable error increases, the allowable uncertainty decreases, necessitating a compromise. The combination selected as being a reasonable compromise is an instrument-caused error, σ_1, of 0.34 km known to within ±20 percent.

The allowable values of each of the six radiometer errors are those values which produce a horizon error not exceeding 0.34 km.

Using the sensitivity coefficients of Table 14, the locator exhibiting the maximum sensitivity for each error was constrained to produce a horizon error of $0.34/\sqrt{6}$ km in order to guarantee that the rss of the six errors did not exceed 0.34 km.

Since a given locator exhibits high sensitivity to one kind of error and low sensitivity to another, the approach described above led to a root sum square horizon error considerably lower than the maximum allowable 0.34 km. Adjustments were made in the errors known to cause difficulty in the radiometer design process (bias calibration and drift) to relieve the requirements and remain with the allowable 0.34 km error.

The resulting allowable radiometer errors and the resultant root-sum-square-horizon standard deviation and overall mean error are shown in Table 15. These results are based on the time and space cells previously defined.

The significance of this table is that the radiometer errors become radiometer specifications, defining the maximum allowable scale and bias errors for calibration drift and noise. For clarity they are given here:

Scale calibration	0.3 percent
Scale drift	0.72 percent
Scale noise	0.27 percent
Bias calibration	0.01 W/m^2-sr
Bias drift	0.01 W/m^2-sr
Bias noise	0.01 W/m^2-sr

TABLE 14. - SENSITIVITY COEFFICIENTS

Standard Deviation	Scale, km/percent			Bias, km/0.01 W/m^2-sr		
	Cal.	Drift	Noise	Cal.	Drift	Noise
L1 (2.0)	.02	.13	.10	.01	.06	.05
L1 (3.0)	.04	.18	.13	.015	.05	.05
L2 (0.15)	0	0	.08	.02	.09	.08
L2 (0.9)	0	0	.48	.002	.008	.10
L3 (4.5)	.006	.07	.026	.06	.04	.15
L3 (20)	.008	.10	.023	.27	.19	.053
L4 (2.5)	0	0	.06	.04	.22	.07
L4 (10)	0	0	.08	.02	.10	.03
Mean Error						
L1 (2.0)	.12	-.02	.004	.06	-.006	-.01
L1 (3.0)	.15	-.03	-.004	.05	-.006	-.008
L2 (0.15)	0	0	-.116	.09	-.01	-.029
L2 (0.9)	0	0	-.625	.008	-.001	-.077
L3 (4.5)	.06	-.007	-.004	.41	-.038	-.006
L3 (20)	.09	-.01	0	.18	-.018	-.003
L4 (2.5)	0	0	-.12	.21	-.02	-.02
L4 (10)	0	0	-.19	.10	-.01	-.03

TABLE 15. - ALLOWABLE INSTRUMENT CAUSED HORIZON ERROR, STANDARD DEVIATION AND MEAN[a]

Locator std. dev.	Sum rss km	Scale km			Bias, all 0.01 W/m^2-sr		
		Cal., 3%	Drift, 0.72%	Noise, 0.27%	Cal. km	Drift km	Noise km
L1(2.0)	.139	.06	.094	.027	.010	.060	.050
L1(3.0)	.197	.12	.130	.035	.015	.050	.050
L2(0.15)	.126	0	0	.022	.020	.090	.080
L2(0.9)	.164	0	0	.130	.002	.008	.100
L3(4.5)	.175	.018	.050	.007	.060	.040	.150
L3(20.0)	.34	.024	.070	.006	.270	.190	.053
L4(2.5)	.235	0	0	.016	.040	.220	.070
L4(10.0)	.109	0	0	.022	.020	.100	.030
Mean	Sum						
L1(2.0)	.393	.36	-.014	.001	.06	-.006	-.01
L1(3.0)	.463	.45	-.002	-.001	.05	-.006	-.008
L2(0.15)	.019	0	0	-.032	.09	-.01	-.029
L2(0.9)	-.239	0	0	-.169	.008	-.001	-.077
L3(4.5)	.54	.18	-.005	-.001	.41	-.038	-.006
L3(20.0)	.422	.27	-.007	0	.18	-.018	-.003
L4(2.5)	.137	0	0	-.003	.21	-.02	-.020
L4(10.0)	-.009	0	0	-.051	.10	-.01	-.030

[a] σ_1 = 0.34 km,
k = 0.2

DATA COLLECTION EFFECTS

The data collection effects are catagorized as data collection effects and data handling effects. The first effect relates to telemetry coverage and spacecraft storage capability constraints while the later relates primarily to profile acquisition rates. The subjects are treated in the following paragraphs.

Orbital Data Collection Effects

Recent studies have shown that there will be an intermittent gap in the data telemetry coverage from the HDS satellite. It has been estimated that over a 28-day map period there are nine occasions, on the average, when the data cannot be telemetered on an every-orbit basis, so that a two-orbit interval of time elapses between data transmission. This telemetry gap, which affects about two percent of the total number of orbits, is a narrow global band some 7° longitude wide which extends sinusoidally around the globe, passing over northern Greenland and over the Antarctic south of Australia, as shown in Figure 14. The tlemetry gap, strictly speaking, extends only over some 80 percent of an orbit, but will be treated here, for convenience, as a one-orbit gap. The question has been raised as to whether this gap seriously affects the data sample and, if so, how the sampling methodology should be modified.

The problem can be approached by first defining the longitudinal dimension of affected space cells for the L4(2.5) and L1(3.0) locators, since these locators represent the two extremes used in defining the overall data sampling requirements. Inspection of maps outlining the no-telemetry band and the space cell distribution for these two locators reveals that the affected space cells have the longitudinal dimensions shown in Table 16.

TABLE 16. - LONGITUDINAL DIMENSIONS OF SPACE CELLS AFFECTED BY THE TELEMETRY GAP

	Locator			
	L4(2.5)		L1(3.0)	
Latitude interval, deg	W long.	E long.	W long.	E long.
0-10	30	15	30	15
10-20	30	15	30	15
20-30	40	40	15	20
30-40	20	20	15	20
40-50	20	20	10	15
50-60	20	20	10	15
60-70	20	20	10	15
70-80	20	20	10	15
80-82.6	45	45	20	20

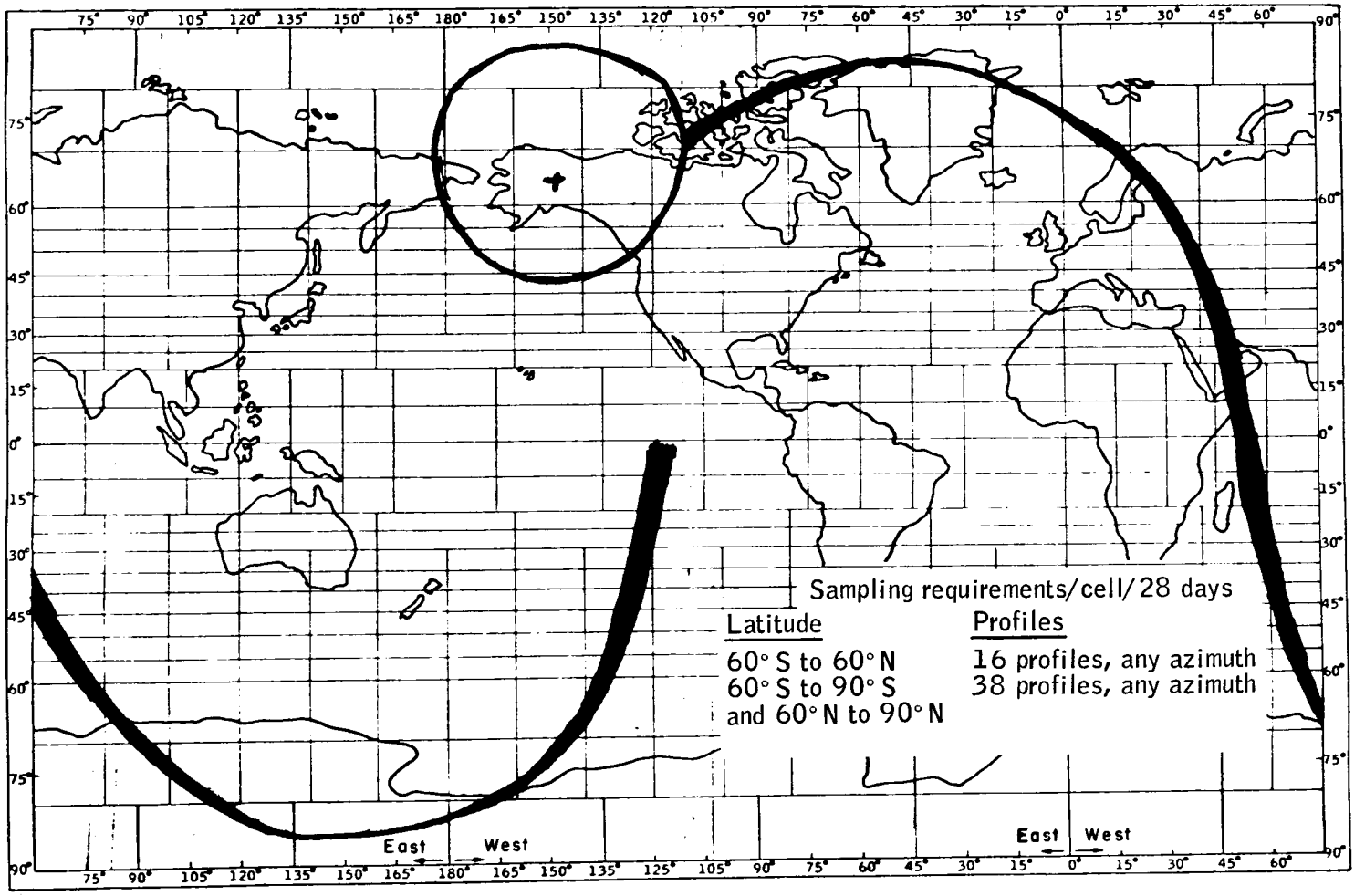

Figure 14. Telemetry Data Gap

The next step in the analysis is to determine the expected number of satellite intercepts, per map period, within a given longitude interval. This can be estimated, for a sufficiently long period of time (i.e., 28 days), by multiplying the number of orbits (429) by the ratio N°/360°, where N is the longitude interval. If both satellite up-passes and down-passes are considered, the number of intercepts is doubled. The following set of values is thereby obtained.

Cell Long. dimension, deg	Expected number of satellite intercepts		
	Down-passes	Up-passes	Total
10	12	12	24
15	18	18	36
20	24	24	48
30	36	36	72
45	54	54	108

Now, if the telemetry gap is associated with a satellite which cannot make contact with a ground station after one orbit during its night-side down-pass in the Western Hemisphere, then nine night-time down-passes are lost per 28-day map period. The following table shows the effect of these telemetry losses.

Expected number of satellite intercepts, considering losses

Cell Long. dimension	Down-passes	Up-passes	Total passes	Overall % decrease
10	3	12	15	38
15	9	18	27	25
20	15	24	39	19
30	27	36	63	13
45	45	54	99	8

It is obvious, from the above table, that the telemetry gap most seriously affects those cells with small longitudinal dimensions. The overall sample (for a given data acquisition rate) is not only considerably reduced within an individual cell, but the balance of night and daytime data to be used for the analysis of diurnal variations is drastically changed for an affected cell in either hemisphere. It must be pointed out, however, that the smaller the longitude dimension, the greater the number of space cells there are within the particular latitude interval. If the worst case is considered, the space cells defined for locator L1(3.0) between 40 to 80° latitude, 38 percent of the data would be lost in each affected Western Hemisphere cell and 25 percent in each Eastern Hemisphere cell. However, within a particular latitude interval, the affected cells would only represent two out of the 30 cells extending around the globe.

Now that the data losses due to the telemetry gap have been defined, the next step is to consider possible ways in which the sampling methodology might be modified to lessen the effect of such losses upon the experiment.

One suggested approach is to spread the data losses over two orbits by temporarily using one-half the normal data acquisition rate to remain within the nominal one-orbit data memory capacity. Thus, the losses due to telemetry gaps could be spread over twice as many space cells (roughly speaking, since successive orbits are displaced 23 1/2° longitude, and, in the case of the 30° and 45° longitude cells, the same cell might be sampled in successive orbits), and the percent data loss could be reduced by one-half within individual cells.

A second approach would be to restrict the data losses during the two-orbit period entirely to the summer hemisphere. Thus, data would be acquired at the normal rate over the winter hemisphere during the two half-orbits, with collection suspended over the summer hemisphere. The winter period is defined here as the half year extending from October to March and the summer period from April to September. This represents the simplest methodology. A more elaborate scheme would involve defining the winter and summer as shorter periods (3 to 4 months) during which time sampling would be confined to the winter hemisphere. During the transitional spring and autumn periods, the sampling rates could be equally reduced over both hemispheres.

A third approach would be to adjust the data acquisition rates on several prior and subsequent orbits to compensate on a broader basis for data losses in the more critically affected space cells, i. e., the 10° and 15° longitude requirements for the various time/space cells as a function of their sensitivity to telemetry losses (by scaling them upward or downward in such a way as to maintain the same total sample/orbit capability).

A fourth possibility would be to merely accept the loss of sample data over one entire meridional band of space cells. This approach could take either of two forms: 1) collect the complete orbital data sample prior to the telemetry gap and then suspend data acquisition during the subsequent orbit; or 2) suspend data collection in the orbit prior to the telemetry gap and then resume data collection on the following orbit. A combination of (1) and (2) also represents another logical alternative, which resembles the first approach in terms of its net effect upon the data sample.

Whichever of the above approaches (or combination thereof) is adopted, some penalty must be paid because of the telemetry gap problem. It must be pointed out, however, that the level of confidence with which the data samples can be analyzed is not unduly sensitive to decreases in sample size (for example, a 17 percent reduction in the data sample size only reduces the level of confidence from 95 to 94 percent). The problem of telemetry gap data losses must, therefore, be kept in the proper context; it is a significant but not a critical problem area. It is premature at this time to specify in

exact terms how the telemetry gap problem should be handled; the experiment design(and spacecraft command capability) should be sufficiently flexible to provide a number of operationally implementable alternatives. The plan, at this time, would be to adopt the second approach described above, and to confine the data losses exclusively to the summer hemisphere during April to September. This approach is consistent with that taken in handling the problem of intermittant orbital periods of no-data collection whenever attitude-error and spin-rate correction are applied.

Data Handling Effects --

The MISER F model has been used to determine the expected coverage of "engineering" data cells within a 28-day map period from a 500 km sun-synchronous orbit. Four different profile acquisition rates were considered, ranging from 0.25 to 0.40 profiles/min. The MISER F results, shown in Table 17 serve to confirm what has been assumed in earlier studies of constant versus variable data acquisition rates: that a smooth, consistent pattern of global data coverage was obtainable from a sun-synchronous orbit during a 28-day period.

The results in Table 17 shows that a constant profile acquisition rate of 0.30/min would provide data cell coverage which is slightly in excess of the nominal data requirements between 30 to 80° latitude and greatly in excess at other latitudes. For a spacecraft rotation of 3 rpm, this acquisition rate means that only every 10th profile would have to be selected to satisfy the nominal requirements. If variable data acquisition rates are considered, then a rate of 0.20/min between 0° to 30° latitude would be more than adequate; this would mean that only every 15th profile would have to be selected within this latitude interval to avoid much of the data redundancy.

The MISER F model has been used to determine the expected coverage of data cells within a 28-day map period from a 500 km, sun-synchronous orbit. Four different data acquisition rates were considered, ranging from 0.25 to 0.40 profiles/min. The results of this study show that: 1) a smooth, consistent pattern of global data coverage is obtainable from this type of orbit; and 2) data acquisition rates of 0.20/min between 0° to 30° latitude and 0.30/min between 30 to 90° latitude are adequate for satisfying the data requirements.

Data Collection Effects on Sampling Requirements

A final step in the analysis was to consider the additional samples required to compensate for data losses resulting from telemetry gaps, garbled transmissions, and other forms of operational degradation. The best available estimate is that such losses will be approximately five percent of the total data sample. A multiplicative factor of 1.05 was applied, therefore, to the sampling requirements listed in Table 6 after they had been adjusted upward to compensate for random radiometer errors. Table 18 lists the data sampling requirements for the various locators which result when errors and losses are both taken into account.

TABLE 17. - RESULTS OF MISER F ANALYSIS OF DATA COVERAGE FROM A 270 N. MI. SUN-SYNCHRONOUS ORBIT

Latitude, °N or °S	"Engineering" data requirement, profiles per space/time cell	Number of profiles per orbit obtained at indicated acquisition rate, min^{-1}				
		0.20 (a)	0.25	0.30	0.35	0.40
0-10 (30° long)	16	37	47	56	56 (b)	56 (b)
0-10 (15° long)	16	18	23	28	32	37
10-20 (30° long)	16	37	47	56	56 (b)	56 (b)
10-20 (15° long)	16	18	23	28	32	37
20-25	16	25	31	37	43	50
25-30	16	25	31	37	44	50
30-35	16	12	15	18	22	25
35-40	16	12	15	18	22	25
40-45	16	12	15	18	22	25
45-50	16	12	15	19	22	25
50-55	16	12	15	19	22	25
55-60	16	13	16	19	22	25
60-70	38	26	32	39	45	52
70-80	38	29	36	44	51	56 (b)
80-90	38	37	47	56	56 (b)	56 (b)

[a]Extrapolated values

[b]These numbers are limited to 56, since MISER F programs ignore values in excess of 2 profiles/cell/day.

TABLE 18. - DATA SAMPLING REQUIREMENTS FOR RECOMMENDED LOCATORS COMPENSATED FOR ERRORS AND LOSSES[a]

Latitude interval, deg	L4 (0.5)	L2 (0.95)	L4 (2.5)	L2 (0.06)	L2 (0.3)	L1 (0.2)	L2 (0.5)	L7	L1 (1.0)	L1 (2.0)	L1 (3.0)
0-10	287	327	286	397	298	291	291	574	357	286	304
10-20	287	327	286	397	298	309	345	574	357	286	321
20-30	303	346	302	514	446	436	917	649	544	857	1 235
30-40	607	692	605	888	811	670	1 442	1 002	758	1 113	1 147
40-50	607	692	605	888	919	763	1 388	1 570	1 546	1 418	2 237
50-60	607	692	605	888	804	1 033	964	1 545	2 078	1 995	4 127
60-70	322	519	510	907	1 346	1 519	1 061	2 757	4 449	4 537	8 255
70-80	512	713	718	1 478	1 871	1 860	1 745	3 703	4 817	5 718	8 633
80-82.6	216	317	353	701	904	834	834	2 450	1 859	2 680	2 539
Totals: Northern hemisphere - 1 time cell	3 793	4 625	4 270	7 058	7 697	7 715	8 987	14 824	16 765	18 890	28 798
Globe - 1 time cell	7 586	9 250	8 540	14 116	15 394	15 430	17 974	29 648	33 530	37 780	57 596
Globe - 13 time cells	98 618	120 250	111 020	183 508	200 122	200 590	233 662	385 424	435 890	491 140	748 748

[a]Based upon a 95 percent confidence level

ATTITUDE CONTROL EFFECTS

An attitude control analysis determined that spin-rate and attitude-error corrections for the HDS satellite are required every five days and can be performed concurrently. Spin-rate correction requires a quarter-orbit period centered over either the south or north magnetic pole. Attitude-error correction requires a half-orbit period which must include one magnetic pole and one magnetic equator. During these correction periods, experiment data collection must be suspended. A basic question, then, is how these corrections can be best incorporated into the mission profile to minimize the effect of intermittent data losses upon the total experiment.

The preferred approach would appear to be one whereby the attitude error correction is applied during a half-orbit period extending from magnetic equator to magnetic equator, with the spin-rate correction being applied during the middle of this period when the satellite is near the magnetic pole. An alternate approach would be to apply these corrections during a half-orbit period extending from 1/8 orbit before (or after) passage at one magnetic pole to 1/8 orbit before (or after) passage at the opposite pole.

The first approach is preferred for two basic reasons. One, the data losses can be confined to either the Northern or Southern Hemisphere (roughly speaking, since the magnetic poles are both located near 70° latitude) during those half-year intervals when the variability of radiance profiles is at a minimum. It was shown in the Part I study, from the analysis of standard deviations in tangent height for locators, L1(3.0) and L4(2.5), that there are two distinct half-year intervals when the variability is either rather high or low. It would appear, from these results, that the spin-rate and attitude corrections should be applied over the Northern Hemisphere during the months April through September and over the Southern Hemisphere during October through March. This approach would not only provide an advantage to the overall data sample but would also avoid the loss of critical data during stratospheric warmings and other important synoptic situations which generally occur during the winter half of the year.

Another reason for favoring the first approach is that it equalizes the loss of day and night data samples since the period of spin-rate and attitude corrections is (broadly speaking) divided between 3:00 a.m. and p.m. local times. With the other approach, the data losses would be mostly concentrated within either a daytime or nighttime period, and this imbalance would have some effect upon the analysis of diurnal variability in the radiance profiles.

SAMPLING AZIMUTH EFFECTS

As currently configured, the radiometer will only scan within the orbit plane. For the 3 o'clock sun-synchronous orbit, which has an inclination of 97.38°, the scan directions with respect to earth coordinates are essentially meridional over low and mid latitudes, although the scan directions become increasingly zonal at high latitudes. As shown by the Part I study results, (ref 3,) the sampling azimuth has an important influence upon the radiance profile; two different viewing paths into the same space cell will reflect whatever differences are present in the atmospheric conditions along each path. Sampling in opposite directions along the same meridian can produce significant differences in the radiance profiles assigned to the same space cell at the low altitude. The constraint imposed upon the experiment by scanning only within the orbit plane could therefore be a significant one, particularly with regard to the diurnal sampling. The uncertainty, σ , is increased by approximately 5 percent at tangent heights below 40 km.

The orbit, as currently defined for the HDS mission, is one wherein the satellite traverses the night (or 3:00 a.m.) side of the earth moving south from the north polar region. Thus, in the Northern Hemisphere the viewing path of the radiometer is, by and large, southward in the direction of the equator. During the Northern Hemisphere fall, winter, and spring seasons, the radiance values measured along the night-side viewing path will generally be higher (especially in winter) than those which would be obtained from the opposite direction of scan. During the Northern Hemisphere summer, the nighttime radiance values would be slightly lower because of the general temperature (and radiance) gradient reversal at stratospheric and mesospheric levels between the polar and equatorial regions.

On the other hand, during the daylight (or 3:00 p.m.) side of the orbit in the Northern Hemisphere, the viewing path will be northward toward the polar region. During the Northern Hemisphere fall, winter, and spring seasons, the radiance values measured along the day-side viewing path will be generally lower (especially in winter) than those which would result from south-looking scans. During the Northern Hemisphere summer, the northward-scanned, daytime radiance values would be slightly higher. The overall result, then, is to obtain, during three seasons of the year, Northern Hemisphere nighttime radiance values which are systematically too high and daytime values which are too low; the diurnal differences in radiance are suppressed, therefore, by the effects of differences in scan direction. In the Northern Hemisphere summer, the diurnal differences are exaggerated by the azimuth direction effects.

For the Southern Hemisphere portion of the orbit, analogous reasoning leads to a reverse result, since the nighttime scans are poleward and daytime scans are equatorward. Thus, during Southern Hemisphere fall, winter, and autumn, the nighttime radiance values will be generally lower, and the daytime values higher, as a result of the differences in scan directions. The diurnal differences in radiance are exaggerated, therefore, during three Southern Hemisphere seasons and suppressed during the Southern Hemisphere summer.

TABLE 19. - AZIMUTHAL SAMPLING EFFECTS UPON DETERMINATION OF DIURNAL (DAY/NIGHT) DIFFERENCES

Hemisphere	Hemispheric season			
	Fall	Winter	Spring	Summer
Northern	Too low	Too low	Too low	Too high
Southern	Too high	Too low	Too high	Too high

radiance is such that suitable Northern Hemisphere and Southern Hemisphere pairs cannot be found which will serve to average out the azimuthal sampling effect for summer and winter time cells. For summer time cells, the diurnal differences measured from the day/night subsamples are consistently too low in both hemispheres; for winter time cells, the diurnal differences are consistently too high. Simple averaging out of opposite hemispheric effects will not work, therefore, in these two seasons.

One straightforward solution to the general problem would be to orbit two HDS satellites concurrently in essentially the same sun-synchronous orbit but travelling in opposite directions (this approach would have other advantages over and above that of statistical separation of azimuthal and diurnal effects). Another solution would be to make up radiometric up-scans as well as down-scans so as to obtain two continuous sets of data at viewing angles 180° apart. There are problems involved in comparing up- and down-scans. For the purposes of diurnal effects analysis, these problems may be relatively insignificant. Further studies of statistical techniques for treating the diurnal samples may yield a simple, reliable solution. It is apparent however, that further study must be directed toward this important problem area.

When viewed collectively for both hemispheres, the azimuth sampling problem appears to be one which can, to a large extent, be adequately handled in the statistical analysis of diurnal radiance variations. This is especially true at lower latitudes, where the diurnal component of radiance variation is largest and where the synoptic variability is sufficiently low so as to permit some reasonable approximations to be made in the analytical treatment.

To illustrate how the statistical separation of azimuth sampling and diurnal effects can be approached at low latitudes, consider the following case involving space cells within ± 10° of the equator during a 28-day time cell period in Northern Hemisphere spring (Southern Hemisphere autumn). All profiles occurring within the 0 to 10° N latitude interval would be separated into a set of day and night subsamples; the samples between 0 to 10° S latitude would be similarly treated. It can be reasonably assumed, for this long a time period, that the effect of synoptic variations within each set would cancel out and no longer be reflected in the differences measured between the day and night subsamples. In the case of the 0 to 10° N day/night subsample differences, the azimuthal sampling effect would suppress the diurnal difference; the 0 to 10° S subsample differences would reflect an additive azimuthal effect. By averaging the two sets of day/night subsample differences, the azimuthal effect can be largely eliminated. In this illustrative case, it was assumed that the Northern Hemisphere underestimate of diurnal differences in the spring was largely compensated for by the Southern Hemisphere overestimate of diurnal differences in the autumn.

The above example represents the simplest case, since the diurnal data samples are drawn from adjacent latitudinal zones in the tropics where the synoptic variability is relatively low. For this reason, the same time cell was used for the Northern Hemisphere and Southern Hemisphere day/night subsamples, since the difference between Northern Hemisphere spring and Southern Hemisphere autumn are relatively insignificant. At higher latitudes, however, the separation of the azimuthal sampling effect from the diurnal variational component is a more formidable problem. Furthermore, the statistical separation problem is more difficult in the case of winter and summer time cells because of the general summer reversal which takes place in the pole-equator radiance gradient (viewed broadly with respect to the range of 30 to 60 km tangent heights which is of main interest). These problems are discussed further below.

At higher latitudes, the statistical separation of azimuthal sampling effects from the diurnal variation component can be performed, in the case of spring and autumn time cells, by pairing sets of day/night subsamples from each hemisphere which apply to the same latitude interval (e.g., 50 to 60°) and to the same hemispheric season. Thus, one set of diurnal subsample differences will be displaced 6 months in time from the other. Further study is required to examine the problem of spatial and temporal correlations for data sets with such large latitudinal and time displacements.

In the case of winter and summer time cells, the statistical separation problem is considerably more difficult. As shown in Table 19, the combined effect of the orbit characteristics and the seasonal gradients in pole-equator

DEFINITION OF EXPERIMENT SAMPLING METHODOLOGY

Development of a recommended data sampling methodology had as its objective a system which would be operationally simple and readily implementable by the data handling subsystem. No attempt was made, therefore, to achieve an abstract level of optimization; instead, the approach was directed toward practical realization of a basic sampling methodology which could be occasionally modified to account for various special situations by means of the command subsystem. Thus, the acquisition rates could be greatly increased over areas where meteorologically significant conditions are occurring, such as stratospheric warming. This type of experimental adaptability and flexibility would appear to be highly desirable.

The starting point for this study was an examination of the profile acquisition rates (profiles/min) needed to satisfy the error and loss compensated set of data-sampling requirements. Table 20 lists these rates for the 11 locators in terms of 10° latitude intervals. These rates cover a range from 0.127 to 3.473 profiles/min. Since the nominal rotation rate of the spacecraft is 3 rpm, it is immediately obvious that a single, passive radiometer operating only in the down-scanning mode cannot completely satisfy the L1 (3.0) data-sampling requirement between 60 to 80° latitude at the desired 95 percent level of confidence.

The implications of very low data acquisition rates must also be carefully examined to avoid too large a space interval between successive samples. At a rate of 0.127 profiles/min, the satellite, with its ground speed of slightly more than 4° latitude/min, would traverse a distance of 32° latitude between profile acquisitions. This separation distance is viewed as too large, even though it has been shown (by recent MISER F computer studies of data coverage from a 270-n.mi. sun-synchronous orbit) that even coverage of all space cells is attainable within a 28-day map period with data-acquisition rates as low as 0.25 profiles/min. A rate of 0.127 profiles/min may also satisfy the data requirements for the Fourier time series analysis. Nevertheless, the separation distance should probably not exceed 10° latitude; otherwise, there would not be a satisfactory basis for studying small-scale time/space correlations between successive radiance profiles and for making detailed error analyses along individual orbits. For this reason, a minimum profile acquisition rate of 0.375 profile/min was adopted, even though this rate does provide 28-day data samples in low-latitude cells which are considerably in excess of the stipulated requirements for Fourier time series analysis at the 95 percent confidence level.

The choice of data-acquisition rates has been restricted, therefore, to a range of 0.375 to 3.0 profiles/min. In addition, selection of specific rates has been limited to the following fractions of the maximum profile acquisition rate: 1/8, 1/7, 1/6, 1/5, 1/4, 1/3, 1/2, and 1/1 (corresponding to rates of 0.375, 0.429, 0.50, 0.60, 0.75, 1.0, 1.5, and 3.0 profiles/min). The use of these fractions serves to provide even spacing between samples acquired at a given rate and also simplifies the mechanization of the data

TABLE 20. - PROFILE ACQUISITION RATES, PROFILE/MIN, NEEDED TO SATISFY COMPENSATED DATA SAMPLING REQUIREMENTS

Latitude interval, deg	Locator										
	L4 (0.5)	L2 (0.95)	L4 (2.5)	L2 (0.06)	L2 (0.3)	L1 (0.2)	L2 (0.5)	L7	L1 (1.0)	L1 (2.0)	L1 (3.0)
0-10	0.128	0.145	0.127	0.177	0.133	0.129	0.129	0.255	0.159	0.127	0.135
10-20	0.127	0.145	0.127	0.176	0.132	0.137	0.153	0.254	0.158	0.127	0.142
20-30	0.133	0.152	0.133	0.226	0.196	0.192	0.403	0.285	0.239	0.377	0.543
30-40	0.265	0.302	0.264	0.388	0.354	0.292	0.629	0.437	0.331	0.486	0.501
40-50	0.263	0.300	0.262	0.385	0.398	0.331	0.601	0.680	0.670	0.614	0.969
50-60	0.263	0.296	0.259	0.380	0.344	0.422	0.413	0.662	0.890	0.855	1.786
60-70	0.135	0.218	0.215	0.382	0.566	0.639	0.446	1.160	1.872	1.909	3.473
70-80	0.197	0.274	0.276	0.568	0.720	0.715	0.671	1.424	1.853	2.199	3.320
80-82.6	0.177	0.215	0.239	0.475	0.612	0.565	0.565	1.660	1.259	1.816	1.720

[a] Based upon a 95% confidence level.

handling subsystem. The use of fractions such as 2/7 or 5/13 would not provide these decisive advantages, although they could provide a nominally closer fit of measured to required numbers of profiles.

By examining Table 20 in terms of the data-acquisition rates listed above, it is obvious that a large number of possible combinations of rates can conceivably be employed. For example, one constant rate can be selected for the entire orbit, or the rate can be varied at 10° latitude intervals. At this stage in the study program, it is largely a matter of judgment as to which rate combination should be selected. Table 21 lists three possible rate combinations which could be applied to three levels of cumulative data-sampling requirements (at the 95-percent confidence level). The use of the "+" notation on the locator identifiers indicates that the requirements for certain other locators have been completely subsumed. At the low end of the cumulative requirements spectrum, a constant sampling rate of 0.375 profiles/min appears to offer a feasible approach. This rate provides a sample excess of 62 percent with respect to the cumulative requirement L2 (0.95) +. This data excess, it must be pointed out, is with regard to the 95 percent confidence level. Such data are not wasted, however, since they can be used to analyze the three designated locators at levels of confidence above 95 percent and to analyze the other locators with nominally higher requirements at levels of confidence below 95 percent.

For the intermediate data requirement level, L2 (0.50) +, two different acquisition rates have been selected. The lower rate serves to reduce the data excess between latitudes 0 to 30°. At the highest cumulative requirement level L1 (3.0) + three acquisition rates are used in order to scale the measured samples down closer to those required over the latitude intervals 0 to 30°, 30 to 50°, and 50 to 82.6°. The variable acquisition rate approach provides a relatively simple but effective data-sampling methodology. The variable data-acquisition rates considered above only differ by integral multiples and should be readily mechanizable by a preprogrammed switching sequence (possibly with periodic resetting by ground command). Also to be considered, for intermediate and highest level data requirements, is the possibility of varying the acquisition rate as a function of season. Thus, during Northern Hemisphere winter and Southern Hemisphere summer (and vice versa) the data-acquisition rate could be increased during the winter half-orbit, possibly at the expense of a lower rate within the summer half-orbit. During the transitional spring-autumn seasons, the acquisition rate could be kept constant throughout the entire orbit.

The total one-year samples obtained by the three data-acquisition schemes outlined above range from 196 586 to 912 702 profiles. For the intermediate requirement level, 336 570 profiles are obtained; this total sample would permit seven of the 11 locators to be analyzed over all latitude intervals at a confidence level of at least 95 percent.

The average radiometer data-acquisition rates, in terms of profiles per orbit, for the three sampling schemes described above are 35.25, 60.35, and 163.28. If an allowance of 5540 bits/profile is made for the radiometric data sample and if an allowance of 100 000 bits/orbit is made for the attitude

TABLE 21. - POSSIBLE COMBINATIONS OF PROFILE ACQUISITION RATES NEEDED TO SATISFY CUMULATIVE DATA SAMPLING REQUIREMENTS, ERROR AND LOSS COMPENSATED

Latitude interval, deg	Cumulative locator identifiers								
	L2 (0.95) + (b)			L2 (0.50) + (c)			L1 (3.0) + (d)		
	Profile acquisition rate, prof/min	No. of samples		Profile acquisition rate, prof/min	No. of samples		Profile acquisition rate, prof/min	No. of samples	
		Measured	Required		Measured	Required		Measured	Required
0-10	0.375	843	327	0.429	963	397	0.600	1 349	574
10-20	0.375	846	327	0.429	976	397	0.600	1 354	574
20-30	0.375	853	348	0.429	975	917	0.600	1 364	1 235
30-40	0.375	859	692	0.750	1 718	1 442	1.00	2 291	1 442
40-50	0.375	865	692	0.750	1 731	1 388	1.00	2 308	2 237
50-60	0.375	875	692	0.750	1 751	1 033	3.00	7 002	4 127
60-70	0.375	891	519	0.750	1 783	1 519	3.00	7 131	8 255
70-80	0.375	975	718	0.750	1 950	1 871	3.00	7 800	8 633
80-82.6	0.375	554	353	0.750	1 107	904	3.00	4 428	2 680
TOTALS:		7 561	4 666		12 945	9 868		35 027	29 757
Globe - 1 time cell		15 122	9 332		25 890	19 736		70 054	59 514
Globe - 13 time cells		196 586	121 316		336 570	256 568		910 702	773 682
Excess percent		62			31			18	

[a] Based upon a 95 percent confidence level

[b] L2 (0.95) + subsumes L4 (0.5), L2 (0.95)

[c] L2 (0.5) + subsumes L2 (0.95), + L2 (0.06), L2 (0.3), L1 (0.2)

[d] L1 (3.0) + subsumes L2 (0.5), + L7, L1 (1.0), L1 (2.0)

determination and spacecraft status data, then the total required memory capacities for the three sampling schemes are 295 285 bits/orbit for L2 (0.95) +; 434 339 for L2 (0.50) +; and 1 004 571 for L1 (3.0) +. These values are all within the range of feasibility for solid-core memories as shown by other Part II project studies.

Further analysis of the sampling methodology problem was based upon an examination of the sensitivity of the 95 percent confidence level to changes in the number of profiles acquired for the various space-cell distributions. It can be shown (ref. 3) that the confidence interval on σ (the measure of uncertainty in the statistical analysis of a cell sample) is given by the following expression:

$$I_c = \left\{ \sqrt{1 + \left[\frac{2}{m\,(N-1)\,(1-P/100)} \right]^{1/2}} - \sqrt{1 - \left[\frac{2}{m\,(N-1)\,(1-P/100)} \right]^{1/2}} \right\} \hat{\sigma}$$

where I_c is the confidence interval, $\hat{\sigma}$ the sample estimate of σ (the true standard deviation), m the number of time cells, N the number of samples per cell, and P the percent level of confidence. It is obvious, for a given value of I_c, that P decreases as (N-1) decreases. If, for example, the value of (N-1) associated with P = 95 percent decreases to (N-1) /2, then P decreases to 90 percent (for a constant I_c). The following table lists some representative multiples of (N-1) versus percent confidence levels:

(N-1) multiple	Percent level of confidence
5	99
2	97.5
1	95
0.67	92.5
0.5	90
0.33	85
0.25	80

It is apparent, from these values, that the cell sample can be considerably reduced and a useful level of confidence will still be obtained. A 95 percent level of confidence is generally regarded as very good (and is the level adopted in the statistical design of many experiments), a 90 percent level can be regarded as good, 85 percent as fair, and 80 percent (or even lower) as still useful. The assignment of these adjectival descriptors is essentially a matter of opinion which reflects the degree of calculated risk which the experimenter is willing to accept that the eventual statements concerning the statistical results are indeed correct. At the 95 percent level of confidence, the odds of being correct regarding the statistical properties of an individual

time/space cell are 19 to 1; at 90 percent, 9 to 1; at 80 percent, 4 to 1; at 50 percent, 1 to 1, or even odds. At this point, the problem changes from one of statistical definition to one of decision making regarding the acceptance of given levels of calculated risk for the many hundreds to time/space cells which constitute the basic HDS experiment. Game theory and value theory can be profitably applied to this decision-making process; this lies outside the scope of this present study but clearly represents an area of further investigation. It should be possible to establish a value function for the different levels of statistical confidence which could be selected for the HDS experiment and thereby provide the basis for trading off experiment value versus system cost.

In the present instance, it is worthwhile to examine possible compromises in confidence level at the high requirement end of the HDS experiment, i. e., as defined by the L7, L1 (1.0), L1 (2.0), and L1 (3.0) locators. As shown in Table 21, the L1 (3.0) + sample is approximately three times as large as the L2 (0.50) + sample. If a level of confidence of at least 95 percent is provided for all 11 locators, this results in extremely high confidence levels for locators such as L2 (0.95) and L4 (0.5) at the lower end of the requirements spectrum. However, if the confidence levels at the high-requirement end can be relaxed so as to still achieve at least a fair to good level of confidence, then a very considerable reduction can be made in the total sampling requirement and data-acquisition rates for all 11 locators.

The sampling problem was re-examined, therefore, in terms of providing a reasonable compromise which would attain a 95 percent level of confidence for most locators, but which could be relaxed in a relatively few instances to values of 90 and 85 percent confidence. The results of this analysis, which was necessarily conducted on a qualitative basis, led to the formulation of the recommended sampling methodology outlined in Table 22. Three data-acquisition rates were selected: 0.429 profiles/min from 0° to 30° latitude, 0.750 profiles/min from 30° to 60°, and 1.00 profiles/min from 60° to 82.6°. The total one-year data sample collectable at these rates amounts to 378 508 profiles a value which includes an overall loss allowance factor of five percent. The useful sample, then, would constitute 360 484 profiles.

The levels of confidence attainable in analyzing the cell samples with the recommended methodology are shown in Table 23 as a function of 10° latitude intervals. These results indicate that a confidence level of at least 98 percent can be achieved for three locators, of at least 95 percent for seven locators, of at least 89 percent for 10 locators, and at least 82 percent for all 11 locators. Over the latitude range 0 to 50°, the confidence levels for all locators exceed 93 percent. These results are regarded as quite satisfactory, overall, since the L1 (3.0) locator has a very demanding set of data-sampling requirements when considered exclusively at the 95 percent confidence level.

The average number of profile samples acquired per orbit with the recommended sampling methodology is 67.88. Based upon an allowance of 5540 bits/profile for the radiometric data, and 100 000 bits/orbit for the attitude determination and spacecraft status data, a total memory capacity of 476 055 bits/orbit would be required, a value well within the limits of feasibility for solid-core memories.

TABLE 22. - NUMBER OF DATA SAMPLES OBTAINABLE WITH RECOMMENDED VARIABLE RATE SAMPLING METHODOLOGY

Latitude interval, deg	Data acquisition rate, profile/min	Number of data samples
0-10	0.429	963
10-20	0.429	967
20-30	0.429	975
30-40	0.750	1718
40-50	0.750	1731
50-60	0.750	1751
60-70	1.00	2377
70-80	1.00	2600
80-82.6	1.00	1476

Totals:

Northern Hemisphere - 1 time cell	-	14 558
Globe - 1 time cell	-	29 116
Globe - 13 time cells	-	378 508

TABLE 23. - LEVEL OF CONFIDENCE IN DATA SAMPLES OBTAINED WITH RECOMMENDED SAMPLING METHODOLOGY, PERCENT

Latitude interval, deg	Locator										
	L4 (0.5)	L2 (0.95)	L4 (2.5)	L2 (0.06)	L2 (0.3)	L1 (0.2)	L2 (0.5)	L7	L1 (1.0)	L1 (2.0)	L1 (3.0)
0-10	98.5	98.3	98.5	97.9	98.5	98.5	98.5	97.0	98.1	98.5	98.4
10-20	98.5	98.3	98.5	97.9	98.5	98.4	98.3	97.0	98.2	98.5	98.3
20-30	98.4	98.2	98.5	97.4	97.2	97.8	95.3	96.7	97.2	95.6	93.7
30-40	98.2	98.0	98.2	97.4	97.6	98.0	95.8	97.1	97.8	96.8	96.7
40-50	98.2	98.0	98.3	97.4	97.3	97.8	96.0	95.5	95.5	95.9	93.5
50-60	98.3	98.0	98.3	97.5	97.7	97.0	97.2	95.6	94.1	94.3	88.2
60-70	99.3	98.9	98.9	98.1	97.2	96.8	97.8	94.2	90.6	90.4	82.6
70-80	99.0	98.6	98.6	97.2	96.4	96.4	96.6	92.9	90.7	89.0	83.4
80-82.6	99.1	98.9	98.8	97.6	96.9	97.2	97.2	91.7	93.7	90.9	91.4

The results of the various studies described above represent a preliminary attempt to size the experiment in such terms as to provide a reasonable basis for potential application to a large number of horizon locators. For convenience, attention has been limited to 11 locators recommended in the Part I study results; the HDS data sample will, of course, be generally applicable to the study of various other locators whose statistical properties are such that their sampling requirements lie within the wide range covered between the L4 (2.5) and L1 (3.0) locators. For example, the recommended sample methodology should provide an adequate basis for Fourier time series analysis of other locators such as L3 (7.5), and of locators in the L1, L2, and L4 families with other values of normalized integral normalized radiance, such as L2 (0.9), L4 (7.5), and L4 (1.0).

In view of the above discussion, the question naturally arises as to whether the so-called basic sampling requirements (i.e., a global, one-year sample of approximately 110 000 profiles, defined on the basis of the L4 (2.5) locator) can fulfill to any satisfactory degree the HDS experiment objectives. To investigate this question, a minimum sampling methodology was defined, based upon a constant data-acquisition rate of 0.21 profiles/min. This rate would provide a global sample of 8472 profiles per 28-day map period, and 110 136 profiles for a one-year operational period. If the number of data samples thereby obtained and compared with those required for the various locators (Table 18), it is possible to compute the level of confidence for each locator within 10° latitude intervals. The results of this computation, presented in Table 24, indicate that levels of confidence of 83 percent or better are obtainable for seven locators. However, for the remaining locators, i.e., L7, L1 (1.0), L1 (2.0), and L1 (3.0), the confidence levels are very drastically reduced at latitudes above 40 to 50°. As pointed out earlier, the problem at this point passes beyond that of statistical definition to one of decision making, wherein follow-on studies are recommended in the areas of game and value theory.

TABLE 24. LEVEL OF PERCENT CONFIDENCE IN DATA SAMPLES BASED UPON MINIMUM METHODOLOGY FOR BASIC DATA REQUIREMENTS

Latitude interval, deg	Locator										
	L4 (0.5)	L2 (0.95)	L4 (2.5)	L2 (0.06)	L2 (0.3)	L1 (0.2)	L2 (0.5)	L7	L1 (1.0)	L1 (2.0)	L1 (3.0)
0-10	97.0	96.5	97.0	95.8	96.8	96.9	96.9	93.9	96.2	97.0	96.8
10-20	97.0	96.5	97.0	95.8	96.9	96.7	96.4	93.9	96.2	97.0	96.6
20-30	96.8	96.4	96.8	94.6	95.3	95.5	90.4	93.2	94.3	91.1	87.1
30-40	93.7	92.8	93.7	90.8	91.6	93.0	85.0	89.6	92.1	88.4	88.1
40-50	93.7	92.9	93.8	90.8	90.5	92.1	85.7	83.8	84.1	85.4	76.9
50-60	93.8	92.9	93.8	90.9	91.8	89.5	90.2	84.2	78.8	79.7	57.9
60-70	96.8	94.8	94.9	90.9	86.5	84.8	89.4	72.4	55.5	54.6	17.3
70-80	95.3	93.5	93.4	86.4	82.8	82.9	84.0	66.9	55.9	47.6	21.0
80-82.6	95.8	94.9	94.3	88.7	85.4	86.5	86.5	60.5	70.1	56.8	59.1

CONCLUSIONS

The comprehensive study of radiometer calibration, drift, and noise errors (both scale and bias types) has shown that the radiometer design specifications are sensitively related to the experiment design requirements. The analysis of located horizon error for several representative horizon locators has indicated that current radiometer error specifications could be, in most cases, considerably relaxed without significantly reducing the level of confidence which can be achieved in the analysis of the space/time cell samples.

The relationship between data-acquisition rate and spacecraft spin rate represents a significant interface. For passive radiometric scanning, the maximum data-acquisition rate is determined by the maximum spin rate, which has been set at 3 rpm on the basis of spacecraft stability considerations. Since variations in the spin rate are directly reflected as variations in the radiance profile resolution, there is an important interface between the experiment and the attitude control subsystem.

The experiment/spacecraft design interface involves the command subsystem, which provides the means whereby the experiment can be operationally modified. The need for building flexibility into the HDS experiment can, at this time, only be justified by general arguments relating to uncertainties in the data-sampling requirements and system operational performance, and to the random character of many atmospheric disturbances such as stratospheric warmings, whose occurrence cannot be reliably predicted but which are sufficiently important to justify temporarily increased data-acquisition rates wherever and whenever they happen to take place.

A major experiment/radiometer design interface is involved in the choice of sampling azimuth. The Part II study has shown that the restriction of profile scans to the orbit plane causes a problem in the diurnal data analysis, especially with regard to the winter and summer time cells. Further exploration of this problem is strongly recommended.

The results of limited studies suggest that interruptions in the data series will not seriously compromise the experiment if they do not exceed the period of one time cell (i.e., 28 days), even in the worst case when the space/cell variances are at a maximum.

Data losses resulting from the telemetry gap in the STADAN network do not have a significant effect upon the experiment data sample. Only two percent of the orbits are affected, and although the telemetry gap affects the same set of space cells, the data losses can be confined, by adaptive reprogramming of the basic sampling methodology, to the summer hemisphere where the variability of radiance is at a minimum.

Data losses resulting from suspended data collection during periods of attitude and spin-rate correction are not significant with respect to the total experiment sample. These losses can be confined to the summer hemisphere by adaptive reprogramming.

The recommended data-sampling methodology is one based upon variable data-acquisition rates ranging from 0.429 profiles/min at low altitudes to 1.00 profiles/min at high latitudes. Rates below 0.375 profiles/min should not be used in order to ensure no more than a 10° latitude separation between successive profiles. The results of the MISER F analysis of data coverage from a 500 km, sun-synchronous orbit has shown that smooth, consistent coverage of 28-day time cells can be obtained even at low acquisition rates of 0.25-0.40 profiles/min.

DATA REDUCTION, ANALYSIS, AND APPLICATIONS

DATA REDUCTION

The data reduction discussed in this section refers to those operations necessary to obtain radiance horizon profiles properly tagged with auxiliary data after the GSFC Data Processing Center has cataloged, screened, ordered, inserted time, and formatted the raw data. Basically, the data reduction functions fall under the control of the experimenter. Figure 15 outlines the data reduction functions to be performed. For purposes of illustration, three data tapes are indicated as inputs; however, this may or not be the case. There are four basic types of data which have to be reduced to provide the final set of horizon profiles. Aside from quality checks, the primary data reduction tasks are those associated with determination of attitude, calculation of tangent heights, calibration of radiometer outputs, generation of horizon radiance profiles, and the auxiliary data tagging as indicated in Figure 39. Further discussion of these areas[a] is presented in the following paragraphs.

Tangent-Height Calculator

The tangent-height calculator as presently envisioned is a mathematical tool for evaluating the minimum earth to scan-line distance when the following data are given:

- The transformation from spacecraft axes to celestial axes (starmapper data reduction output)
- The radiometer scan vector in spacecraft axis components
- The geocentric spacecraft vector

The tangent-height calculation is basically a sequence of coordinate transformations where the output consists of tangent height and latitude, longitude of the sub-tangent point tagged with time and any other useful auxiliary data. The accuracies associated with this approach have not been evaluated; however, it is expected that an earth oblateness correction will be necessary. Depending on the accuracy required, second and higher order iterations of an oblateness correction procedure may be necessary. The efficiency of this approach is important to the cost and time involved in this particular data reduction function. This factor has not been considered in the approach prescribed; however, a basis has been formed for future adaptions and/or improvements.

Generation of Radiance Profiles

Generation of radiance profiles is basically referred to as "merging of the data" to obtain the radiance profiles. The radiometer data is inputted as a function of time and the corresponding tangent heights are inputted as a function of time. These two sets of data are merged to provide radiance

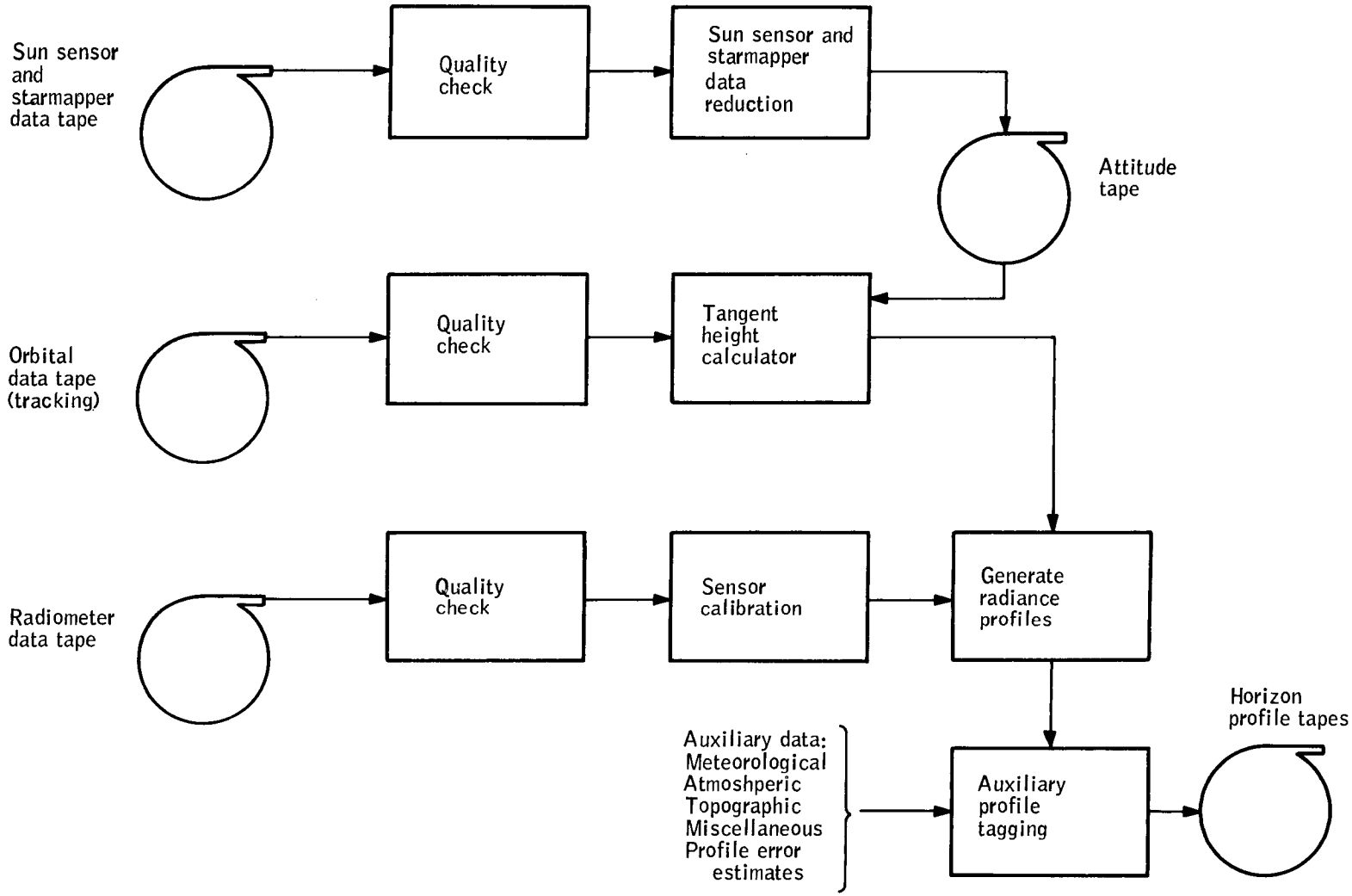

Figure 15. Experimenter Data Reduction Function

levels as a function of tangent height, which results in a horizon radiance profile for each two sets of input data (i. e., data associated with one scan of the horizon). Although not mentioned, it is assumed that any profile identifiers (latitude, longitude, time, etc.) are carried along through the process. If certain errors have been identified (i. e., calibration, tangent height, etc.) these too should be identified and recorded with the resulting profile.

Profile Tagging

Profile tagging is not a data reduction function per se but rather a merging process of profiles and auxiliary data which will be useful in subsequent data analysis. Various types of auxiliary data have been identified in Figure 15. It is expected that this data will be available in abundance by the early 1970's, due to increased activity in meteorological measurement programs. The merged data, horizon profiles and auxiliary information, will then be stored on magnetic tapes for later data analysis and/or utilization by industry and various investigators.

DATA ANALYSIS AND UTILIZATION

The analyses associated with collection of horizon profiles will be primarily those of model verification (comparison to phase I results), model extension, and scientific analysis. The general analysis and data utilization considered is outlined in Figure 16. The results of each analysis will be utilized in a different manner as indicated. The purpose of data analysis is to summarize or reduce the horizon profile data to information which is useful to industry and scientific investigation. Certainly the profiles themselves are useful to industry for analysis and comparison of locators as indicated in the figure. Further discussion of model verification, scientific analyses and associated data utilization is presented in the following paragraphs.

Model Verification and Extension

This portion of the analysis consists of selecting types or classes of locators whose outputs best characterize the profile and which are useful to the horizon sensor users. The profiles are then processed by the locators and reduced to located horizon altitudes, and analyzed for space-time deterministic variations as indicated by Figure 17. Note that the amount of data to be analyzed is multiplied by the number of locators that one wishes to use to describe the profile. The basic operations performed in data analysis are indicated in Figure 18. The preliminary data analysis consists of obtaining gross characteristics of the data (i. e., early trends, etc.) with which to plan portions

---

[a] Inputs relating to starmapper data reduction and radiometer calibration data reduction were not received in time for inclusion in this report. For information relating to these data reduction functions, the reader is referred to those portions of the Part II report describing the experiment package.

of the final analysis and to make decisions with regard to the operation of the experiment in case of unexpected events. Portions of the data analysis can begin as soon as the first orbit of data is processed. Certain space correlations could be performed, as well as some preliminary space series analysis (auto correlation analysis). Short-term variations (e.g., diurnal) can be performed as the measurement program progresses; however, the analysis of long-term time variations must wait until all data is available.

The analysis of diurnal variability is expected to proceed along these lines: 1) Identification of all profile samples with respect to sunrise and sunset times over the 0 to 80 km interval; 2) grouping of profiles, for each time cell, into day and night subsamples covering suitable aggregates of space cells, i.e., 5° or 10° latitude zones; 3) separate studies of twilight samples, including those with partial day or night components influencing a portion of the profile 4) statistical analysis of the day and night subsamples in terms of sampling azimuth effects; 5) comparative analysis of diurnal effects measured from HDS profile samples and those derived from selected high-resolution time series of synthesized radiance profiles; and 6) comprehensive error analysis, including all errors and uncertainties which affect the determination (or estimation) of diurnal components.

The importance of the diurnal analysis is to be judged not only in terms of providing a basis for empirical time-of-day corrections for horizon sensors (as a function of latitude and season) but also in terms of normalizing (or standardizing) the entire experimental set of radiance profiles on such a basis that they can be properly interpreted and applied by various potential users.

The final result of the total analysis will consist of a functional relationship between indicated altitudes, space, time, and other influencing factors. In the event that variations appear that were not predicted from the analysis of synthesized profiles, the results may be used to update the basic functional model or be the basis for the definition of further experiments.

The form of the presented data for utilization has not been considered beyond recognition that the types of outputs of this analysis would be functional relationships, plots of selected parameters, and tables of certain variables or coefficients.

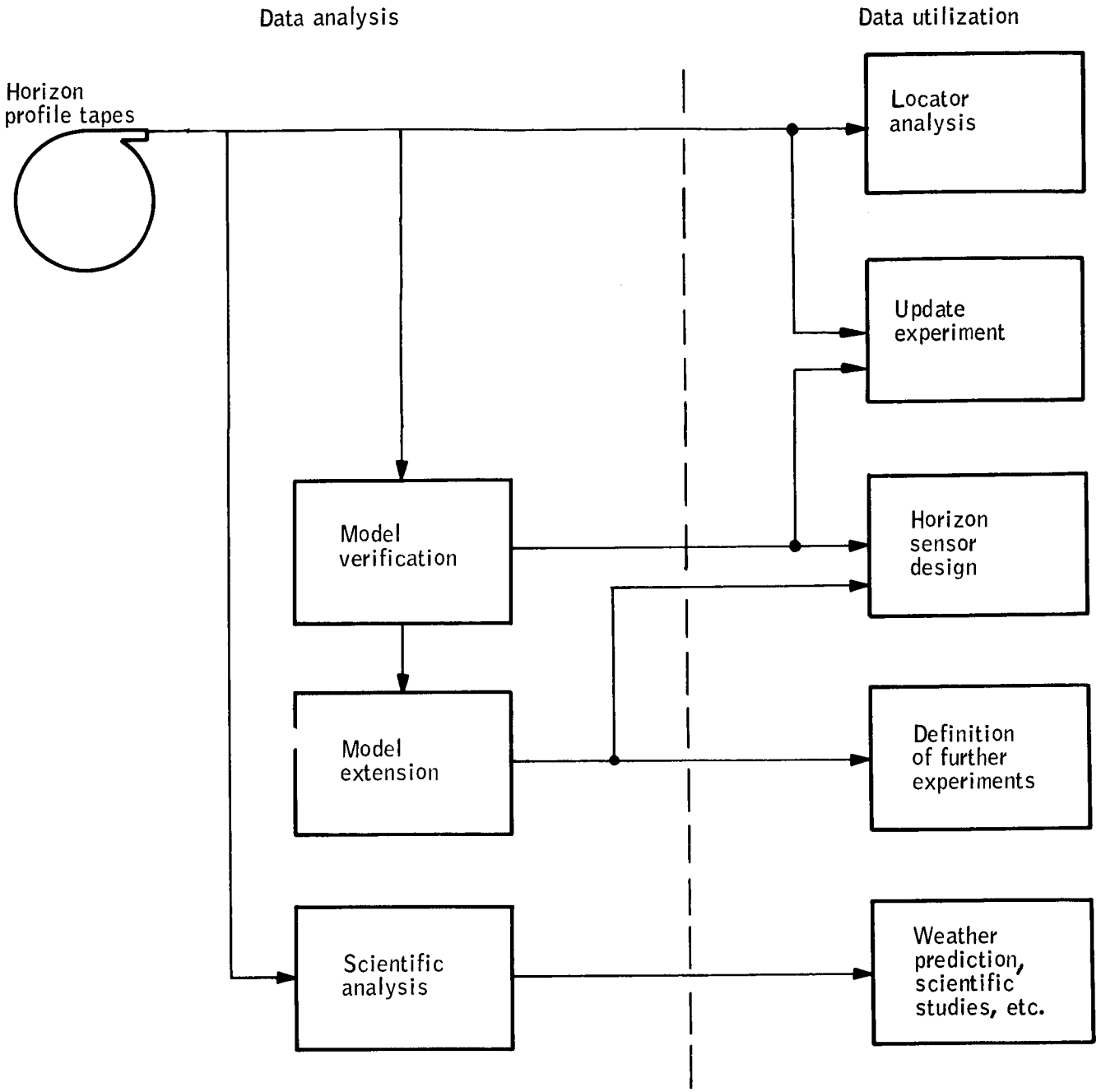

Figure 16. Data Analysis and Utilization

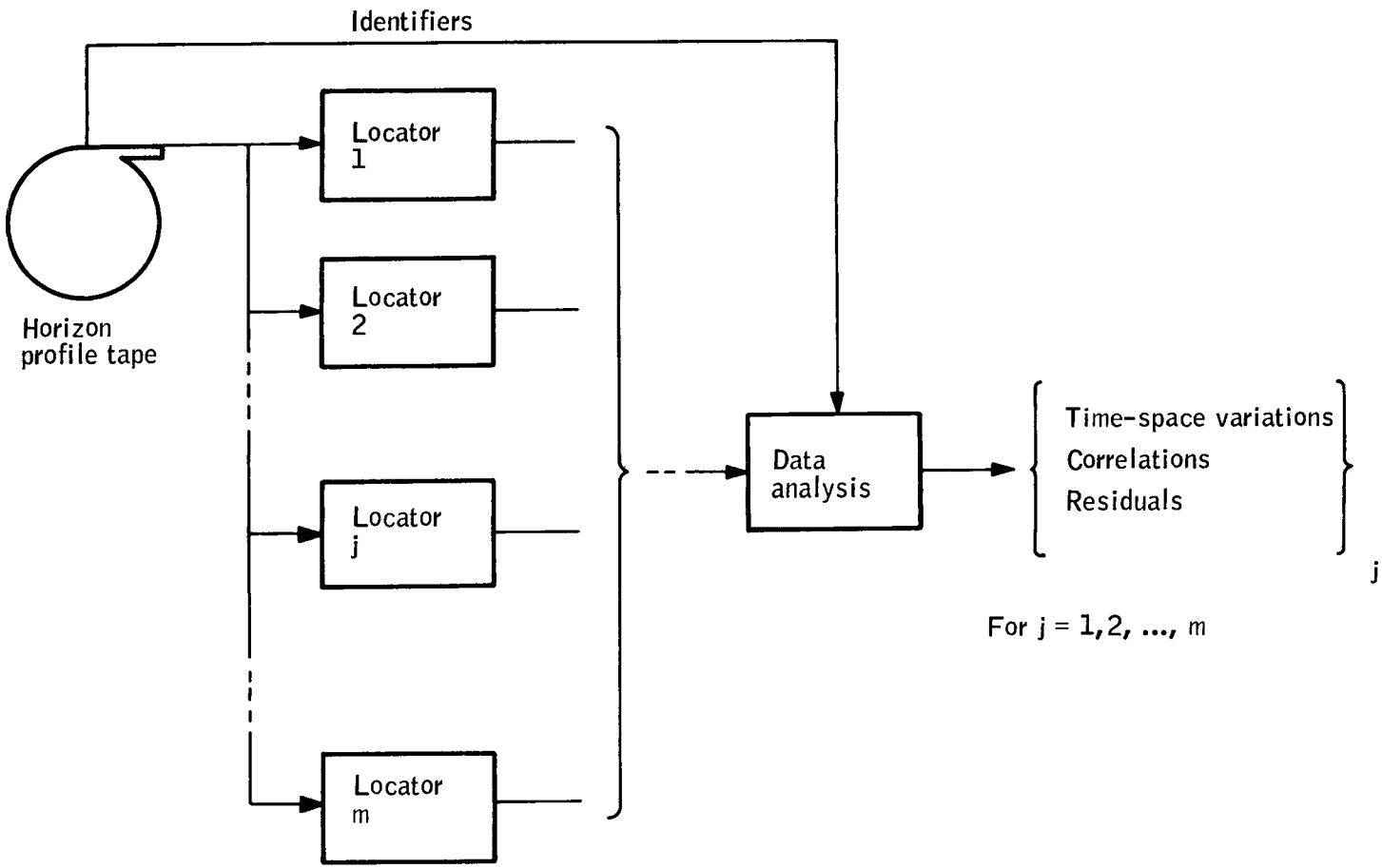

Figure 17. Model Verification

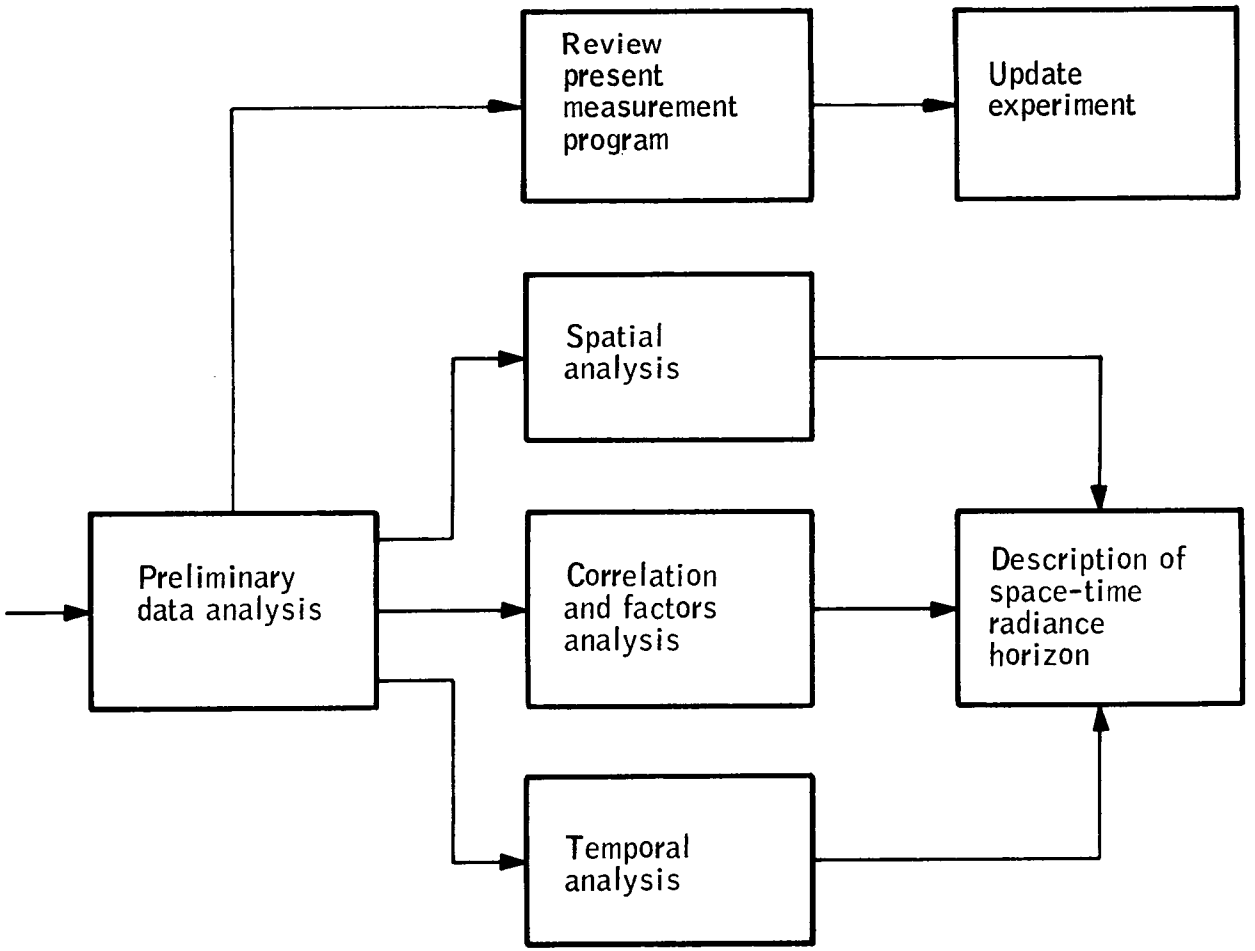

Figure 18. Data Analysis

Applications of HDS Results to Design of Further Experiments

The results of the HDS experiment will essentially establish empirical guidelines and ground rules for future experiments, since additional experiments should provide for general consistency and comparability of their results with those obtained in the HDS experiment.

There are many possible ways in which to apply the HDS results to the design of further horizon radiance experiments. The simplest possibility is to use the results of the initial HDS flight(s) to make minor modifications in the hardware and/or mission profile for subsequent HDS flights. The most obvious types of modification would be to alter the data acquisition rate, increase the data storage capacity, or change the orbit configuration. Another possibility would be to design a second-generation spacecraft which would significantly extend the experiment sampling capability, e. g., increase the profile resolution, or provide for simultaneous sampling in several different azimuthal directions. In the latter case, the HDS results would provide an empirical data base for experiment definition vastly superior to that which was necessarily used in shaping the pioneer experiment.

There are other possible experiment applications which must also be recognized. Among these might be design of advanced Scanner-type rocket probes for high-resolution profile measurement; design of meteorological rocket sounding systems specifically aimed at using the data in the derivation of synthesized radiance profiles; design of multi-channel radiometric satellite systems to measure radiance at several discrete wavelength intervals in the CO_2 absorption band, similar to the weather bureau infrared spectrometer (SIRS), but aimed at the use of inversion analysis to determine the vertical temperature structure in the higher stratosphere and mesosphere.

Application to Scientific Studies

It is expected that the most extensive effort ever undertaken to gather data on the earth's atmosphere will be made in 1972. This effort, which will employ both new and conventional observing techniques, will entail two programs, the Global Atmospheric Research Program (GARP), and the World Weather Watch (WWW) program. If it is launched in 1972, a 15-micron horizon scanning satellite system will be able to play a vital role in this atmospheric observation effort. In order to define the role then of GARP-WWW effort, in the satellite horizon scanner program, the nature of the atmospheric observation program and the capabilities of the scanning satellite system will be discussed.

World Weather Watch. - The WWW will be an international effort by member nations of the World Meteorological Organization to secure weather data for the entire globe and to communicate it for use on a real-time basis (ref. 6). The program calls for expanding observations of basic weather elements to eliminate the large data-void regions that presently exist. The ocean areas presently comprise the greatest part of the data-void region.

Even over much of the land area of the world, no observations are made of conditions in the upper air. The optimum radiosonde station density exists nowhere except perhaps in Europe, which is a very small part of the total surface of the earth. A large gap even exists in the surface observation network over some land areas, due to lack of financial support or lack of population. Many islands in remote areas, which are either uninhabited or sparsely inhabited, exist without a weather station.

It is the objective of the WWW program to eliminate completely the larger data-void regions, and to trim down gaps between observing stations wherever possible. For complete weather prediction, observation gaps and time gaps must be filled in, since old information is useless to a weather forecaster. Thus, communications are a vital part of WWW. It is the objective of WWW to establish a global observing system, employing all possible techniques of information acquisition and timely communication.

Global Atmospheric Research Program (GARP). - Nearly every atmospheric research project and program relies on operational weather data to supplement its data collection. Since 1972 is the year in which the massive WWW effort to obtain global atmospheric information will take place, global atmospheric research interests will give special consideration to conducting special programs in that particular year so as to benefit from the extra supplemental data. Systems machinery has been established to coordinate the research eforts of the many atmospheric research laboratories under the acronym GARP. GARP will collect data for use of researchers back in the laboratory, and not for real time use as with the WWW data.

GARP is being coordinated internationally by the International Union of Geodesy and Geophysics (IUGG), and nationally by the American branch, the Committee on Atmospheric Sciences (CAS-IUGG). To coordinate the activities of participating and interested agencies, the IUGG has announced a world congress to be held in the fall of 1967 in Geneva. At this congress, the IUGG will ask geophysicists to promote immediate work on prerequisite studies and ask them to design experiments. The congress will also reach tentative agreements on communications and coordination of national efforts. The National Center for Atmospheric Research (NCAR), ESSA, and NASA are already participating in the program on a national level.

NCAR is presently conducting a pilot research study in the Line Islands, where they are gathering data on the atmosphere for comparison with Advanced Technology satellite observations. For the past year, NCAR has also been launching transosondes at Christchurch, New Zealand as a pilot study to gather global wind data at several levels in the atmosphere.

It is, therefore, the aim of GARP to enlarge upon the information gathered by WWW by obtaining more data in both horizontal and vertical coordinates. Unlike WWW, GARP is not concerned with the speed with which this information can be communicated, since it is being collected for research purposes at a later date.

Having examined the atmospheric data gathering programs to be undertaken in 1972, attention can now be directed to the observing systems which will be employable in that year. In order to project meaningfully the potential uses of the satellite scanner data, it is necessary to examine the projections of what is expected in terms of atmospheric data-gathering by other techniques in 1972.

Cloud photography. -- In the 1972 time period, satellites which photograph the earth to obtain cloud information will be in their second decade of operation. Unlike satellites of the first decade, these satellites will each be part of a system to maintain constant surveillance of the earth.

The system will be composed of two basic satellite types. One type will consist of two satellites in a near-polar, sun-synchronous orbit. These satellites will have day-night cloud observing capability, and will cover each part of the globe every six hours. Polar regions would be covered more frequently, however, since each satellite would cross poleward of latitudes 80°N and 80°S on each orbit.

The tropics and middle latitudes will be continuously observed with three or four satellites in synchronous orbit, presenting readouts similar to the present Advanced Technology Satellite. These satellites provide synoptic coverage of all of the earth except for the polar regions. Besides observing cloud systems on the global scale, these satellites will be able to study the evolution of smaller-scale, short-lived cloud sybsystems.

Ghost system. - The Global Horizontal Sounding Technique (GHOST) system is perhaps this period's most advanced meteorological innovation, creating the same stir that weather radar did with its display of precipitation areas laterally over regions hitherto in "silent areas" between weather stations. In between these two developments, atmospheric sounding rockets probed upward into the high stratosphere in the late 1950's. The Tiros satellite, with its cloud pictures from around the world, was introduced in the early 1960's. Several years later the Nimbus satellite added another dimension and provided tropospheric and stratospheric temperature information from its radiometers. Ghost consists of super-pressure balloons which float at pre-designated constant density levels in the stratosphere and higher troposphere, and carry sensors to monitor pressure, temperature, and humidity. In addition, wind can be obtained by measuring the changes in the position of the balloon from one interrogation to the next.

Although the balloons are now interrogated by land stations, plans call for satellite interrogation by the Interrogation, Recording and Locating System (IRLS) which is expected to be on board a Nimbus satellite to be launched by France, called EOLE, may also be made using a French FR-2 satellite.

With the planned expansion of the system, these data will make available for the first time observations of pressure, temperature, humidity, and wind on a global basis, enabling global atmospheric charts to be drawn to sufficient accuracy for the first time.

Automatic weather stations. - IRLS is also expected to obtain surface weather information from buoys such as the US Navy Nomad and from other buoy configurations currently under development. Also, plans are underway to integrate into the system automatic weather stations on uninhabited islands and other remote land locations which can be interrogated directly by satellites.

Radiation-sensing systems. - Satellites which collect earth radiation data to obtain temperature information in the troposphere and stratosphere can be expected to continue in operation. The sensor which will obtain the data to enable more precise vertical temperature profiles to be made will probably be a version of the Satellite Infrared Spectrometer (SIRS) which will sample eight channels in the 15-micron CO_2 region. Through inversion of the radiative transfer equation, radiance data from this spectrometer can be transformed into temperature profiles from cloud-top altitude to an altitude of about 50 km. Where no clouds exist, the temperature profiles can be calculated to the vicinity of the earth's surface.

Research vehicles. - In addition to the above, continued launching of research vehicles such as Nimbus can be expected to continue. Although these satellites will continue to add new types of sensors, increased emphasis may be placed on installation of more conventional, improved sensors for gathering data for special projects. Thus, emphasis will shift from testing the sensor to using the sensor in different contexts to obtain information for specific atmospheric research investigations.

The role of a satellite horizon scanning system. -- Above the stratosphere, extending upward from about 50 km to 80 km, is the mesosphere. In this region, the atmospheric pressure varies from about 1 millibar at the lower end to about 0.01 millibar at the top. Its atmosphere is too light to support a balloon, but it is much too dense for sustained satellite operations.

Current economical rocket systems explore only the lowest portion of the mesosphere. The only economical state-of-the-art probe which can currently penetrate its vertical extent is the "big gun" on Barbados Island (a gun-fired sounding projectile). It is, therefore, a region about which very little is known. However, some facts about its general makeup are known from earlier indirect measurements and the few direct measurements made in the past decade. The mesosphere behaves in many respects much as does the troposphere. Its temperature profile is characterized by a general decrease of temperature with altitude, with the warm temperatures at the bottom being the result of ozone absorption of ultraviolet. The mesosphere is a region in which nitrogen and oxygen comprise the overwhelming bulk of the atmosphere,

and where conventional atmosphere mixing processes account for the chemical composition. The heated ozone layers result in convection currents, which rise up to heat the upper portion. The mesopause marks the upper boundary of the troposphere. Similar to the lower stratosphere above the tropopause, the lower thermosphere above the mesosphere is a generally isothermal region.

The mesosphere is, however, a cloudless region, except for noctilucent clouds which form in the vicinity of the mesopause. The exact nature and composition of these highly stratified clouds which are frequently seen in the polar atmosphere is not yet completely understood. Perhaps they are composed of water vapor which has been carried upward by convection currents created by ozone-rich air which heats up under the perpetually sunlit polar day. Thus heated, the atmosphere may then rise from the bottom of the mesophere to the mesopause, where the water vapor carried upward then condenses into ice crystals which spread out beneath the temperature inversion.

Leovy (ref. 7) notes that the mesosphere is a "region where a close relationship exists between photochemical, radiative, and dynamical processes", and where "global scale motions are largely determined by the distribution of radiative heating, while the motions themselves influence the infrared radiation through modification of the temperature". The value of temperature measurements in the mesosphere is quite apparent.

Thiele (ref. 8) concludes that there is a strong solar influence on the lower mesosphere. His data, taken from White Sands rocket data indicate that the diurnal oscillations of pressure and density are almost as large as the seasonal variability.

The importance of the mesosphere extends well beyond special applications for radiowave propagation and occasional experiments in which its behavior is important. Gregory (ref. 9) noted that changes in electron densities in winter in the mesosphere are larger than simple theory predicts. In an investigation, he found that mesosphere electron densities were correlated with stratospheric temperatures between 20 and 30 millibars. In the situation investigated, electron density throughout the mesosphere lowered considerably while the temperature at 20 to 30 millibars rose by 8.3° C in 24 hours. Because of lack of information concerning the mesosphere, Gregory was unable to document the reason for the coupling. However, he suggests that the relationship possibly occurred as a result of simultaneous sinking of the air in both the mesosphere and stratosphere. Based on the findings of other investigators, Gregory surmises that the westerly circulation of the winter mesosphere is responsible for this ionospheric effect.

Considering the evidence which shows that sudden warmings in the stratosphere frequently precede tropospheric blocking highs, the implications for understanding the mesosphere and medium-range and long-range weather forecasting become extremely interesting.

Other questions and conjectures concerning the mesosphere are also of interest. The exact upper boundary of the mesosphere is not yet certain. Schilling (ref. 10) suggests that although the height over the polar regions may be around 82 km (as suggested by the mean height of noctilucent clouds near latitude 60° in summer), the height of the mesopause may be as high as 100 km over the equator. He also suggests the possibility of a double mesopause.

It has also been surmised that a high dust particle concentration may be located at the mesopause, since this is the upper region of what is evidently a turbulent region (Schilling, ref. 10).

Wave phenomena also evidently exist in the mesosphere. Lettau (ref. 11), using Robin sounding data obtained at White Sands, New Mexico, has found indications of extended waves in the mesosphere which he believes to be very important to the small-scale dynamics of the mesosphere. The conclusion is based upon small oscillations which show up in his analysis.

Lack of information about the mesosphere, however, far surpasses what is known about it, since so few measurements have been made of its vertical extent, save for an occasional rocket or gun-fired projectile. Many questions are as yet unanswered. Because of its temperature decrease with altitude, how strong are the convection currents which form within it when the ozone region is heated? Into what kind of circulation systems are these currents organized? - perhaps they are quite different from those in the highly-stratified stratosphere and bear some resemblence to some systems found in the troposphere. What is the temperature field? How does it vary in time and space? What effect does the aurora have on its temperature field?

More important, perhaps, is a question that concerns medium-range and long-range forecasting. That question is: what interactions and couplings does the mesosphere have with the stratosphere and troposphere? Will it be possible to forecast general weather patterns up to two weeks in advance without knowing at least some general conditions about the mesosphere?

The 1972 global observation program and the sensing systems which will be used have been reviewed in the previous two subsections. As can be seen, observations will be made on a global basis throughout the troposphere and stratosphere far surpassing the last major data-gathering program, IGY-1957. Through use of a horizon-scanning 15-micron sensor in 1972, the mesosphere could be added to the trosposphere and stratosphere as a region from which knowledge and understanding can be gained during the WWW-GARP programs.

Although it is difficult to predict exactly the impact the mesospheric data might have on understanding of the atmosphere, it is still possible to predict with near certainty what effect the launch data of the HDS satellite will have on the use that is made of the data. If it is launched by 1972, it can be expected that its information will join the pool of WWW-GARP data which scientists will scrutinize for years to come.

If it is true that the mesosphere is coupled to any appreciable degree with the stratosphere and troposphere, then the loss of mesospheric information in 1972 would be an unfortunate blow to hopes for medium and long-range forecasting. In speaking of numerical forecasting for a week or longer, Smagorinsky (ref. 12) states that "it would be unavoidable that dynamic models for the entire fluid envelope of the earth be employed". Hence, if forecasts of circulation patterns are to be extended to anywhere near two weeks, and if the WWW-GARP program hopes to examine the possibilities of such forecasts, a mesospheric temperature-field sensing system is necessary.

In conclusion, a radiometer scanning the horizon and vicinity in the 15-micron region would be the only sensor which could feasibly gather mesospheric data on a global scale in 1972. If such a device can give even a qualitative measure of the mesospheric temperature field, it will be of great value.

In view of the great potential of this satellite, it would be most desirable to conduct an intensive investigation to determine precisely the information that can be obtained from it, and to determine how this information would best be integrated into the WWW-GARP programs. Action should be taken to ensure that information is integrated into the program by coordination with the IUGG and other participating agencies at the proper time.

CONCLUSIONS AND RECOMMENDATIONS

The objectives of this study were to amplify the Part I data requirement results to satisfy the requirements of broad-scale horizon sensor and scientific applications and to assure experiment and measurement system compatibility. These objectives were met by defining a new set of temporal, spatial, and statistical sampling requirements necessary to describe the earth's radiance profile with a high degree of certainty for the 15-μ carbon dioxide obsorption band using the 615 to 715 cm^{-1} spectral region. With respect to data requirements, the following conclusions and recommendations have been reached:

The Part I study specification of 13 time cells (28 days/cell) still appears to be valid as the basis for the Fourier time series analysis of systematic seasonal variations.

The newly defined set of recommended data requirements, based upon a global distribution of 588 space cells and a total sample of approximately 378 000 profiles/year, provides an adequate data base for analyzing 11 locators at approximately the 95 percent confidence level.

The study of diurnal temperature variations in the stratosphere and mesosphere has shown that the associated radiance variations, expressed in terms of tangent height changes for select horizon locators, can be significant, especially at low and mid latitudes. Specific provision should be made, therefore, for a diurnal sampling mode.

The recommended approach todiurnal data sampling is one based upon a 3 o'clock sun-synchronous orbit. This orbit can provide daytime samples near the time of the diurnal temperature (and radiance) maxima and nighttime samples near the corresponding minima.

Conclusions related to constraints and operational methodology are as follows:

In the determination of data-sampling requirements, compensation must be made for the effects of random errors in the radiometer data and for miscellaneous data losses. In the latter instance, an overall allowance of 5 percent appears to provide adequate data-loss compensation.

The recommended data-sampling methodology is one based upon variable data-acquisition rates ranging from 0.429 profiles/min at low latitudes to 1.00 profiles/min at high latitudes.

A major experiment/radiometer design interface is involved in the choice of sampling azimuth. The restriction of profile scans to the orbit plane causes a problem in the diurnal data analysis, especially with regard to the winter and summer time cells. Further exploration of this problem is strongly recommended.

Data losses resulting from the telemetry gap in the STADAN network do not have a significant effect upon the experiment data sample.

Data losses resulting from suspended data collection during periods of attitude and spin-rate correction are not significant with respect to the total experiment sample. These losses can be confined to the summer hemisphere by adaptive reprogramming.

Studies relating to system effectiveness have shown the advantages of prescheduling thelaunch of standby spacecraft at such times as to maintain a high probability of continuing themission without interruption.

A major operational contingency which must be accounted for in the detailed experiment planning is the possibility of not attaining the proper orbit. The experimenter must be provided with a set of tolerance limits within which the experiment can be defined as a normal mode operation.

Conclusions and recommendations associated with the data reduction and data utilization study are as follows:

An operational system of data reduction and analysis is required to provide information feedback, as the experiment progresses, for the experimenter to use in determining the adequacy of the telemetered data, in modifying the data-acquisition methodology, and in developing improved methods for data reduction.

A basic end-product of the HDS experiment is the radiance profile catalog. The profiles included in this catalog should be identified not only with such descriptions as data, time, latitude, longitude, and scan azimuth but also with estimates of all systematic and random errors which apply to the tabulated radiance and tangent-height values.

The radiance profiles can be used directly to test operational characteristics of new locator designs and thus aid in the stability optimization of the locator.

The reduction and analysis of HDS data should be approached as a continuing phase of the experiment, and not merely as a task of compiling and routine processing of the data.

A very significant part of the data analysis will involve the use of meteorological data gathered by conventional ground-based observational systems, e.g., radiosondes and rocketsondes. Also, the current plans for WWW and GARP indicates that the HDS experiment will coincide with the time period of these intensified meteorological observations and thus a mutual data exchange may enhance all programs.

PRECEDING PAGE BLANK NOT FILMED.

APPENDIX A

THE EFFECTS OF TEMPERATURE ERRORS UPON SYNTHESIZED RADIANCE PROFILES

PRECEDING PAGE BLANK NOT FILMED

APPENDIX A

THE EFFECTS OF TEMPERATURE ERRORS UPON SYNTHESIZED RADIANCE PROFILES

STUDY OBJECTIVES

There are two basic reasons for studying the effects of temperature sounding and extrapolation errors upon synthesized radiance profiles. First, the overall data sampling requirements for the HDS experiment are based upon an extensive set of 1039 synthesized profiles which were derived from Meteorological Rocketsonde Network (MRN) and radiosonde observational data and from extrapolated temperatures above the level of effective MRN data coverage. It is important, therefore, to assess the effects of temperature errors upon these synthesized profiles since they were used to determine statistical properties of horizon locators (i. e., L4 (2.5) and L1 (3.0) in the Part I study and several additional locators in the Part II study) which were used as the basis for determining the required global distribution of space and time cells, as well as the sample sizes required within each cell.

The second basic reason for examining the temperature error effects problem is to help determine a realistic methodology for comparing samples of radiance profiles measured by the HDS experiment with synthesized profiles calculated from meteorological sounding data at coincident times and locations. This comparison of measured and synthesized profiles is a necessary part of the experiment data analysis in order to check the validity and representativeness of the HDS radiance profiles. Obviously, only a relatively small number of profiles can be subjected to this type of comparative analysis. It is important, therefore, that the temperature error effect in synthesized profiles be clearly established so that the radiance (and tangent height) deviations resulting from such comparisons can be reasonably analyzed and interpreted.

STUDY APPROACH

The altitude range over which meteorological data are used to calculate synthesized radiance profiles extends from 0 to 90 km. This range can be divided into three altitude intervals where distinctly different types of temperature data are available: 1) 0 to 30 km, covered by relatively accurate radiosonde data from a global network of upper-air reporting stations; 2) 30 to 60 km, covered by less accurate rocketsonde data mostly concentrated over North America, but also including some European stations and a few other widely scattered locations; and 3) 60 to 90 km, covered by infrequent mesospheric soundings made at widely diverse times and places.

During the Part I study (ref. 4), some attention was directed toward estimating the likely temperature errors within the three altitude intervals as defined above. From 0 to 30 km, the observational error in radiosonde temperatures increases with altitude; however, an error standard deviation,

σ_T, of ±1°C is a good working estimate for the entire interval. If interpolation error is considered, i.e., the error in temperatures interpolated at grid points some distance removed from the observed radiosonde data, then an overall σ_T value of ±2°C would appear to provide a representative estimate.

Temperature error estimation for MRN observations is considerably more difficult and uncertain (ref. 5). Of overwhelming importance in determining the basic accuracy of an MRN temperature sounding is whether or not corrections like the Wagner correction (ref. 13) have been applied. Without this correction, extremely high-positive (warm-side) temperature errors are possible: a mean error of 4.5°C at 45 km increasing to 33.5°C at 65 km, for the bead thermistor most widely used in MRN observations. With the Wagner correction applied, the temperature error can be drastically reduced to an estimated value of ±2°C or less below 65 km. A detailed evaluation of the MRN temperature data used in deriving the body of synthesized profiles during the Part I study is beyond the scope of this current effort. Such a study would necessarily have to examine the flight and ground equipment used, the data reduction techniques employed, and the processes of data analysis and interpolation applied in deriving the grid point emperature data during the Part I study. For these reasons, a σ_T value of ±4°C was adopted as a working estimate of MRN temperature error; since $3\sigma_T$ values of ±12°C were also used, the analysis of temperature error effects can be generalized over a wide range.

From 60 to 90 km, the temperature errors are considerably larger than those which apply to the two lower altitude intervals. In the Part I study, the temperatures were estimated above 60 km by an extrapolation technique based upon only 14 data points in the summer period (May - October) and 16 points in the winter period (November - April) for which mesospheric sounding data were available. The estimated σ_T between 60 to 90 km is ±7°C in summer and ±10°C in winter.

For the purposes of this preliminary study, it was decided to apply the $+\sigma_T$ and $\pm 3\sigma_T$ temperature errors separately to each of the three altitude intervals for one selected profile, Profile 943 (July, 20°N, 90°W). By assuming a particular size temperature error in one altitude interval and no error in the other two intervals, the error effects could then be separately examined. Thus, values of σ_T = 2.0°C and $3\sigma_T$ = ±12.0°C applied from 30 to 60 km (with zero error elsewhere); and σ_T = 7.0°C and $3\sigma_T$ = ±21.0°C applied from 60 to 90 km (with zero error elsewhere). Profile 943 represented a convenient choice since this summer, low-latitude profile was also used in the study of diurnal temperature variability effects, discussed elsewhere in this report. In order to provide a winter, high-latitude comparison for 60 to 90 km error effects, Profile 883 (Jan., 75°N, 90°W) was selected as the baseline case for evaluating σ_T = 10.0°C and $3\sigma_T$ = ±30.0°C.

The 12 error-perturbed profiles, as defined above, were calculated by applying the various plus of minus temperature deviations to the basic sets of temperature values determined for Profiles 943 and 883 in the Part I study.

The study approach taken was designed to reveal the more important features of temperature error effects upon synthesized radiance profiles. This analysis could then provide the basis for more comprehensive studies involving a larger number of profiles and a greater variety of temperature error combinations.

PERCENTAGE DEVIATIONS IN RADIANCE FOR PERTURBED VERSUS BASELINE PROFILES

Figure A1 shows a set of curves expressing the percent deviations in radiance for Profile 943 when the $+\sigma_T$ and $+3\sigma_T$ temperature errors are separately applied to each altitude interval. Figure A2 presents comparable curves for $+\sigma_T$ and $+3\sigma_T$ temperature errors in the 60 to 90 km altitude interval for Profile 883. Table A1 provides a list of the percent radiance deviations per 1°C temperature error at 10 km tangent height intervals for the 12 cases included in the study. The error effects within each altitude interval are discussed below.

0 to 30 km Temperature Error

For 2°C and 6°C temperature errors in this altitude interval, which will be abbreviated as (2, 6:0-30), the percent deviation in radiance is approximately constant over the -30 to +20 km tangent height range, as shown by both curves in Figure A1. At these tangent heights, the percent radiance deviation is roughly equal to one-half the temperature error in °C, although, as shown in Table A1, the absolute value of the radiance deviation/temperature error ratio is lowest for the -6°C error case (-0.03), increases slightly for the +2°C error case (0.04) and is considerably higher for the +6°C error case (0.07).

30 to 60 km Temperature Error

The (4, 12:30-60) curves of percent radiance deviation in Figure A1 exhibit some interesting characteristics. The slopes of these curves gradually increase from -30 to 20 km tangent height, sharply increase from 20 to 30 km tangent height, gradually decrease from 30 to 50 km tangent height and then decrease at a rapidly increasing rate to 60 km tangent height. As shown in Table A1, the percent radiance deviation from -30 to 20 km tangent height is approximately equal to 0.7-1.0 times the temperature error in °C. From 30 to 50 km tangent height, the absolute value of the ratio of radiance deviation to temperature error varies between 1.4 to 1.9 for the three types of error considered; the comparable range of values at 60 km tangent height is 0.4 to 0.5

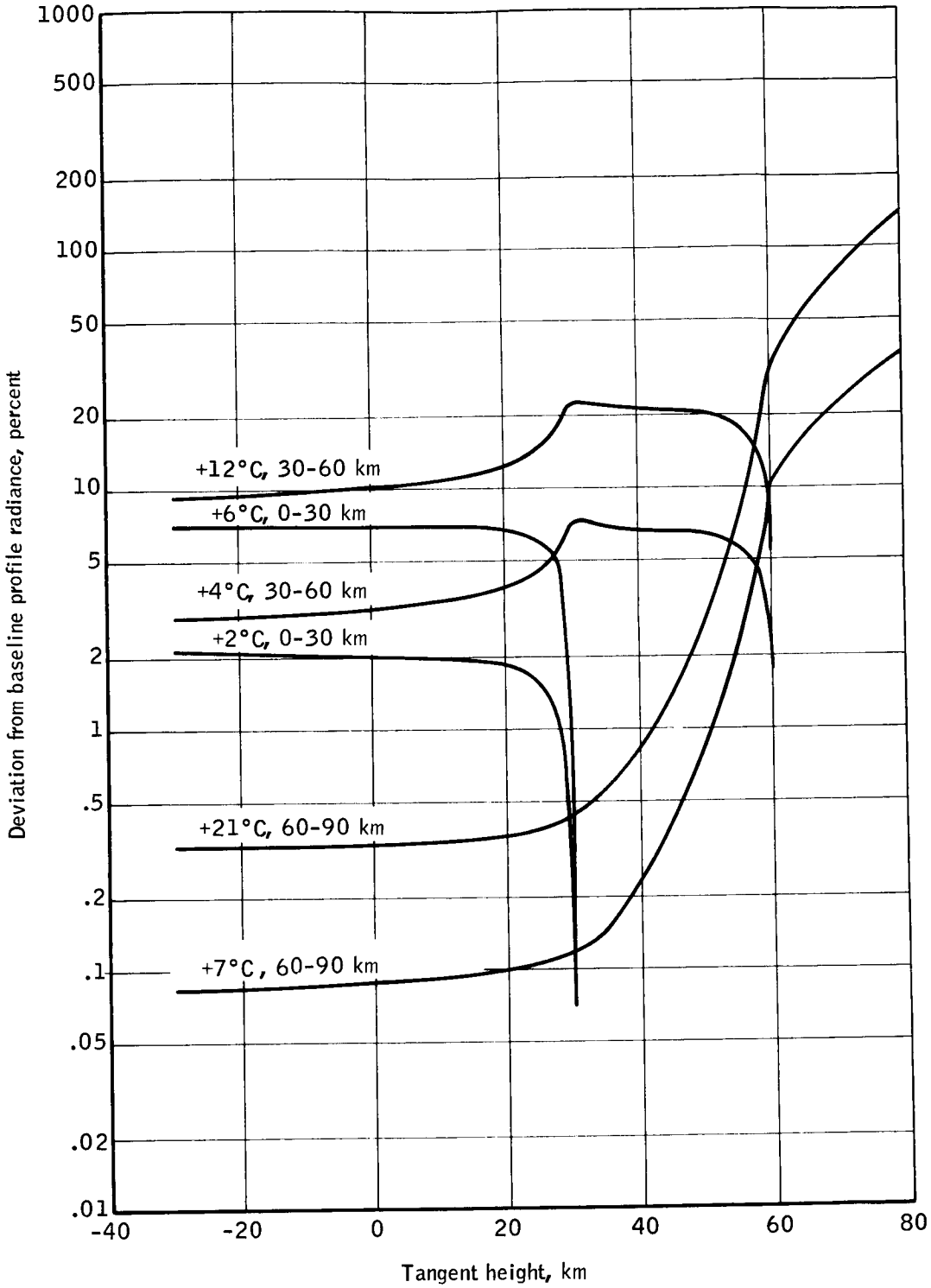

Figure A1. Percent Deviations in Radiance for Various Assumed Temperature Error Distributions, Profile 943

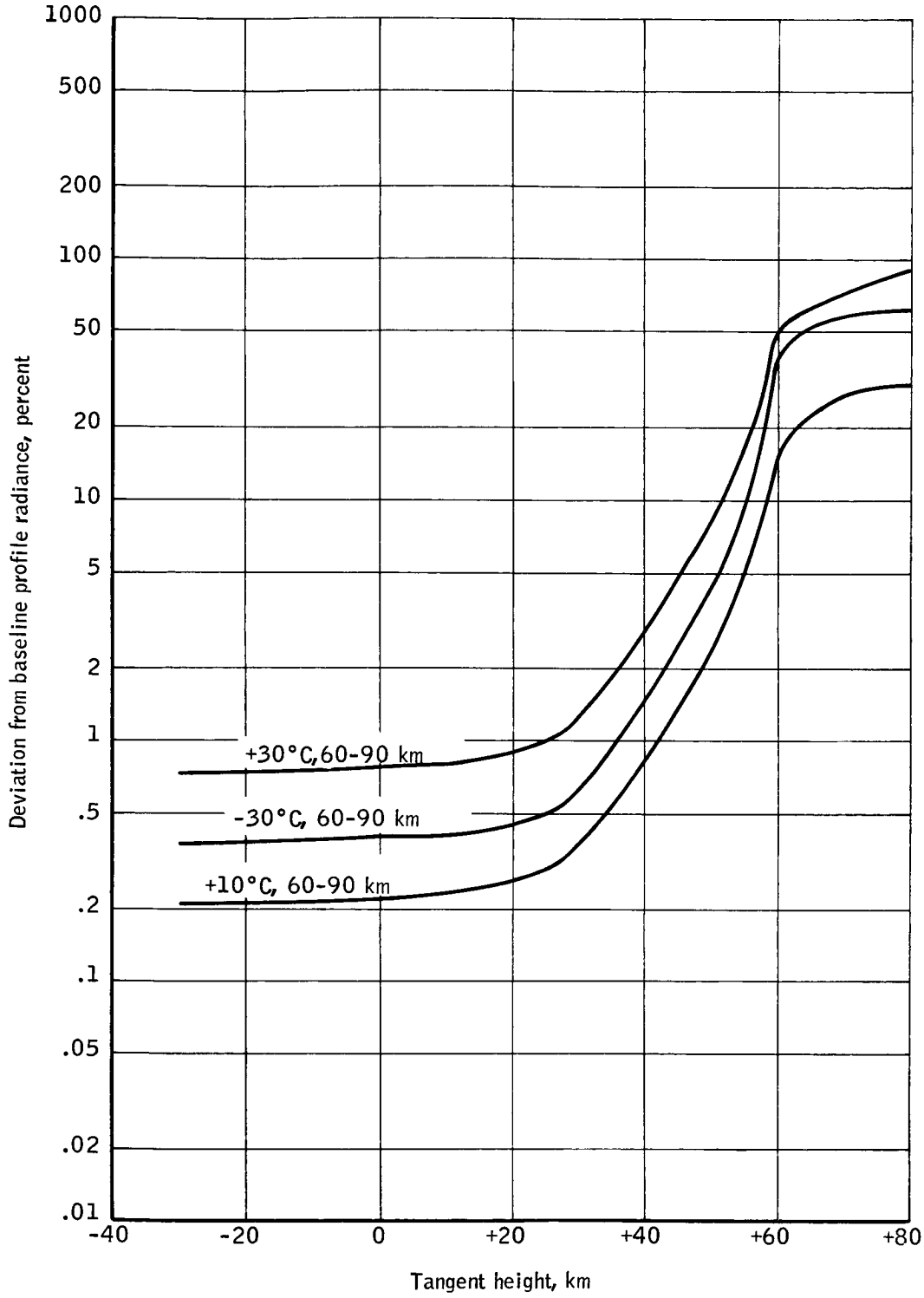

Figure A2. Percent Deviations in Radiance for Various Assumed Temperature Error Distributions, Profile 883

TABLE A1. - PERCENT RADIANCE DEVIATION PER 1°C TEMPERATURE ERROR VERSUS TANGENT HEIGHT

Temperature error identifier	Tangent height, km											
	-30	-20	-10	0	10	20	30	40	50	60	70	80
Profile 943:												
2°, 0-30 km	1.1	1.0	1.0	1.0	1.0	0.9	0.04	-	-	-	-	-
6°, 0-30 km	1.2	1.2	1.2	1.2	1.1	1.1	0.07	-	-	-	-	-
-6°, 0-30 km	-1.0	-1.0	-1.0	-1.0	-1.0	-0.9	-0.03	-	-	-	-	-
4°, 30-60 km	0.7	0.7	0.8	0.8	0.9	1.0	1.8	1.7	1.6	0.5	-	-
12°, 30-60 km	0.8	0.8	0.8	0.9	0.9	1.0	1.9	1.8	1.7	0.5	-	-
-12°, 30-60 km	-0.7	-0.8	-0.8	-0.8	-9.9	-1.0	-1.9	-1.5	-1.4	-0.4	-	-
7°, 60-90 km	0.01	0.01	0.01	0.01	0.01	0.01	0.02	0.03	0.1	1.5	3.0	5.1
21°, 60-90 km	0.02	0.02	0.02	0.02	0.02	0.02	0.02	0.04	0.2	1.6	3.2	6.7
-21°, 60-90 km	-0.01	-0.01	-0.01	-0.01	-0.01	-0.01	-0.01	-0.02	-0.09	-1.2	-2.0	-3.1
Profile 883:												
10°, 60-90 km	0.02	0.02	0.02	0.02	0.02	0.03	0.04	0.09	0.2	1.5	2.8	3.1
30°, 60-90 km	0.02	0.02	0.02	0.03	0.03	0.03	0.04	0.1	0.3	1.7	2.3	3.1
-30°, 60-90 km	-0.01	-0.01	-0.01	-0.01	-0.01	-0.02	-0.02	-0.05	-0.1	-1.3	-1.9	-2.0

60 to 90 km Temperature Error

The (7, 21:60-90) curves in Figure A1 clearly indicate that temperature errors in this highest altitude interval produce a relatively low percent radiance deviation over the -30 to 30 km tangent height range. As shown in Table A1, the absolute value of the ratio of percent radiance deviation to temperature error is 0.01 to 0.02, or as much as two orders of magnitude less than the comparable ratios for radiosonde and MRN temperature errors over this tangent height range. However, there is a sharp increase in the deviation/error ratio from 30 to 60 km tangent height, with a continuing increase, although at a slower rate, above 60 km tangent height. As shown in Figure A1, the percent radiance deviation at 50 km tangent height becomes approximately equal to the value of temperature error in °C. It is also interesting to note that from -30 to 54 km tangent height, a (4:30-60) temperature error produces a larger percent radiance deviation than a (21:60-90) temperature error.

The (10, 30:60-90) curves in Figure A2 are very similar in their general characteristics to the (7, 21:60-90) curves discussed above. The normalized values of percent radiance deviation per 1°C temperature error, as shown in Table A1, permit a direct comparison for the summer and winter profile cases. From -30 to 60 km tangent height, the absolute magnitudes of the deviation/error ratios are slightly larger for the winter, lower-radiance profile; above 60 km tangent height, the reverse is true. However, the ratios for both profiles are sufficiently close below 60 km tangent height to provide useful approximations of the temperature error effect upon radiance profiles until more thorough analyses can be carried out to develop a complete set of estimation curves. It should be pointed out that the horizon locators of primary interest in the HDS study are those which operate at or below 60 km tangent height; thus, the estimates of temperature error effect provided by these preliminary results are of immediate benefit.

ABSOLUTE DEVIATIONS IN RADIANCE FOR PERTURBED VERSUS BASELINE PROFILES

The description of percent radiance devications, presented above, is most helpful in analyzing the behavior of normalized and integral normalized horizon locators, whose tangent height deviations can be readily determined by the differences in the percent radiance deviations at the level of peak radiance and at higher levels. However, for non-normalized locators, the absolute radiance deviations are of basic interest, since the absolute deviation, together with the slope of the radiance function (e.g., radiance or integral radiance) versus tangent height, essentially determines the equivalent tangent height deviation. Figures A3 through A6 show curves of absolute radiance deviation per 1°C temperature error, for the 12 cases included in this study. In terms of maximum absolute radiance deviations per °C, the (2, 6:0-30) and (4, 12:30-60) temperature errors show the greatest effect: in the former instance, a broad region of 0.051-0.065 W/m^2-sr per °C occurring between -20 to 20 km tangent height; in the latter instance, a sharp peak of

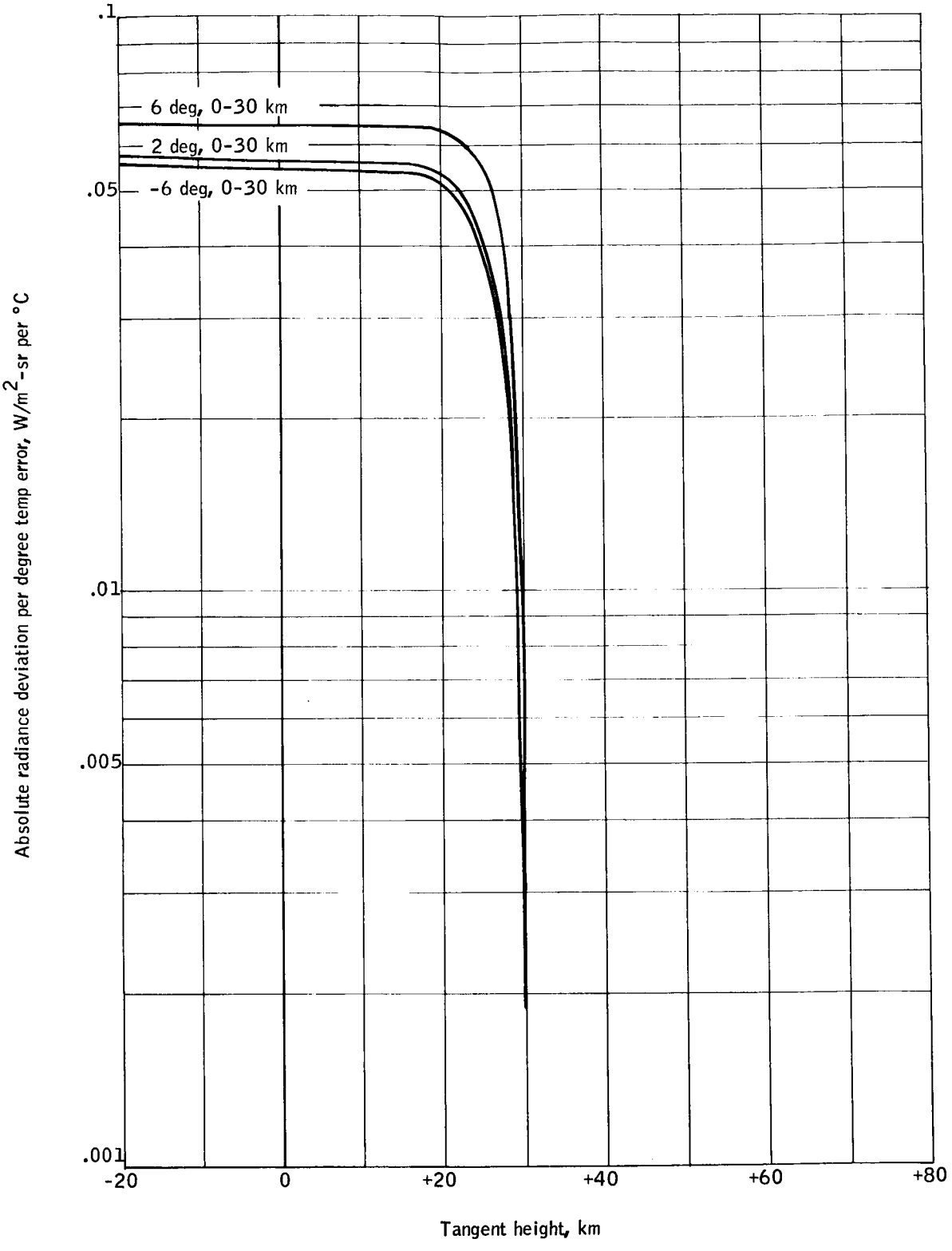

Figure A3. Absolute Radiance Deviation per 1° C for Temperature Error in the 0 to 30 km Region, Profile 943

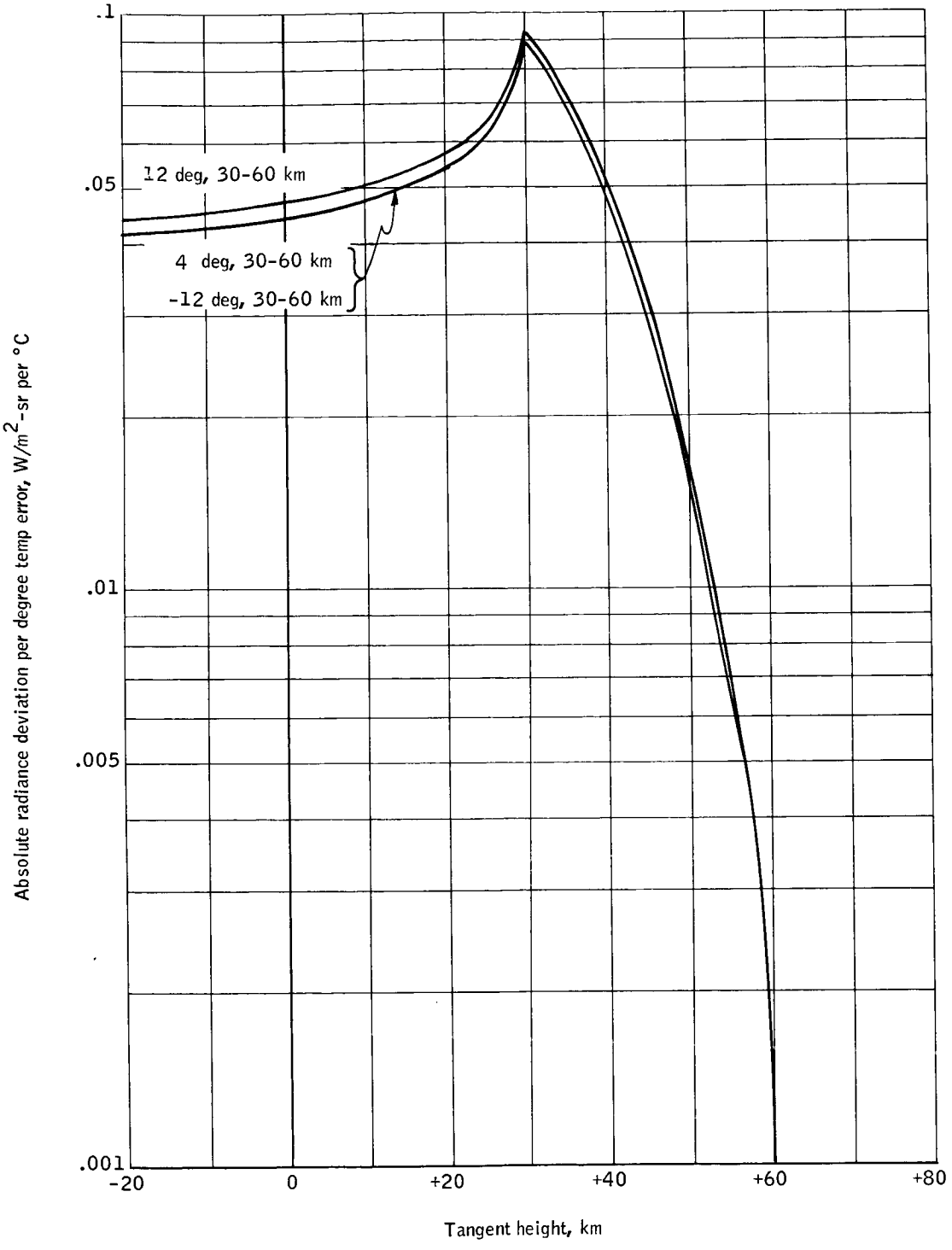

Figure A4. Absolute Radiance Deviation per 1° C for Temperature Error in the 30 to 60 km Region, Profile 943

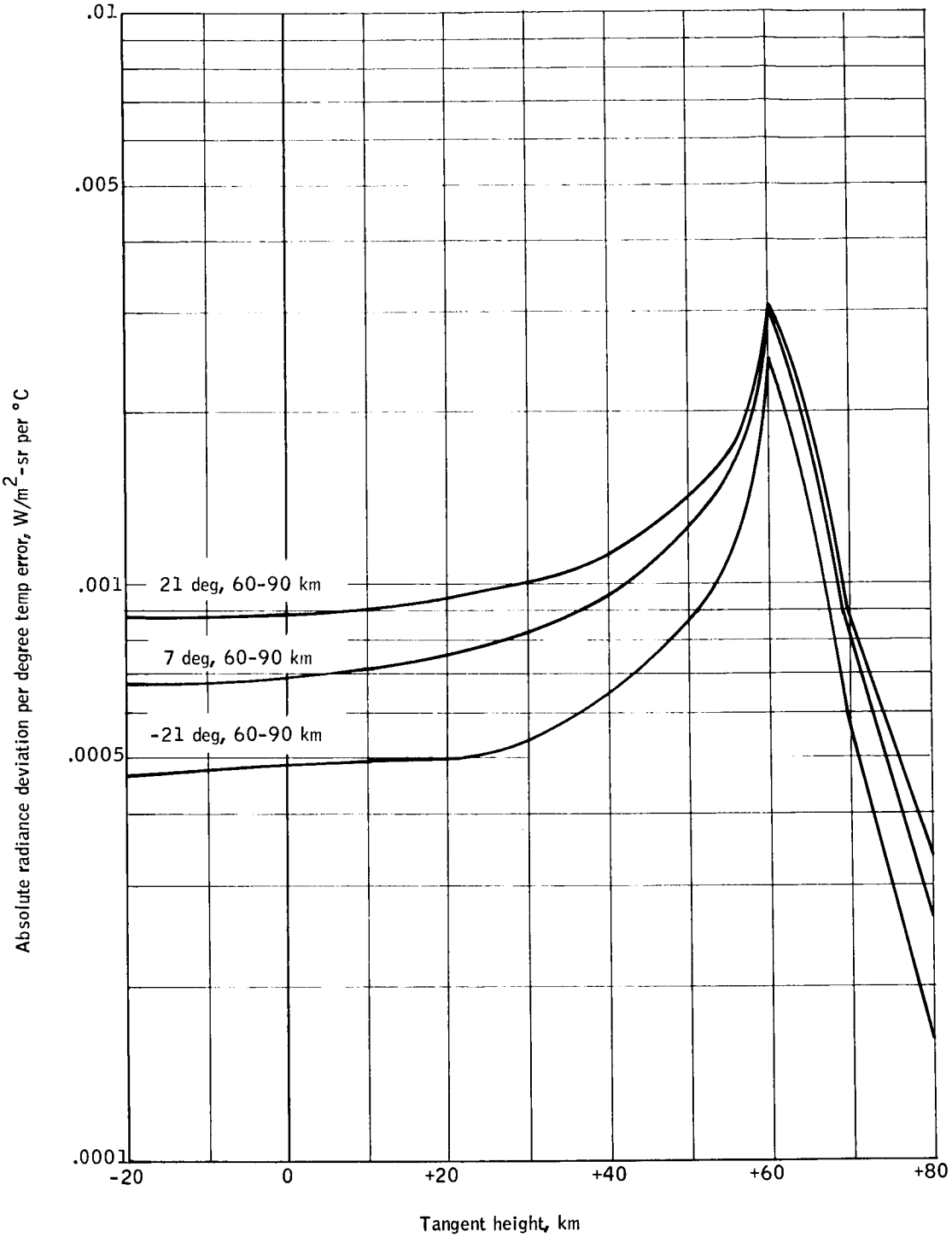

Figure A5. Absolute Radiance Deviation per 1°C for Temperature Error in the 60 to 90 km Region, Profile 943

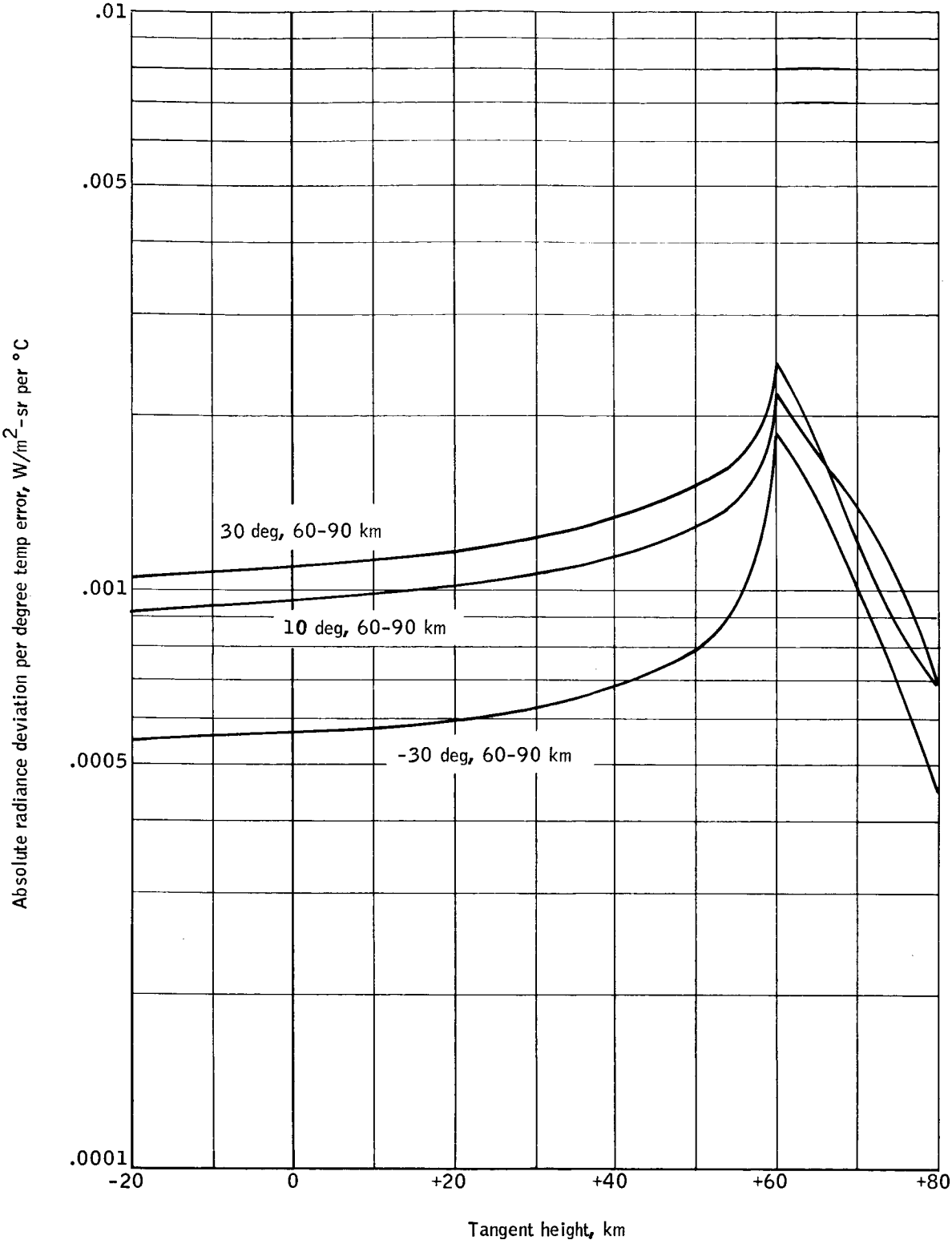

Figure A6. Absolute Radiance Deviation per 1° C for Temperature Error in the 60 to 90 km Region, Profile 883

start 0.089-0.094 W/m^2 -sr per °C occurring at 30 km tangent height. The maximum absolute radiance deviations per °C for the (7, 21:60-90) and (10, 30: 60-90 cases are not as large as those for lower altitude temperature errors: in the former instance, a sharp peak of 0.0025-0.0031 W/m^2 -sr per °C occurs at 60 km tangent height; in the latter instance, a peak of 0.0019-0.0025 W/m^2 -sr per °C occurs, also centered at 60 km tangent height.

EFFECTS OF TEMPERATURE ERRORS UPON HORIZON LOCATORS FROM SYNTHESIZED RADIANCE PROFILES

In order to explore more fully the effects of temperature errors upon the HDS experiment, a set of calculations was made, for the Profile 943 error cases, to determine the associated deviations in tangent height for 12 specific horizon locators. These locators included four of the fixed radiance (L1) type, four of the normalized radiance (L2) type, one of the integral radiance (L3) type, two of the integral normalized radiance (L4) type, and one of the slope extrapolation (L7) type.

The methods used to calculate the tangent heights for the perturbed profiles, and their departures from the basic unperturbed profile, followed the general lines described elsewhere in this report for the study of radiometer error and diurnal temperature variability effects upon horizon locators. In brief, the radiance deviations were determined from the computer printout of Profile 943 for each temperature error case and were converted into the function of radiance appropriate to each locator, i.e., fixed radiance, normalized radiance, integral radiance, integral normalized radiance, and slop extrapolated radiance (in the last instance, involving two levels of fixed radiance). The equivalent tangent height deviations were then calculated on the basis of the change in radiance function with tangent height for each horizon locator considered. Table A2 outlines the results of these calculations, which are discussed in detail below.

Fixed Radiance (L1) Locators

Temperature errors in the 0 to 30 km altitude interval do not affect the L1 locators considered here, all of which operate at tangent heights above 30 km.

Temperature errors between 30 to 60 km most affect the L1 (3.0) locator, with the tangent height departures per 1°C error gradually decreasing for the higher level L1 locators. This result agrees with what would be generally expected on the basis of Figure A4, which shows a decrease over the 30 to 60 km tangent height interval in absolute radiance deviation per °C. The effect of these deviations is, of course, moderated by the values of radiance/tangent height slope which apply at each locator level; these slope changes are relatively small, however, compared to the dominant effect of changes in absolute

TABLE A2. - TEMPERATURE ERROR EFFECTS UPON HORIZON LOCATORS FOR SYNTHESIZED RADIANCE, PROFILE 943

Locator	Tangent height, km, basic profile	Temperature error, °C and applicable altitude interval, km								
		2, 0-30	6, 0-30	-6, 0-30	4, 30-60	12, 30-60	-12, 30-60	7, 60-90	21, 60-90	-21, 60-90
L1 (3.0)	39.37	--	--	--	40.24 (0.22)	41.86 (0.21)	36.11 (-0.27)	39.40 (0.004)	39.47 (0.005)	39.31 (-0.003)
L1 (2.0)	44.05	--	--	--	44.69 (0.16)	45.85 (0.15	41.99 (-0.17)	44.09 (0.01)	44.19 (0.01)	43.98 (-0.003)
L1 (1.0)	49.88	--	--	--	50.36 (0.12)	51.27 (0.12)	48.33 (-0.13)	49.94 (0.01)	50.11 (0.01)	49.75 (-0.006)
L1 (0.2)	59.98	--	--	--	60.11 (0.03)	60.39 (0.03)	59.64 (-0.03)	60.78 (0.11)	62.20 (0.11)	59.02 (-0.05)
L2 (0.95)	26.05	25.69 (-0.18)	25.41 (-0.11)	27.70 (0.28)	26.80 (0.19)	30.25 (0.35)	24.06 (-0.17)	26.05 (±0)	26.07 (0.001)	26.04 (±0)
L2 (0.50)	40.18	39.93 (-0.13)	39.31 (-0.15)	40.94 (0.13)	40.56 (0.10)	41.24 (0.09)	39.05 (-0.09)	40.20 (0.003)	40.25 (0.003)	40.14 (-0.002)
L2 (0.30)	45.62	45.46 (-0.08)	45.04 (-0.10)	46.10 (0.08)	45.84 (0.06)	46.30 (0.06)	44.93 (-0.06)	45.65 (0.004)	45.73 (0.005)	45.56 (-0.003)
L2 (0.06)	57.07	56.95 (-0.06)	56.65 (-0.07)	57.41 (0.06)	57.15 (0.02)	57.26 (0.02)	56.83 (-0.02)	57.30 (0.03)	57.83 (0.04)	56.57 (-0.02)
L3 (4.5)	52.40 [E] (a)	--	--	--	52.60 (0.05)	52.97 (0.05)	51.74 (-0.06)	52.94 (0.08)	54.27 (0.09)	51.32 (-0.05)
L4 (2.5)	44.60 [E] (a)	44.45 (-0.08)	44.06 (-0.09)	44.99 (0.07)	44.73 (0.03)	45.01 (0.03)	44.31 (0.02)	44.81 (0.03)	45.39 (0.04)	44.18 (-0.02)
L4 (0.5)	55.60 [E] (a)	55.47 (-0.07)	55.12 (-0.08)	55.95 (0.06)	55.52 (-0.02)	55.35 (-0.02)	55.96 (0.03)	56.30 (0.10)	57.92 (0.11)	54.13 (-0.07)
L7	57.25	--	--	--	57.61 (0.09)	58.14 (0.07)	56.36 (-0.07)	57.38 (0.02)	57.72 (0.02)	57.01 (-0.01)

[a] Estimated

radiance produced by the temperature errors. The absolute magnitudes of the tangent height deviations for the +4°C error case are roughly one third as large as those for the +12°C error cases.

For 60 to 90 km temperature errors, the tangent height deviations per 1°C error are relatively small in all cases for locators L1 (3.0), L1 (2.0), and L1 (1.0); however, L1 (0.2) is rather seriously affected, most expecially for positive temperature errors, where the tangent height deviation is approximately 0.11 km per 1°C error. It is also notable that the deviations for -21°C error are, in terms of their absolute magnitude, roughly one-half those for +21°C error. Much of the difference is explainable by reference to the curves of absolute radiance deviation per °C shown in Figure A5, where a considerable degree of offset may be noted between the +21° and -21°C error curves. The remainder of this difference is explained, especially in the case of locators L1 (1.0) and L1 (0.2) by the higher values of the radiance profile slopes which apply to these two higher levels for the -21°C versus +21°C error cases (i.e., 0.1404 and 0.0540 W/m^2 -sr per km, versus 0.1189 and 0.0295 W/m^2 -sr per km, respectively).

Normalized Radiance (L2) Locators

Here, for 0 to 30 km temperature errors, the process of normalization produces an interesting sign reversal: the tangent height deviations are negative for positive temperature errors, and vice versa. By referring to Figure A1, this result can be explained by the fact that the absolute magnitude of the percent radiance change is higher at the peak radiance, $N_{max.}$ (near 20 km), than at any of the other radiance levels where the four different L2 locators operate. Now, since the normalized radiance is, by definition, $N/N_{max,}$, the effect of larger positive percent errors in the denominator, as compared to the numerator, is to produce (for a given value of $N/N_{max.}$, say, 0.50) a proportionally larger increase in N and a negative deviation in tangent height. Correspondingly larger negative percent errors in $N_{max,}$ will produce a proportionally larger decrease in N, along with a positive tangent height deviation.

It is also significant to note, for the (2, 6:0-30) error cases, that the absolute magnitude of the tangent height deviation per 1°C generally decreases for the higher level L2 locators. This results from the fact that N becomes a smaller multiple of $N_{max,}$ for higher level L2 locators. If, for example, the (6:0-30) error case is considered for locators L2 (0.50) and L2 (0.06), the radiance error in $N_{max,}$ is approximately 6.7 percent, whereas the radiance error in N is zero percent in both instances. In the first instance, the erroneous N value (reflecting the $N_{max.}$ error) is 1.067 (0.5) $N_{max,}$; in the second instance, 1.067 (0.06) $N_{max.}$. In other words, the error in N for L2 (0.50)

is, in absolute terms, more than eight times larger than the error in N for L2 (0.06). If we examine Table A2, however, it is seen that the (6:0-30) tangent height departure for L2 (0.50) is only twice as large as that for L2 (0.06). This difference (i.e., 8 versus 2) is accounted for by differences in the slope of the radiance profile at the levels to which these two locators apply: in other words, at the higher level (57.07 km) a given size radiance error has an equivalent tangent height error which is four times larger than that at the lower level (40.18 km). The slope of the radiance profile is, therefore, an important factor in determining the ultimate tangent height departure for radiance deviations attributable to temperature errors.

In the case of 30 to 60 km temperature errors, it may be noted from Table A2 that the tangent height deviations decrease smoothly for higher level L2 locators. As contrasted with the 0 to 30 km temperature errors, there is in this instance no sign reversal in the tangent height deviations. By reference to Figure A1, this difference in behavior can be explained by the fact that the absolute magnitudes of the percent radiance deviation at the four locator levels (i.e., 26.05, 40.18, 45.62, and 57.07 km) exceed those at the peak radiance level (i.e., 18 to 20 km). Considerations similar to those already discussed for the (2, 6:0-30) error effects for L2 locators also apply here.

Temperature errors in the 60 to 90 km altitude interval produce but a very small tangent height deviation for L2 locators. Only in the case of L2 (0.06) does the tangent height departure exceed a value of 0.01 km/°C. This result is understandable in terms of the (7, 21:60-90) curves presented in Figure A1, which show relatively small percent radiance deviations at the peak radiance level (18-20 km) and at 26.05, 40.18, and 45.62 km where the lower three L2 locators operate. It is expected that an analysis of the (10, 30:60-90) error cases for Profile 883 would yield a distribution of tangent height deviations rather similar to that obtained here for Profile 943 (7, 21:60-90).

Integral Radiance (L3) Locators

Only the L3 (4.5) locator was included in this analysis; however, the analysis can be readily extended to estimate tangent height deviations for other levels of integral radiance.

Temperature errors in the 0 to 30 km altitude interval do not affect L3 (4.5), nor would they affect L3 locators up to an integral radiance level of 20.0. Temperature errors in both the 30 to 60 and 60 to 90 km altitude intervals produce a relatively modest effect: 0.05-0.09 km tangent height deviation per 1°C temperature error, with the deviation and the error having the same algebraic sign. If one examines the (7, 21:60-90) curves in Figure A1, it might appear strange at first glance that the tangent height deviations are not considerably greater in view of the large percent radiance deviations which apply between 52.40 to 80 km, the interval over which the radiance is integrated for L3 (4.5). However, some 60 percent or more of the integral radiance for L3 (4.5) is contributed within the 52.4 to 60 km interval, and at higher levels the contributions become extremely small as the percent radiance deviations become extremely large. Thus, the results obtained for L3 (4.5) are regarded as entirely reasonable.

Integral Normalized Radiance (L4) Locators

For 0 to 30 km temperature errors, the L4 (2.5) and L4 (0.5) locators show the sign reversal noted earlier for the L2 locators affected by errors within this altitude interval. Thus, for positive temperature errors, a negative tangent height deviation of -0.07 to -0.09 km/°C can be expected, and for negative errors, a value of 0.06 to 0.07 km/°C.

For (4, 12:30-60) temperature errors, the distribution of algebraic signs for the tangent height deviations revert to the normal pattern for L4 (2.5) but show a sign reversal for L4 (0.5). This interesting result arises as follows. Since L4 locators are defined in terms of $\Sigma Ni/N_{max.}$, percent errors of the same magnitude and algebraic sign in the numerator and denominator will cancel out with no resultant tangent height deviation. However, if as an example the (4:30-60) error case is considered, the deviation in peak radiance is 3.74 percent. For L4 (2.5), the integrated percent deviation in radiance from 44.6-80 km is 5.55 percent, or somewhat larger. This excess in the numerator term, ΣNi, with respect to the denominator term, $N_{max.}$, translates into a positive tangent height deviation. A helpful way to consider this effect is to consider L4 (2.5) as the area under the radiance profile within the tangent height limits 44.6 to 80 km. If positive errors cause an upward displacement in the radiance profile (which represents the upper boundary of the area), then, for a constant value of 2.5 W-km/m^2-sr, the lower tangent height limit is shifted to a higher value. If L4 (0.5) is now considered, the integrated percent deviation in radiance is 2.46 percent, or lower than the percent deviation in peak radiance. By analogous reasoning, it can be shown that the lower tangent height limit is shifted so as to produce a negative deviation. The analysis of error effects upon normalized locators such as L2 and L4 is complicated, therefore, by the fact that the percent radiance deviation in peak radiance must be subtracted out from the individual or integral deviations at higher altitudes to determine the residual effect.

For (7, 21:60-90) temperature errors, the tangent height deviations in both L4 locators have the same algebraic sign as the errors. The absolute magnitudes of the tangent height deviations for L4 (2.5) are relatively small (i.e., 0.02 to 0.04 km). Comparable values for L4 (0.5) are larger by a factor of three, reflecting the combined influence of three factors: 1) the integrated percent radiance deviation in L4 (0.5) is more than three times as large as that for L4 (2.5); 2) the integral normalized radiance value of L4 (0.5) is five times as small as that of L4 (2.5); and 3) the slope of integral normalized radiance per tangent height interval for L4 (2.5) is five times as large as that for L4 (0.5).

Slope Extrapolation (L7) Locators

As shown in Table A2, 0 to 30 km temperature errors have no effect upon the tangent height of locator L7 (1.5; 0.75). This results from the fact that the fixed radiance levels used for this locator both occur well above 30 km.

As shown by the Part I study results, the 1.5 and 0.75 W/m^2 -sr radiance levels do not occur below 35 and 44 km, respectively.

The effect of 30 to 60 temperature errors upon the L7 locator is to produce fair-sized tengent height deviations with the same algebraic sign as the error. The absolute magnitudes of these deviations, per °C, range between 0.07 to 0.09 km. Because the L7 locator involves slope extrapolation from the 1.5 and 0.75 to the zero W/m^2 -sr radiance levels, it is possible to obtain complete error cancellation whenever the magnitude of the tangent height deviation at 1.5 W/m^2 -sr is twice that at the 0.75 W/m^2 -sr radiance level and is of the same algebraic sign. On the other hand, the slope extrapolation process can produce relatively large tangent height deviations at the zero radiance level whenever the deviations at the two higher radiance levels have the opposite algebraic sign.

The effect of constant temperature error within the 60 to 90 km altitude interval is to produce a relatively insignificant tangent height deviation in locator L7. The absolute magnitude of this deviation, per °C, is only 0.01 to 0.02 km.

DISCUSSION OF OVERALL RESULTS

This study has shown that the effect of temperature errors upon locator tangent heights can vary over wide limits. Temperature errors between 0 to 30 km have the greatest impact upon locators L2 (0.95) and L2 (0.50); for three σ temperature errors of +6°C, the absolute values of the tangent height deviations for these locators lie within the range 0.6 to 1.7 km. Temperature errors between 30 to 60 km mostly affect locators L1 (3.0), L1 (2.0), L1 (1.0) and L2 (0.95); for 3σ errors of +12°C, the deviations in tangent height for these locators fall within an absolute value range of 1.4 to 4.2 km. Temperature errors between 60 to 90 km produce the largest tangent height deviations in locators L1 (0.2), L3 (4.5), and L4(0.5); for 3σ errors of ±21°C, the absolute values of these deviations lie within a range of 1.0 to 2.3 km. Overall, temperature errors between 30 to 60 km appear to have the greatest effect upon the locators included in this study. This result is entirely reasonable since, with the exception of L2 (0.95), all locators operate within the tangent height range of 30 to 60.

In addition, this study has revealed a remarkable consistency, in terms of the tangent height deviations per °C temperature error which are produced upon a given horizon locator by errors of different signs and magnitudes. Locator L2 (0.95) is the only one to exhibit any real inconsistencies in the normalized deviations; these occur in the (2, 6: 0-30) and 4, 12: 30-60) error cases. The overall results suggest that a nomogram could be developed, for each class of locators, which would permit rapid, accurate estimation of tangent height deviations as a function of 1) basic temperature error combinations within the 0 to 90 km altitude interval, and 2) some general profile

descriptor such as peak radiance which would sufficiently identify the radiance profile slope characteristics in order to take into account the functional relationship between the tangent height deviation and the radiance deviation caused by temperature errors. The development of such a series of monograms could proceed on the basis of 1) selecting a representative number of radiance profiles which cover a range of different latitudes and seasons, 2) defining a greater number of plus and minus error combinations, and 3) establishing firmer estimates of σ_T, the error standard deviation in temperature, over the 0 to 90 km interval.

EFFECTS OF TEMPERATURE ERRORS UPON EXPERIMENT DESIGN

The results of the analysis of tangent height deviations for various locators provide a basis for estimating possible effects which temperature errors in synthesized profiles may have produced upon the experiment design. Of specific interest are: 1) The data requirements which were established in the Part I study for the "scientific" and "engineering" measurement program, based upon the time series analysis of locators L1 (3.0) and L3 (2.5), respectively, and 2) the data requirements defined in the Part II study for other additional locators.

The tangent height deviations which were determined for the 12 different locators can be identified as error standard deviations in tangent height, σ_{h_T}, which correspond to the assigned values of error standard deviation in temperature, σ_T. Thus, the following three types of tangent height error can be defined: 1) σ_{h_T} (0-30), associated with a constant value of σ_T = 2°C between 0 to 30 km; 2) σ_{h_T} (30-60), which correspond to σ_T = 4°C between 30 to 60 km; and 3) σ_{h_T} (60-90), which is associated with σ_T = 7°C between 60 to 90 km. Estimates of σ_{h_T} are provided by the recent study results (even though the analysis only included positive $1\sigma_T$ errors, the values for negative $1\sigma_T$ errors are expected to be approximately the same over this small a total error interval).

The ideal basis for examining the relative influence of the three σ_{h_T} values would be set of σ_h values which denote the standard deviation in tangent height for the various locators within specific space/time cells. This type of information is not available, however, because of basic data limitations. It is necessary, therefore, to draw inferences from the locator tangent height statistics which were generated during the Part I study. Values of standard deviation σ_h for the locators of interest were

determined: 1) over an extensive North American grid area for eight synoptic cases; 2) at specific stations (i.e., Cape Kennedy, Ft. Churchill and White Sands Missile Range) over various time periods extending from two days to one year; and 3) at specific times along a space cross section extending from White Sands Missile Range to Antigua. For purposes of illustration, σ_h values were selected for the June and January synoptic cases, the May time-series case for Cape Kennedy, and the October cross-section case. These values, together with σ_{h_T} values for each interval and for the entire 0 to 90 km altitude range, are presented in Table A3.

There are some notable features in the distribution of σ_h and σ_{h_T} values shown in this table. Of the 12 locators considered, the σ_{h_T} (0-90) values exceed the June synoptic case σ_h values in seven instances, exceed the May Cape Kennedy σ_h values in eight instances, and exceed the October WSMR-Antigua σ_h values in six instances. This result has some interesting implications, since these three sets of σ_h values represent either periods of the year or locations when σ_h is at a near minimum. It would normally be expected that these σ_h values would be larger than the σ_{h_T} (0-90) values, so as to reflect the combined influence of natural variability as well as temperature error effects upon the synthesized radiance profiles. The σ_h values for the January synoptic case (where the natural variability is at a near maximum) does indeed exceed the σ_{h_T} (0-90) values by a considerable margin, with but one exception, the L4 (0.5) locator. In this January case, the error component in σ_h which can be attributed to the assumed temperature error distribution is relatively small; for example, if we subtract out the effect of σ_{h_T} = 0.87 km, for the L1 (3.0) locator, from σ_h = 4.79 km, we obtain a value of 4.71 km, representing only a very minor correction.

In the three cases where the σ_{h_T} (0-90) values frequently exceed the σ_h values, there are some important inferences to be drawn regarding the magnitude of temperature errors which were adopted within the three altitude intervals. Most noteworthy are the results obtained for the L1 (0.2), L3 (4.5), and L4 (0.5) locators; here, the σ_{h_T} (0-90) values typically exceed the three sets of σ_h values by a factor of three. In each instance, the σ_{h_T} (60-90) error is the major contributor. This suggests

TABLE A3. - TANGENT HEIGHT AND TANGENT HEIGHT ERROR STATISTICS FOR VARIOUS LOCATORS

Locator	Tangent height standard deviations, km, caused by temperature error				Tangent height standard deviations, km, for Part I study cases			
	σ_{h_T}, 10-30, 2°C	σ_{h_T}, 30-60, 4°C	σ_{h_T}, 60-90, 7°C	σ_{h_T}, 0-90	σ_h, June synoptic case	σ_h, January synoptic case	σ_h, May Cape Kennedy	σ_h, October WSMR-Antigua
L1 (3.0)	--	0.87	0.03	0.87	0.58	4.79	0.75	1.36
L1 (2.0)	--	0.64	0.04	0.64	0.53	3.80	0.59	1.32
L1 (1.0)	--	0.48	0.06	0.48	0.51	2.97	0.40	0.63
L1 (0.2)	--	0.13	0.80	0.81	0.27	1.71	0.29	0.27
L2 (0.95)	0.36	0.75	0	0.83	1.24	2.98	0.42	0.48
L2 (0.50)	0.25	0.38	0.02	0.46	0.60	2.34	0.62	0.78
L2 (0.30)	0.16	0.22	0.03	0.27	0.32	2.35	0.48	0.74
L2 (0.06)	0.12	0.08	0.23	0.27	0.18	1.18	0.23	0.10
L3 (4.5)	--	0.20	0.54	0.58	0.25 (a)	1.41 (a)	0.21 (a)	0.27 (a)
L4 (2.5)	0.15	0.13	0.21	0.29	0.22	1.50	0.29	0.30
L4 (0.5)	0.13	0.08	0.70	0.72	0.13	0.66	0.18	0.07
L7 (0.75, 1.5)	--	0.36	0.13	0.38	0.70	1.86	0.50	0.29

[a] Interpolated from L3 (1.5) and L3 (7.5) values

that the value of 7°C adopted as the temperature error between 60 to 90 km may be too large by a considerable factor, possible as much as three. A similar analysis of the σ_h values with respect to σ_{h_T} (30-60) suggests that the value of 4°C adopted between 30 to 60 km may also be too large by a factor of 1.5 or possible more. It may also be inferred that the σ_{h_T} value of 2°C adopted for the 0 to 30 km interval is possible too large by a factor of 1.5.

There are certain inherent limitations to the inferences which can be made from the available information. The most important question is whether or not the σ_h values derived for the synoptic time-series and space cross-section cases can be regarded as representative. This question is discussed in detail below.

Between 30 to 60 km, MRN temperature data is quite sparse. The spatial analyses for the synoptic cases were typically based upon temperature data coverage at six stations covering the entire North American continent and adjacent ocean areas. The space cross-section and time-series cases were also based upon relatively incomplete data which did not usually provide the nominal resolution. Thus, a considerable amount of interpolative analysis was used to fill in the data gaps at levels between 30 to 60 km. This analysis served to smooth out the effects of errors and of small-scale components of natural variability contained in the individual temperature observations. Thus, the large-scale patterns of spatial and temporal variability in temperature were depicted. The process of interpolating and extrapolating temperature values at spatial grid points or at designated times between adjacent observations does not, however, add any resolution to that to which the original data is inherently limited. For example, six widely spaced observations for a synoptic case cannot really provide the type of resolution which is implied by the use of a 56-point grid. Thus, the set of synthesized radiance profiles which are derived at these 56 points do not necessarily represent the scale of temperature variability which is associated with the selected grid spacing. Nevertheless, the standard deviations in locator tangent height derived from such a highly interpolated (and extrapolated) set of synthesized profiles will be reasonably close to the comparable statistics which would be obtained from an ideal, high-resolution set of profiles as long as the predominant features of the temperature field between 30 to 60 km have been adequately resolved and have not been distorted by large systematic errors at individual stations. Since the temperature analyses in the Part I study were conducted by experienced meterologists, the σ_h values which were obtained for the various cases are regarded as reasonably representative in terms of the 30 to 60 km temperature contributions to the radiance profiles.

For the 60 to 90 km altitude interval, an extrapolation process of temperature estimation was developed, whereby the observed 50 km temperature and the temperature at the highest point in the sounding were used to

estimate the remainder of the temperature profile to 90 km. Since the extrapolation process was based upon a limited number of high-altitude rocket woundings, considerable concern has been expressed that the temperature errors from 60 to 90 km may be very large and therefore, adversely affect the accuracy of the synthesized radiance profiles and the derived tangent height statistics. The results presented in Table A3 suggest, however, that the value of 7°C associated with σ_{h_T} (60-90) may be too large by a factor of as much as three. This inference is essentially based upon a comparison of σ_{h_T} (60-90) values observed during periods when the natural atmospheric variability is relatively low. If the σ_h values used for this comparison are too low, then the inference is incorrect. There does not appear to be any reason to doubt the general validity of these values.

Overall, the analysis of temperature error effects has revealed that they do not unduly influence the tangent height statistics derived from the set of synthesized radiance profiles in the Part I study. Temperature errors do not appear to seriously affect the higher values of σ_h which were the major factor in determining the data sampling requirements for the HDS experiment.

USE OF SYNTHESIZED PROFILES IN COMPARATIVE STUDIES WITH OBSERVED PROFILES

The results of this preliminary study werve to identify many of the problems involved in the computation and application of synthesized radiance profiles. Further study is recommended to develop improved methods whereby synthesized profiles can be more accurately computed and more definitive error limits established. This would provide a firm basis for using such profiles for comparative studies with profiles observed by the HDS experiment.

APPENDIX B

DETERMINATION OF DIURNAL DATA SAMPLING REQUIREMENTS

APPENDIX B

DETERMINATION OF DIURNAL DATA SAMPLING REQUIREMENTS

Available evidence strongly suggests that diurnal effects upon horizon locators may be almost as important as seasonal and latitudinal effects. Thus, the proposed HDS experiment has as one of its objectives the collection of radiance profile data on such a basis that diurnal effects can be statistically evaluated. This will provide a means for making deterministic corrections to horizon sensor outputs.

The term diurnal is applied to the daily component of variation in radiance profiles associated with the 24-hour period of alternate warming, and cooling of the atmosphere. Daily changes in solar energy input, resulting from the effect of the earth's rotation, serve to generate a 24-hour cycle of temperature variation. This daily cycle is most regular in the tropical zone where the level of incoming solar radiation is least variable throughout the year and where the duration of night and day intervals is relatively constant.

REVIEW OF DIURNAL TEMPERATURE VARIABILITY

The first step in determining the diurnal data sampling requirements was to review information sources relating to the diurnal variability of atmospheric parameters between 30 to 70 km. The general nature of the diurnal temperature component, including amplitude and phase, was established as a function of altitude, latitude, and time of year (i.e., solstices and equinoxes). The results of significant studies which have been made of diurnal temperature variability are summarized below.

Theoretical

Johnson, F. S. (ref. 14). --

Method: (1) Heating effect due to absorption of solar energy by atmospheric ozone.

(2) Assumed constant rate of heat loss due to day and night infrared emission.

(3) Based upon WSMR rocket flight data (June 14, 1949) of zone concentration and solar uv spectral intensity.

Results: (1) Maximum diurnal temperature change of 5.3°C at 48 km.

(2) Diurnal temperature change 1°C at 31 km and 70 km.

Pressman, J. (ref. 15). --

Method: (1) Solar energy absorption by ozone based upon solar spectrum, ozone distribution, and density distribution.

(2) Assumed uniform cooling rate over 24-hour period exactly balancing heating due to ozone absorption of solar energy.

Results: (1) 24-hour curves of diurnal temperature variation for

(a) latitudes 0°, 45°, and 75°

(b) altitudes 30, 42.5, 57.5 km

(c) dates March 21, May 1, June 21

(2) Maximum diurnal variation occurs near 45 km between 0 to 45° latitude and does not exceed 5 to 6°C.

(3) Below 30 km and above 58 km diurnal temperature variation is less than 1.5°C.

(4) No seasonal changes at 0° latitude.

(5) Modest seasonal changes at 45° latitude.

(6) Pronounced seasonal changes at 75° latitude (order-of-magnitude from vernal equinox to summer solstice).

Leovy, C. (ref. 16). --

Method: (1) Based upon calculations of joint photochemical radiative equilibrium in mesosphere and upper stratosphere.

(2) Assumed that only oxygen allotropes are involved in chemical changes.

(3) Assumed radiative balance between absorption of solar radiation by molecular oxygen and ozone and infrared emission by carbon dioxide and ozone.

(4) Calculations made for short periods following summer and winter solstices.

Results: (1) Maximum diurnal temperature range at both solstices is 4.5 to 5.0°C/day, occurring between 45 to 55 km and latitudes 0° to 15°.

(2) Minimum diurnal range of less than 0.5°C/day between 30 to 70 km at both solstices from 75° to pole.

Observational

Beyers and Miers (ref. 17). --

Data: (1) Primary - 11 meteorological rocket soundings at 2-hour intervals over White Sands Missile Range, from 0400 MST, 7 February 1964 to 0205 MST, 8 February 1964.

(2) Secondary - four soundings at 1400 and 1600 MST, 21 November 1964 and 0400 and 0600 MST, 22 November 1964 over WSMR.

Results: (1) Primary data indicate

(a) Maximum temperatures occurred around 1400 MST

(b) Minimum temperatures recorded near 0400-0600 MST

(c) Diurnal temperature range 5°C at 35 km, increasing to 15°C at 45 km and near 20°C at 55 km.

(d) Significant non-diurnal heating also present.

(2) Secondary data indicate

(a) Essentially no diurnal variation from 30 to 50 km (masked by snyoptic variation?)

(b) Day to night variation of 15°C from 55 to 63 km

Beyers, Miers, and Reed (ref. 18). --

Data: Eight temperature soundings at WSMR from 1400 MST, 30 June 1965 to 1100 MST, 2 July 1965.

Results: (1) Amplitude of temperature oscillation increases from less than 2.0°C at 40 km to 5.5°C at 48 km and averages 7.5°C up to 56 km with a sharp increase above 56 km to about 9°C near 60 km.

(2) Time of maximum temperature shows a consistent trend from 1715 MST at 44 km to 1200 MST at 60 km.

(3) A relatively large synoptic trend of temperature variation was noted at higher levels - 25°C/24 hour at 56 km (synoptic trends were removed before making harmonic analysis).

Webb, et al. (ref. 19). --

(1) Descriptive article

(2) Cites Beyers and Miers (1965) re diurnal temperature variation

(3) Qualitative description of diurnal heat wave resulting from "geometric and rotational aspects of interaction between the ozonosphere heat exchanges and the solar radiant flux".

(4) Pictorial representation of wind circulation and temperature structure at North American summer solstice.

(5) Earth's diurnal rotation described as producing a ridge of heated air in the ozonosphere sweeping around the earth in the 24-hour period.

(6) There is a rather sharp leading edge of this heat wave beginning about sunrise and ending shortly after noon.

Finger and Woolf (ref. 20). --

Data: Sixteen meteorological rocket soundings at Wallops Island, extending from 1645 EST, 8 September 1965 to 0738 EST, 10 September 1965 (20 to 52 km).

Results: (1) Analysis indicates a daily temperature range varying from about 3°C at 30 km to about 9°C at 48 km.

(2) Minimum temperatures occur near sunrise (0500 EST) and maximum near sunset (1900 EST).

(3) The greatest rate of temperature increase occurs within one to two hours after sunrise; of temperature decrease within one to two hours after sunset.

Finger (ref. 21). --

Data: Extensive sample of USA radiosonde observations at 30 mb (24 km), 10 mb (30 km) and 5 mb (36 km).

Results: (1) At 40 mb, the diurnal range of temperature is 0.5°C between 30 to 50°N, decreasing with higher latitude to a value of 0.2°C between 60 to 80°N.

(2) At 10 mb, the diurnal range of temperature is 1.0°C between 30 to 50°N, decreasing to a value of 0.4° between 70 to 80°N.

(3) At 5 mb, the diurnal range of temperature is 2.0°C between 30 to 60°N, decreasing to 1.3°C between 60 to 80°N.

Based upon an evaluation and synthesis of these various study results, a set of curves has been derived which depicts the amplitude of the diurnal temperature oscillation as a function of altitude (24 to 90 km), latitude (0, 45, and 75°N) and time of year (solstices and equinoxes). These curves are shown in Figure B1. The altitude interval covered by these curves includes the portion of the stratosphere and mesosphere which exerts the greatest relative influence upon 14-to 16-micron radiance profiles. No attempt has been made to extend the curves below 24 km; however, the diurnal temperature amplitude at 24 km may be taken as generally representative of conditions extending down to the lower few kilometers.

Figure B1 shows the following important features: 1) overall, the amplitude of diurnal temperature variation is largest near 55 km; 2) the maximum value of diurnal temperature amplitude is approximately 7°C, occurring throughout the year near 55 km in the equatorial region, 3) mean diurnal temperature amplitude at 45°N is 0.5 to 1.5°C less than that at the equator, with somewhat higher values occurring at the vernal and autumnal equinozes; 4) diurnal temperature amplitude at 75°N is considerably less than at lower latitudes, with extremely large seasonal changes from relative minima at the solstices to relative maxima at the equinoxes; and 5) the smallest diurnal temperature variation occurs in the polar region at the solstices, where the peak value near 55 km probably does not exceed 1°C. Therefore, the diurnal variation in temperature represents a complex phenomenon which cannot be grossly oversimplified in view of the significant altitudinal, latitudinal, and seasonal changes which produce over an order of magnitude spread in amplitude.

In addition to the amplitude, the phase of the diurnal temperature variation is a significant factor affecting the HDS data sampling requirements. Figure B2 presents a curve showing the phase of diurnal temperature variation as a function of local time. This curve, which represents a composite derived from a variety of information sources, indicates a broad plateau of maximum temperature occurring early to midafternoon, with a broad minimum occurring near 3:00 a.m. local time. The greatest rates of diurnal temperature increase and decrease are shown to occur within the two to three hour periods following sunrise and sunset, respectively. As noted on Figure B2, the phase is expected to vary within ± one to five hours as a function of latitude, altitude, and time of year. Beyers, Miers and Reed's analysis of WSMR temperature data indicated, for example, that the maximum temperature occurred in late afternoon at 44 km and near noon at 60 km. Thus, the phase relationship shown in Figure B2 depicts an average, representative condition.

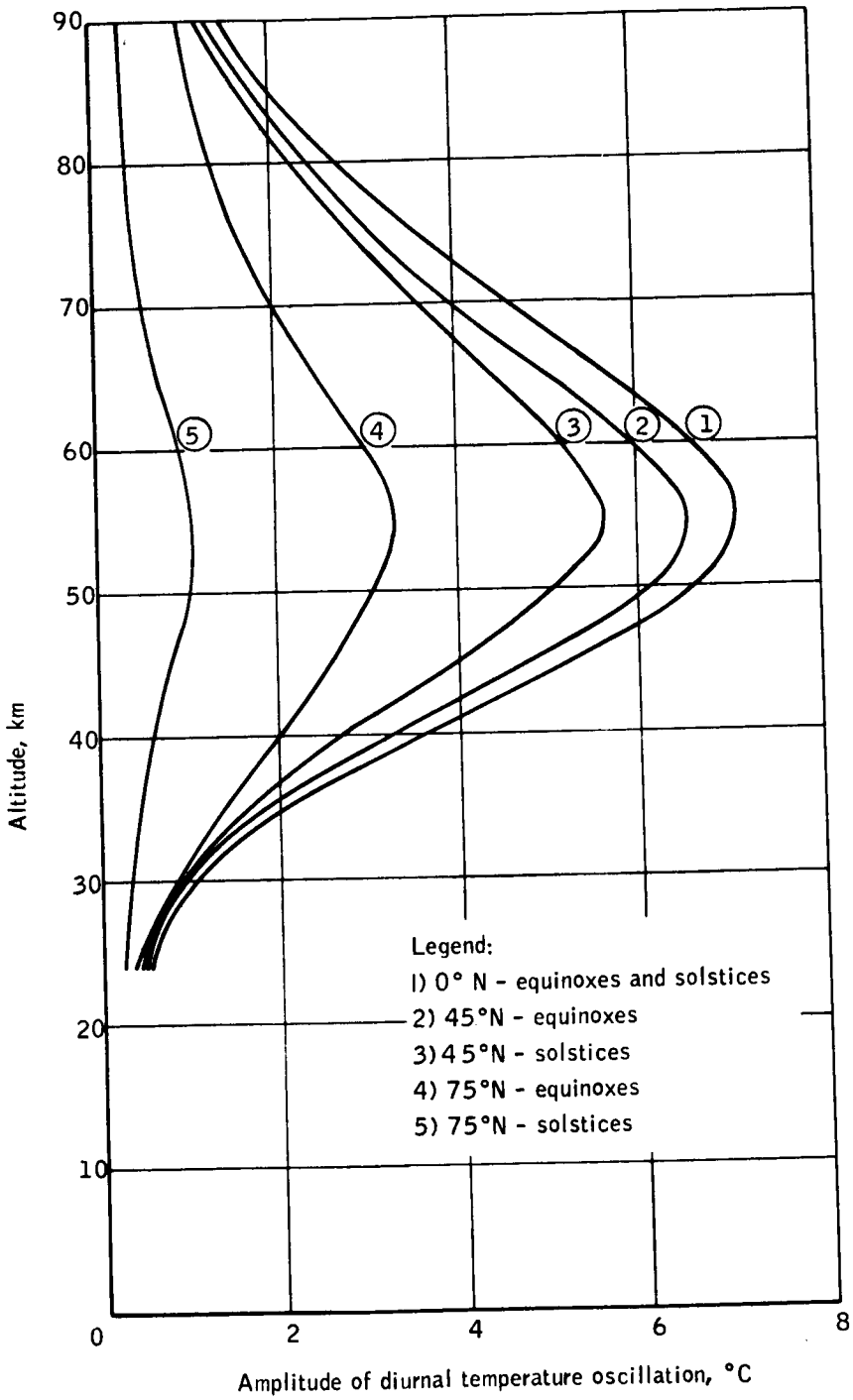

Figure B1. Variation of Diurnal Temperature Amplitude with Altitude as a Function of Latitude and Time of Year

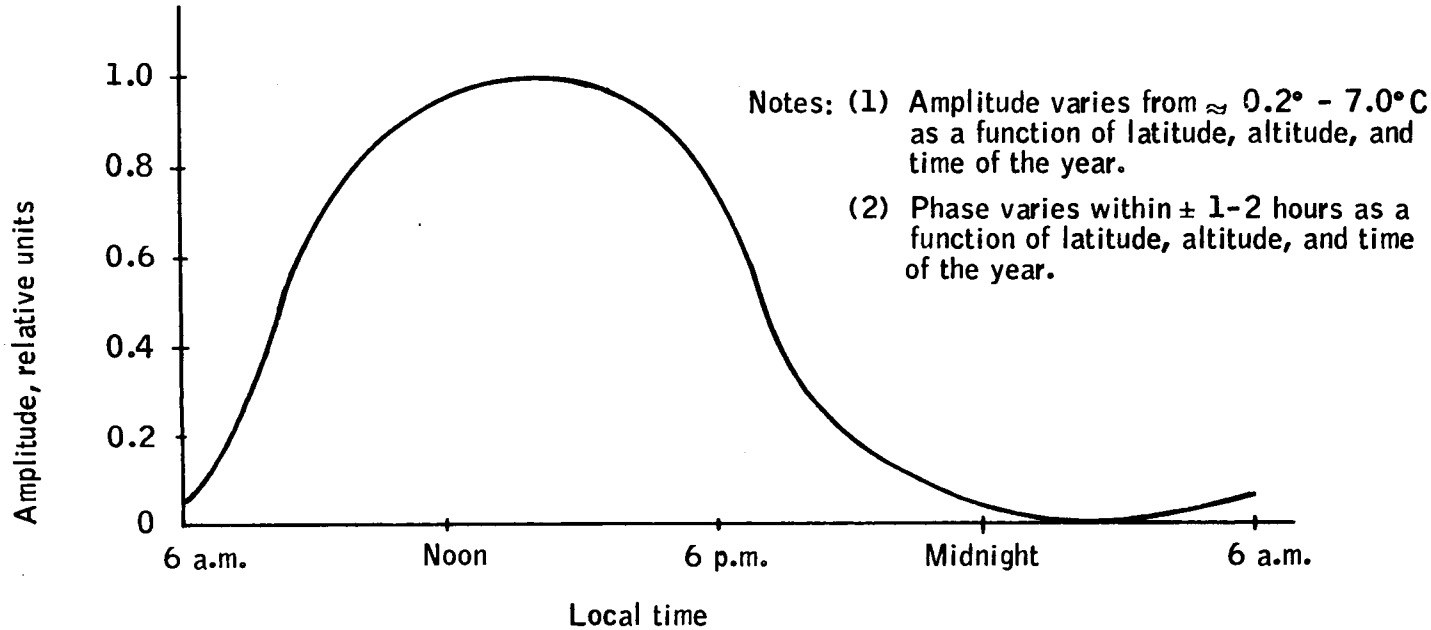

Figure B2. Typical Curve of Diurnal Temperature Variation

REVIEW OF HDS DIURNAL SAMPLING REQUIREMENTS IN PART I STUDY

HDS Part I Study results (ref. 3), were reviewed to determine the extent to which diurnal effects were defined and reflected in the data sampling requirements. Analysis of diurnal effects upon radiance profiles performed in Part I included 1) evaluation of overall differences in the amplitude of radiance profiles determined from samples of daytime and nighttime data at Cape Kennedy and White Sands Missile Range, and 2) significance tests of the diurnal frequency component in high resolution time series.

Results of the analysis performed under item (1) above were described as "doubtful", since the nighttime radiance was apparently greater than the daytime radiance. These results can be explained as reflecting basic inadequacies in the temperature sounding data: either the data were not available at local times closely corresponding to the expected temperature maxima and minima (Cape Kennedy), or the nighttime sample was so inadequate that subjective interpolation may have inadvertently introduced higher temperatures (and radiance) during the evening hours (WSMR).

Results of the study under item (2) above gave strong evidence of the fact that diurnal frequency components are statistically significant at the 95 percent level for those locators and identifiers which relate to altitude above 45 km. Thus, the L4 (2.5) locator, in addition to 15 other specific locators and two profile identifiers, appeared to be significantly influenced by diurnal variations in the radiance profile. On the other hand, the L1 (3.0) locator, along with other locator and identifiers which pertain to mean altitudes at 40 km and below, did not show any detectable diurnal effect, at the 95 percent significance level.

As a consequence of these results, the following statement was made in the Part I Study report (ref. 3) regarding diurnal sampling requirements:

> "For any diurnal effects, the reduction in uncertainty due to a deterministic fit to daily variations was insignificant in the case of locator L1 (3.0) and only slightly significant in the case of locator L4 (2.5). Since these uncertainties are inherent in the Cape Kennedy one-year sequence, no additional uncertainty value is included in that determined for Cape Kennedy to account for diurnal variations. In terms of diurnal sampling requirements, the number of samples required for determination of spatial and seasonal variations will provide sufficient samples of day and night variations to obtain average diurnal effects."

RECENT REASSESSMENT OF DIURNAL SAMPLING REQUIREMENTS

The approach outlined in the Part I study report for handling the diurnal effects problem was a sound one at the time it was developed. Recently, however, more detailed examination of the mission profile and of specific orbit configurations has served to point out that a sun-synchronous orbit (which appears highly desirable from the spacecraft design viewpoint) will only provide radiance data samples at local times spaced 12 hours apart. The twilight sun-synchronous orbit, which was the type first considered, provides data samples near 6:00 a.m. and 1:00 p.m. local time.

Basic questions were raised as to whether the twilight sun-synchronous orbit could provide adequate diurnal sampling and, indeed, whether any sun-synchronous orbit could provide diurnal component coverage comparable to that obtained from a more inclined, precessing orbit where the local sampling times would change appreciably within a given space cell during a 28-day map period. The latter type of orbit was considered in terms of a 70° inclined orbit with 2.63° westward precession, which provides diurnal coverage at local times extending over 13 to 15 hours out of 24 within a given map period. On the basis of the study made of diurnal temperature variability, the recommendation was made that a 3 o'clock sun-synchronous orbit be adopted in place of the twilight orbit. This study indicated that the expected time of maximum diurnal temperature, at stratospheric and lower mesospheric levels, probably occurs midway between noon and 6:00 p.m., local time. Empirical data favor earlier times, whereas theoretical calculations indicate times more toward sunset. Available evidence also suggests that the phase of the diurnal temperature (and associated radiance) oscillation varies appreciably with altitude, latitude, and time of the year. A twilight sun-synchronous orbit, with sampling near 6:00 p.m., would be offset with respect to the average time of the diurnal maximum. Thus, the daytime sample from a twilight orbit would, in many instances (i.e., whenever sunset occurs prior to 6:00 p.m.) be taken during the time of maximum temperature decrease near and subsequent to sunset. The daytime sample would contain, therefore, a mixture of diurnal maxima as well as intermediate values. A similar argument applies at the sunrise side of a twilight orbit with respect to the diurnal minima. The 3 o'clock sun-synchronous orbit, on the other hand, seems to provide a considerably larger percentage of true daylight samples by avoiding sunset (except at very high latitudes near the winter solstice).

The other basic question considered is whether or not a 3 o'clock sun-synchronous orbit can provide an adequate sample for analyzing the diurnal component of radiance profile variability. Here, comparison was made with a 70 degree inclined maximum precession orbit, since this orbit provides a daily shift in the local times at which samples are taken with a given time/space cell. The 70 degree inclined orbit essentially provides two periods of approximately six hours each, wherein the local sampling time gradually changes during a 28-day map interval.

Figure B3 illustrates the dirunal data coverage which would be obtained within a typical time/space cell from a 3 o'clock sun-synchronous orbit and a 70° inclined maximum precession orbit. The total sample of 16 points divides, in both cases, into two equal clusters of daytime and nighttime data. It is assumed that the points, as plotted here, represent values from which the synoptic and seasonal trends have been removed, i. e., the reduced data from which the diurnal component is to be evaluated. The sun-synchronous orbit data sample, it may be noted, is highly concentrated with respect to local time, whereas the 70° inclined orbit data are scattered throughout two 6-hour periods. Because of their highly time-concentrated nature, the synoptic and seasonal components can be more easily and accurately removed from the sun-synchronous profile data. In the case of the 70° inclined orbit data, the local time spread renders the analysis of the diurnal component more difficult and less certain, since there is no reliable "anchor point" for separating the synoptic from the diruanl variance within relatively small samples from individual time/space cells. Thus, the 70° inclined orbit for a given sample size does not provide (as might originally have been supposed) better determination of the amplitude and phase of the diurnal variation, because of the "time-smear" problem.

The sun-synchronous orbit does provide relatively accurate statistics at two points in loca time spaced 12 hours apart. These points can be selected at the local times which, on the average, correspond to the diurnal maxima and minima. Delineation of the complete diurnal curve connecting these two points will depend upon theory and rocketsonde observations. As shown in Table B1, because of the inclination required for a sun-synchronous orbit, there will be a change in the local time of satellite crossings at higher latitudes, with respect to the nominal local time for nodal crossings. However, from 0 to 63° latitude, the local times of satellite crossings are within one hour of the nodal time (one hour earlier in the 3:00 a. m. case; one hour earlier in the 3:00 p. m. case).

Special series of high-level rocket soundings (including some taken above the nominal 60 km range of MRN flight equipment) represent the most straightforward and reliable means for determining the complete curve of diurnal temperature (and radiance) variation. Series of rocketsonde observations, taken systematically at low, mid, and high latitudes at representative times during the four seaons and during select synoptic conditions, would provide a highly desirable supplement to HDS diurnal component data obtained from a 3 o'clock sun-synchronous orbit.

Table B2 provides a brief summary of the relative advantages and disadvantages of the 3 o'clock sun-synchronous and 70° inclination maximum precession orbits.

1) 3 p.m./3 a.m. sun-synchronous orbit

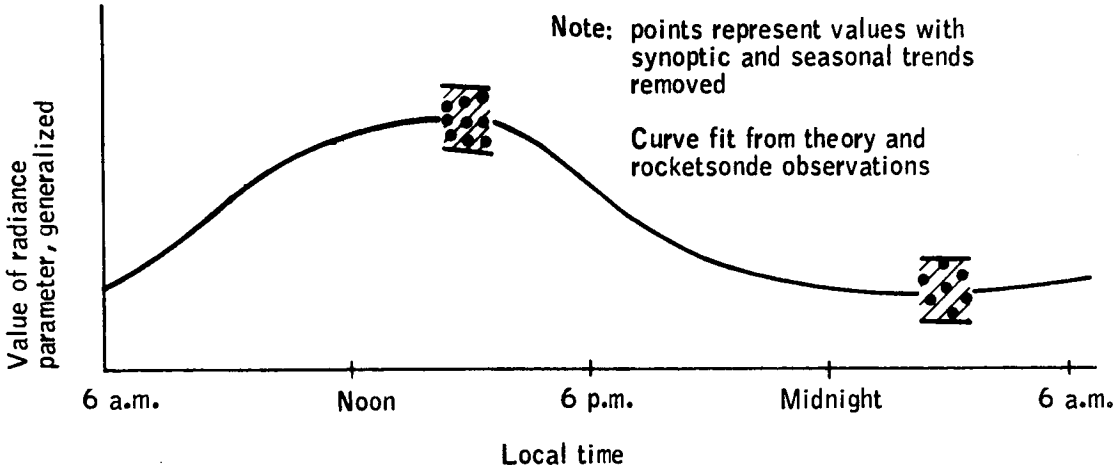

2) 70 deg inclined maximum precession orbit

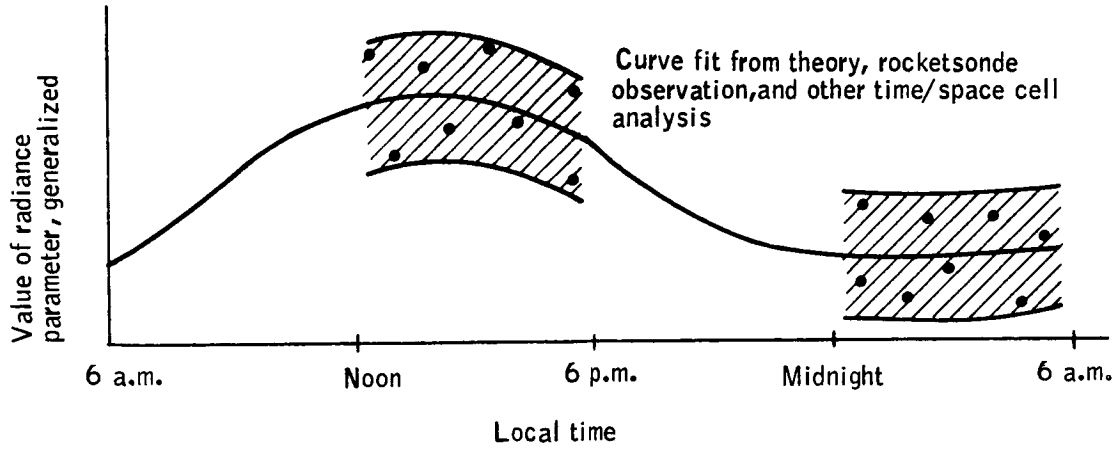

Figure B3. Illustrative Example of Diurnal Data Coverage in a Time/Space Cell

TABLE B1. - APPROXIMATE LOCAL TIMES OF LATITUDE CROSSINGS, 3 O'CLOCK SUN-SYNCHRONOUS ORBIT

Latitude	Local time
0	3:00 a. m.
10	2:56 a. m.
20	2:52 a. m.
30	2:46 a. m.
40	2:40 a. m.
50	2:28 a. m.
60	2:12 a. m.
70	1:40 a. m.
80	11:56 p. m.
82.6	9:00 p. m.
80	6:04 p. m.
70	4:20 p. m.
60	3:48 p. m.
50	3:32 p. m.
40	3:20 p. m.
30	3:14 p. m.
20	3:08 p. m.
10	3:04 p. m.
0	3:00 p. m.

COMPARISON OF DIURNAL COVERAGE OBTAINED FROM 3 AND 4 O'CLOCK SUN-SYNCHRONOUS ORBITS

The selection of a 3 o'clock sun-synchronous orbit was based upon a general requirement ot obtain day and night radiance profile samples which would permit calculation of the diurnal component of variability. The study of theoretical and empirical evidence relating to the diurnal variability of temperature led to the choice of a 3 o'clock local time as one which would provide daytime near-maxima and nighttime near-minima and which would generally avoid the problem of skirting near relatively sharp sunrise and sunset discontinuities. However, a shift to a later local time could provide spacraft design advantages. The diurnal sampling problem was re-examined, therefore, to determine the annual latitudinal distribution of night and daytime samples obtained with 3 and 4 o'clock orbits and to examine the sensitivity of changes in the diurnal sample size for different local times, ranging from 0230 to 0430.

TABLE B2. - RELATIVE ADVANTAGES AND DISADVANTAGES OF TWO DIFFERENT ORBITS FOR DIURNAL DATA SAMPLING[a]

3 o'clock sun-synchronous	70° inclination maximum precession
Advantages	**Advantages**
• Concentrated data samples are provided at or near times of expected maximum and minimum values.	• Data samples in each time/space cell cover two 6-hour periods centered at expected times of maximum and minimum values.
• Time-concentrated data samples facilitate statistical separation of diurnal from synoptic (and seasonal) variability.	• Diurnal trends can be calculated for two 6-hour time periods within each time/space cell.
• Data samples provide more reliable determination of diurnal variability at the two most significant points, i. e., maximum and minimum.	• During a one-year program, samples will be obtained during the entire 24-hour diurnal cycle.
• More reliable determination of the limits of diurnal variability can be made within a given time/space cell.	• Overall analysis of global sample does not necessarily depend upon theory and rocketsonde observations to determine shape of diurnal variability curve.
Disadvantages	**Disadvantages**
• Only provides two-point determination of diurnal variability. Complete curve must be inferred from theory and rocketsonde observations.	• It is more difficult to separate diurnal from synoptic (and seasonal) variability within a given time/space cell.
• Phase changes in diurnal variability are difficult to assess.	• Less reliable determinations are made of diurnal variability at the times covered by sun-synchronous orbit sample.
μ • Expected times of maximum and minimum values may be in error.	• Aggregates of sampling cells must be used to obtain an acceptable level of statistical confidence.

[a]Only considers data analysis; does not include spacecraft design factors.

Reference 22 was used as the basis for this recent study. This reference consists of a series of charts and overlays which enable the rapid computation of onset times for periods of complete darkness (defined as beginning at the end of astronomical twilight) and complete light (defined as beginning at zero sun declination). By superimposing the overlay, which contains a circular and local time grid, upon the series of charts, which outline the areas of sunlight, darkness, and three twilight levels at select 1 to 3 week intervals, it is possible to determine the latitudes where the selected local times intersect the darkness and sunlight areas. Five local times were used in this analysis: 0230, 0300, 0330, 0400, and 0430 on the darkness side, and 1430, 1500, 1530, 1600, and 1630 on the sunlight side.

Figure B4 presents sets of nighttime and daytime curves as a function of latitude and time of the year. The latitude values denote the limits below which samples will be obtained in either the night or daytime periods. It should be noted that the daytime samples can be obtained, even at the 1630 local time, throughout the entire year over latitudes 0 to 45°; during the period from the vernal equinox to the autumnal equinox, daytime samples can be obtained at all latitudes. The nighttime samples are far more sensitive to changes in local time, especially during the several week period centered at the summer solstice were nighttime samples can only be obtained over latitudes 0 to 40° at 0230 local time, the most favorable case considered. During the three-month period centered at the winter solstice, nighttime samples can be obtained over all latitudes for all five local times considered.

If the relative merits of 3 versus 4 o'clock local times for diurnal sampling are examined, the losses incurred by switching to the later time are obvious in Figure B4. The latitude range wherein nighttime samples can be obtained during the several-week period near the summer solstice is reduced from 0 to 34° to 0 to 14°. Correspondingly, the latitude range within which daytime samples can be obtained is reduced during the period near the winter solstice from 0 to 61° to 0 to 52°. The losses incurred in the nighttime samples at the later local time are obviously more serious.

In order to explore the problem in greater detail, the 3 and 4 o'clock local time curves shown in Figure B4 were used to determine the percent of day and nighttime samples obtained within 10° latitude intervals for each 28-day time cell (or map period). These time cells are outlined on Figure B4, with the initial cell beginning on 1 January. The analysis was based upon a constant orbital data acquisition rate, where the number of samples obtained in each 10° latitude interval were expressed as a percentage of the total number of samples per orbit.

Tables B3 and B4 present the results of this analysis, which permits the assessment of the diurnal sample losses for 4 o'clock versus 3 o'clock sun-synchronous orbits as a function of latitude interval and time cell. On an annual basis, with the 3 o'clock orbit, 91 percent of the 3:00 p. m. radiance profiles fall within the daylight period, and some 72 percent of the 3:00 a. m. profiles occur during darkness. With the 4 O'clock orbit, these percentages are reduced to 87 and 60 percent, respectively.

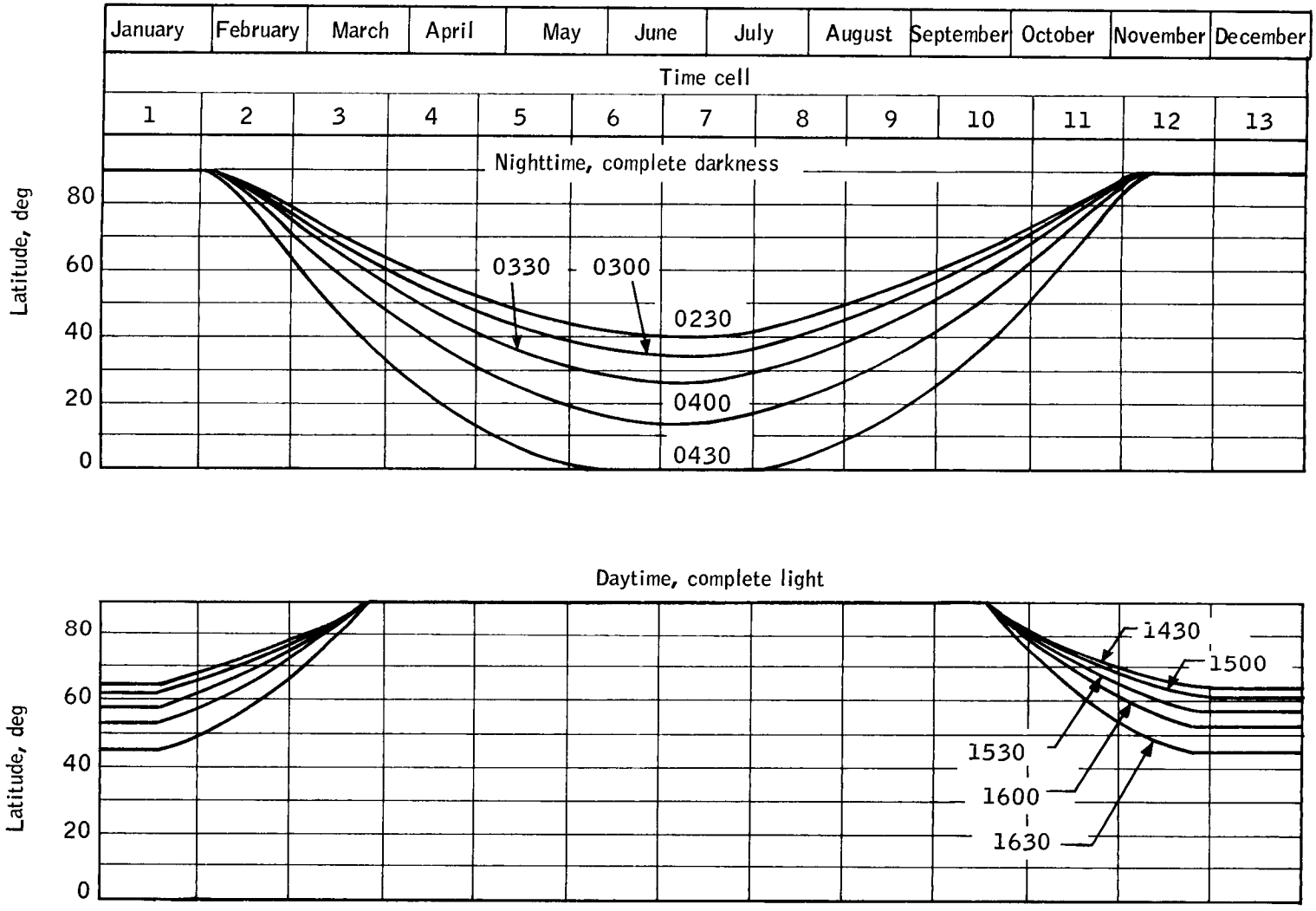

Figure B4. Annual Distribution of Latitude Limits Below which Nighttime and Daytime Radiance Samples Can be at Various Local Times of Nodal Crossings

TABLE B3. - DIURNAL COVERAGE STATISTICS FOR 3 AND 4 O'CLOCK ORBITS AS A FUNCTION OF LATITUDE INTERVAL

Latitude interval, deg	Average percent coverage - all time cells, annual			
	Nighttime		Daytime	
	3 o'clock	4 o'clock	3 o'clock	4 o'clock
0-10	100	100	100	100
10-20	100	93.2	100	100
20-30	100	74.3	100	100
30-40	93.2	62.8	100	100
40-50	71.5	53.9	100	100
50-60	58.2	46.5	100	85.8
60-70	48.1	39.5	82.5	71.1
70-80	37.7	32.7	67.0	62.1
80-82.6	31.3	28.2	59.7	57.2
Average - all latitudes	72.0	59.6	90.7	86.9

TABLE B4.- DIURNAL COVERAGE STATISTICS FOR 3 AND 4 O'CLOCK ORBITS AS A FUNCTION OF TIME OF YEAR, 13 TIME CELLS

Time cell, successive 28-day periods beginning 1 January	Average percent coverage, all latitudes, 0-82.6 deg			
	Nighttime		Daytime	
	3 o'clock	4 o'clock	3 o'clock	4 o'clock
1	100	100	71.5	61.0
2	97.9	93.2	81.4	73.2
3	79.3	67.4	97.5	95.0
4	61.6	43.5	100	100
5	48.3	28.1	100	100
6	40.9	18.3	100	100
7	39.8	16.8	100	100
8	45.8	24.2	100	100
9	56.8	38.3	100	100
10	73.0	58.8	100	99.1
11	92.4	86.0	87.0	79.5
12	100	100	72.6	62.9
13	100	100	69.5	59.3
Average - all time cells	72.0	59.6	90.7	86.9

Another important aspect of the diurnal sampling problem is to define the latitudinal limits within which both day and night radiance samples can be obtained concurrently. Daytime samples within a given time cell and latitude interval are of relatively limited value without their counterpart nighttime samples (and vice versa). Figure B5 was prepared, therefore, to show the annual distribution of latitudinal limits for concurrent day and night samples. Above these latitudinal limits, either twilight or opposite lighting conditions are occurring. It may be seen that the shift from a 3 o'clock to a 4 o'clock orbit results, throughout the year, in a loss of 5 to 20° latitude within which concurrent diurnal sampling coverage can be obtained; this loss is least in late February and mid-October and greatest during the several-week period centered at the summer solstice.

The basic question is how serious are these relative diurnal data losses incurred in shifting from a 3 o'clock to a 4 o'clock orbit. These losses must be regarded as significant, and should be avoided, if at all possible; they can be reluctantly tolerated, however, if the earlier local time can be shown to impose inordinately heavy design penalties. In either case, the HDS experiment is not capable of satisfying completely an ideal set of diurnal sampling requirements. For this reason, auxiliary experiments of diurnal variability, involving special MRN radiosonde and high mesosphere sounding observations are definitely recommended. These observations would not only provide temperature data and allow syntehsized radiance profiles therefrom for correlation studies with HDS data, but would extend the analysis of diurnal variability to those latitudes and times of year which lie outside the effective range of the HDS experiment.

THE EFFECT OF DIURNAL TEMPERATURE VARIABILITY UPON THE DETERMINATION OF HORIZON LOCATORS

A representative number of climatological profiles were selected to serve as the basis for evaluating the effect of diurnal temperature variability upon the determination of several recommended horizon locators. The selected profiles, all of which lie along the 90°W meridian, are listed below:

Profile no.	Month	Latitude, °N	Diurnal curve no.	Maximum diurnal ampl. °C
843	Jan.	20	1	7.0
863	Jan.	45	2S	5.6
883	Jan.	75	3S	1.0
913	Apr.	45	2E	6.5
933	Apr.	75	3E	3.3
943	July	75	3E	3.3
963	July	45	2S	5.6
983	July	75	3S	1.0

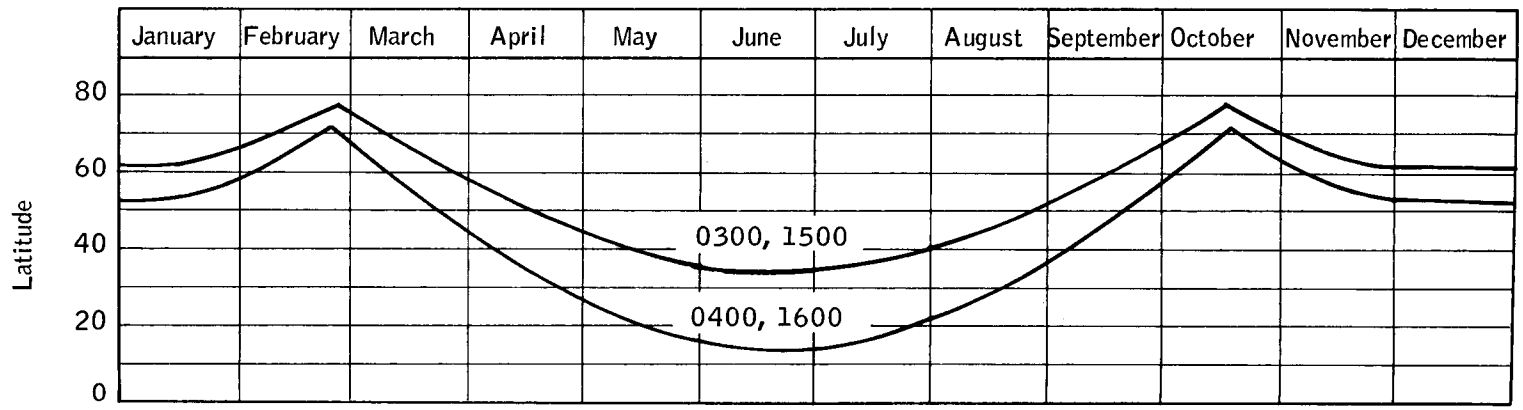

Figure B5. Annual Distribution of Latitudinal Limits Below which Day and Night Radiance Samples Can be Obtained Concurrently for Two Sun-Synchronous Orbits

Also shown here is the diurnal curve number, which refers to one of the specific curves of diurnal temperature oscillation presented in Figures B6 and B7. The maximum amplitude of diurnal temperature variation for each diurnal curve is also listed here.

The complete rationale underlying the definition of the diurnal temperature curves is described earlier in this section. In brief, these are significant latitudinal and seasonal changes in the amplitude of diurnal temperature variation. The selection of representative cases for this study was designed, therefore, to include latitudes 20°, 45°, and 75°N, and to include months near the times of the winter solstice, vernal equinox, and summer solstice. These cases provide a good range of combinations with respect to the basic radiance profiles and the superimposed diurnal variations.

Computation of diurnal range in tangent heights for the L1, L2 and L7 locators involved straightforward interpolation from the "plus" and "minus" pairs of radiance profiles. For the L1 locators, tangent heights for each profile pair were interpolated at each fixed radiance value (i.e., 3.0, 2.0, 1.0, and 0.2 W/m^2 - sr) and diurnal ranges were obtained by subtraction. For the L2 locators, the interpolation was performed with respect to the values of normalized radiance, i.e., 0.95, 0.50, 0.30, and 0.06. The peak radiances were multiplied by these factors and the interpolation of tangent heights made directly from the computer printouts at the fixed radiance levels corresponding to the assigned values of normalized radiance. For the L7 locator, interpolations were carried out in each instance at the 1.5 and 0.75 W/m^2 - sr radiance levels and slope extrpolation was made to determine the zero radiance level intercept.

Computation of diurnal tangent height range for the integral normalized radiance locators L4 (2.5) and L4 (0.5) necessarily involved a more elaborate process. Since no computer program was available to permit direct calculation, the mean tangent heights of the Lr (2.5) and Lr (0.5) locators, for the "plus" and "minus" pairs, were first estimated by interpolation based upon their values of peak radiance with respect to the peak radiance of the minimum, mean, and maximum profiles, the tangent heights for which had been determined in the Part I study. Then, weighted averages of the percent radiance deviations (plus or minus) were obtained over the interval extending from the estimated locator tangent height to 80 km. The percent deviation in the peak radiance was then subrracted from the weighted average deviation to determine the net percent deviation for each profile pair and locator. This deviation, multiplied by the value of integral normalized radiance, (i.e., 2.4 or 0.5 $W\text{-}km/m^2$ - sr) yielded a value of deviation expressed in the proper units. An average value of the slope of integral normalized radiance per km was then determined for the "plus" and "minus" profiles at the estimated locator tangent height. The slope value was used to convert the integral normalized radiance deviation into an equivalent tangent height deviation.

The results of the analysis of locator tangent height deviations attributable to diurnal temperature variability are presented in Table B5. These results indicated that a significant diurnal variability in locator tangent heights will

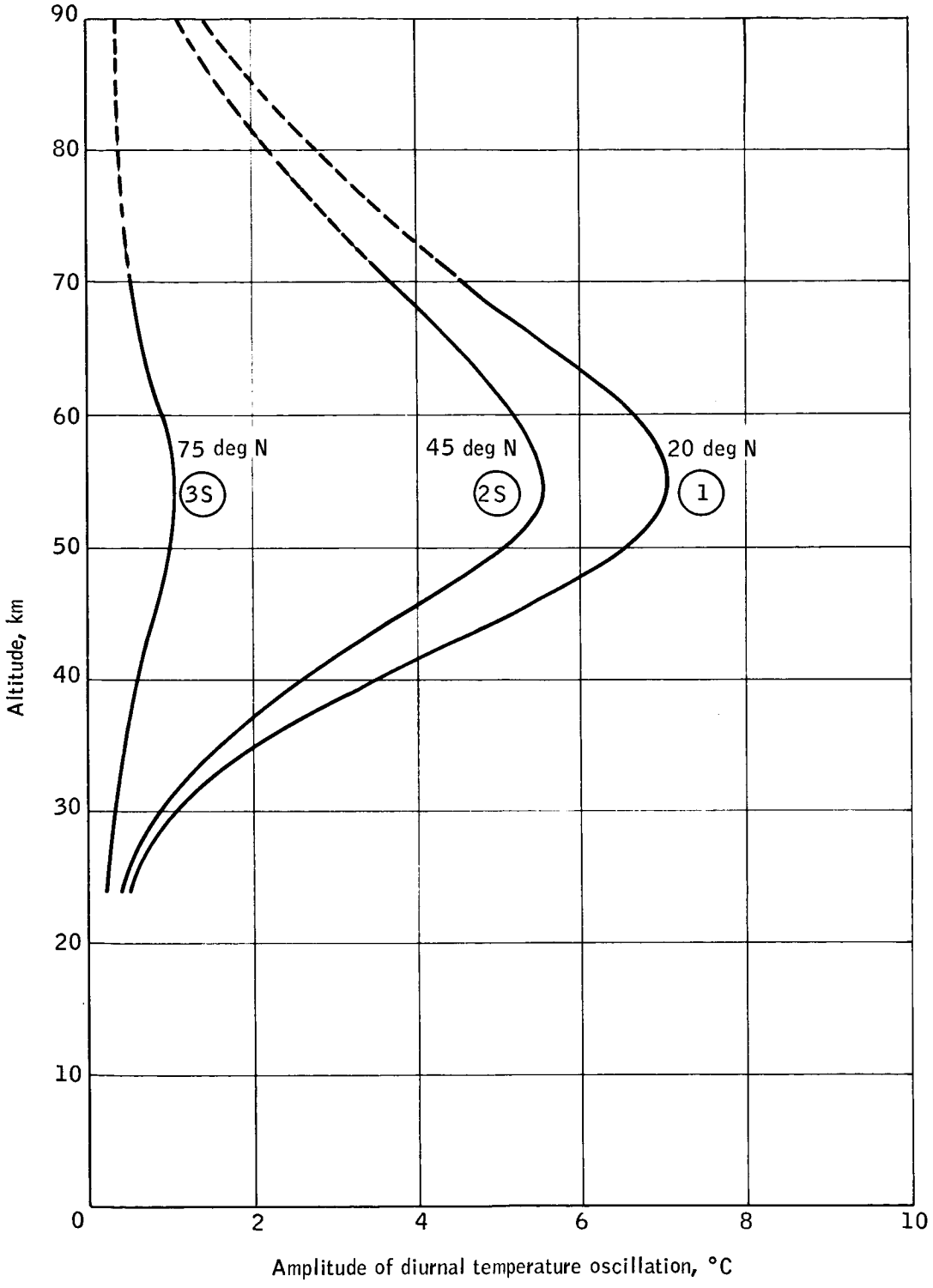

Figure B6. Amplitude of Diurnal Temperature Oscillation during Summer and Winter Solstice, June 21 and December 21

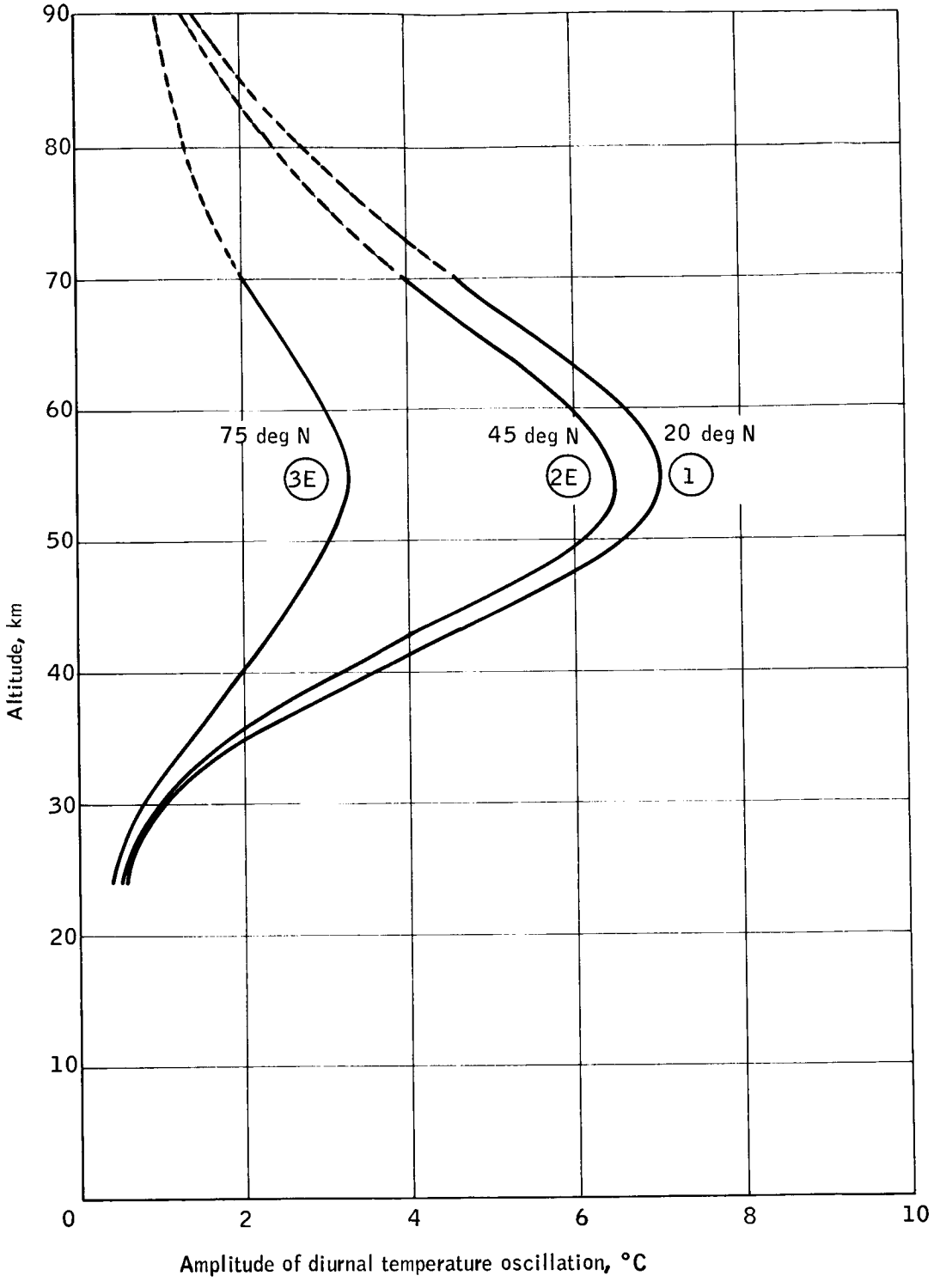

Figure B7. Amplitude of Diurnal Temperature Oscillation for Vernal and Autumnal Equinox, March 21 and September 21

TABLE B5. - DIURNAL RANGE OF LOCATOR TANGENT HEIGHT, km, ATTRIBUTABLE TO DIURNAL TEMPERATURE VARIATION

Locator	Locator tangent height parameter, km	Maximum amplitude of diurnal temperature variation, °C								
			1.0		3.3	5.6		6.5	7.0	
		Profile no.	883	983	933	863	963	913	843	943
		Month/latitude	Jan/75	Jul/75	Apr/75	Jan/45	July/45	Apr/45	Jan/20	July/20
		Peak radiance W/m^2-sr	4.3041	7.0477	5.6357	5.1366	6.0699	5.7634	5.3696	5.6445
L1 (1.0)	Diurnal range		0.19	0.16	0.15	0.67	0.79	0.83	1.50	1.06
	Mean height		29.9	43.4	36.8	34.7	41.3	39.4	39.0	39.4
L1 (0.0)	Diurnal range		0.14	0.13	0.14	0.70	0.62	0.64	0.99	0.97
	Mean height		35.1	47.0	42.2	40.2	45.5	43.8	44.7	44.1
L1 (1.0)	Diurnal range		0.18	0.11	0.16	0.98	0.66	0.70	0.76	0.86
	Mean height		43.1	52.7	49.1	47.7	51.0	50.0	50.3	49.9
L1 (0.2)	Diurnal range		0.11	0.07	0.08	0.55	0.61	0.65	0.58	0.71
	Mean height		57.5	62.7	59.8	59.1	61.2	60.2	59.8	60.1
L2 (0.95)	Diurnal range		0.02	0.06	0.04	0.19	0.34	0.28	0.12	0.48
	Mean height		18.2	23.0	20.3	20.4	24.3	21.8	26.8	26.0
L2 (0.50)	Diurnal range		0.06	0.08	0.07	0.44	0.47	0.49	0.79	0.64
	Mean height		34.3	41.5	37.6	37.0	41.1	40.0	41.0	40.2
L2 (0.30)	Diurnal range		0.05	0.07	0.09	0.37	0.43	0.47	0.57	0.60
	Mean height		40.4	46.6	43.8	42.8	46.2	45.1	46.6	45.6
L2 (0.06)	Diurnal range		0.08	0.04	0.06	0.06	0.34	0.41	0.47	0.41
	Mean height		55.6	58.3	56.7	56.1	57.6	57.0	57.1	57.1
L4 (2.5)	Diurnal range		0.11	0.07	0.08	0.50	0.45	0.50	0.46	0.59
	Mean height (a)		42.1	46.6	44.6	43.8	45.2	44.8	44.2	44.6
L4 (0.5)	Diurnal range		0.07	0.04	0.05	0.35	0.41	0.43	0.49	0.56
	Mean height (a)		54.2	56.7	55.6	55.1	55.9	55.7	55.4	55.6
L7	Diurnal range		0.32	0.11	0.06	0.65	0.57	0.43	0.39	0.69
	Mean height		54.6	59.8	58.0	57.7	58.2	57.5	56.8	57.3

[a] Estimated

occur in those cases where the maximum amplitude of the diurnal temperature oscillation exceeds a value of 3.3°C. The tangent height deviations in Table B5 show a definite break point between maximum temperature amplitude (MTA) values of 3.3° and 4.5°C. For lower MTA values, the tangent height deviations (THD's) are for the most part in the range of 0.05 - 0.15 km. The median values for the different classes of locator are as follows: L1, 0.14; L2, 0.06; Lr, 0.07, and L7, 0.11. In the case of locator L7 the THD value for Profile 883 (1°C MTA) is considerably higher than for Profile 983 (1°C MTA) and Profile 933 (3.3°C), i.e., 0.32 versus 0.11 and 0.06 km. respectively. This interesting result is discussed below in terms of Profiles 883 and 983 since it exemplifies the way in which various factors influence the magnitude of the tangent height deviation.

The L7 locator tangent height is calculated by extrapolating from the 1.5 and 0.75 W/m^2 - sr radiance levels. The THD value for L7 (at zero radiance) is sensitive, therefore, to the relative magnitude of the THD values at the two higher radiance levels. In the case of Profile 883, the radiance deviations at 1.5 and 0.75 W/m^2 - sr are 0.0166 and 0.0128, respectively, for a relative difference factor of 1.3 However, because of differences in the slope of the radiance profile at these two levels, a given size radiance deviation at 0.75 W/m^2 - sr produces an equivalent tangent height deviation which is 2.1 times larger than at the higher radiance level. The combination of these two factors yields a relatively larger THD value at 0.75 W/m^2 - sr which, in turn, by extrapolation, increases the THD at zero radiance. For Profile 983, on the other hand, the radiance deviation at 1.5 versus 0.75 W/m^2 - sr is larger by a factor of 1.9; the profile slope differences are such that a given radiance deviation at 0.75 versus W/m^2 - sr produces an equivalent THD which is larger by a factor of 1.8. The combination of these two factors, which are almost equal, produces an extrapolated THD at zero radiance which is slightly less than atthe two higher radiance levels. The THD values for the other locators, i.e., L1, L2, and L4, are not affected by the extrapolation process; nevertheless, in comparing relative differences for different profiles and locators, it should be kept in mind that difference in absolute radiance deviations and radiance profile slope characteristics are both involved in the determination of THD values.

For MTA's of 6.5° and 7°C, Table B5 shows typical THD values of 0.80 km for the L1 locators, 0.48 km for L2 locators, 0.50 km for the L4 locators, and 0.43 km for the L7 locator. The highest overall THD values, i.e., 1.06 and 1.50 km, were obtained for the L1 (3.0) locator. The magnitude of the THD's for the L1 class of locators appears to decrease gradually over the range of fixed levels from 3.0 to 0.2 W/m^2 - sr. For the L2 locators, the highest THD's occur at the 0.50 normalized radiance level. The THD's for the two L4 locators are approximately the same.

It would appear from the results presented above that, at low and mid latitudes, the tangent height deviations for most locators, attributable to the diurnal cycle of temperature variation in the stratosphere, lie within the range of 0.50 - 1.00 km throughout most or all of the year. At very high latitudes, where the MTA of diurnal variability is relatively small, THD's of 0.1 - 0.2 km can be normally expected. The higher THD values at low and mid latitudes are especially significant since they are comparable in magnitude to the tangent height standard deviations which occur at locations and during time periods when the synoptic variability of the atmosphere is relatively low (see Table B5 which presents sample values of tangent height standard deviations for various locators, based upon representative synoptic, time cross section and space cross section cases). During periods of high synoptic variability, the diurnal component of tangent height variation is relatively small and difficult to isolate, but it should be statistically easier to separte within space/time cells of relatively low synoptic variability.

PRECEDING PAGE BLANK NOT FILMED.

APPENDIX C

EFFECTS OF ERRORS AND UNCERTAINTIES ON DATA REQUIREMENTS

PRECEDING PAGE BLANK NOT FILMED.

APPENDIX C

EFFECTS OF ERRORS AND UNCERTAINTIES ON DATA REQUIREMENTS

THE EFFECT OF RANDOM RADIOMETER ERRORS UPON SAMPLE SIZE REQUIREMENTS FOR HORIZON LOCATORS

A preliminary error analysis was made to determine the effect upon the experiment sampling requirements of random errors associated with the operation of the radiometer instrument. This effect was appraised in terms of equivalent tangent height error in 11 recommended horizon locators. This error, in turn, can be expressed in terms of an additional number of profile samples which must be taken within each space/time cell to maintain the same level of confidence as that designated for the no-radiometer-error case. The error analysis was conducted on a parametric basis, covering a range of error standard deviation in radiance from 0.0001 to 0.1 W/m^2 - sr.

The results of this preliminary analysis were used to make working estimates of the additional samples required for radiometer error compensation; they also provided a basis for the more extensive study of radiometer error effects, the results of which are presented in a subsequent section of this report. The results of this preliminary analysis and those obtained in the subsequent analysis are not directly comparable since, in the latter case, the analysis was aimed at specification of radiometer design requirements and at predicting horizon sensor performance.

The approach which was taken in the preliminary analysis was to compute the equivalent tangent height error for three representative cases: the minimum, mean, and maximum profiles which were determined by computer analysis in the Part I study from an extensive series of 839 synoptic profiles. The three radiance profiles, illustrated in Figure C1, are statistical conglomerates. The mean profile consists of mean radiance values determined at one km tangent height intervals between 0 to 50 km and at 2 and 5 km intervals elsewhere. The maximum (minimum) profile consists of a series of maximum (minimum) radiance values selected at each designated tangent height level from the entire set of 839 profiles.

The maximum and minimum profiles are sensitive, over the 0 to 50 km tangent height interval, to small-scale fluctuations within each of the 839 input profiles; as a result, the level-by-level selection of maximum and minimum values by the computer tends to produce irregularities in the derived profiles which do effect to a limited degree the representativeness of radiance profile slope values used to convert radiance error into equivalent tangent height error.

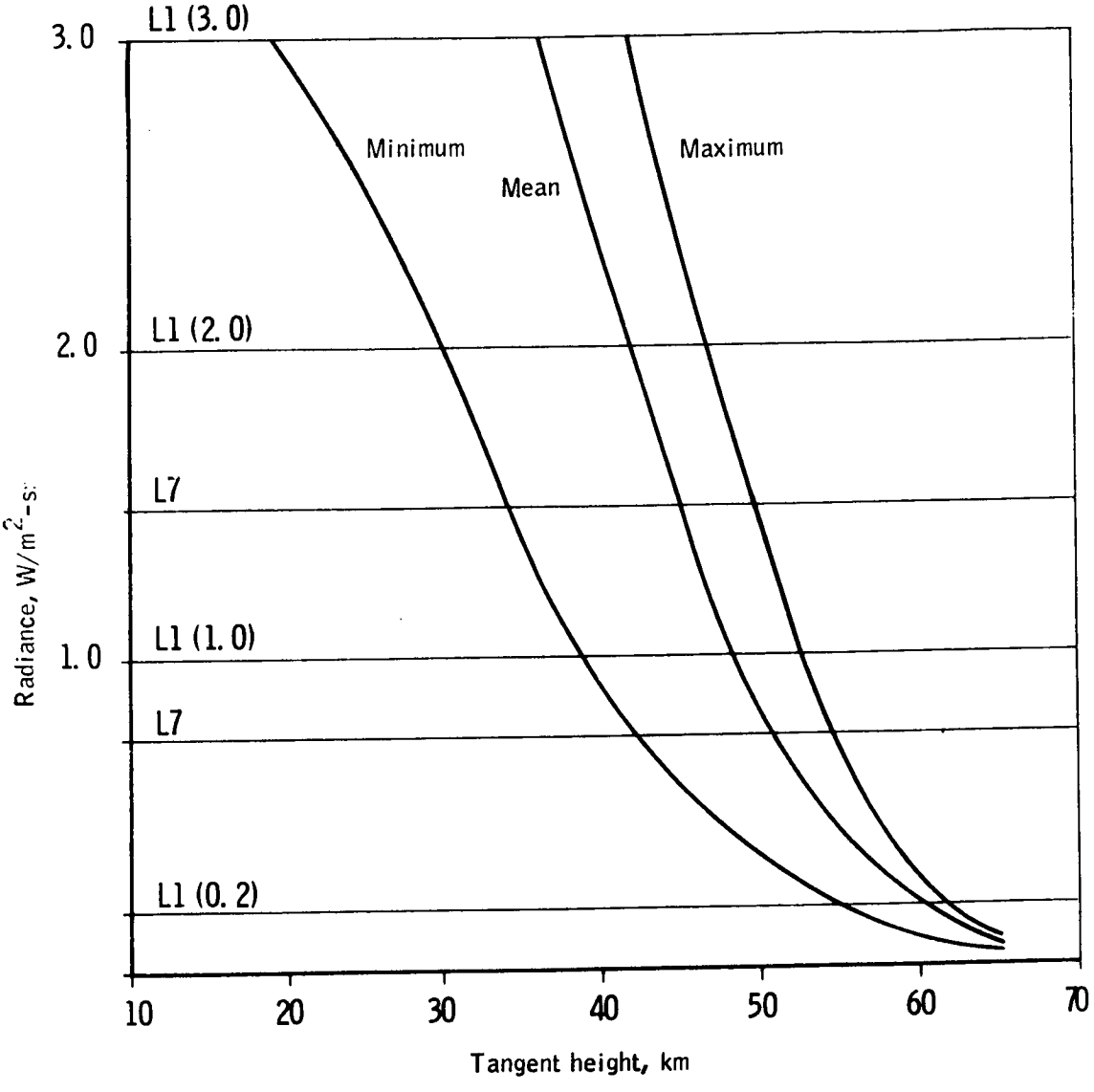

Figure C1. Distribution of Minimum, Mean, and Maximum Radiance Profiles in 0-3.0 W/m^2-sr Interval, Based upon 839 Synoptic Cases

A far more important effect was introduced into the preliminary error analysis by the use of minimum, maximum, and mean slope valued, dN/dh, (where N is radiance in W/m^2 - sr and h is tangent height in km) in computations involving the L1 and L7 locators. These slope values, which were available from the computer analysis of the 839 synoptic profiles, were plotted as a function of tangent height. The mean slope values were analyzed subjectively with a least-square type of curve fit; the plots of maximum and minimum slope values were analyzed in terms of smoothed boundary curves drawn on the outer side of all extreme values. The maximum slope values (which represented small negative or positive numbers) were used in the analysis of L1 and L7 locators for the minimum radiance profile. The minimum slope values (which represented large negative numbers) were used in the analysis start of L1 and L7 locators for the maximum radiance profile. Subsequent re-examination of this procedure has revealed that the slope values used in the minimum profile case to compute equivalent tangent height errors for locators L1(3.0) and L1(2.0) were completely non-representative. Analysis of several individual profiles with low peak radiance (i.e., of the order of 3.5 W/m^2 - sr) revealed that the slope values applied to locators L1 (3.0) and L1 (2.0) for the minimum profile case in the prelimimary analysis were too low by factors of 20 and 22.5, respectively. On the other hand, the slope values applied to the L1 (1.0), L1 (0.2) and L7 locators for the minimum profile were found to be representative, as were the slope values for the maximum profile case. This interesting result reflects the occurrence of occasional irregularities in the radiance profiles in the vicinity of the 2.0 and 3.0 W/m^2 - sr fixed radiance levels. Thus, the computer analysis of the slopes for 839 individual profiles systematically selected the largest negative numbers for the minimum slope and the small positive or negative numbers in the profile set for the maximum slope. In the latter instance, where the slope numbers are very small (e.g., 0.004 W/m^2 - sr per km) the computation of equivalent tangent height error from the radiance error is extremely sensitivie to the effect of profile irregularities. This effect was further compounded by the type of boundary smoothing which was used to analyze the slope values used for the minimum profile. In the discussion of the random radiometer error analysis presented below, amended slope values have been used to calculate the L1 (2.0) and L1 (3.0) tangent height errors for the minimum profile case.

The calculation of random error effects must be carried out differently for each major class of locator, i.e., L1, L2, L4, and L7. Briefly described below are the methods, assumptions and input data involved in the calculation of σ_h as a function of σ_N.

L1 Locators

The L1 locators are only sensitive to the radiance error which applies to their designated radiance levels, i.e., 3.0, 2.0, 1.0, and 0.2 W/m^2 - sr. The calculation of σ_h versus σ_N is based, therefore, upon an assumed set of σ_N values and the measured slope values of $\Delta N/\Delta h$ as determined at the

various radiance levels for the mean, maximum, and minimum profile cases. The results are shown in Figure C2 through C4.

L7 Locators

The L7 (slope extrapolation) locator is sensitive to the radiance errors at both points in the profile (i.e., 0.75 and 1.5 W/m^2 - sr) which provide the basis for the slope extrapolation to zero radiance. The tangent height for L7 at the zero radiance intercept can be expressed as:

$$h_0 = h_{0.75} + (h_{0.75} - h_{1.5}) = 2h_{0.75} - h_{1.5} \tag{C1}$$

where the subscripts for h indicate the radiance levels to which the tangent height value applies. If it is assumed that the random errors in $h_{0.75}$ and $h_{1.5}$ are independent, the following error equation applies:

$$\sigma_{h_0} = \sqrt{4\,\sigma^2_{h_{0.75}} + \sigma^2_{h_{1.5}}} \tag{C2}$$

The σ_h values are calculable from the assigned valued of σ_N at the 0.75 and 1.5 W/m^2 - sr levels by means of the slopes, $\Delta N/\Delta h$, measurable at these points from the mean, maximum, and minimum profiles.

As an illustrative example, consider the mean profile case with an assigned value of $\sigma_N = 0.1$ W/m^2 - sr at both extrapolation points in the profile. The slope determined values of σ_h at the 0.75 and 1.5 W/m^2 - sr levels are 1.05 and 0.69 km, respectively. By substitution in equation (3), a σ_h value of 2.21 km is obtained. The other calculations were similarly performed. The results for this locator are presented in Figures C2 through C4.

L2 Locators

The L2 locator involved the determination of tangent height at the normalized radiance level where R, the ratio of radiance to peak radiance, is equal to a preassigned value. The four locators of this type recommended in the Part I study are L2 (0.95), L2 (0.50), L2 (0.30), and L2 (0.06). The calculation of σ_h versus σ_N errors for these locators was formulated as follows. Since $R = N/N_{max.}$ the error standard deviation for R can be expressed, for independent errors, as:

$$\sigma_R = \sqrt{\sigma^2_N + \sigma^2_{N_{Max.}}} \tag{C3}$$

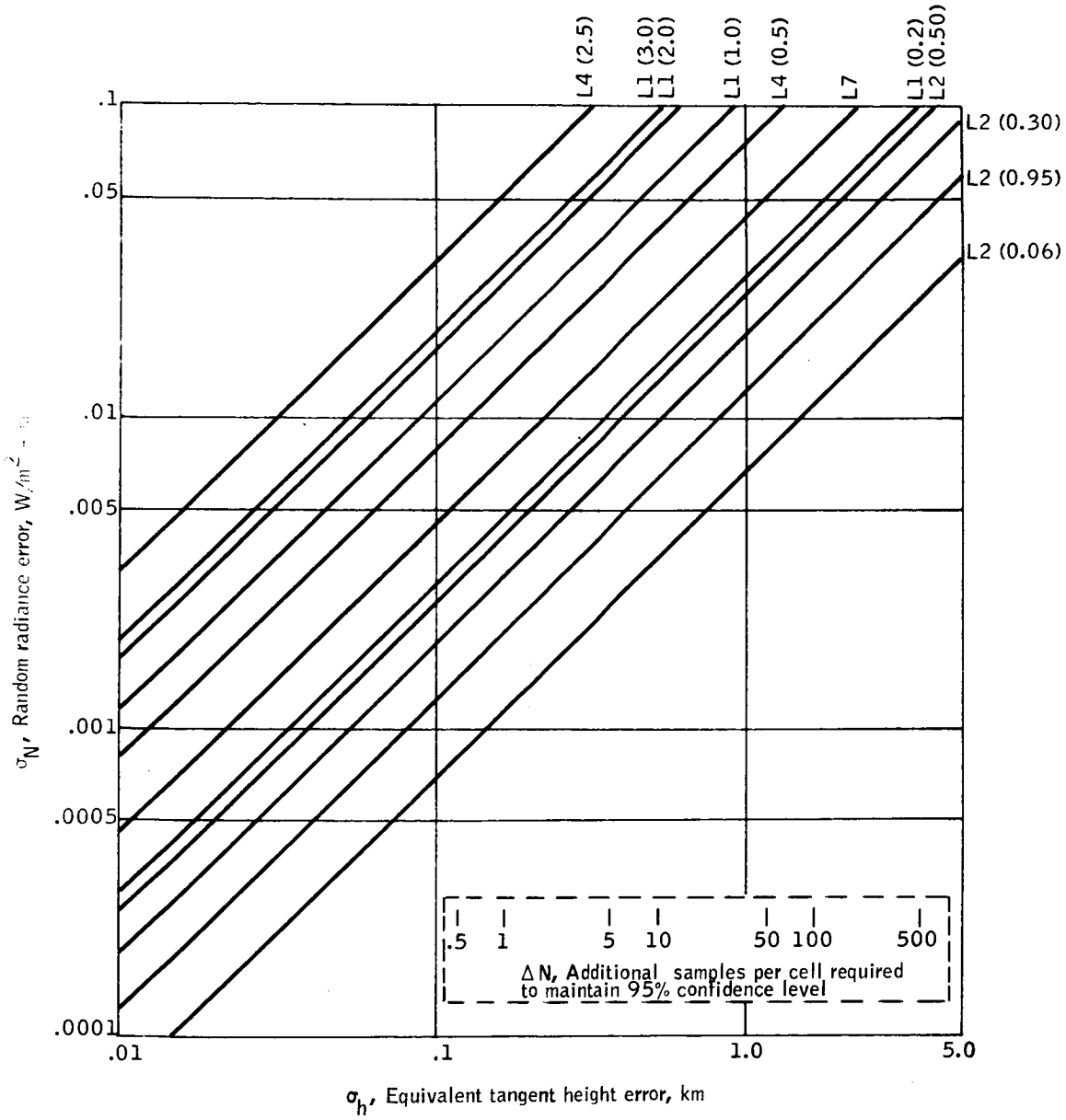

Figure C2. Effects of Random Radiance Errors, Mean Profile Case, All Locators

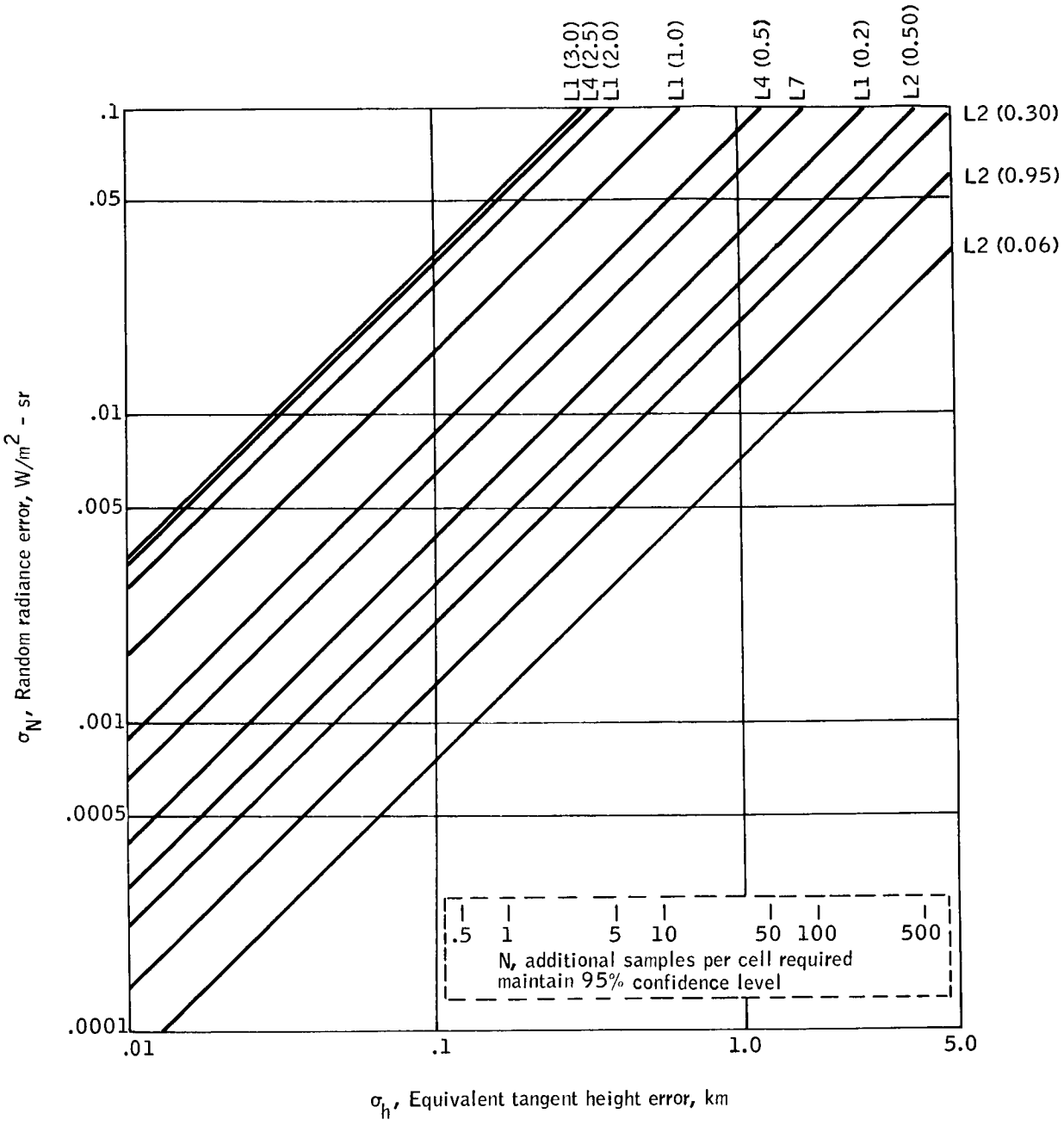

Figure C3. Effects of Random Radiance Errors, Maximum Profile Case, All Locators

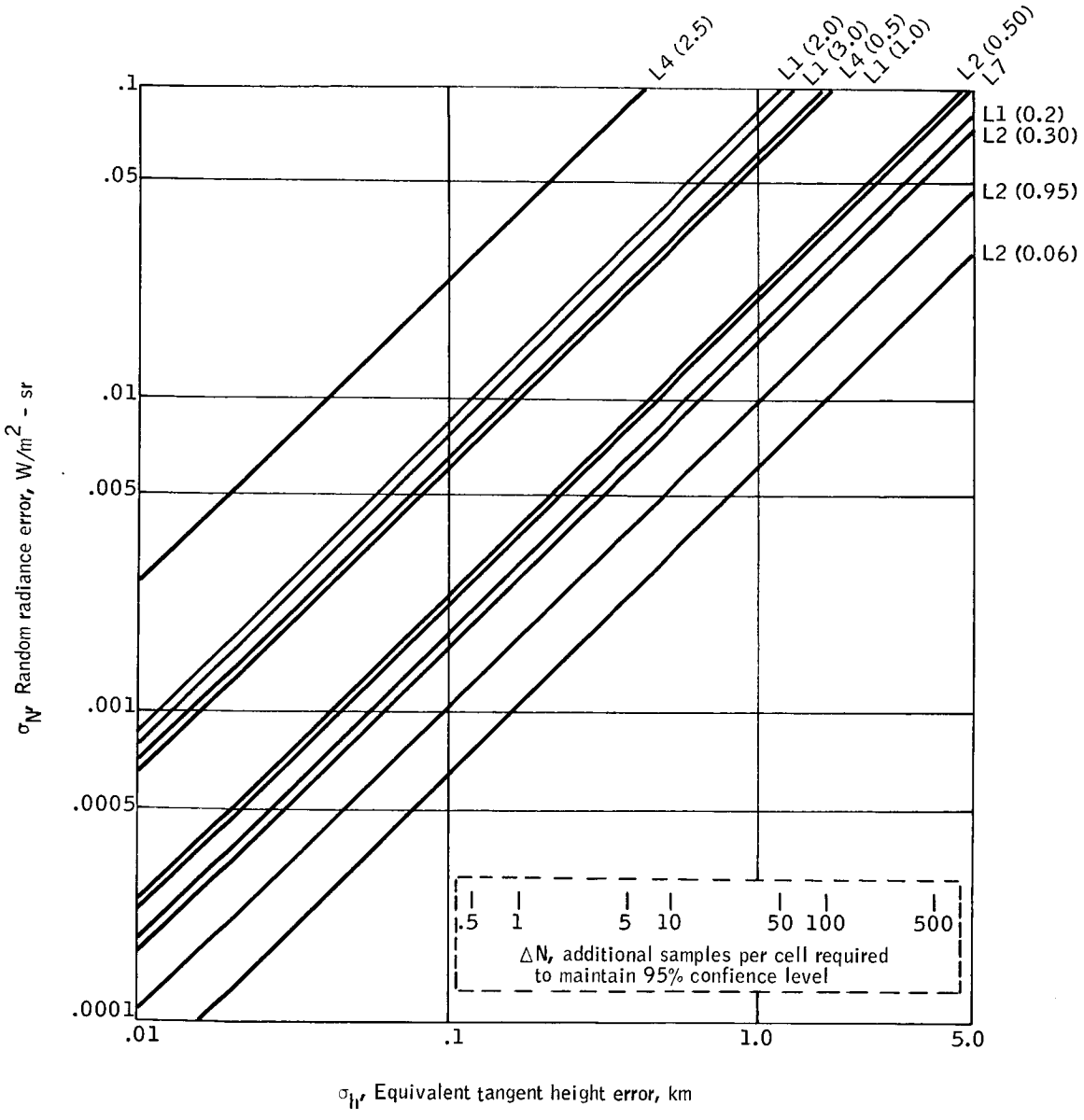

Figure C4. Effects of Random Radiance Errors, Minimum Profile Case, All Locators

where it has been reasoned that the measurements of N and $N_{max.}$ are sufficiently far apart to justify the assumption of their independency. It is further assumed that $\sigma_N^2 = \sigma_{N_{max.}}^2$, then:

$$\sigma_R = \sqrt{2}\,\sigma_N \tag{C4}$$

The calculation σ_h as a function of σ_R then proceeds by determining R versus h slope values at the designated levels of R on the mean, maximum, and minimum profiles. The results of these calculations are shown in Figures C2 through C4.

L4 Locators

The tangent heights for the L4 locators are definable in terms of the following expression.

$$h = f\,(\Sigma\, R_i\, \Delta\, h_i), \tag{C5}$$

where h represents the integral of the normalized radiance values, R_i, for intervals of Δh_i from 80 km to the tangent height h, and where the area under the R versus h curve equals a preassigned value. It will be assumed that there are no intrinsic errors in Δh_i. On this basis, the following error equation can be formulated:

$$\sigma^2_{\sum R_i} = \sigma^2_{\overline{N}} + \sigma^2_{N_{max.}} \tag{C6}$$

where σ_{R_i} is the error standard deviation (ESD) in the integral normalized radiance, $\sigma_{\overline{N}}$ is the ESD for the average radiance level in the integration interval, and $\sigma_{N_{max.}}$ is the ESD of the peak radiance. However, σ_N can be expressed as follow (ref. 23):

$$\sigma_N = \frac{\sigma_N}{\sqrt{K}} \tag{C7}$$

where σ_N is the ESD in an individual radiance measurement and K is the number of independent measurements. The term, 1/ K, thus represents the statistical advantage which accrues for an increasing number of independent measurements.

It has been assumed here that individual radiance measurements are to be taken during the HDS experiment at tangent height intervals of every 0.5 km. This provides a significant statistical advantage in terms of reducing the effect of radiance error in the L4 locators, which are integrated over tangent height intervals of some 25 to 40 km. The following is a list of the tangent height intervals as determined for locators L4 (2.5) and L4 (0.5) in the Part I study, the number of individual radiance measurements to be included in each interval, and values of σ_N/σ_N:

Locator	Profile	Tangent height interval, km	No. of independent measurements, K	$\sigma_{\overline{N}}/\sigma_N$
L4 (2.5)	Mean	44.1 - 80	72	0.118
L4 (2.5)	Max.	46.3 - 80	68	0.121
Lr (2.5)	Min.	40.1 - 80	80	0.112
L4 (0.5)	Mean	55.3 - 80	50	0.141
L4 (0.5)	Max.	56.5 - 80	47	0.146
L4 (0.5)	Min.	53.2 - 80	54	0.136

It is obvious from the small size of the $\sigma_{\overline{N}}/\sigma_N$ values that the $\sigma_{\overline{N}}^2$ term in equation (C6) exerts an almost negligible influence upon the size of $\sigma^2_{\sum R_i}$, and that $\sigma^2_{\overline{N}_{max.}}$ is the predominant term for the K values considered here. If we assume that $\sigma_{N_{max.}} = \sigma_N$, we obtain the following values of $\sigma_{\sum R_i}/\sigma_N$:

Locator	Profile	$\sigma_{\sum R_i}/\sigma_N$
L4 (2.5)	Mean	1.014
L4 (2.5)	Max.	1.015
L4 (2.5)	Min.	1.013
L4 (0.5)	Mean	1.020
L4 (0.5)	Max.	1.021
L4 (0.5)	Min.	1.018

Values of σ_{R_i} were readily calculated for the assigned range of σ_N values. Then, by means of the slope relationship, R_i/km, as determined from computer analysis in the Part I study, the ESD's in tangent height were determined. The results of these calculations are shown in Figures C2 through C4.

Discussion of Results

The overall results of the parametric random error analysis for the 11 locators, clearly show a wide range of tangent height ESD's for a given value of radiance ESD. For the mean profile, the tangent height ESD's vary by a factor of 46 from the least to the most effective locator; and for the maximum profile, by a factor of 43; and for the minimum profile, by a factor of 41. For the mean profile case, the tangent height error sensitivity of the 11 locators follows this ascending order: L4 (2.5), L1 (3.0), L1 (2.0), L1 (1.0), Lr (0.5), L7, L1 (0.2), L2 (0.50), L2 (0.30), L2 (0.95), and L2 (0.06). Approximately the same order applies to the maximum and minimum profile cases.

Some important implications can be drawn from this parametric analysis regarding design goals for random radiance error. As pointed out in the earlier section of this report, "Determination of Data Sampling Requirements for Additional Locators", the time/space cell sample size can be increased to compensate for random experimental errors, thereby maintaining an estimated uncertaintiy of δ_h = 0.5 km at a 95 percent level of confidence. The scale shown in the lower right corner of Figures C2 through C4 shows the additional number of profiles, ΔN, required per sampling cell to maintain this level of confidence.

A 3 σ value of 0.01 W/m^2 - sr has been established in other project studies as the radiometer design requirement with respect to random error. Based upon this value, a set of calculations has been made to determine the equivalent error standard deviation in tangent height and ΔN, the additional samples required (profiles per cell) to compensate for the error effect. These results, which cover 11 recommended locators for the mean, minimum and maximum profile cases, are presented in Table C1. These results, which were used in making the final determination of the total sampling requirements for the various locators (discussed later), indicate that all the L2 locators are most affected by radiometer errors, along with locators L1 (0.2) and L7.

Although random error effects can be compensated for by increasing the cell samples, it is undesirable to have any sizeable error components in the HDS data sample which could be possibly eliminated by more exacting design and calibration of the radiometer. The separation of error variance from the variance of naturally occurring radiance fluctuations, although statistically possible, still represents a difficult, time-consuming and often uncertain process. For this reason, random radiance errors should be kept to a minimum.

TABLE C1.- TANGENT HEIGHT ERROR STANDARD DEVIATION AND ADDITIONAL CELL SAMPLES REQUIRED FOR AN ASSUMED RADIANCE ERROR STANDARD DEVIATION OF 0.0033 W/m^2-sr

Locator	Tangent height error standard deviation, km			ΔN, additional samples required, profiles/cell			Total no. of space/time cells, 10^3
	Mean profile	Minimum profile	Maximum profile	Mean profile	Minimum profile	Maximum profile	
L1 (3.0)	0.02	0.04	0.01	0.01	0.06	<0.01	10.0
L1 (2.0)	0.02	0.04	0.01	0.01	0.05	0.01	8.3
L1 (1.0)	0.03	0.05	0.02	0.03	0.11	0.01	7.2
L1 (0.2)	0.12	0.18	0.08	0.48	1.23	0.24	6.5
L2 (0.95)	0.27	0.32	0.25	2.66	3.69	2.18	5.3
L2 (0.50)	0.13	0.14	0.12	0.62	0.71	0.50	6.9
L2 (0.30)	0.18	0.21	0.16	1.14	1.51	0.86	6.6
L2 (0.06)	0.48	0.54	0.42	8.29	10.31	6.35	5.9
L4 (2.5)	0.01	0.01	0.01	<0.01	0.01	<0.01	5.3
L4 (0.5)	0.04	0.05	0.04	0.06	0.09	0.05	5.3
L7	0.07	0.15	0.05	0.19	0.81	0.09	7.6

PRECEDING PAGE BLANK NOT FILMED.

APPENDIX D

EFFECT OF INSTRUMENT ERROR ON DATA REQUIREMENTS - STATISTICAL ANALYSIS

PRECEDING PAGE BLANK NOT FILMED.

APPENDIX D

EFFECT OF INSTRUMENT ERROR ON DATA REQUIREMENTS - STATISTICAL ANALYSIS

This analysis is an extension of that presented in Appendix C, pp. 211 to 221 of reference 3. Detailed derivations are omitted here. The notation adopted uses a bar over a quantity such as $\bar{x}$ to indicate the ensemble average or mean of the random variable. The circumflex, e.g., $\hat{x}$, is used to designate an estimate of a random variable.

Measurements are made to determine the indicated altitude of the infrared horizon. This indicated altitude is obtained from a horizon profile, using various locators as discussed in the text. It is assumed the resultant indicated altitude x has an uncertainty ζ_1 due to the instrument and an additional independent uncertainty ζ_2 due to "nature". Hence, the ith observation x_i is given by

$$x_i = \bar{x} + \zeta_{1i} + \zeta_{2i}$$

when systematic corrections are not considered. The two cases of a zero mean instrument error and a non-zero mean instrument error are discussed separately in the following two sections.

ZERO MEAN INSTRUMENT ERROR

It is assumed that ζ_1 and ζ_2 are zero mean random variables with variances σ_1^2 and σ_1^2, respectively. An estimate of σ_1^2, $\hat{\sigma}_1^2$, is obtained prior to any flight program and this estimate has an uncertainty that is related to the variance, β^2, of $\hat{\sigma}_1^2$. That is, $\hat{\sigma}_1^2$ is a random variable with mean $\hat{\sigma}_1^2$ and variance β^2.

The available data is a sequence of independent samples, x_1, x_2 ---x_n and $\hat{\sigma}_1^2$ and β^2. From this data an estimate of $\bar{x}$, σ_2 and the uncertainty in $\bar{x}$ and σ_2 is desired. The sample mean, M_n, given by

$$M_n = \frac{1}{n} \sum_{i=1}^{n} x_i$$

is an unbiased estimate of $\bar{x}$ and this estimate has a variance $(\sigma_1^2 + \sigma_2^2)/n$. The confidence interval on this estimate then goes to zero as n goes to ∞.

The sample variance, S_n^2, is given by

$$S_n^2 = \frac{1}{n} \sum_{i=1}^{n} (x_i - M_n)^2.$$

It can be shown that

$$\langle S_n^2 \rangle = \frac{n-1}{n} (\sigma_1^2 + \sigma_2^2).$$

Let the estimate of σ_2^2, $\hat{\sigma}_2^2$, be given by

$$\hat{\sigma}_2^2 = \left(\frac{n}{n-1}\right) S_n^2 - \hat{\sigma}_1^2.$$

This estimate is unbiased since

$$\langle \hat{\sigma}_2^2 \rangle = \left\langle \left(\frac{n}{n-1}\right) S_n^2 - \hat{\sigma}_1^2 \right\rangle$$

$$= \left(\frac{n}{n-1}\right) \left(\frac{n-1}{n}\right) (\sigma_1^2 + \sigma_2^2) - \sigma_1^2 = \sigma_2^2.$$

The variance of the estimate of σ_2^2 is needed to obtain the confidence interval on σ_2.

Consider variance $(\hat{\sigma}_2^2)$,

$$\text{variance } (\hat{\sigma}_2^2) = \left\langle \left[\sigma_2^2 - \left(\frac{n}{n-1} S_n^2 - \hat{\sigma}_1^2\right) \right]^2 \right\rangle.$$

It should be noted that S_n and $\hat{\sigma}_1$ are independent random variables since S_n is obtained from in-flight measurements and $\hat{\sigma}_1$ is obtained from pre-flight measurements. It should also be remembered that σ_2 is fixed, a real number, although it is not known.

Expanding the indicated expected value gives

$$\text{variance } (\hat{\sigma}_2^{\,2}) = \sigma_2^{\,4} - 2\sigma_2^{\,2} \frac{n}{n-1} \langle S_n^{\,2} \rangle + 2\sigma_2^{\,2} \langle \hat{\sigma}_1^{\,2} \rangle$$

$$+ \left(\frac{n}{n-1}\right)^2 \langle S_n^{\,4} \rangle - 2 \frac{n}{n-1} \langle \hat{\sigma}_1^{\,2} \rangle \langle S_n^{\,2} \rangle + \langle \hat{\sigma}_1^{\,4} \rangle .$$

It can be shown that

$$\langle \hat{\sigma}_1^{\,2} \rangle = \sigma_1^{\,2}$$

$$\langle \hat{\sigma}_1^{\,4} \rangle = \beta^2 + \sigma_1^{\,4}$$

and

$$\left(\frac{n}{n-1}\right)^2 \langle S_n^{\,4} \rangle = \frac{1}{n} (\mu_{41} + \mu_{42}) + \frac{n^2 - 2_n + 3}{n(n-1)} (\sigma_1^{\,4} + \sigma_2^{\,4}) + \frac{2(n+1)}{n-1} \sigma_1^{\,2} \sigma_2^{\,2}$$

where μ_{41} and μ_{42} are the forth moments about the mean of ζ_1 and ζ_2, respectively.

Therefore,

$$\text{variance } (\hat{\sigma}_2^{\,2}) = \frac{1}{n} (\mu_{41} + \mu_{42}) + \beta^2 - \frac{n-3}{n(n-1)} (\sigma_1^{\,4} + \sigma_2^{\,4}) + \frac{4}{n-1} \sigma_1^{\,2} \sigma_2^{\,2}.$$

If ζ_1 and ζ_2 are assumed gaussian then

$$\mu_{41} = 3\sigma_1^{\,4}$$

$$\mu_{42} = 3\sigma_2^{\,4}$$

and the above reduces to

$$\text{variance } (\hat{\sigma}_2^{\,2}) = \frac{2(\sigma_1^{\,2} + \sigma_2^{\,2})^2}{n-1} + \beta^2$$

It should be remembered that β is known but σ_1 and σ_2 are not. If the estimates of σ_1 and σ_2 are used, then the estimate of variance $(\hat{\sigma}_2^2)$ becomes

$$\text{variance } (\hat{\sigma}_2^2) = \left(\frac{2}{n-1}\right) (\hat{\sigma}_1^2 + \hat{\sigma}_2^2)^2 + \beta^2$$

The expected value of this estimate is

$$\text{variance } (\hat{\sigma}_2^2) = \text{variance } (\hat{\sigma}_2^2) + \frac{4}{n-1} \left[\frac{(\sigma_1^2 + \sigma_2^2)^2}{n-1} + \beta^2 \right]$$

The estimate is, therefore, biased with a bias

$$\left[4/(n-1)\right] \left[(\sigma_1^2 + \sigma_2^2)^2/(n-1) + \beta^2 \right]$$

which is equal to

$$\left[2/(n-1)\right] \left[\text{variance } (\hat{\sigma}_2^2) + \beta^2 \right]$$

which goes to zero as n gets large.

Let us consider a numerical example,

$\bar{x}$	= 30		
σ_2	= 0.5,	σ_2^2	= 0.25
σ_1	= 0.2,	σ_1^2	= 0.04
β	= 0.01,	β^2	= 0.0001

In this case the standard deviation in our apriori estimate of σ_1^2 is 0.01.

The standard deviations and mean values of the estimated quantities are tabulated below for various values of n.

n	$\bar{x}$		σ_2^2		variance $(\hat{\sigma}_2^2)$	
	mean	s. d.	mean	s. d.	mean	bias
10	30	0. 17	0. 25	0. 137	0. 0187	0. 0042
20	30	0. 12	0. 25	0. 094	0. 0089	0. 00095
50	30	0. 076	0. 25	0. 059	0. 0034	0. 000143
100	30	0. 054	0. 25	0. 043	0. 0017	0. 0000364
	30	0	0. 25	0. 01	0. 0001	0

It should be noted that the standard deviation of $\bar{x}$ and the bias on variance $(\hat{\sigma}_2^2)$ go to zero as n goes to ∞ but the other quantities do not. If β were zero the standard deviation of σ_2^2 would go to zero as n goes to infinity.

Consider now the case when a systematic variation in x (as a function of t for example) is removed. Let the systematic variation be represented by a series of functions, ϕ_i (t), or the normal over the n samples. That is

$$\sum_{k=1}^{M} \phi_i (t_k) \, d_j (t_\beta) = \zeta_{ij}$$

The correction series is

$$\sum_{i=1}^{M} a_i \, \phi_i (t)$$

where

$$a_i = \sum_{k=1}^{n} x (t_k) \, \phi_i (t_k).$$

The above a_i is an unbiased estimate of the true correction coefficient $\bar{a}_i$, that is

$$\langle a_i \rangle = \bar{a}_i$$

The variance of this estimate is,

$$\text{variance } (a_i) = \sigma_1^2 + \sigma_2^2$$

and is independent of n as long as the normality of the basis functions is maintained.

The residual, r, is the variation in x that remains after the systematic variation is removed, that is

$$r^2 = \sum_{k=1}^{n} \left[x(t_k) - \sum_{i=1}^{m} a_i \phi_i (t_k) \right]^2 .$$

It can be shown that

$$\langle r^2 \rangle = (n-m) (\sigma_1^2 + \sigma_2^2).$$

An unbiased estimate of σ_2^2 is, therefore,

$$\hat{\sigma}_2^2 = \frac{r^2}{n-m} - \hat{\sigma}_1^2 .$$

For ζ_1 and ζ_2 gaussian the variance of this estimate becomes

$$\text{variance } (\hat{\sigma}_2^2) = \frac{2(\sigma_1^2 + \sigma_2)^2}{n-m} + \beta^2 .$$

To obtain confidence intervals on $\hat{\sigma}_2^2$, Chebychev's inequality is applied to obtain

$$\text{probability} \left\{ \left| \hat{\sigma}_2^2 - \sigma_2^2 \right| \geq \gamma \right\} \leq \frac{\text{variance } (\hat{\sigma}_2^2)}{\gamma^2}$$

If p is the per unit error in σ_2^2 the confidence interval on σ_2 is defined as

$$I_c = (\sqrt{1+p} - \sqrt{1-p}) \sigma_2$$

and it is clear that

$$\text{probability } (\sigma_2 \text{ is } \underline{\text{not}} \text{ on the confidence interval } I_c)$$

$$= \text{ probability } \left\{ \left| \hat{\sigma}_2^{\,2} + \sigma_2^{\,2} \right| \geq p\ \sigma_2^{\,2} \right\}$$

Using this with the expression for variance $(\hat{\sigma}_2^{\,2})$ in the above

$$1 - \frac{P}{100} \leq \left[\frac{2\,(\sigma_1^{\,2} + \sigma_2^{\,2})^2}{n-m} + \beta^2 \right] \Big/ \ p^2 \sigma_2^{\,4}$$

where p is the probability that $\hat{\sigma}_2$ is in the confidence interval.

Therefore, for fixed percent confidence P

$$p \leq \left[\frac{2\,(\sigma_1^{\,2} + \sigma_2^{\,2})^2 + (n-m)\,\beta^2}{(n-m)\ \sigma_2^{\,4}\ (1-P/100)} \right]^{1/2}$$

If P is small an approximate expression for the confidence interval is

$$I_c = p\,\sigma_2$$

so finally

$$I_c \leq \left\{ \frac{2\left[1 + \left(\frac{\sigma_1}{\sigma_2}\right)^2\right]^2 + (n-m)\left(\frac{\beta}{\sigma_2^{\,2}}\right)^2}{(n-m)\ (1 - P/100)} \right\}^{1/2} \sigma_2$$

If σ_2 is assumed gaussian the confidence interval for $P = 95$ becomes

$$I_c = \frac{2\sqrt{2}}{\sqrt{n-m}} \left[1 + \frac{\sigma_1}{\sigma_2} \right)^2 + (n-m)\left(\frac{\beta}{\sigma_2^{\,2}}\right)^2 \Bigg]^{1/2} \sigma_2$$

If n_0 samples gives a confidence I_c when there is no instrument error ($\sigma_1 = \beta = 0$) then to obtain the same confidence interval with an instrument error the number of samples needed is given by n,

$$n = \frac{(n_0 - m)\left[1 + \frac{\sigma_1^2}{\sigma_2^2}\right]^2}{1 - \frac{\beta^2}{\sigma_2^4}(n_0 - m)} + m$$

In the special case when σ_1 is known exactly, that is $\beta = 0$, this becomes

$$n = (n_0 - m)\left[1 + \frac{\sigma_1^2}{\sigma_2^2}\right]^2 + m = n_0\left[1 + \frac{\sigma_1^2}{\sigma_2^2}\right] = 2m\frac{\sigma_1^2}{\sigma_2^2}\left(1 - \frac{\sigma_1^2}{2\sigma_2^2}\right)$$

Let us consider some numerical examples. Let $\beta = 0$, then the following table is obtained for the expression for n.

$\frac{\sigma_1}{\sigma_2}$	$m = 1$	$m = 3$	$m = 10$
0.1	$1.02\ n_0 - 0.02$	$1.02\ n_0 - 0.06$	$1.02\ n_0 - 0.2$
0.5	$1.56\ n_0 - 0.44$	$1.56\ n_0 - 1.3$	$1.56\ n_0 - 4.4$
1.0	$4\ n_0 - 1$	$4\ n_0 - 3$	$4\ n_0 - 10$

In the example previously used,

$\bar{x} = 30$

$\sigma_2 = 0.5$ $\qquad$ $\sigma_2^2 = 0.25$

$\sigma_1 = 0.2$ $\qquad$ $\sigma_1^2 = 0.04$

$\beta = 0.01$ $\qquad$ $\beta^2 = 0.0001$

and with $m = 10$

The equation for n becomes

$$n = \frac{(n_0 - 10)\ (1.35)}{1 - 0.0016\ (n_0 - 10)} + 10$$

Tabulating the above gives

n_0	n
20	24
50	68
100	152
200	379

It is clear that when

$$\frac{\beta^2}{\sigma_2^4} \quad (n_0 - m) = 1$$

n goes to infinity. This means that a small confidence interval attainable with no instrument error is not attainable with an uncertainty in the spread of the instrument error. That is, for $\beta > 0$, the limit on the confidence interval occurs when

$$n_0 = \frac{\sigma_2^4}{\beta^2} + m$$

i.e., the minimum attainable confidence interval is

$$I_c\ (\min) = \frac{2\sqrt{2\beta}}{\sigma_2}$$

NON-ZERO INSTRUMENT ERROR

The instrument may cause an uncertainty in the indicated altitude that has a non-zero mean. In this case let m, be the bias in the indicated altitude due to the instrument and δ, be the zero mean uncertainty due to the instrument. Therefore, the observed altitude at the ℓth observation is

$$x_\ell = \bar{x} + m_1 + \delta_{1\ell} + \delta_{2\ell}$$

Prior to any flight the ensemble statistics on the m, are determined and assume it has a mean $\hat{m}$, and a variance α. These are analogous to δ^2, and β^2, the a-priori information about the distribution of δ_1.

If M_n, is the sample mean, then an unbiased estimate of the true indicated altitude, $\bar{x}$, is

$$\hat{\bar{x}} = M_n - \hat{m},$$

The variance of M_n is

$$\mathrm{Var}(M_n) = \langle (M_n - \bar{x} - m_1)^2 \rangle = \frac{1}{n} (\sigma_1^2 + \sigma_2)^2$$

and the variance of $\hat{\bar{x}}$ is

$$\mathrm{Var}(x) = \langle (\hat{\bar{x}} - \bar{x})^2 \rangle = \frac{1}{n} (\sigma_1^2 + \sigma_2^2) + \alpha$$

Note that the uncertainty in $\bar{x}$ does not go to zero as the number of samples but rather approaches the uncertainty in the a-priori estimate of the instrument bias.

The statistics of the estimate of σ_2^2 remain unchanged with the addition of this instrument bias.

If x has a systematic variation with time, for example, $x = x(t)$ and this variation is corrected using orthonormal basis functions the following occurs: The correction coefficients, a_i^m, are made up of two parts, a_{ix} that due to the variations in nature and a_{im}, that due to the variation in the bias due to instrument error. It can be shown that

$$A_{ix} = \sum_k \phi_i (t_k) \bar{x} (t_k)$$

$$A_{im} = \sum_k \phi_i (t_k) m_i (t_k)$$

An unbiased estimate of A_{ix} , the desired correction coefficient is,

$$\hat{A}_{ix} = \sum_k \left[x (t_k) - m_1 (t_k) \right] \phi_i (t_k)$$

The variance of this estimate, Var $(\hat{A}_{ix})$, is, .

$$\text{Var} (\hat{A}_{ix}) = \langle (A_{ix} - \hat{A}_{ix} - \hat{A}_{ix})^2 \rangle$$

$$= \sigma_1^2 + \sigma_2^2 + \alpha$$

That is, the correction coefficients have an additional uncertainty that is the uncertainty in our a-priori knowledge of the bias due to the instrument.

It should be noted that it was assumed that the bias is a function of time and space. Hence an analysis should be performed to determine the bias a-priori in each time-space cell. It was also assumed that the uncertainty in the estimate of this bias did not change from one cell to another, α = constant. If α is not a constant an average value of α is suitable in the preceeding equations.

As before the estimate of the uncertainty in the corrected indicated altitude is not affected by the bias. Therefore, the existence of the bias does not change the sampling requirements since these were based on the estimate of uncertainty.

The existence of the bias does require some mathematical exercises to determine ensemble averages of the bias as a function of time and space, $\hat{m}_1$ (t) . This can be done using Monte-Carlo techniques on classes of radiance profiles peculiar to a given space time cell. An estimate of α should be obtained at the same time.

The most that can be known prior to any flight (as regards effect of instrument error) is

$\hat{m}_1$ (t) - average bias due to instrument as function of time and space.

α - uncertainty in $\hat{m}$.

$\hat{\sigma}_1^2$ - uncertainty, due to instrument, in the indicated altitude.

β^2 - uncertainty of $\hat{\sigma}_1^2$.

On a given flight m_1 will be fixed, i.e. only one ensemble member will be chosen, and the Var $(\hat{\bar{x}})$ and Var $(\hat{A}_{iz})$ will not be $\frac{i}{n}(\sigma_1^2 + \sigma_2^2) + \alpha$ or $\sigma_1^2 + \sigma_2^2 + \beta$ but rather some number for which the above constitute an ensemble average. That is, if many flights were performed then Var $(\hat{\bar{x}})$ and Var $(\hat{A}_{ix})$ would in fact be these quantities. Since only one flight will be used to ascertain the desired information $\frac{1}{n}(\sigma_1^2 + \sigma_2^2) + \alpha$ and $\sigma_1^2 + \sigma_2^2 + \alpha$ represent the best estimate of the Var $(\hat{\bar{x}})$ and Var $(\hat{A}_{ix})$, respectively.

Also since δ_1 varies from measurement to measurement in a given flight program the estimate of σ_2 and confidence intervals on σ_2 are as given and will be the same for any flight programs with a similar instrument. In summary:

1. The uncertainity in the corrected indicated altitude and the uncertainity in the correction coefficients may vary from flight to flight due to the a-priori uncertainity in the instrument caused bias.

2. The estimate of correction coefficients, mean corrected indicated altitude, uncertainity in the corrected indicated altitude due to nature (σ_2) , and the confidence interval on σ_2 should not vary from one flight to another when performed under similar conditions.

APPENDIX E

PROFILES, ERRORS, LOCATORS, AND COMPUTATIONS

APPENDIX E

PROFILES, ERRORS, LOCATORS, AND COMPUTATIONS

This appendix contains listings of profiles, errors, locators, and computations used in determining radiometer-caused errors.

PROFILES

Table E1, called "Profile Set B."

LOCATORS

Locators and input constants to be used are L1 (2.0), L1 (3.0), L2 (0.15), L2 (0.9), L3 (4.5), L3 (20), L4 (2.5), and L4 (10.0).

ERRORS

Error Type 1-Calibration Scale Error

Multiply all radiance values by $(1 + \Delta N/N)$

1 a $\frac{\Delta N}{N} = 0.004$

1 b $\frac{\Delta N}{N} = 0.01$

1 c $\frac{\Delta N}{N} = 0.02$

1 d $\frac{\Delta N}{N} = 0.05$

Error Type 2 - Calibration Bias Error

Add ΔN to all radiance values

2 a $\Delta N = 0.001$

2 b $\Delta N = 0.004$

2 c $\Delta N = 0.01$

2 d $\Delta N = 0.04$

Error Type 3 - Drift Scale Error

Multiply radiance values by $(1 + \Delta N/N)$

$\Delta N/N$ is selected from gaussian distributions of zero mean with standard deviations given below.

$\Delta N/N$ is selected once for each profile; within a given profile it remains constant but it changes from profile to profile.

3a	$\Delta N/N = 0.004$	Standard deviations of gaussian distributions from which the value of $\Delta N/N$ is selected.
3b	$\Delta N/N = 0.01$	
3c	$\Delta N/N = 0.02$	
3d	$\Delta N/N = 0.05$	

Error Type 4 - Drift Bias Error

Add ΔN to all radiance values.

ΔN is selected from gaussian distributions with zero mean with standard deviations given below.

ΔN is selected once for each profile; within a given profile it remains constant but changes from profile to profile.

4a	$\Delta N = 0.001$	Standard deviations of gaussian distributions from which the value of ΔN is selected.
4b	$\Delta N = 0.004$	
4c	$\Delta N = 0.01$	
4d	$\Delta N = 0.04$	

Error Type 5 - Noise Scale Error

Multiply all radiance values by $(1 + \Delta N/N)$

$\Delta N/N$ is selected from gaussian distributions of zero mean with standard deviations given below.

$\Delta N/N$ is selected once for each radiance value on each profile; i.e., it changes from point to point.

5a	$\Delta N/N = 0.004$	Standard deviation of gaussian distributions from which the value of $\Delta N/N$ is selected.
5b	$\Delta N/N = 0.01$	
5c	$\Delta N/N = 0.02$	
5d	$\Delta N/N = 0.05$	

Error Type 6 - Noise Bias Error

Add ΔN to all radiance values.

ΔN is selected from gaussian distributions with zero mean and standard deviations given below.

ΔN is selected once for each radiance value on each profile; i.e., it changes from point to point.

6a	$\Delta N = 0.001$	Standard deviation of gaussian distributions from which the value of ΔN is selected.
6b	$\Delta N = 0.004$	
6c	$\Delta N = 0.01$	
6d	$\Delta N = 0.04$	

COMPUTATIONS

For each of the 24 error values, and for the case where $\frac{\Delta N}{N} = \Delta N = 0$ (reference) perform the following computations

A. Modify Profile Set B as indicated.

B. Compute located horizons, h_1, for the specified locators.

C. Compute the following:

1. $\bar{h}_1$, σ_{h_1}, $(h_{1\,max.} - h_{1\,min})$

2. Δh_1, $\sigma_{\Delta h_1}$, $\Delta h_{1\,max.}$, $\Delta h_{1\,min}$

3. $\bar{\theta}$, σ_θ, $(\theta_{max.} - \theta_{min})$

4. $\overline{\Delta\theta}$, $\sigma_{\Delta\theta}$, $\Delta\theta_{max.}$, $\Delta\theta_{min}$

where the following definitions apply

$$\bar{h}_1 = \frac{1}{n} \sum h_{1_i}$$

$$\sigma_{h_1} = \left[\frac{1}{n} \sum (h_{1_i} - \bar{h}_1)^2 \right]^{1/2}$$

h_{1_i} = located horizon for a given locator for the ith profile.

$$\Delta h_{1_i} = h_{1_i} (\epsilon) - h_{1_i} (\epsilon = 0)$$

h_{1_i} (ϵ) is the value of located horizon for the ith profile with ϵ = the specified value of $\Delta N/N$ or ΔN.

$$\Delta\bar{h}_1 = \frac{1}{n} \sum \Delta h_{1_i}$$

$$\sigma_{\Delta h_1} = \left[\frac{1}{n} \sum (\Delta h_{1_i} - \Delta\bar{h}_1)^2 \right]^{1/2}$$

$$\theta_i = \left[h_{1_i} - h_{1_{i+1}} \right] \left[\frac{1}{2} \times 0.0225 \right] \qquad i = 1, 3, 5--$$

$$\bar{\theta} = \frac{1}{n} \sum \theta_i$$

$$\sigma_\theta = \left[\frac{1}{n} \sum (\theta_i - \bar{\theta})^2 \right]^{1/2}$$

$$\Delta\theta_i = \left[\Delta h_{1_i} - \Delta h_{1_{i+1}} \right] \left[\frac{1}{2} \times 0.0225 \right] \qquad i = 1, 3, 5--$$

$$\Delta\bar{\theta} = \frac{1}{n} \sum \Delta\theta_i$$

$$\sigma_{\Delta\theta} = \left[\frac{1}{n} \sum (\Delta\theta_i - \Delta\bar{\theta})^2 \right]^{1/2}$$

Identify, by profile identification number, the profile or profile set for which maximum and minimum values of h_1, Δh, θ, and $\Delta\theta$ occur.

Suggested Output Format. --

Line no.	Run	Error	h_1	h_1	Δh_1	Δh_1	θ	θ	$\Delta\theta$	$\Delta\theta$
1	1	Type	Mean	σ	Mean	σ	Mean	σ	Mean	σ
2	1	Value	Max.	Min	Max.	Min	Max.	Min	Max.	Min
3	1	———	ID	ID	ID	ID	ID	ID	ID	ID
Skip line										
1	2									
2	2				1					
3	2									
1	25									
2	25				1					
3	25									

TABLE E1. - PROFILE SET B

Pair no.	i	Profile no.	Lat	Long.	Time
1	1	01010001	63.75	165	April 8
	2	01010020	41.25	105	
2	3	01030001			Aug. 12
	4	01030020			
3	5	01040001			Oct. 21
	6	01040020			
4	7	01070001			Jan. 20
	8	01070020			
5	9	01010002	52.5	165	April 8
	10	01010031	63.75	90	
6	11	01030002			Aug. 12
	12	01030031			
7	13	01040002			Oct. 21
	14	01040031			
8	15	01070002			Jan. 20
	16	01070031			
9	17	01010003	75	150	April 8
	18	01010049	48.75	75	
10	19	01030003			Aug. 12
	20	01030049			
11	21	01040003			Oct. 21
	22	01040049			
12	23	01070003			Jan. 20
	24	01070049			
13	25	01010005	45	150	April 8
	26	01010022	26.25	105	
14	27	01030005			Aug. 12
	28	01030022			

TABLE E1. - PROFILE SET B - Continued

Pair no.	i	Profile no.	Lat	Long.	Time
15	29	01040005			Oct. 21
	30	01040022			
16	31	01070005			Jan. 20
	32	01070022			
17	33	01010006	30	150	April 8
	34	01010018	56.75	105	
18	35	01030006			Aug. 12
	36	01030018			
19	37	01040006			Oct. 21
	38	01040018			
20	39	01070006			Jan. 20
	40	01070018			
21	41	01010008	37.5	135	April 8
	42	01010040	26.25	90	
22	43	01030008			Aug. 12
	44	01030040			
23	45	01040008			Oct. 21
	46	01040040			
24	47	01070008			Jan. 20
	48	01070040			
25	49	01010010	75	120	April 8
	50	01010056	45	60	
26	51	01030010			Aug. 12
	52	01030056			
27	53	01040010			Oct. 21
	54	01040056			
28	55	01070010			Jan. 20
	56	01070056			
29	57	01010013	45	120	April 8
	58	01010043	15	90	

TABLE E1. - PROFILE SET B - Continued

Pair no.	i	Profile no.	Lat	Long.	Time
30	59	01030013			Aug. 12
	60	01030043			
31	61	01040013			Oct. 21
	62	01040043			
32	63	01070013			Jan. 20
	64	01070043			
33	65	01010014	37.5	120	April 8
	66	01010052	26.25	75	
34	67	01030014			Aug. 12
	68	01030052			
35	69	01040014			Oct. 21
	70	01040052			
36	71	01070014			Jan. 20
	72	01070052			
37	73	01010016	15	120	April 8
	74	01010035	45	90	
38	75	01030016			Aug. 12
	76	01030035			
39	77	01040016			Oct. 21
	78	01040035			
40	79	01070016			Jan. 20
	80	01070035			
41	81	01010046	3.75	90	April 8
	82	01010050	41.25	75	
42	83	01030046			Aug. 12
	84	01030050			
43	85	01040046			Oct. 21
	86	01040050			
44	87	01070046			Jan. 20
	88	01070050			

TABLE E1. - PROFILE SET B - Concluded

Pair no.	i	Profile no.	Lat	Long.	Time
45	89	01010027	78.75	90	April 8
	90	01010037	37.5	90	
46	91	01030027			Aug. 12
	92	01030037			
47	93	01040027			Oct. 21
	94	01040037			
48	95	01070027			Jan. 20
	96	01070037			
49	97	01010036	41.25	90	April 8
	98	01010047	0	90	
50	99	01030036			Aug. 12
	100	01030047			
51	101	01040036			Oct. 21
	102	01040047			
52	103	01070036			Jan. 20
	104	01070047			
53	105	01010042	18.75	90	April 8
	106	01010048	56.25	75	
54	107	01030042			Aug. 12
	108	01030048			
55	109	01040042			Oct. 21
	110	01040048			
56	111	01070042			Jan. 20
	112	01070048			
57	113	01010024	90	90	April 8
	114	01010019	48.75	105	
58	115	01030024			Aug. 12
	116	01030019			
59	117	01040024			Oct. 21
	118	01040019			
60	119	01070024			Jan. 20
	120	01070019			

PRECEDING PAGE BLANK NOT FILMED.

APPENDIX F

PARAMETRIC ERROR ANALYSIS - PLOTTED RESULTS

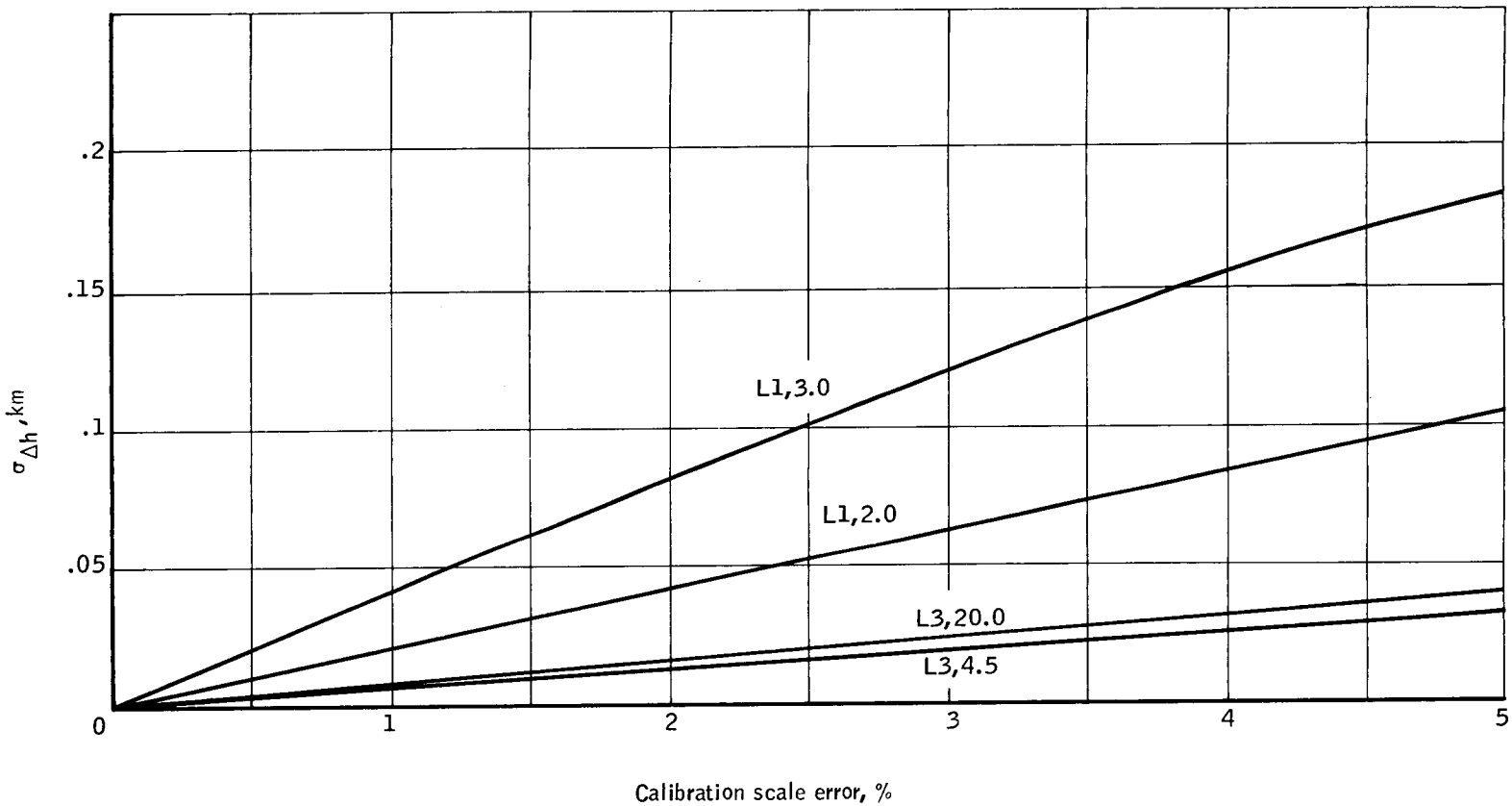

Figure F1. Located Horizon Error Standard Deviation Caused by Instrument Calibration Scale

PRECEDING PAGE BLANK NOT FILMED

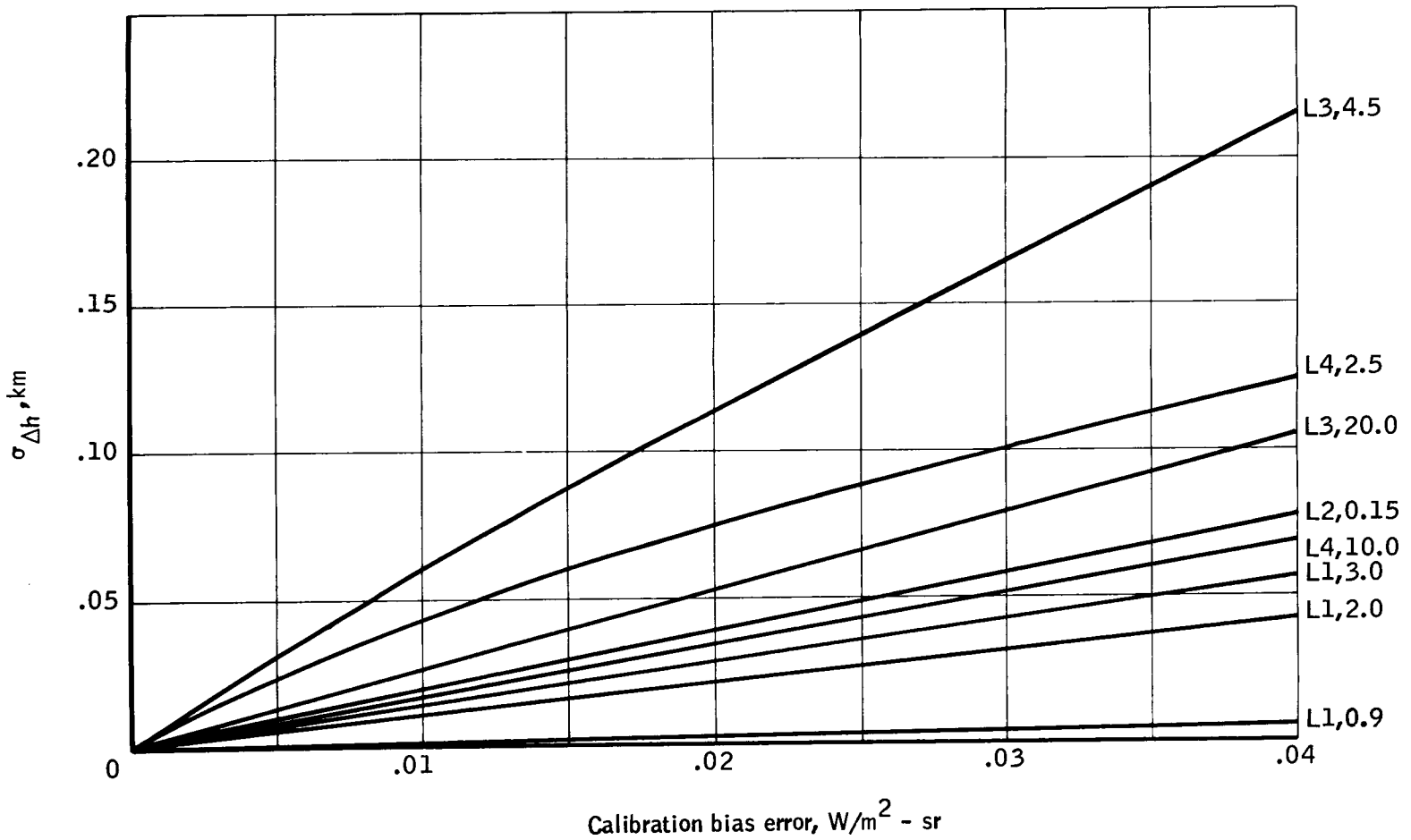

Figure F2. Located Horizon Error Standard Deviation Caused by Instrument Calibration Bias

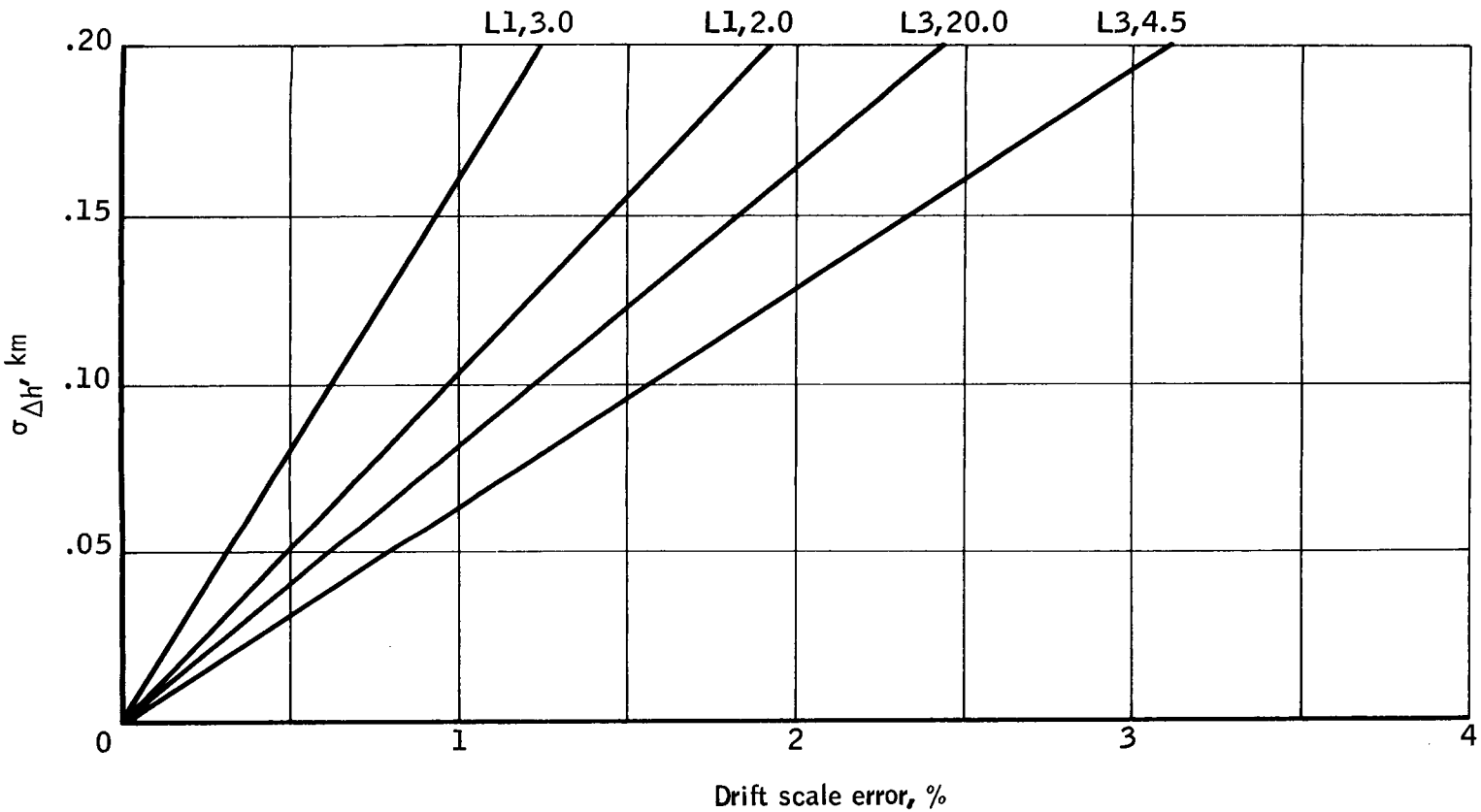

Figure F3. Located Horizon Error Standard Deviation Caused by Instrument Scale Drift

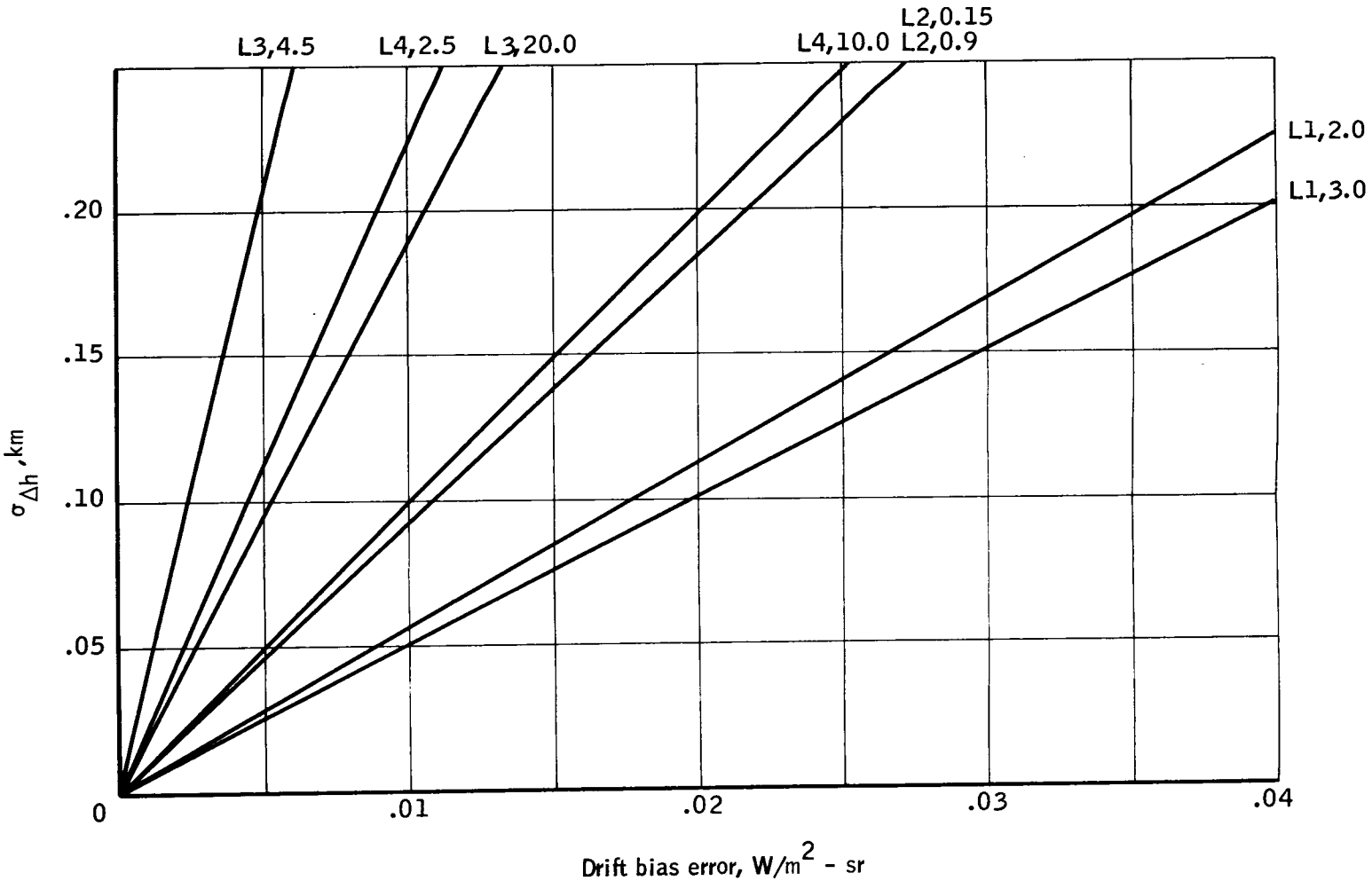

Figure F4. Located Horizon Error Standard Deviation Caused by Instrument Bias Drift

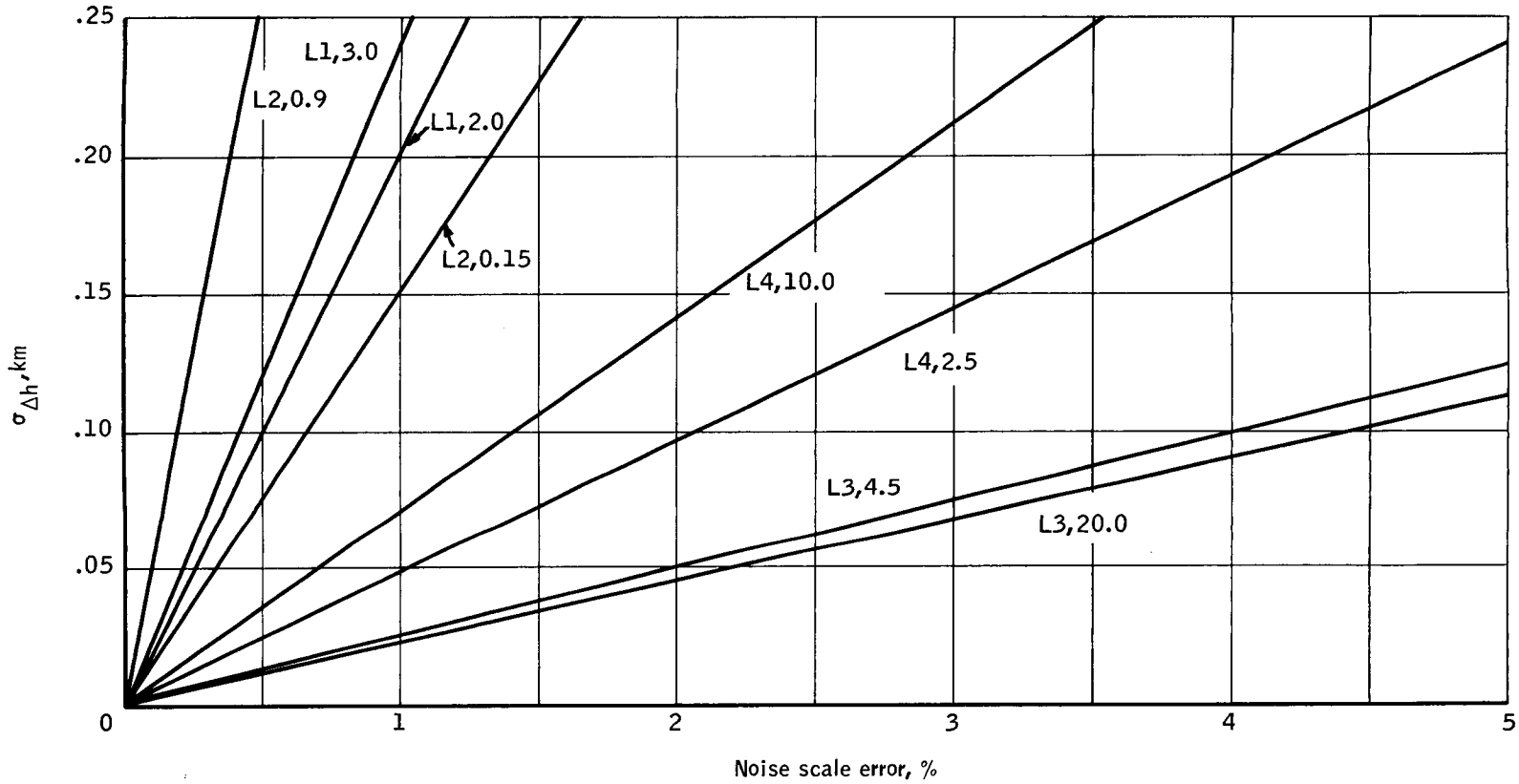

Figure F5. Located Horizon Error Standard Deviation Caused by Instrument Scale Noise

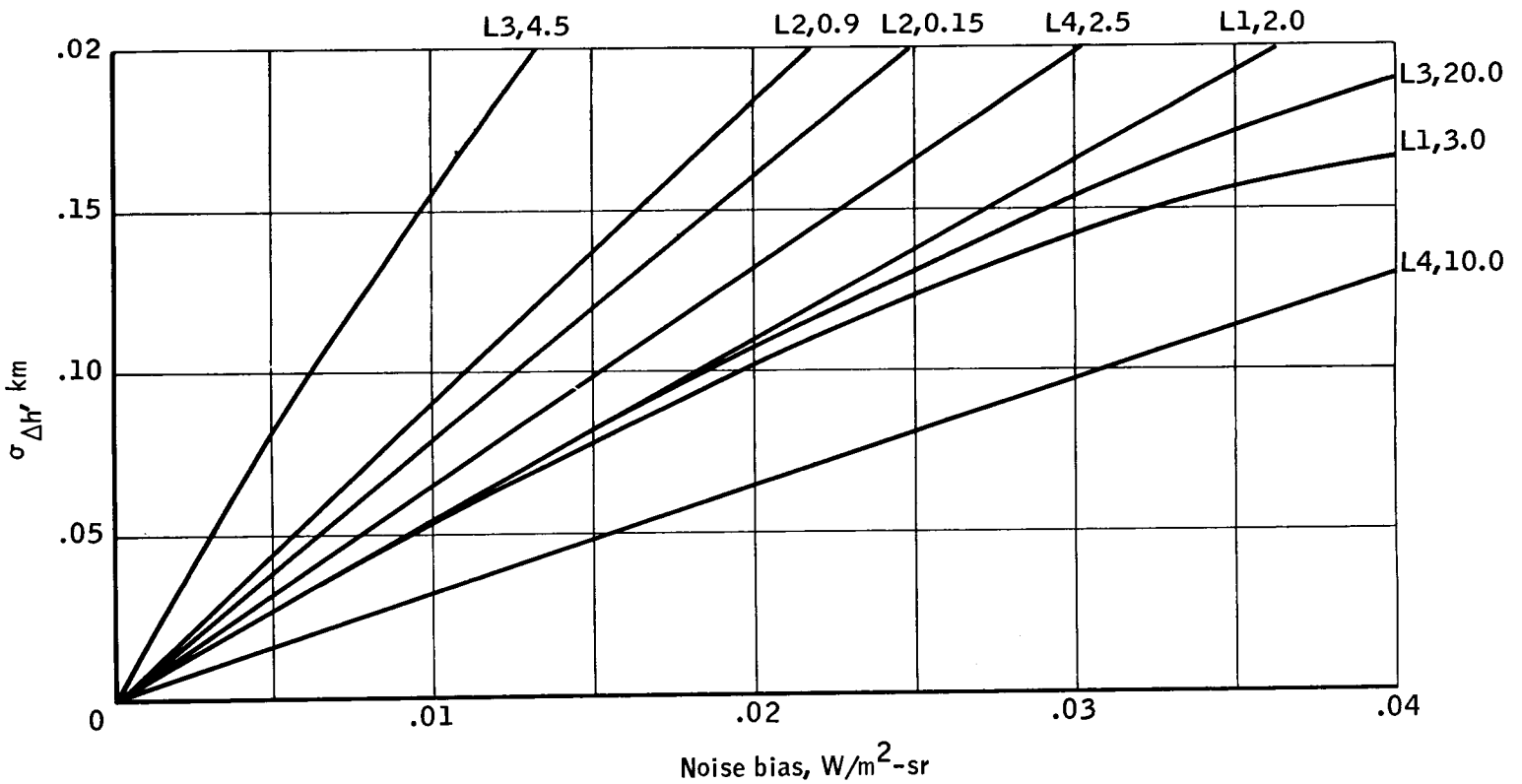

Figure F6. Located Horizon Error Standard Deviation Caused by Instrument Bias Noise

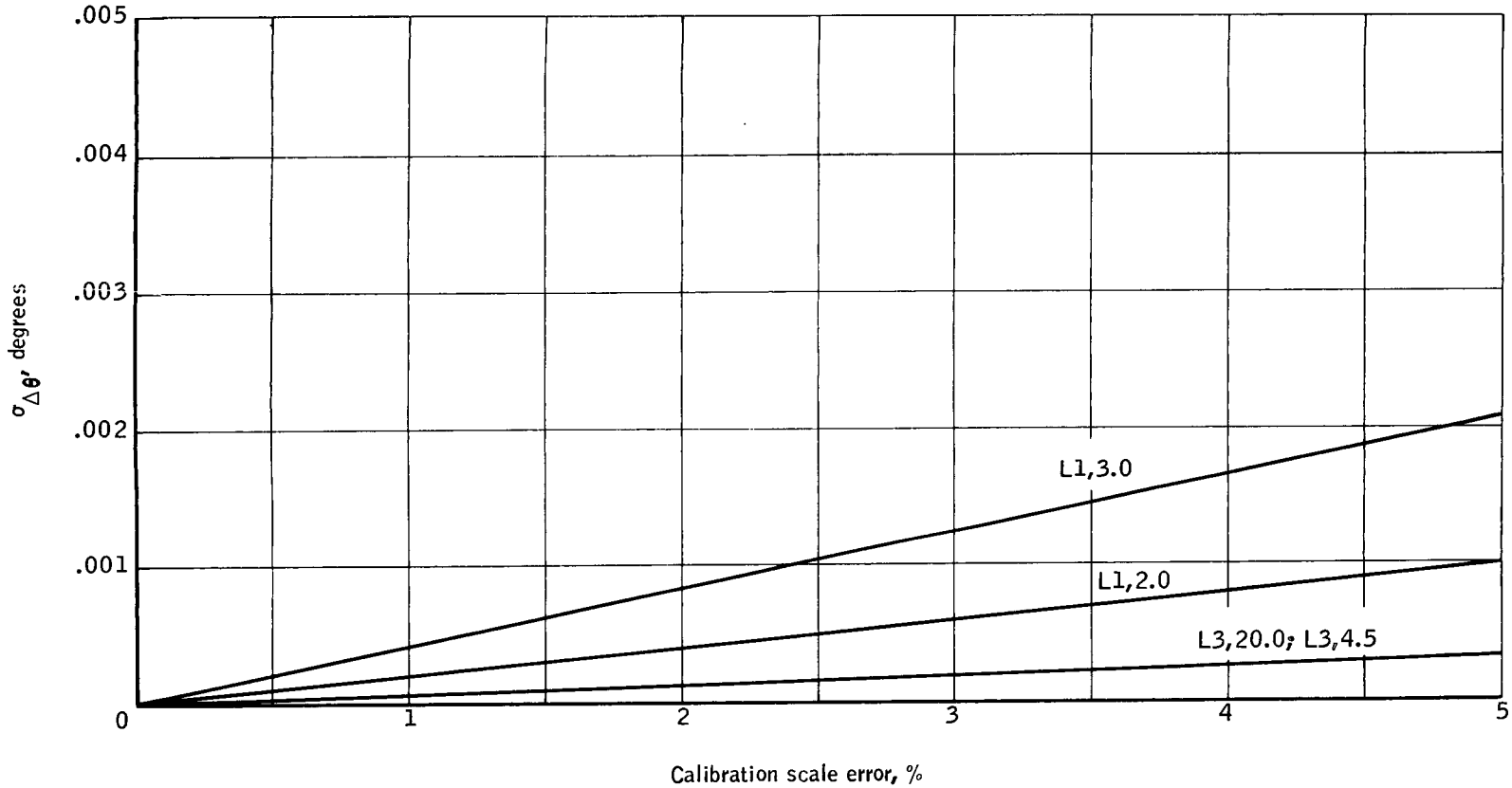

Figure F7. Local Vertical Error Standard Deviation Caused by Instrument Scale Calibration Error

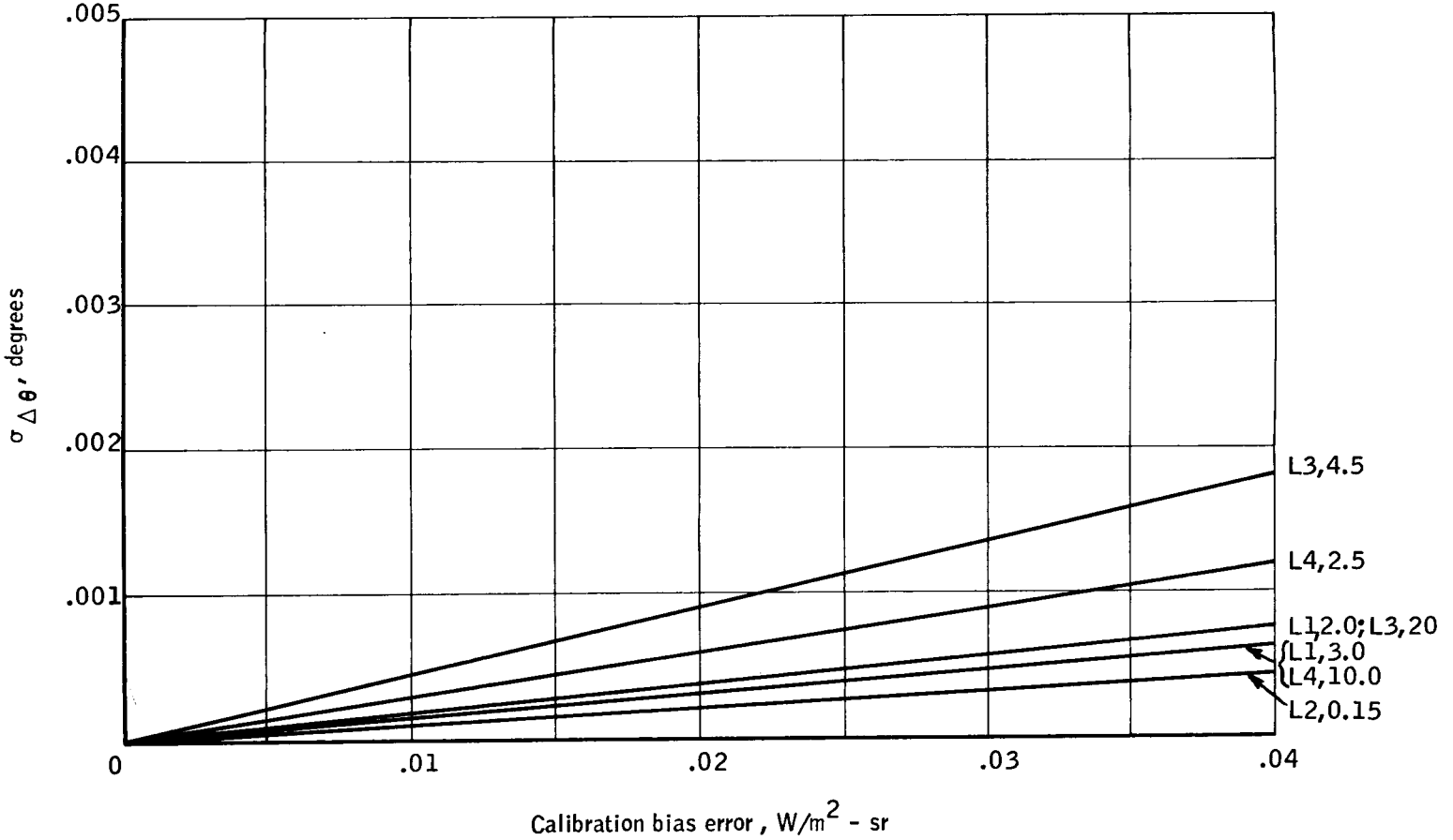

Figure F8. Local Vertical Error Standard Deviation Caused by Instrument Calibration Bias Error

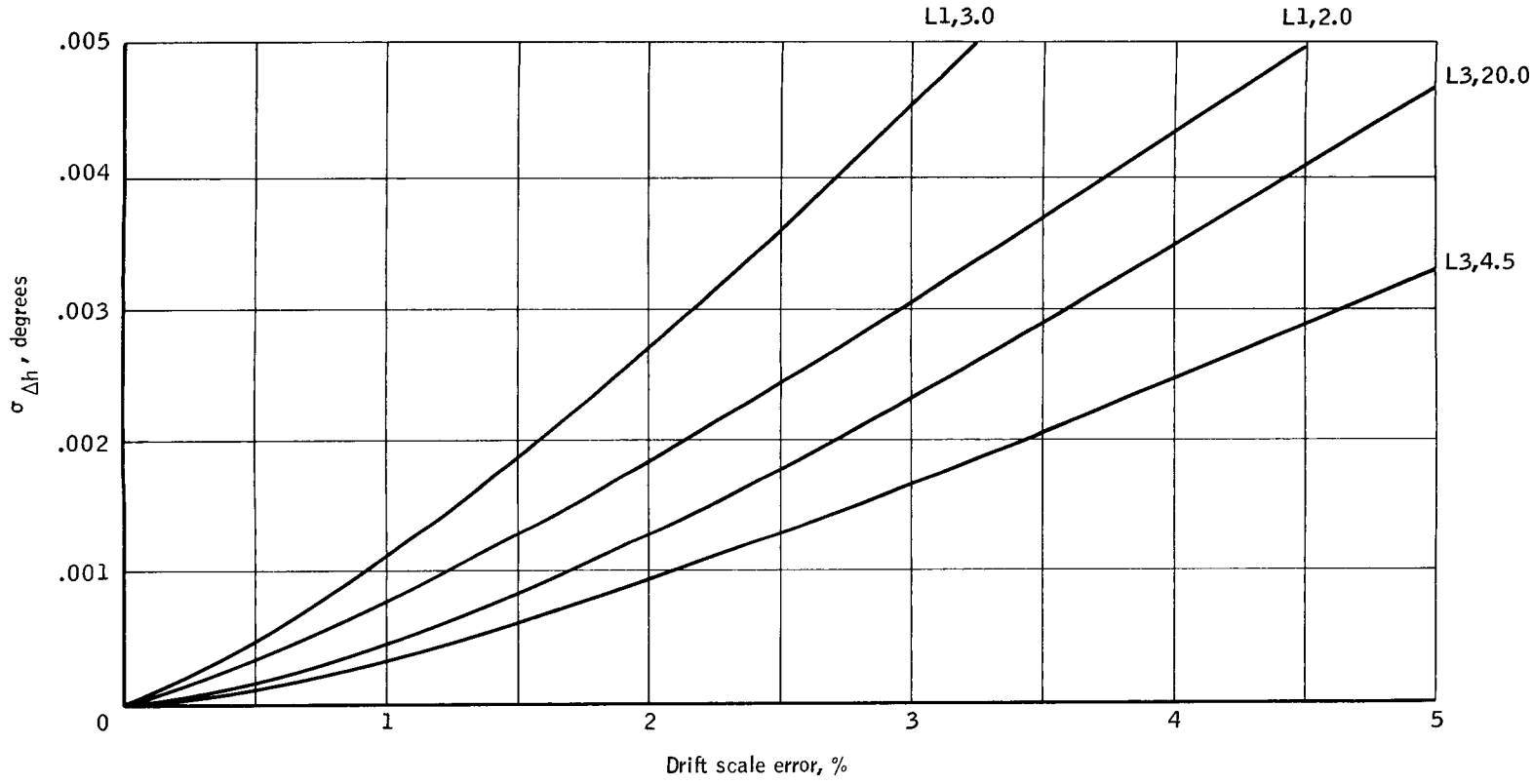

Figure F9. Local Vertical Error Standard Deviation Caused by Instrument Scale Drift

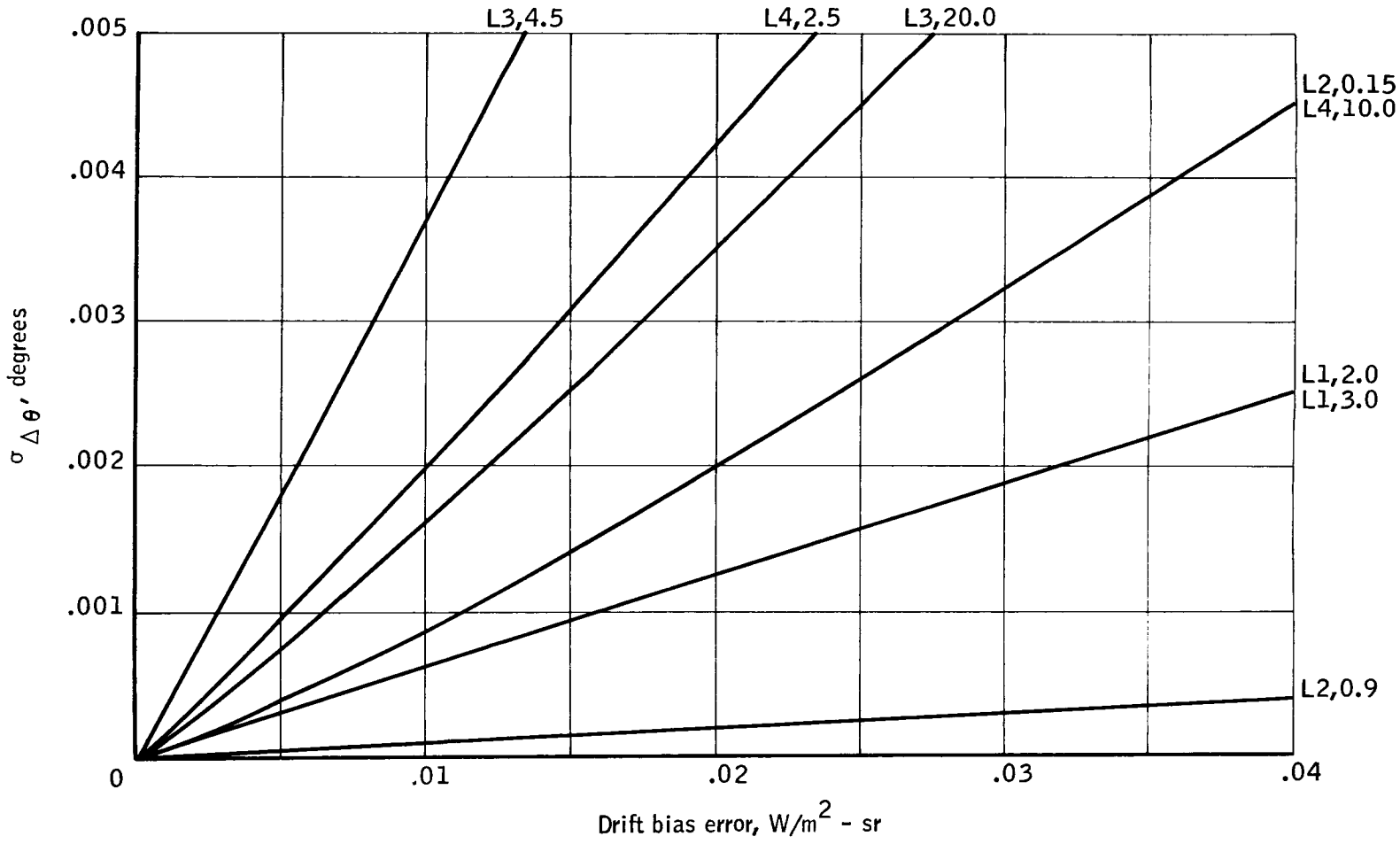

Figure F10. Local Vertical Error Standard Deviation Caused by Instrument Bias Drift

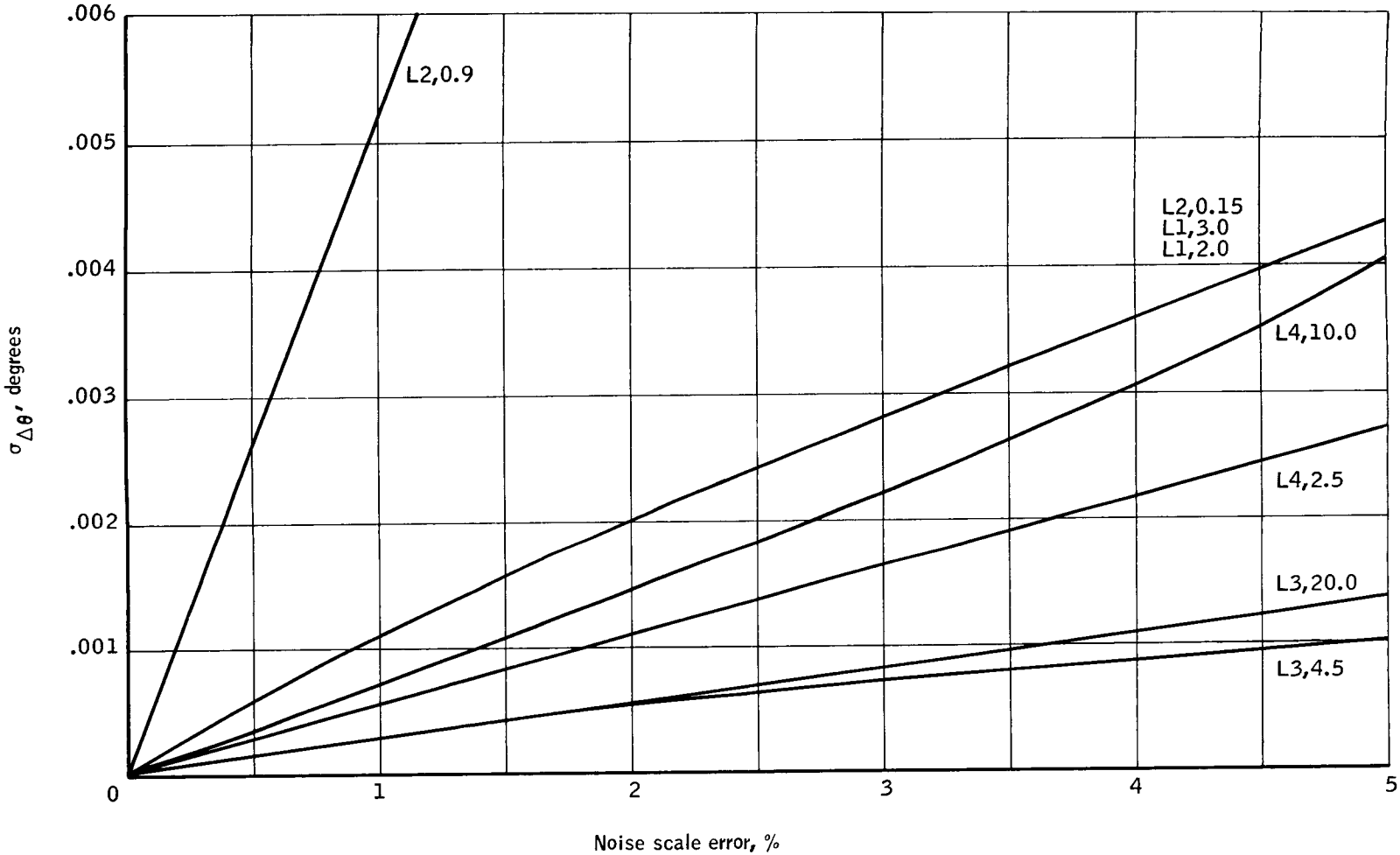

Figure F11. Local Vertical Error Standard Deviation Caused by Instrument Scale Noise

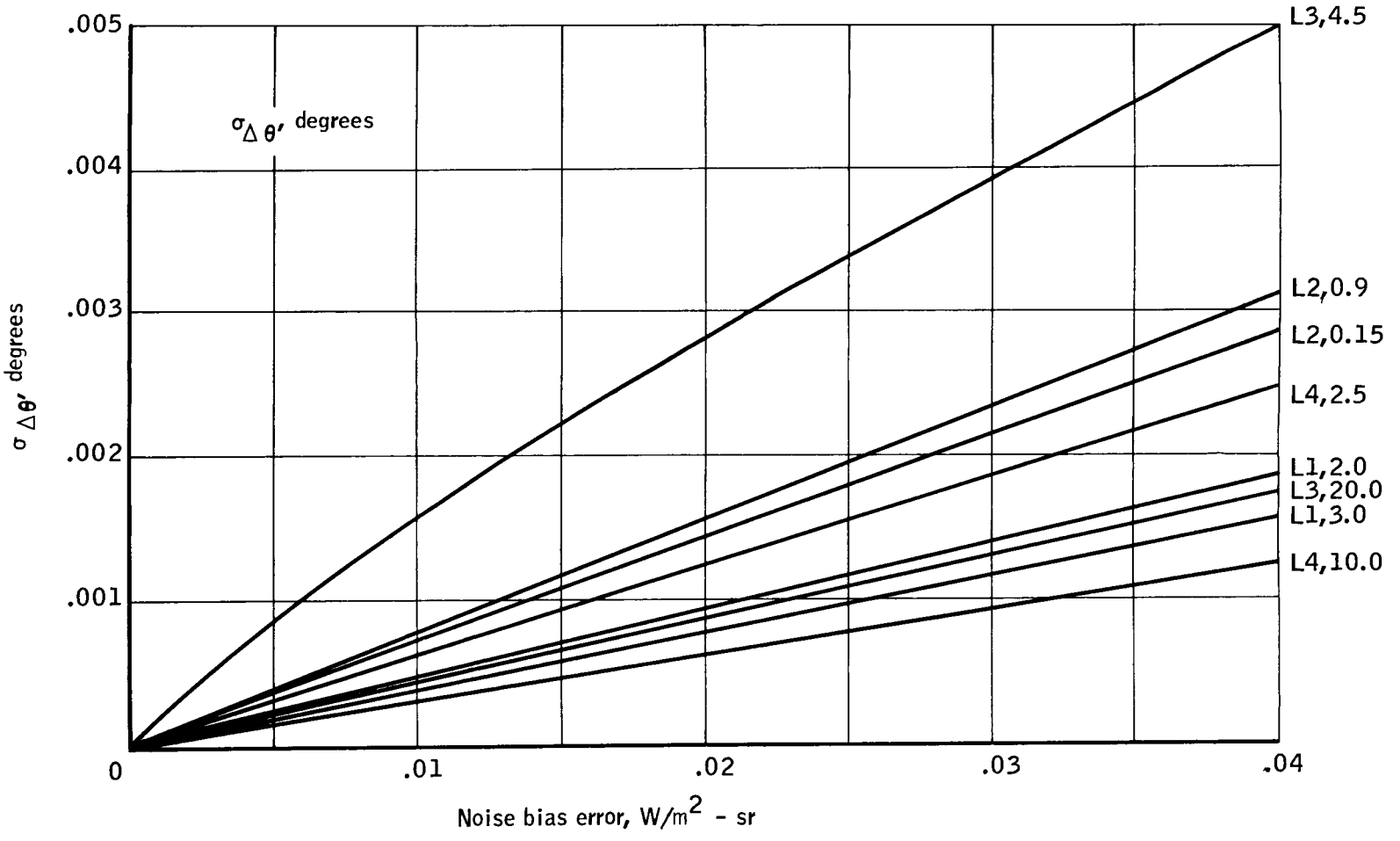

Figure F12. Local Vertical Error Standard Deviation Caused Instrument Bias Noise

APPENDIX G
PARAMETRIC ERROR ANALYSIS - TABULAR RESULTS

APPENDIX G

PARAMETRIC ERROR ANALYSIS - TABULAR RESULTS

Complete statistics on located horizon and local vertical calculated for 24 radiometric errors, as discussed in the section on radiometer errors, are given here. The tables are reproductions of actual computer outputs and the following key will be necessary for complete understanding.

Computer Parameter	Interpretation
Locator L1 Value 3.0	Radiance threshold locator Radiance threshold = 3.0 W/m^2-sr
Locator L2 Value 0.15	Normalized radiance threshold Threshold at 15% of peak radiance
Locator L3 Value 4.50	Integral of radiance threshold Threshold at integrated radiance = 4.5 W-km/m^2-sr
Locator L4 Value 2.50	Integral of normalized radiance threshold Threshold at integrated normalized radiance = 2.5 km
H mean	Mean value of located horizon, km
H sigma	Standard deviation of located horizon, km
DH mean	Mean value of located horizon error, km
DH sigma	Standard deviation of located horizon error, km
Theta mean	Mean value of sensed local vertical direction, degrees
Theta sigma	Standard deviation of sensed local vertical direction, degrees
Dtheta mean	Mean value of local vertical error, degrees
Dtheta sigma	Standard deviation of local vertical error, degrees

Computer Parameter	Interpretation
Seq. No.	Profile number which produced the minimum or maximum value. See references 24 and 25.
Error No. 0	No errors applied, disregard statistics for DH and Dtheta
Error No. 1	Calibration scale error = +0.4%
Error No. 2	Calibration scale error = +1%
Error No. 3	Calibration scale error = +2%
Error No. 4	Calibration scale error = +5%
Error No. 5	Calibration bias error = +0.001 W/m^2-sr
Error No. 6	Calibration bias error = +0.004 W/m^2-sr
Error No. 7	Calibration bias error = +0.01 W/m^2-sr
Error No. 8	Calibration bias error = +0.04 W/m^2-sr
Error No. 9	Scale drift error, $\sigma = \pm 0.4\%$
Error No. 10	Scale drift error, $\sigma = \pm 1\%$
Error No. 11	Scale drift error, $\sigma = \pm 2\%$
Error No. 12	Scale drift error, $\sigma = \pm 5\%$
Error No. 13	Bias drift error, $\sigma = \pm 0.001$ W/m^2-sr
Error No. 14	Bias drift error, $\sigma = \pm 0.004$ W/m^2-sr
Error No. 15	Bias drift error, $\sigma = \pm 0.01$ W/m^2-sr

Computer Parameter	Interpretation
Error No. 16	Bias drift error, $\sigma = \pm 0.04$ W/m^2-sr
Error No. 17	Scale noise error, $\sigma = \pm 0.4\%$
Error No. 18	Scale noise error, $\sigma = \pm 1\%$
Error No. 19	Scale noise error, $\sigma = \pm 2\%$
Error No. 20	Scale noise error, $\sigma = \pm 5\%$
Error No. 21	Bias noise error, $\sigma = \pm 0.001$ W/m^2-sr
Error No. 22	Bias noise error, $\sigma = \pm 0.004$ W/m^2-sr
Error No. 23	Bias noise error, $\sigma = \pm 0.01$ W/m^2-sr
Error No. 24	Bias noise error, $\sigma = \pm 0.04$ W/m^2-sr

Numbers printed in floating point format; i.e.,

$$.\text{xxxxxx yy} = (.\text{xxxxxx})(10^{yy})$$

TABLE G1. - RADIOMETRIC ERROR ANALYSIS RESULTS

ERROR NO. 0
LOCATOR L1
VALUE 2.00

	H MEAN	H SIGMA	DH MEAN	DH SIGMA	THETA MEAN	THETA SIGMA	DTHETA MEAN	DTHETA SIGMA
APR-	.437237E 02	.880917E 00	.437237E 02	.880917E 00	.125073E-01	.863713E-02	.125073E-01	.863713E-02
AUG-	.429815E 02	.140310E 01	.429815E 02	.140310E 01	.231515E-01	.942286E-02	.231515E-01	.942286E-02
OCT-	.411536E 02	.236268E 01	.411536E 02	.236268E 01	.344379E-01	.140071E-01	.344379E-01	.140071E-01
JAN-	.382158E 02	.348939E 01	.382158E 02	.348939E 01	.511998E-01	.234231E-01	.511998E-01	.234231E-01
TOT-	.415187E 02	.311360E 01	.415187E 02	.311360E 01	.303241E-01	.207956E-01	.303241E-01	.207956E-01

MAX H	MIN H	MAX DH	MIN DH	MAX THETA	MIN THETA	MAX DTHETA	MIN DTHETA
.451654E 02	.313031E 02	.451654E 02	.313031E 02	.104340E 00	.245002E-03	.104340E 00	.245002E-03
SEQ. NO.	SEQ. NO.	SEQ. NO.	SEQ. NO.	SEQ. NO.	SEQ. NO.	SEQ. NO.	SEQ. NO.
139	36	139	360	378	16	378	16

ERROR NO. 0
LOCATOR L1
VALUE 3.00

	H MEAN	H SIGMA	DH MEAN	DH SIGMA	THETA MEAN	THETA SIGMA	DTHETA MEAN	DTHETA SIGMA
APR-	.386537E 02	.132159E 01	.386537E 02	.132159E 01	.212194E-01	.126119E-01	.212194E-01	.126119E-01
AUG-	.382515E 02	.135146E 01	.382515E 02	.135146E 01	.199663E-01	.790361E-02	.199663E-01	.790361E-02
OCT-	.354493E 02	.261211E 01	.354493E 02	.261211E 01	.386917E-01	.139719E-01	.386917E-01	.139719E-01
JAN-	.321419E 02	.421256E 01	.321419E 02	.421256E 01	.574860E-01	.322839E-01	.574860E-01	.322839E-01
TOT-	.361241E 02	.372088E 01	.361241E 02	.372088E 01	.343409E-01	.244562E-01	.343409E-01	.244562E-01

MAX H	MIN H	MAX DH	MIN DH	MAX THETA	MIN THETA	MAX DTHETA	MIN DTHETA
.406696E 02	.192432E 02	.406696E 02	.192432E 02	.122499E 00	.233473E-02	.122499E 00	.233473E-02
SEQ. NO.	SEQ. NO.	SEQ. NO.	SEQ. NO.	SEQ. NO.	SEQ. NO.	SEQ. NO.	SEQ. NO.
56	360	56	360	360	6	360	6

TABLE G1. - RADIOMETRIC ERROR ANALYSIS RESULTS -

ERROR NO. 0
LOCATOR L2
VALUE .15

	H MEAN	H SIGMA	DH MEAN	DH SIGMA	THETA MEAN	THETA SIGMA	DTHETA MEAN	DTHETA SIGMA
APR=	.518478E 02	.207861E 00	.518478E 02	.207861E 00	.324858E-02	.260235E-02	.324858E-02	.260235E-02
AUG=	.510546E 02	.443123E 00	.510546E 02	.443123E 00	.724196E-02	.504764E-02	.724196E-02	.504764E-02
OCT=	.509757E 02	.395655E 00	.509757E 02	.395655E 00	.117287E-01	.783762E-02	.117287E-01	.783762E-02
JAN=	.497236E 02	.149626E 01	.497236E 02	.149626E 01	.215601E-01	.141664E-01	.215601E-01	.141664E-01
TOT=	.509004E 02	.118242E 01	.509004E 02	.118242E 01	.109448E-01	.109614E-01	.109448E-01	.109614E-01

MAX H	MIN H	MAX DH	MIN DH	MAX THETA	MIN THETA	MAX DTHETA	MIN DTHETA
.525990E 02	.470000E 02	.525990E 02	.470000E 02	.455519E-01	.233733E-03	.455519E-01	.233733E-03
SEQ. NO.	SEQ. NO.	SEQ. NO.	SEQ. NO.	SEQ. NO.	SEQ. NO.	SEQ. NO.	SEQ. NO.
214	367	214	367	378	337	378	337

ERROR NO. 0
LOCATOR L2
VALUE .90

	H MEAN	H SIGMA	DH MEAN	DH SIGMA	THETA MEAN	THETA SIGMA	DTHETA MEAN	DTHETA SIGMA
APR=	.267705E 02	.216363E 01	.267705E 02	.216363E 01	.315550E-01	.128629E-01	.315550E-01	.128629E-01
AUG=	.269241E 02	.467035E 00	.269241E 02	.467035E 00	.653089E-02	.492592E-02	.653089E-02	.492592E-02
OCT=	.253770E 02	.225817E 01	.253770E 02	.225817E 01	.331035E-01	.151659E-01	.331035E-01	.151659E-01
JAN=	.240723E 02	.260249E 01	.240723E 02	.260249E 01	.380512E-01	.185954E-01	.380512E-01	.185954E-01
TOT=	.257860E 02	.235265E 01	.257860E 02	.235265E 01	.273101E-01	.184678E-01	.273101E-01	.184678E-01

MAX H	MIN H	MAX DH	MIN DH	MAX THETA	MIN THETA	MAX DTHETA	MIN DTHETA
.297327E 02	.190415E 02	.297327E 02	.190415E 02	.793130E-01	.593267E-03	.793130E-01	.593267E-03
SEQ. NO.	SEQ. NO.	SEQ. NO.	SEQ. NO.	SEQ. NO.	SEQ. NO.	SEQ. NO.	SEQ. NO.
52	360	52	360	378	125	378	125

TABLE G1. - RADIOMETRIC ERROR ANALYSIS RESULTS - Continued

ERROR NO. 0
LOCATOR L3
VALUE 4.50

	H MEAN	H SIGMA	DH MEAN	DH SIGMA	THETA MEAN	THETA SIGMA	DTHETA MEAN	DTHETA SIGMA
APR=	.530685E 02	.308151E 00	.530685E 02	.308151E 00	.502904E-02	.254690E-02	.502904E-02	.254690E-02
AUG=	.525151E 02	.672403E 00	.525151E 02	.672403E 00	.103030E-01	.695284E-02	.103030E-01	.695284E-02
OCT=	.518622E 02	.102717E 01	.518622E 02	.102717E 01	.138992E-01	.795857E-02	.138992E-01	.795857E-02
JAN=	.504934E 02	.154180E 01	.504934E 02	.154180E 01	.218838E-01	.119255E-01	.218838E-01	.119255E-01
TOT=	.519848E 02	.138513E 01	.519848E 02	.138513E 01	.127788E-01	.101332E-01	.127788E-01	.101332E-01

MAX H	MIN H	MAX DH	MIN DH	MAX THETA	MIN THETA	MAX DTHETA	MIN DTHETA
.537011E 02	.468519E 02	.537011E 02	.468519E 02	.342222E-01	.713364E-04	.342222E-01	.713364E-04
SEQ. NO.	SEQ. NO.	SEQ. NO.	SEQ. NO.	SEQ. NO.	SEQ. NO.	SEQ. NO.	SEQ. NO.
56	360	56	360	372	27	372	27

ERROR NO. 0
LOCATOR L3
VALUE 20.00

	H MEAN	H SIGMA	DH MEAN	DH SIGMA	THETA MEAN	THETA SIGMA	DTHETA MEAN	DTHETA SIGMA
APR=	.421647E 02	.507595E 00	.421647E 02	.507595E 00	.826742E-02	.406274E-02	.826742E-02	.406274E-02
AUG=	.415211E 02	.972911E 00	.415211E 02	.972911E 00	.146241E-01	.767853E-02	.146241E-01	.767853E-02
OCT=	.402919E 02	.156621E 01	.402919E 02	.156621E 01	.224867E-01	.899807E-02	.224867E-01	.899807E-02
JAN=	.382122E 02	.252408E 01	.382122E 02	.252408E 01	.367516E-01	.169515E-01	.367516E-01	.169515E-01
TOT=	.405475E 02	.218578E 01	.405475E 02	.218578E 01	.205325E-01	.149667E-01	.205325E-01	.149667E-01

MAX H	MIN H	MAX DH	MIN DH	MAX THETA	MIN THETA	MAX DTHETA	MIN DTHETA
.431497E 02	.328485E 02	.431497E 02	.328485E 02	.675801E-01	.165422E-02	.675801E-01	.165422E-02
SEQ. NO.	SEQ. NO.	SEQ. NO.	SEQ. NO.	SEQ. NO.	SEQ. NO.	SEQ. NO.	SEQ. NO.
139	360	139	360	378	158	378	158

TABLE G1. - RADIOMETRIC ERROR ANALYSIS RESULTS - Continued

ERROR NO. 0
LOCATOR L4
VALUE 2.50

	H MEAN	H SIGMA	DH MEAN	DH SIGMA	THETA MEAN	THETA SIGMA	DTHETA MEAN	DTHETA SIGMA
APR=	.449041E 02	.326113E 00	.449041E 02	.326113E 00	.478340E-02	.387008E-02	.478340E-02	.387008E-02
AUG=	.442812E 02	.438909E 00	.442812E 02	.438909E 00	.742503E-02	.506140E-02	.742503E-02	.506140E-02
OCT=	.441469E 02	.967722E 00	.441469E 02	.967722E 00	.128385E-01	.791234E-02	.128385E-01	.791234E-02
JAN=	.430771E 02	.139227E 01	.430771E 02	.139227E 01	.196072E-01	.128954E-01	.196072E-01	.128954E-01
TOT=	.441023E 02	.110701E 01	.441023E 02	.110701E 01	.111635E-01	.997841E-02	.111635E-01	.997841E-02

MAX H	MIN H	MAX DH	MIN DH	MAX THETA	MIN THETA	MAX DTHETA	MIN DTHETA
.457329E 02	.406683E 02	.457329E 02	.406683E 02	.395527E-01	.783960E-04	.395527E-01	.783960E-04
SEQ. NO.	SEQ. NO.	SEQ. NO.	SEQ. NO.	SEQ. NO.	SEQ. NO.	SEQ. NO.	SEQ. NO.
56	367	56	367	378	182	378	182

ERROR NO. 0
LOCATOR L4
VALUE 10.00

	H MEAN	H SIGMA	DH MEAN	DH SIGMA	THETA MEAN	THETA SIGMA	DTHETA MEAN	DTHETA SIGMA
APR=	.311921E 02	.952755E 00	.311921E 02	.952755E 00	.133628E-01	.106988E-01	.133628E-01	.106988E-01
AUG=	.306694E 02	.408427E 00	.306694E 02	.408427E 00	.586102E-02	.500316E-02	.586102E-02	.500316E-02
OCT=	.299877E 02	.151098E 01	.299877E 02	.151098E 01	.218236E-01	.101504E-01	.218236E-01	.101504E-01
JAN=	.294885E 02	.186514E 01	.294885E 02	.186514E 01	.267820E-01	.154305E-01	.267820E-01	.154305E-01
TOT=	.300844E 02	.165542E 01	.300844E 02	.165542E 01	.169573E-01	.135727E-01	.169573E-01	.135727E-01

MAX H	MIN H	MAX DH	MIN DH	MAX THETA	MIN THETA	MAX DTHETA	MIN DTHETA
.328338E 02	.253631E 02	.328338E 02	.253631E 02	.603502E-01	.142127E-03	.603502E-01	.142127E-03
SEQ. NO.	SEQ. NO.	SEQ. NO.	SEQ. NO.	SEQ. NO.	SEQ. NO.	SEQ. NO.	SEQ. NO.
56	367	56	367	378	128	378	128

TABLE G1. - RADIOMETRIC ERROR ANALYSIS RESULTS - Continued

ERROR NO. 1
LOCATOR L1
VALUE 2.00

	H MEAN	H SIGMA	DH MEAN	DH SIGMA	THETA MEAN	THETA SIGMA	DTHETA MEAN	DTHETA SIGMA
APR-	.437669E 02	.877245E 00	.431064E-01	.452979E-02	.124473E-01	.859983E-02	.669381E-04	.455582E-04
ALG-	.430251E 02	.144237E 01	.435083E-01	.638756E-02	.231279E-01	.942907E-02	.833634E-04	.714593E-04
OCT-	.412019E 02	.235519E 01	.482178E-01	.986505E-02	.343187E-01	.139458E-01	.127230E-03	.993379E-04
JAN-	.382695E 02	.348687E 01	.536415E-01	.668138E-02	.511731E-01	.234253E-01	.807518E-04	.684970E-04
TOT-	.415659E 02	.310823E 01	.471142E-01	.830027E-02	.302667E-01	.207851E-01	.895709E-04	.771178E-04

MAX H	MIN H	MAX DH	MIN DH	MAX THETA	MIN THETA	MAX DTHETA	MIN DTHETA
.452159E 02	.313815E 02	.343963E-01	.359436E-01	.104260E 00	.260666E-03	.429025E-03	.804828E-06
SEQ. NO.	SEQ. NO.	SEQ. NO.	SEQ. NO.	SEQ. NO.	SEQ. NO.	SEQ. NO.	SEQ. NO.
139	360	195	48	378	16	195	182

ERROR NO. 1
LOCATOR L1
VALUE 3.00

	H MEAN	H SIGMA	DH MEAN	DH SIGMA	THETA MEAN	THETA SIGMA	DTHETA MEAN	DTHETA SIGMA
APR-	.387115E 02	.131302E 01	.578349E-01	.137124E-01	.211056E-01	.125589E-01	.144472E-03	.166077E-03
ALG-	.393028E 02	.135466E 01	.512352E-01	.784727E-02	.200207E-01	.795811E-02	.115113E-03	.555632E-04
OCT-	.355154E 02	.260583E 01	.661419E-01	.145530E-01	.325834E-01	.139650E-01	.220935E-03	.117334E-03
JAN-	.322107E 02	.419525E 01	.687955E-01	.233291E-01	.572925E-01	.320819E-01	.297257E-03	.274421E-03
TOT-	.361851E 02	.371016E 01	.610019E-01	.173077E-01	.342505E-01	.243429E-01	.194444E-03	.186953E-03

MAX H	MIN H	MAX DH	MIN DH	MAX THETA	MIN THETA	MAX DTHETA	MIN DTHETA
.407139E 02	.193918E 02	.148642E 00	.363393E-01	.121462E 00	.229863E-02	.103658E-02	.672833E-05
SEQ. NO.	SEQ. NO.	SEQ. NO.	SEQ. NO.	SEQ. NO.	SEQ. NO.	SEQ. NO.	SEQ. NO.
56	360	360	134	360	6	360	349

TABLE G1. - RADIOMETRIC ERROR ANALYSIS RESULTS - Continued

ERROR NO. 1
LOCATOR L2
VALUE .15

	H MEAN	H SIGMA	DH MEAN	DH SIGMA	THETA MEAN	THETA SIGMA	DTHETA MEAN	DTHETA SIGMA
APR-	.519479E 02	.207961E 00	-.585134E-05	.291053E-04	.324858E-02	.260235E-02	.403493E-06	.328035E-06
AUG-	.510546E 02	.443123E 00	-.271557E-05	.271165E-04	.724196E-02	.504764E-02	.419840E-06	.165133E-06
OCT-	.509757E 02	.895655E 00	.147099E-05	.276509E-04	.117287E-01	.783762E-02	.209948E-06	.161033E-06
JAN-	.497236E 02	.149626E 01	.384113E-05	.330951E-04	.215601E-01	.141664E-01	.383542E-06	.269528E-06
TOT-	.509004E 02	.113242E 01	-.206370E-05	.294903E-04	.101448E-01	.109614E-01	.354203E-06	.255861E-06

MAX H	MIN H	MAX DH	MIN DH	MAX THETA	MIN THETA	MAX DTHETA	MIN DTHETA
.525990E 02	.470000E 02	.488551E-04	-.499997E-04	.455519E-01	.233733E-03	.958104E-06	.328728E-08
SEQ. NO.	SEQ. NO.	SEQ. NO.	SEQ. NO.	SEQ. NO.	SEQ. NO.	SEQ. NO.	SEQ. NO.
214	367	342	346	378	337	1	346

ERROR NO. 1
LOCATOR L2
VALUE .30

	H MEAN	H SIGMA	DH MEAN	DH SIGMA	THETA MEAN	THETA SIGMA	DTHETA MEAN	DTHETA SIGMA
APR-	.267705E 02	.216363E 01	-.116173E-04	.269498E-04	.315550E-01	.128629E-01	.435460E-06	.264662E-06
AUG-	.269241E 02	.467035E 00	.473050E-05	.301541E-04	.654089E-02	.492592E-02	.414597E-06	.352380E-06
OCT-	.253770E 02	.225817E 01	.996358E-05	.267224E-04	.331035E-01	.151659E-01	.304501E-06	.183189E-06
JAN-	.240723E 02	.268249E 01	-.106163E-05	.298654E-04	.395512E-01	.185954E-01	.285334E-06	.207293E-06
TOT-	.257960E 02	.235265E 01	.278701E-06	.281096E-04	.273101E-01	.184678E-01	.359993E-06	.268359E-06

MAX H	MIN H	MAX DH	MIN DH	MAX THETA	MIN THETA	MAX DTHETA	MIN DTHETA
.297327E 02	.189415E 02	.490567E-04	-.497715E-04	.793130E-01	.593267E-03	.103497E-05	.261934E-11
SEQ. NO.	SEQ. NO.	SEQ. NO.	SEQ. NO.	SEQ. NO.	SEQ. NO.	SEQ. NO.	SEQ. NO.
52	360	43	371	378	125	9	178

TABLE G1. - RADIOMETRIC ERROR ANALYSIS RESULTS - Continued

ERROR NO. 1
LOCATOR L3
VALUE 4.50

	H MEAN	H SIGMA	DH MEAN	DH SIGMA	THETA MEAN	THETA SIGMA	DTHETA MEAN	DTHETA SIGMA
APR-	.530928E 02	.306998E 00	.242871E-01	.117506E-02	.501032E-02	.253576E-02	.188432E-04	.113356E-04
AUG-	.525397E 02	.672208E 00	.245960E-01	.226199E-02	.103029E-01	.695230E-02	.275532E-04	.206094E-04
OCT-	.518881E 02	.102664E 01	.259049E-01	.172417E-02	.138906E-01	.796238E-02	.195555E-04	.141621E-04
JAN-	.505214E 02	.153950E 01	.280233E-01	.309325E-02	.218431E-01	.119078E-01	.419980E-04	.351313E-04
TOT-	.520105E 02	.138329E 01	.257029E-01	.263121E-02	.127617E-01	.101222E-01	.269875E-04	.241620E-04

MAX H	MIN H	MAX DH	MIN DH	MAX THETA	MIN THETA	MAX DTHETA	MIN DTHETA
.537229E 02	.468827E 02	.319987E-01	.202668E-01	.341336E-01	.722772E-04	.127236E-03	.103721E-05
SEQ. NO. 56	SEQ. NO. 360	SEQ. NO. 356	SEQ. NO. 378	SEQ. NO. 372	SEQ. NO. 27	SEQ. NO. 378	SEQ. NO. 24

ERROR NO. 1
LOCATOR L3
VALUE 20.00

	H MEAN	H SIGMA	DH MEAN	DH SIGMA	THETA MEAN	THETA SIGMA	DTHETA MEAN	DTHETA SIGMA
APR-	.421995E 02	.506233E 00	.347618E-01	.171677E-02	.825030E-02	.404889E-02	.211057E-04	.157568E-04
AUG-	.415561E 02	.971376E 00	.350020E-01	.226274E-02	.145947E-01	.768239E-02	.324153E-04	.217450E-04
OCT-	.403287E 02	.156343E 01	.368361E-01	.334356E-02	.224418E-01	.899089E-02	.460539E-04	.263552E-04
JAN-	.382519E 02	.252156E 01	.396717E-01	.291894E-02	.367143E-01	.169410E-01	.389201E-04	.275569E-04
TOT-	.405840E 02	.218296E 01	.365679E-01	.328583E-02	.205003E-01	.149570E-01	.346237E-04	.250590E-04

MAX H	MIN H	MAX DH	MIN DH	MAX THETA	MIN THETA	MAX DTHETA	MIN DTHETA
.431941E 02	.328914E 02	.439684E-01	.316160E-01	.674778E-01	.159839E-02	.102057E-03	.256101E-05
SEQ. NO. 139	SEQ. NO. 360	SEQ. NO. 355	SEQ. NO. 52	SEQ. NO. 378	SEQ. NO. 158	SEQ. NO. 378	SEQ. NO. 5

TABLE G1. - RADIOMETRIC ERROR ANALYSIS RESULTS - Continued

ERROR NO. 1
LOCATOR L4
VALUE 2.50

	H MEAN	H SIGMA	DH MEAN	DH SIGMA	THETA MEAN	THETA SIGMA	DTHETA MEAN	DTHETA SIGMA
APR-	.449041E 02	.326113E 00	-.144978E-04	.257174E-04	.478340E-02	.387008E-02	.361675E-06	.275984E-06
AUG-	.442912E 02	.438909E 00	.424016E-06	.261728E-04	.742503E-02	.506140E-02	.321273E-06	.186738E-06
OCT-	.441469E 02	.967722E 00	-.537455E-05	.297973E-04	.128385E-01	.791234E-02	.379516E-06	.204205E-06
JAN-	.430771E 02	.139227E 01	-.223637E-05	.270184E-04	.196072E-01	.128954E-01	.319482E-06	.193767E-06
TOT-	.441023E 02	.110701E 01	-.542117E-05	.277984E-04	.111635E-01	.997841E-02	.345496E-06	.243836E-06

MAX H	MIN H	MAX DH	MIN DH	MAX THETA	MIN THETA	MAX DTHETA	MIN DTHETA
.457329E 02	.406683E 02	.494218E-04	-.480996E-04	.395527E-01	.783960E-04	.104952E-05	.778469E-08
SEQ. NO.	SEQ. NO.	SEQ. NO.	SEQ. NO.	SEQ. NO.	SEQ. NO.	SEQ. NO.	SEQ. NO.
56	367	376	5	378	182	2	184

ERROR NO. 1
LOCATOR L4
VALUE 10.00

	H MEAN	H SIGMA	DH MEAN	DH SIGMA	THETA MEAN	THETA SIGMA	DTHETA MEAN	DTHETA SIGMA
APR-	.311921E 02	.952755E 00	.791273E-05	.324469E-04	.133628E-01	.106988E-01	.421804E-06	.285114E-06
AUG-	.306694E 02	.408427E 00	.607756E-05	.266293E-04	.586102E-02	.500316E-02	.386802E-06	.285855E-06
OCT-	.299977E 02	.151099E 01	-.122926E-05	.294777E-04	.219236E-01	.101504E-01	.404585E-06	.247520E-06
JAN-	.294985E 02	.186514E 01	.380552E-05	.294665E-04	.267820E-01	.154305E-01	.411408E-06	.294796E-06
TOT-	.300844E 02	.165542E 01	.414164E-05	.295301E-04	.169573E-01	.135727E-01	.406192E-06	.279208E-06

MAX H	MIN H	MAX DH	MIN DH	MAX THETA	MIN THETA	MAX DTHETA	MIN DTHETA
.328338E 02	.253631E 02	.497270E-04	-.494143E-04	.603502E-01	.142127E-03	.104810E-05	.465981E-08
SEQ. NO.	SEQ. NO.	SEQ. NO.	SEQ. NO.	SEQ. NO.	SEQ. NO.	SEQ. NO.	SEQ. NO.
56	367	20	126	378	128	46	139

TABLE G1. - RADIOMETRIC ERROR ANALYSIS RESULTS - Continued

ERROR NO. 2
LOCATOR L1
VALUE 3.00

	H MEAN	H SIGMA	DH MEAN	DH SIGMA	THETA MEAN	THETA SIGMA	DTHETA MEAN	DTHETA SIGMA
APR-	.438314E 02	.477045E 00	.197674E 00	.115691E-01	.123626E-01	.854886E-02	.162162E-03	.113578E-03
AUG-	.430900E 02	.[illegible]E 01	.198471E 00	.168093E-01	.230843E-01	.943368E-02	.216495E-03	.196652E-03
OCT-	.412741E 02	.[illegible]E 01	.120576E 00	.245745E-01	.341507E-01	.133428E-01	.317428E-03	.241533E-03
JAN-	.383494E 02	.348316E 01	.133513E 00	.164954E-01	.511303E-01	.233259E-01	.200141E-03	.168675E-03
TOT-	.416362E 02	.310[illegible]E 01	.117559E 00	.208347E-01	.306820E-01	.207675E-01	.224057E-03	.194641E-03

MAX H	MIN H	MAX DH	MIN DH	MAX THETA	MIN THETA	MAX DTHETA	MIN DTHETA
.452911E 02	.314035E 02	.210205E 00	.892538E-01	.104143E 00	.289658E-03	.107518E-02	.812557E-05
SEQ. NO.	SEQ. NO.	SEQ. NO.	SEQ. NO.	SEQ. NO.	SEQ. NO.	SEQ. NO.	SEQ. NO.
139	36[illegible]	195	48	378	16	195	6

ERROR NO. 2
LOCATOR L1
VALUE 3.00

	H MEAN	H SIGMA	DH MEAN	DH SIGMA	THETA MEAN	THETA SIGMA	DTHETA MEAN	DTHETA SIGMA
APR-	.387975E 02	.[illegible]E 01	.143837E 00	.335310E-01	.209209E-01	.124834E-01	.344130E-03	.415614E-03
AUG-	.383790E 02	.135334E 01	.127446E 00	.194744E-01	.291017E-01	.804756E-02	.286386E-03	.137283E-03
OCT-	.356116E 02	.26[illegible]E 01	.162355E 00	.319964E-01	.384651E-01	.139347E-01	.497825E-03	.229266E-03
JAN-	.42312[illegible]E 02	.31[illegible]E 01	.170865E 00	.576222E-01	.570063E-01	.317875E-01	.734686E-03	.679787E-03
TOT-	.362752E 02	.35[illegible]E 01	.151131E 00	.416364E-01	.341255E-01	.241785E-01	.465757E-03	.454580E-03

MAX H	MIN H	MAX DH	MIN DH	MAX THETA	MIN THETA	MAX DTHETA	MIN DTHETA
.407797E 02	.19[illegible]E 02	.363594E 00	.903757E-01	.119934E 00	.222525E-02	.256493E-02	.124419E-04
SEQ. NO.	SEQ. NO.	SEQ. NO.	SEQ. NO.	SEQ. NO.	SEQ. NO.	SEQ. NO.	SEQ. NO.
56	36[illegible]	360	134	360	337	360	16

TABLE G1. - RADIOMETRIC ERROR ANALYSIS RESULTS - Continued

ERROR NO. 2
LOCATOR L2
VALUE .15

	H MEAN	H SIGMA	DH MEAN	DH SIGMA	THETA MEAN	THETA SIGMA	DTHETA MEAN	DTHETA SIGMA
APR-	.518478E 02	.207861E 00	-.585134E-05	.281053E-04	.324858E-02	.260235E-02	.403483E-06	.328035E-06
AUG-	.510546E 02	.443123E 00	-.771557E-05	.271165E-04	.724196E-02	.504764E-02	.419840E-06	.165133E-06
OCT-	.509757E 02	.895655E 00	.147099E-05	.276509E-04	.117287E-01	.783762E-02	.209948E-06	.161033E-06
JAN-	.497236E 02	.149626E 01	.384113E-05	.330951E-04	.215601E-01	.141664E-01	.383542E-06	.269528E-06
TOT-	.509004E 02	.118242E 01	-.206370E-05	.294903E-04	.109448E-01	.109614E-01	.354203E-06	.255861E-06

MAX H	MIN H	MAX DH	MIN DH	MAX THETA	MIN THETA	MAX DTHETA	MIN DTHETA
.525990E 02	.470000E 02	.488551E-04	-.499997E-04	.454519E-01	.233733E-03	.958104E-06	.328728E-08
SEQ. NO.	SEQ. NO.	SEQ. NO.	SEQ. NO.	SEQ. NO.	SEQ. NO.	SEQ. NO.	SEQ. NO.
214	367	342	346	378	337	1	346

ERROR NO. 2
LOCATOR L2
VALUE .90

	H MEAN	H SIGMA	DH MEAN	DH SIGMA	THETA MEAN	THETA SIGMA	DTHETA MEAN	DTHETA SIGMA
APR-	.267705E 02	.216363E 01	-.115173E-04	.269698E-04	.315550E-01	.128629E-01	.435460E-06	.264662E-06
AUG-	.269241E 02	.467035E 00	.473050E-05	.301541E-04	.653089E-02	.492592E-02	.414587E-06	.352380E-06
OCT-	.253770E 02	.225817E 01	.906358E-05	.267224E-04	.331035E-01	.151659E-01	.304591E-06	.183189E-06
JAN-	.240723E 02	.260249E 01	-.106163E-05	.238654E-04	.380512E-01	.185954E-01	.285334E-06	.207293E-06
TOT-	.257860E 02	.235255E 01	.278791E-06	.281096E-04	.273101E-01	.184678E-01	.359993E-06	.268359E-06

MAX H	MIN H	MAX DH	MIN DH	MAX THETA	MIN THETA	MAX DTHETA	MIN DTHETA
.297327E 02	.190415E 02	.490567E-04	-.497715E-04	.793130E-01	.593267E-03	.103497E-05	.261934E-11
SEQ. NO.	SEQ. NO.	SEQ. NO.	SEQ. NO.	SEQ. NO.	SEQ. NO.	SEQ. NO.	SEQ. NO.
52	360	43	371	378	125	8	178

TABLE G1. - RADIOMETRIC ERROR ANALYSIS RESULTS - Continued

ERROR NO. 2
LOCATOR L3
VALUE 4.50

	H MEAN	H SIGMA	DH MEAN	DH SIGMA	THETA MEAN	THETA SIGMA	DTHETA MEAN	DTHETA SIGMA
APR-	.531288E 02	.305292E 00	.603525E-01	.292530E-02	.498285E-02	.251912E-02	.466236E-04	.283103E-04
AUG-	.525767E 02	.671540E 00	.616095E-01	.542867E-02	.102915E-01	.695287E-02	.682309E-04	.399438E-04
OCT-	.519269E 02	.102537E 01	.646542E-01	.449823E-02	.138842E-01	.797589E-02	.548523E-04	.375695E-04
JAN-	.505633E 02	.153618E 01	.699304E-01	.729345E-02	.217853E-01	.118841E-01	.101595E-03	.793230E-04
TOT-	.520489E 02	.138051E 01	.641366E-01	.644201E-02	.127360E-01	.101095E-01	.678254E-04	.544494E-04

MAX H	MIN H	MAX DH	MIN DH	MAX THETA	MIN THETA	MAX DTHETA	MIN DTHETA
.537554E 02	.469254E 02	.794718E-01	.540981E-01	.340028E-01	.746154E-04	.241865E-03	.945400E-06
SEQ. NO.	SEQ. NO.	SEQ. NO.	SEQ. NO.	SEQ. NO.	SEQ. NO.	SEQ. NO.	SEQ. NO.
56	361	356	122	372	27	378	24

ERROR NO. 2
LOCATOR L3
VALUE 20.00

	H MEAN	H SIGMA	DH MEAN	DH SIGMA	THETA MEAN	THETA SIGMA	DTHETA MEAN	DTHETA SIGMA
APR-	.422511E 02	.584232E 00	.364348E-01	.426269E-02	.822468E-02	.402723E-02	.527625E-04	.390218E-04
AUG-	.416081E 02	.969137E 00	.870451E-01	.554377E-02	.145500E-01	.768949E-02	.790352E-04	.555049E-04
OCT-	.403839E 02	.155948E 01	.920433E-01	.806293E-02	.223776E-01	.898826E-02	.111900E-03	.589709E-04
JAN-	.383115E 02	.251749E 01	.993252E-01	.769613E-02	.366552E-01	.169289E-01	.100396E-03	.706438E-04
TOT-	.406387E 02	.217852E 01	.912121E-01	.836427E-02	.204518E-01	.149442E-01	.860235E-04	.614470E-04

MAX H	MIN H	MAX DH	MIN DH	MAX THETA	MIN THETA	MAX DTHETA	MIN DTHETA
.432352E 02	.339551E 02	.110359E 00	.784965E-01	.673263E-01	.151510E-02	.253537E-03	.448864E-06
SEQ. NO.	SEQ. NO.	SEQ. NO.	SEQ. NO.	SEQ. NO.	SEQ. NO.	SEQ. NO.	SEQ. NO.
139	360	363	52	378	158	378	338

TABLE G1. - RADIOMETRIC ERROR ANALYSIS RESULTS - Continued

ERROR NO. 2
LOCATOR L4
VALUE 2.50

	H MEAN	H SIGMA	DH MEAN	DH SIGMA	THETA MEAN	THETA SIGMA	DTHETA MEAN	DTHETA SIGMA
APR-	.449041E 02	.326113E 00	-.144978E-04	.287174E-04	.478340E-02	.387008E-02	.361675E-06	.275984E-06
AUG-	.442812E 02	.438[illegible]9E 00	.424016E-06	.261729E-04	.742503E-02	.506140E-02	.321273E-06	.186738E-06
OCT-	.441469E 02	.967722E 00	-.537455E-05	.297978E-04	.128385E-01	.791234E-02	.379516E-06	.294205E-06
JAN-	.430771E 02	.139227E 01	-.223637E-05	.270184E-04	.196072E-01	.128954E-01	.319482E-06	.193767E-06
TOT-	.441023E 02	.110701E 01	-.542117E-05	.277984E-04	.111635E-01	.997841E-02	.345486E-06	.243836E-06

MAX H	MIN H	MAX DH	MIN DH	MAX THETA	MIN THETA	MAX DTHETA	MIN DTHETA
.457329E 02	.406683E 02	.494218E-04	-.480996E-04	.395527E-01	.783960E-04	.104952E-05	.778469E-08
SEQ. NO. 56	SEQ. NO. 367	SEQ. NO. 376	SEQ. NO. 5	SEQ. NO. 378	SEQ. NO. 182	SEQ. NO. 2	SEQ. NO. 184

ERROR NO. 2
LOCATOR L4
VALUE 10.00

	H MEAN	H SIGMA	DH MEAN	DH SIGMA	THETA MEAN	THETA SIGMA	DTHETA MEAN	DTHETA SIGMA
APR-	.311921E 02	.957755E 00	.791273E-05	.324468E-04	.133628E-01	.106988E-01	.421894E-06	.285114E-06
AUG-	.306694E 02	.408427E 00	.607756E-05	.266293E-04	.586102E-02	.500316E-02	.386802E-06	.285855E-06
OCT-	.299877E 02	.151098E 01	-.122926E-05	.294777E-04	.218236E-01	.101504E-01	.404585E-06	.247520E-06
JAN-	.284885E 02	.186514E 01	.380552E-05	.284665E-04	.267820E-01	.154305E-01	.411488E-06	.294796E-06
TOT-	.300844E 02	.165532E 01	.414164E-05	.295301E-04	.169573E-01	.135727E-01	.406192E-06	.279208E-06

MAX H	MIN H	MAX DH	MIN DH	MAX THETA	MIN THETA	MAX DTHETA	MIN DTHETA
.328338E 02	.253631E 02	.497270E-04	-.494143E-04	.603502E-01	.142127E-03	.104810E-05	.465981E-08
SEQ. NO. 56	SEQ. NO. 367	SEQ. NO. 20	SEQ. NO. 126	SEQ. NO. 378	SEQ. NO. 128	SEQ. NO. 46	SEQ. NO. 139

TABLE G1. - RADIOMETRIC ERROR ANALYSIS RESULTS - Continued

ERROR NO. 3
LOCATOR L1
VALUE 2.00

	H MEAN	H SIGMA	DH MEAN	DH SIGMA	THETA MEAN	THETA SIGMA	DTHETA MEAN	DTHETA SIGMA
APR=	.439373E 02	.863684E 00	.213582E 00	.233726E-01	.122272E-01	.846776E-02	.315899E-03	.234884E-03
AUG=	.431970E 02	.147918E 01	.215447E 00	.336908E-01	.230054E-01	.946863E-02	.424550E-03	.403380E-03
OCT=	.413931E 02	.232676E 01	.239560E 00	.490717E-01	.338666E-01	.136731E-01	.627828E-03	.481620E-03
JAN=	.394819E 02	.347649E 01	.266080E 00	.318200E-01	.510281E-01	.234226E-01	.408844E-03	.303593E-03
TOT=	.417523E 02	.308705E 01	.233667E 00	.416011E-01	.300318E-01	.207296E-01	.444280E-03	.385301E-03

MAX H	MIN H	MAX DH	MIN DH	MAX THETA	MIN THETA	MAX DTHETA	MIN DTHETA
.454143E 02	.316932E 02	.416225E 00	.176750E 00	.103944E 00	.329396E-03	.213288E-02	.175416E-04
SEQ. NO.	SEQ. NO.	SEQ. NO.	SEQ. NO.	SEQ. NO.	SEQ. NO.	SEQ. NO.	SEQ. NO.
139	36[illegible]	195	48	378	16	195	6

ERROR NO. 3
LOCATOR L1
VALUE 3.00

	H MEAN	H SIGMA	DH MEAN	DH SIGMA	THETA MEAN	THETA SIGMA	DTHETA MEAN	DTHETA SIGMA
APR=	.389386E 02	.127902E 01	.284935E 00	.644207E-01	.206451E-01	.123227E-01	.669963E-03	.813476E-03
AUG=	.385060E 02	.136668E 01	.254427E 00	.373591E-01	.202369E-01	.820697E-02	.532591E-03	.264365E-03
OCT=	.357688E 02	.250335E 01	.319489E 00	.590896E-01	.383062E-01	.139323E-01	.923029E-03	.442544E-03
JAN=	.324795E 02	.413114E 01	.337612E 00	.111547E 00	.565693E-01	.313389E-01	.141445E-02	.131710E-02
TOT=	.364232E 02	.367213E 01	.299116E 00	.799614E-01	.339391E-01	.239328E-01	.885008E-03	.882386E-03

MAX H	MIN H	MAX DH	MIN DH	MAX THETA	MIN THETA	MAX DTHETA	MIN DTHETA
.408877E 02	.190732E 02	.730036E 00	.179021E 00	.117417E 00	.204507E-02	.508212E-02	.384018E-04
SEQ. NO.	SEQ. NO.	SEQ. NO.	SEQ. NO.	SEQ. NO.	SEQ. NO.	SEQ. NO.	SEQ. NO.
56	348	360	134	360	337	360	13

TABLE G1. - RADIOMETRIC ERROR ANALYSIS RESULTS -
Continued

ERROR NO. 3
LOCATOR L2
VALUE .15

	H MEAN	H SIGMA	DH MEAN	DH SIGMA	THETA MEAN	THETA SIGMA	DTHETA MEAN	DTHETA SIGMA
APR-	.518478E 02	.207861E 00	-.585134E-05	.281053E-04	.324858E-02	.260235E-02	.403483E-06	.328035E-06
AUG-	.510546E 02	.443123E 00	-.771557E-05	.271165E-04	.724196E-02	.504764E-02	.419840E-06	.165133E-06
OCT-	.509757E 02	.895495E 00	.147099E-05	.276509E-04	.117287E-01	.783762E-02	.209948E-06	.161033E-06
JAN-	.497236E 02	.149626E 01	.384113E-05	.330951E-04	.215601E-01	.141664E-01	.383542E-06	.269528E-06
TOT-	.509004E 02	.118242E 01	-.206370E-05	.294903E-04	.109448E-01	.109614E-01	.354203E-06	.255861E-06

MAX H	MIN H	MAX DH	MIN DH	MAX THETA	MIN THETA	MAX DTHETA	MIN DTHETA
.525990E 02	.470000E 02	.488851E-04	-.499997E-04	.455519E-01	.233733E-03	.958104E-06	.328728E-08
SEQ. NO.	SEQ. NO.	SEQ. NO.	SEQ. NO.	SEQ. NO.	SEQ. NO.	SEQ. NO.	SEQ. NO.
214	367	342	346	378	337	1	346

ERROR NO. 3
LOCATOR L2
VALUE .90

	H MEAN	H SIGMA	DH MEAN	DH SIGMA	THETA MEAN	THETA SIGMA	DTHETA MEAN	DTHETA SIGMA
APR-	.267705E 02	.216363E 01	-.116173E-04	.269698E-04	.315550E-01	.128629E-01	.435460E-06	.264662E-06
AUG-	.269241E 02	.467035E 00	.473050E-05	.301541E-04	.653089E-02	.492592E-02	.414587E-06	.352380E-06
OCT-	.253770E 02	.225417E 01	.906358E-05	.267224E-04	.331035E-01	.151659E-01	.304591E-06	.183189E-06
JAN-	.240723E 02	.260249E 01	-.106163E-05	.238654E-04	.380512E-01	.185954E-01	.285334E-06	.207293E-06
TOT-	.257860E 02	.235265E 01	.278791E-06	.281096E-04	.273161E-01	.184678E-01	.359993E-06	.268359E-06

MAX H	MIN H	MAX DH	MIN DH	MAX THETA	MIN THETA	MAX DTHETA	MIN DTHETA
.297327E 02	.190415E 02	.490567E-04	-.497715E-04	.793130E-01	.593267E-03	.103497E-05	.261934E-11
SEQ. NO.	SEQ. NO.	SEQ. NO.	SEQ. NO.	SEQ. NO.	SEQ. NO.	SEQ. NO.	SEQ. NO.
52	368	43	371	378	125	8	178

TABLE G1. - RADIOMETRIC ERROR ANALYSIS RESULTS - Continued

ERROR NO. 3
LOCATOR L3
VALUE 4.50

	H MEAN	H SIGMA	DH MEAN	DH SIGMA	THETA MEAN	THETA SIGMA	DTHETA MEAN	DTHETA SIGMA
APR-	.531880E 02	.302489E 00	.119538E 00	.579751E-02	.493744E-02	.249190E-02	.924633E-04	.560762E-04
AUG-	.526389E 02	.669205E 00	.123807E 00	.106431E-01	.102657E-01	.692913E-02	.145145E-03	.838148E-04
OCT-	.519907E 02	.102464E 01	.128512E 00	.884337E-02	.138670E-01	.799602E-02	.119714E-03	.784025E-04
JAN-	.506322E 02	.153085E 01	.138895E 00	.140921E-01	.216932E-01	.113487E-01	.196636E-03	.149187E-03
TOT-	.521125E 02	.137591E 01	.127688E 00	.125643E-01	.126908E-01	.100868E-01	.138490E-03	.105439E-03
	MAX H	MIN H	MAX DH	MIN DH	MAX THETA	MIN THETA	MAX DTHETA	MIN DTHETA
	.538087E 02	.470039E 02	.157353E 00	.107174E 00	.337869E-01	.778564E-04	.471869E-03	.345184E-05
	SEQ. NO.	SEQ. NO.	SEQ. NO.	SEQ. NO.	SEQ. NO.	SEQ. NO.	SEQ. NO.	SEQ. NO.
	56	360	356	122	372	27	342	24

ERROR NO. 3
LOCATOR L3
VALUE 20.00

	H MEAN	H SIGMA	DH MEAN	DH SIGMA	THETA MEAN	THETA SIGMA	DTHETA MEAN	DTHETA SIGMA
APR-	.423365E 02	.501178E 00	.171765E 00	.851037E-02	.918160E-02	.398707E-02	.108525E-03	.764218E-04
AUG-	.416942E 02	.965845E 00	.173144E 00	.102910E-01	.144793E-01	.770649E-02	.153700E-03	.984557E-04
OCT-	.404755E 02	.155336E 01	.183602E 00	.153806E-01	.229772E-01	.898613E-02	.214914E-03	.112160E-03
JAN-	.384101E 02	.251033E 01	.197950E 00	.159458E-01	.365506E-01	.169048E-01	.201706E-03	.151818E-03
TOT-	.407291E 02	.217116E 01	.181616E 00	.166488E-01	.203722E-01	.149208E-01	.169711E-03	.120654E-03
	MAX H	MIN H	MAX DH	MIN DH	MAX THETA	MIN THETA	MAX DTHETA	MIN DTHETA
	.433191E 02	.330645E 02	.219515E 00	.155476E 00	.670772E-01	.137871E-02	.502641E-03	.240006E-05
	SEQ. NO.	SEQ. NO.	SEQ. NO.	SEQ. NO.	SEQ. NO.	SEQ. NO.	SEQ. NO.	SEQ. NO.
	139	360	338	52	378	158	378	360

TABLE G1. - RADIOMETRIC ERROR ANALYSIS RESULTS - Continued

ERROR NO. 3
LOCATOR L4
VALUE 2.50

	H MEAN	H SIGMA	DH MEAN	DH SIGMA	THETA MEAN	THETA SIGMA	DTHETA MEAN	DTHETA SIGMA
APR-	.449041E 02	.326113E 00	-.144978E-04	.257174E-04	.478340E-02	.387008E-02	.361675E-06	.275984E-06
AUG-	.442812E 02	.438[illegible]E 00	.424016E-06	.261728E-04	.742503E-02	.506140E-02	.321273E-06	.186738E-06
OCT-	.441469E 02	.967722E 00	-.537455E-05	.297978E-04	.128385E-01	.791234E-02	.379516E-06	.294205E-06
JAN-	.430771E 02	.139227E 01	-.223637E-05	.270184E-04	.196072E-01	.128954E-01	.319482E-06	.193767E-06
TOT-	.441023E 02	.110701E 01	-.542117E-05	.277984E-04	.111635E-01	.997841E-02	.345486E-06	.243836E-06

MAX H	MIN H	MAX DH	MIN DH	MAX THETA	MIN THETA	MAX DTHETA	MIN DTHETA
.457329E 02	.406683E 02	.494218E-04	-.480996E-04	.395527E-01	.783960E-04	.104952E-05	.778469E-08
SEQ. NO.	SEQ. NO.	SEQ. NO.	SEQ. NO.	SEQ. NO.	SEQ. NO.	SEQ. NO.	SEQ. NO.
56	367	376	5	378	182	2	184

ERROR NO. 3
LOCATOR L4
VALUE 10.00

	H MEAN	H SIGMA	DH MEAN	DH SIGMA	THETA MEAN	THETA SIGMA	DTHETA MEAN	DTHETA SIGMA
APR-	.311921E 02	.952758E 00	.791273E-05	.324468E-04	.133623E-01	.106988E-01	.421894E-06	.285114E-06
AUG-	.306694E 02	.403427E 00	.607756E-05	.266293E-04	.586102E-02	.500316E-02	.386802E-06	.285855E-06
OCT-	.299877E 02	.151028E 01	-.122926E-05	.294777E-04	.218236E-01	.101504E-01	.404585E-06	.247520E-06
JAN-	.284885E 02	.196514E 01	.380552E-05	.284665E-04	.267820E-01	.154305E-01	.411488E-06	.294796E-06
TOT-	.300844E 02	.165542E 01	.414164E-05	.295301E-04	.169573E-01	.135727E-01	.406192E-06	.279208E-06

MAX H	MIN H	MAX DH	MIN DH	MAX THETA	MIN THETA	MAX DTHETA	MIN DTHETA
.328338E 02	.253631E 02	.497270E-04	-.494143E-04	.603503E-01	.142127E-03	.104810E-05	.465981E-08
SEQ. NO.	SEQ. NO.	SEQ. NO.	SEQ. NO.	SEQ. NO.	SEQ. NO.	SEQ. NO.	SEQ. NO.
56	367	20	126	378	128	46	139

TABLE G1. - RADIOMETRIC ERROR ANALYSIS RESULTS - Continued

ERROR NO. 4
LOCATOR L1
VALUE 2.00

	H MEAN	H SIGMA	DH MEAN	DH SIGMA	THETA MEAN	THETA SIGMA	DTHETA MEAN	DTHETA SIGMA
APR=	.442481E 02	.846464E 00	.524372E 00	.513675E-01	.119772E-01	.824455E-02	.674913E-03	.512517E-03
AUG=	.435199E 02	.146016E 01	.938389E 00	.759018E-01	.226007E-01	.939552E-02	.105292E-02	.959782E-03
OCT=	.417488E 02	.225[illegible]4E 01	.595228E 00	.143189E 00	.329461E-01	.129123E-01	.166709E-02	.148825E-02
JAN=	.388679E 02	.345776E 01	.652068E 00	.674333E-01	.508156E-01	.234266E-01	.878855E-03	.636850E-03
TOT=	.420962E 02	.303881E 01	.577514E 00	.104495E 00	.295834E-01	.205706E-01	.106844E-02	.104328E-02

MAX H	MIN H	MAX DH	MIN DH	MAX THETA	MIN THETA	MAX DTHETA	MIN DTHETA
.457689E 02	.321715E 02	.114008E 01	.449199E 00	.103335E 00	.443726E-03	.567764E-02	.314904E-04
SEQ. NO.	SEQ. NO.	SEQ. NO.	SEQ. NO.	SEQ. NO.	SEQ. NO.	SEQ. NO.	SEQ. NO.
139	360	192	131	378	16	192	114

ERROR NO. 4
LOCATOR L1
VALUE 3.00

	H MEAN	H SIGMA	DH MEAN	DH SIGMA	THETA MEAN	THETA SIGMA	DTHETA MEAN	DTHETA SIGMA
APR=	.393456E 02	.122614E 01	.591972E 00	.144743E 00	.198663E-01	.119512E-01	.154452E-02	.176277E-02
AUG=	.388755E 02	.139732E 01	.623988E 00	.912809E-01	.207184E-01	.863523E-02	.119618E-02	.766053E-03
OCT=	.362260E 02	.253[illegible]8E 01	.776710E 00	.133357E 00	.380552E-01	.138703E-01	.219444E-02	.995340E-03
JAN=	.329604E 02	.409[illegible]0E 01	.813506E 00	.256048E 00	.555469E-01	.302986E-01	.315063E-02	.314849E-02
TOT=	.366519E 02	.361241E 01	.727794E 00	.183921E 00	.335467E-01	.233658E-01	.202144E-02	.205008E-02

MAX H	MIN H	MAX DH	MIN DH	MAX THETA	MIN THETA	MAX DTHETA	MIN DTHETA
.412033E 02	.21[illegible]E 02	.181589E 01	.434863E 00	.109671E 00	.213913E-02	.128276E-01	.154147E-04
SEQ. NO.	SEQ. NO.	SEQ. NO.	SEQ. NO.	SEQ. NO.	SEQ. NO.	SEQ. NO.	SEQ. NO.
56	340	360	134	360	6	360	14

TABLE G1. - RADIOMETRIC ERROR ANALYSIS RESULTS - Continued

ERROR NO. 4
LOCATOR L2
VALUE .15

	H MEAN	H SIGMA	DH MEAN	DH SIGMA	THETA MEAN	THETA SIGMA	DTHETA MEAN	DTHETA SIGMA
APR-	.518478E 02	.207961E 00	-.585134E-05	.281053E-04	.324868E-02	.260235E-02	.403483E-06	.328035E-06
AUG-	.510546E 02	.443123E 00	-.771557E-05	.271165E-04	.724196E-02	.504764E-02	.419840E-06	.165133E-06
OCT-	.509757E 02	.895655E 00	.147099E-05	.276509E-04	.117287E-01	.783762E-02	.209948E-06	.161033E-06
JAN-	.497236E 02	.149626E 01	.384113E-05	.330951E-04	.216601E-01	.141664E-01	.383542E-06	.269528E-06
TOT-	.509004E 02	.118242E 01	-.206370E-05	.294903E-04	.109448E-01	.109614E-01	.354903E-06	.255861E-06

MAX H	MIN H	MAX DH	MIN DH	MAX THETA	MIN THETA	MAX DTHETA	MIN DTHETA
.525990E 02	.470000E 02	.488551E-04	-.499997E-04	.455519E-01	.233733E-03	.958104E-06	.328728E-08
SEQ. NO.	SEQ. NO.	SEQ. NO.	SEQ. NO.	SEQ. NO.	SEQ. NO.	SEQ. NO.	SEQ. NO.
214	347	342	346	378	337	1	346

ERROR NO. 4
LOCATOR L2
VALUE .90

	H MEAN	H SIGMA	DH MEAN	DH SIGMA	THETA MEAN	THETA SIGMA	DTHETA MEAN	DTHETA SIGMA
APR-	.267705E 02	.215363E 01	-.116173E-04	.269698E-04	.315550E-01	.128629E-01	.435460E-06	.264662E-06
AUG-	.269241E 02	.467035E 00	.473050E-05	.301541E-04	.653089E-02	.492592E-02	.414587E-06	.352380E-06
OCT-	.253770E 02	.225817E 01	.906358E-05	.267224E-04	.331035E-01	.151659E-01	.304591E-06	.183189E-06
JAN-	.240723E 02	.260249E 01	-.106163E-05	.238654E-04	.380512E-01	.185954E-01	.285334E-06	.207293E-06
TOT-	.257860E 02	.235255E 01	.278791E-06	.281096E-04	.273101E-01	.184678E-01	.359993E-06	.268359E-06

MAX H	MIN H	MAX DH	MIN DH	MAX THETA	MIN THETA	MAX DTHETA	MIN DTHETA
.297327E 02	.190415E 02	.490567E-04	-.497715E-04	.793130E-01	.593267E-03	.103497E-05	.261934E-11
SEQ. NO.	SEQ. NO.	SEQ. NO.	SEQ. NO.	SEQ. NO.	SEQ. NO.	SEQ. NO.	SEQ. NO.
52	360	43	371	378	125	8	178

TABLE G1. - RADIOMETRIC ERROR ANALYSIS RESULTS - Continued

ERROR NO. 4
LOCATOR L3
VALUE 4.50

	H MEAN	H SIGMA	DH MEAN	DH SIGMA	THETA MEAN	THETA SIGMA	DTHETA MEAN	DTHETA SIGMA
APR-	.533588E 02	.294418E 00	.290294E 00	.140794E-01	.480705E-02	.241347E-02	.224019E-03	.136727E-03
AUG-	.528193E 02	.661755E 00	.304201E 00	.276638E-01	.101720E-01	.685270E-02	.377295E-03	.264820E-03
OCT-	.521786E 02	.101939E 01	.316373E 00	.216790E-01	.137804E-01	.803040E-02	.298874E-03	.216949E-03
JAN-	.508343E 02	.151440E 01	.340978E 00	.332313E-01	.214369E-01	.117455E-01	.461348E-03	.298506E-03
TOT-	.522977E 02	.136113E 01	.312962E 00	.313247E-01	.125491E-01	.100166E-01	.340384E-03	.253109E-03

MAX H	MIN H	MAX DH	MIN DH	MAX THETA	MIN THETA	MAX DTHETA	MIN DTHETA
.539623E 02	.472449E 02	.392957E 00	.260098E 00	.331668E-01	.268256E-04	.105570E-02	.593318E-05
SEQ. NO.	SEQ. NO.	SEQ. NO.	SEQ. NO.	SEQ. NO.	SEQ. NO.	SEQ. NO.	SEQ. NO.
56	360	360	122	372	173	372	24

ERROR NO. 4
LOCATOR L3
VALUE 20.00

	H MEAN	H SIGMA	DH MEAN	DH SIGMA	THETA MEAN	THETA SIGMA	DTHETA MEAN	DTHETA SIGMA
APR-	.435873E 02	.493536E 00	.422642E 00	.197237E-01	.805473E-02	.393048E-02	.268713E-03	.171815E-03
AUG-	.419459E 02	.955615E 00	.424850E 00	.242588E-01	.142545E-01	.776269E-02	.391081E-03	.228771E-03
OCT-	.407432E 02	.153766E 01	.451329E 00	.343639E-01	.220111E-01	.895276E-02	.488423E-03	.280291E-03
JAN-	.386981E 02	.249850E 01	.485936E 00	.403463E-01	.362260E-01	.167811E-01	.529183E-03	.383087E-03
TOT-	.409936E 02	.215019E 01	.446189E 00	.400070E-01	.201366E-01	.148359E-01	.419350E-03	.294746E-03

MAX H	MIN H	MAX DH	MIN DH	MAX THETA	MIN THETA	MAX DTHETA	MIN DTHETA
.435612E 02	.333910E 02	.542467E 00	.392108E 00	.662836E-01	.984954E-03	.129627E-02	.100572E-04
SEQ. NO.	SEQ. NO.	SEQ. NO.	SEQ. NO.	SEQ. NO.	SEQ. NO.	SEQ. NO.	SEQ. NO.
139	360	360	211	378	158	378	338

TABLE G1. - RADIOMETRIC ERROR ANALYSIS RESULTS - Continued

ERROR NO. 4
LOCATOR L4
VALUE 2.50

	H MEAN	H SIGMA	DH MEAN	DH SIGMA	THETA MEAN	THETA SIGMA	DTHETA MEAN	DTHETA SIGMA
APR-	.449041E 02	.326113E 00	-.144978E-04	.257174E-04	.478340E-02	.387008E-02	.361675E-06	.275984E-06
AUG-	.442812E 02	.438[illegible]9E 00	.424016E-06	.261728E-04	.742503E-02	.506140E-02	.321273E-06	.186738E-06
OCT-	.441469E 02	.967[illegible]2E 00	-.537455E-05	.297978E-04	.128385E-01	.791234E-02	.379516E-06	.294205E-06
JAN-	.430771E 02	.139227E 01	-.223637E-05	.270184E-04	.196072E-01	.128954E-01	.319482E-06	.193767E-06
TOT-	.441023E 02	.110701E 01	-.542117E-05	.277984E-04	.111635E-01	.997841E-02	.345486E-06	.243836E-06

MAX H	MIN H	MAX DH	MIN DH	MAX THETA	MIN THETA	MAX DTHETA	MIN DTHETA
.457329E 02	.406633E 02	.494218E-04	-.480996E-04	.395527E-01	.783960E-04	.104952E-05	.778469E-08
SEQ. NO.	SEQ. NO.	SEQ. NO.	SEQ. NO.	SEQ. NO.	SEQ. NO.	SEQ. NO.	SEQ. NO.
56	367	376	5	378	182	2	184

ERROR NO. 4
LOCATOR L4
VALUE 10.00

	H MEAN	H SIGMA	DH MEAN	DH SIGMA	THETA MEAN	THETA SIGMA	DTHETA MEAN	DTHETA SIGMA
APR-	.311021E 02	.952755E 00	.791273E-05	.324468E-04	.133628E-01	.106988E-01	.421894E-06	.285114E-06
AUG-	.306694E 02	.408427E 00	.607756E-05	.266293E-04	.586102E-02	.500316E-02	.386802E-06	.285855E-06
OCT-	.299877E 02	.151038E 01	-.122926E-05	.294777E-04	.218236E-01	.101504E-01	.404585E-06	.247520E-06
JAN-	.284885E 02	.196514E 01	.380552E-05	.284665E-04	.267820E-01	.154305E-01	.411488E-06	.294796E-06
TOT-	.300844E 02	.165542E 01	.414164E-05	.295301E-04	.169573E-01	.135727E-01	.406192E-06	.279208E-06

MAX H	MIN H	MAX DH	MIN DH	MAX THETA	MIN THETA	MAX DTHETA	MIN DTHETA
.328338E 02	.253631E 02	.497270E-04	-.484143E-04	.603502E-01	.142127E-03	.104810E-05	.465981E-08
SEQ. NO.	SEQ. NO.	SEQ. NO.	SEQ. NO.	SEQ. NO.	SEQ. NO.	SEQ. NO.	SEQ. NO.
56	367	20	126	378	128	46	139

TABLE G1. - RADIOMETRIC ERROR ANALYSIS RESULTS - Continued

ERROR NO. 5
LOCATOR L1
VALUE 2.00

	H MEAN	H SIGMA	DH MEAN	DH SIGMA	THETA MEAN	THETA SIGMA	DTHETA MEAN	DTHETA SIGMA
APR=	.437291E 02	.880444E 00	.539951E-02	.580616E-03	.125001E-01	.863197E-02	.819751E-05	.605015E-05
AUG=	.429969E 02	.148332E 01	.540189E-02	.732134E-03	.231491E-01	.942303E-02	.979799E-05	.788148E-05
OCT=	.411596E 02	.236175E 01	.601035E-02	.117796E-02	.344229E-01	.140005E-01	.160722E-04	.107851E-04
JAN=	.382225E 02	.349999E 01	.667919E-02	.869463E-03	.511964E-01	.234230E-01	.110374E-04	.897460E-05
TOT=	.415245E 02	.311299E 01	.587981E-02	.101629E-02	.303171E-01	.207941E-01	.112763E-04	.908716E-05

MAX H	MIN H	MAX DH	MIN DH	MAX THETA	MIN THETA	MAX DTHETA	MIN DTHETA
.451717E 02	.313129E 02	.999160E-02	.482916E-02	.104330E 00	.247105E-03	.469477E-04	.176531E-06
SEQ. NO.	SEQ. NO.	SEQ. NO.	SEQ. NO.	SEQ. NO.	SEQ. NO.	SEQ. NO.	SEQ. NO.
139	36[illegible]	195	48	378	16	195	6

ERROR NO. 5
LOCATOR L1
VALUE 3.00

	H MEAN	H SIGMA	DH MEAN	DH SIGMA	THETA MEAN	THETA SIGMA	DTHETA MEAN	DTHETA SIGMA
APR=	.396589E 02	.132956E 01	.482198E-02	.116750E-02	.212097E-01	.126075E-01	.125258E-04	.138487E-04
AUG=	.392558E 02	.135175E 01	.423248E-02	.682630E-03	.199711E-01	.790867E-02	.105278E-04	.413681E-05
OCT=	.354548E 02	.261153E 01	.554824E-02	.131642E-02	.386817E-01	.139716E-01	.190105E-04	.115651E-04
JAN=	.321476E 02	.421117E 01	.573309E-02	.199210E-02	.574690E-01	.322680E-01	.253715E-04	.232132E-04
TOT=	.361292E 02	.371[illegible]E 01	.508395E-02	.149578E-02	.343329E-01	.244469E-01	.168589E-04	.159488E-04

MAX H	MIN H	MAX DH	MIN DH	MAX THETA	MIN THETA	MAX DTHETA	MIN DTHETA
.406733E 02	.19[illegible]E 02	.123831E-01	.288904E-02	.122413E 00	.233020E-02	.563490E-04	.132789E-05
SEQ. NO.	SEQ. NO.	SEQ. NO.	SEQ. NO.	SEQ. NO.	SEQ. NO.	SEQ. NO.	SEQ. NO.
56	360	360	134	360	6	360	349

TABLE G1. - RADIOMETRIC ERROR ANALYSIS RESULTS - Continued

ERROR NO. 5
LOCATOR L2
VALUE .15

	H MEAN	H SIGMA	DH MEAN	DH SIGMA	THETA MEAN	THETA SIGMA	DTHETA MEAN	DTHETA SIGMA
APR-	.518551E 02	.208056E 00	.725689E-02	.231180E-02	.325759E-02	.259779E-02	.293194E-04	.227195E-04
AUG-	.510625E 02	.441793E 00	.789635E-02	.232503E-02	.722487E-02	.502882E-02	.396359E-04	.218506E-04
OCT-	.509855E 02	.894911E 00	.979260E-02	.280187E-02	.117268E-01	.781501E-02	.335422E-04	.301284E-04
JAN-	.497339E 02	.149443E 01	.103578E-01	.341621E-02	.215331E-01	.141653E-01	.503883E-04	.333701E-04
TOT-	.509093E 02	.118086E 01	.882442E-02	.303715E-02	.109341E-01	.109478E-01	.382214E-04	.285748E-04

MAX H	MIN H	MAX DH	MIN DH	MAX THETA	MIN THETA	MAX DTHETA	MIN DTHETA
.526057E 02	.470065E 02	.182091E-01	.427792E-02	.455132E-01	.274994E-03	.136716E-03	.198531E-06
SEQ. NO.	SEQ. NO.	SEQ. NO.	SEQ. NO.	SEQ. NO.	SEQ. NO.	SEQ. NO.	SEQ. NO.
214	367	195	134	378	2	360	169

ERROR NO. 5
LOCATOR L2
VALUE .90

	H MEAN	H SIGMA	DH MEAN	DH SIGMA	THETA MEAN	THETA SIGMA	DTHETA MEAN	DTHETA SIGMA
APR-	.267709E 02	.216357E 01	.381203E-03	.868920E-03	.315522E-01	.128609E-01	.910564E-05	.121898E-04
AUG-	.269251E 02	.467858E 00	.101724E-02	.171332E-02	.654162E-02	.492885E-02	.137941E-04	.181175E-04
OCT-	.253776E 02	.225811E 01	.596017E-03	.120670E-02	.331064E-01	.151698E-01	.119158E-04	.169819E-04
JAN-	.240733E 02	.260193E 01	.943418E-03	.160543E-02	.380363E-01	.186059E-01	.197434E-04	.206986E-04
TOT-	.257867E 02	.235213E 01	.734469E-03	.141347E-02	.273090E-01	.184662E-01	.136397E-04	.177092E-04

MAX H	MIN H	MAX DH	MIN DH	MAX THETA	MIN THETA	MAX DTHETA	MIN DTHETA
.297327E 02	.190417E 02	.522670E-02	-.497715E-04	.793130E-01	.639373E-03	.585586E-04	.261934E-11
SEQ. NO.	SEQ. NO.	SEQ. NO.	SEQ. NO.	SEQ. NO.	SEQ. NO.	SEQ. NO.	SEQ. NO.
52	360	339	371	378	125	339	178

TABLE G1. - RADIOMETRIC ERROR ANALYSIS RESULTS - Continued

ERROR NO. 5
LOCATOR L3
VALUE 1.50

	H MEAN	H SIGMA	DH MEAN	DH SIGMA	THETA MEAN	THETA SIGMA	DTHETA MEAN	DTHETA SIGMA
APR-	.531049E 02	.306014E 00	.364539E-01	.216413E-02	.999489E-02	.252678E-02	.347756E-04	.202960E-04
AUG-	.525528E 02	.571[illegible]E 00	.376923E-01	.362[illegible]E-02	.102882E-01	.694345E-02	.441347E-04	.317921E-04
OCT-	.519029E 02	.102[illegible]E 01	.407299E-01	.345796E-02	.138688E-01	.795645E-02	.405996E-04	.254826E-04
JAN-	.505396E 02	.153559E 01	.462960E-01	.699206E-02	.217825E-01	.118778E-01	.101401E-03	.688240E-04
TOT-	.520251E 02	.133032E 01	.402932E-01	.584006E-02	.127335E-01	.100998E-01	.552277E-04	.492343E-04

MAX H	MIN H	MAX DH	MIN DH	MAX THETA	MIN THETA	MAX DTHETA	MIN DTHETA
.537331E 02	.469048E 02	.568791E-01	.319974E-01	.340303E-01	.730728E-04	.250753E-03	.219779E-05
SEQ. NO.	SEQ. NO.	SEQ. NO.	SEQ. NO.	SEQ. NO.	SEQ. NO.	SEQ. NO.	SEQ. NO.
56	36[illegible]	360	122	372	27	378	27

ERROR NO. 5
LOCATOR L3
VALUE 20.00

	H MEAN	H SIGMA	DH MEAN	DH SIGMA	THETA MEAN	THETA SIGMA	DTHETA MEAN	DTHETA SIGMA
APR-	.421812E 02	.506727E 00	.165070E-01	.100099E-02	.825571E-02	.405437E-02	.131294E-04	.910967E-05
AUG-	.415380E 02	.971736E 00	.169171E-01	.143407E-02	.146033E-01	.767715E-02	.212653E-04	.120049E-04
OCT-	.403103E 02	.156409E 01	.183763E-01	.231738E-02	.224535E-01	.898913E-02	.333094E-04	.164943E-04
JAN-	.382330E 02	.252153E 01	.208482E-01	.265153E-02	.367147E-01	.169375E-01	.369481E-04	.199737E-04
TOT-	.405656E 02	.218332E 01	.181622E-01	.259856E-02	.205068E-01	.149540E-01	.261630E-04	.177438E-04

MAX H	MIN H	MAX DH	MIN DH	MAX THETA	MIN THETA	MAX DTHETA	MIN DTHETA
.331656E 02	.328239E 02	.253763E-01	.147489E-01	.674940E-01	.162574E-02	.858718E-04	.113150E-06
SEQ. NO.	SEQ. NO.	SEQ. NO.	SEQ. NO.	SEQ. NO.	SEQ. NO.	SEQ. NO.	SEQ. NO.
139	36[illegible]	360	52	378	158	378	114

TABLE G1. - RADIOMETRIC ERROR ANALYSIS RESULTS - Continued

ERROR NO. 5
LOCATION L4
VALUE 2.50

	H MEAN	H SIGMA	DH MEAN	DH SIGMA	THETA MEAN	THETA SIGMA	DTHETA MEAN	DTHETA SIGMA
APR=	.349223E 02	.325256E 00	.181370E-01	.112876E-02	.377423E-02	.386145E-02	.162120E-04	.961607E-05
AUG=	.342997E 02	.433257E 00	.184703E-01	.187546E-02	.742011E-02	.504869E-02	.258483E-04	.118798E-04
OCT=	.331684E 02	.965565E 00	.214393E-01	.278958E-02	.128070E-01	.790098E-02	.387328E-04	.191236E-04
JAN=	.431027E 02	.133727E 01	.255843E-01	.513290E-02	.195385E-01	.128735E-01	.742375E-04	.284670E-04
TOT=	.441232E 02	.113312E 01	.209080E-01	.432115E-02	.111352E-01	.995276E-02	.387576E-04	.289113E-04

MAX H	MIN H	MAX DH	MIN DH	MAX THETA	MIN THETA	MAX DTHETA	MIN DTHETA
.457196E 02	.405933E 02	.385923E-01	.154609E-01	.394174E-01	.423464E-04	.135381E-03	.167426E-06
SEQ. NO.	SEQ. NO.	SEQ. NO.	SEQ. NO.	SEQ. NO.	SEQ. NO.	SEQ. NO.	SEQ. NO.
55	367	360	139	378	182	378	42

ERROR NO. 5
LOCATION L4
VALUE 10.00

	H MEAN	H SIGMA	DH MEAN	DH SIGMA	THETA MEAN	THETA SIGMA	DTHETA MEAN	DTHETA SIGMA
APR=	.312006E 02	.952170E 00	.154019E-02	.660205E-03	.133539E-01	.106953E-01	.937997E-05	.617778E-05
AUG=	.306780E 02	.408036E 00	.357558E-02	.673214E-03	.585695E-02	.499945E-02	.954434E-05	.431771E-05
OCT=	.299077E 02	.150997E 01	.100583E-01	.117143E-02	.218077E-01	.101488E-01	.169605E-04	.861095E-05
JAN=	.285000E 02	.163300E 01	.114210E-01	.201655E-02	.267577E-01	.154275E-01	.256712E-04	.182718E-04
TOT=	.300941E 02	.165203E 01	.964889E-02	.173419E-02	.160438E-01	.135661E-01	.153890E-04	.126815E-04

MAX H	MIN H	MAX DH	MIN DH	MAX THETA	MIN THETA	MAX DTHETA	MIN DTHETA
.328614E 02	.253700E 02	.189379E-01	.741138E-02	.603115E-01	.151123E-03	.706146E-04	.649191E-06
SEQ. NO.	SEQ. NO.	SEQ. NO.	SEQ. NO.	SEQ. NO.	SEQ. NO.	SEQ. NO.	SEQ. NO.
56	367	360	136	378	128	360	337

TABLE G1. - RADIOMETRIC ERROR ANALYSIS RESULTS - Continued

ERROR NO. 6
LOCATION 11
VALUE 1.00

	H MEAN	H SIGMA	DH MEAN	DH SIGMA	THETA MEAN	THETA SIGMA	DTHETA MEAN	DTHETA SIGMA
APR=	.437454E 02	.473374E 00	.216246E-01	.228039E-02	.124753E-01	.861790E-02	.335503E-04	.234716E-04
AUG=	.[illegible]33E 02	[illegible]	.217452E-01	.301660E-02	.231410E-01	.942416E-02	.405164E-04	.325289E-04
OCT=	.411776E 02	[illegible]	.241825E-01	.491581E-02	.243767E-01	.139777E-01	.654442E-04	.476217E-04
JAN=	.382427E 02	[illegible]	.263664E-01	.339157E-02	.511843E-01	.234236E-01	.412955E-04	.346954E-04
TOT=	.415423E 02	[illegible]	.235797E-01	.418950E-02	.302955E-01	.207901E-01	.452016E-04	.376277E-04

MAX H	MIN H	MAX DH	MIN DH	MAX THETA	MIN THETA	MAX DTHETA	MIN DTHETA
.451907E 02	[illegible]	.413726E-01	.190889E-01	.104300E 00	.253414E-03	.210655E-03	.187905E-05
SEQ. NO.	SEQ. NO.	SEQ. NO.	SEQ. NO.	SEQ. NO.	SEQ. NO.	SEQ. NO.	SEQ. NO.
139	[illegible]	195	48	378	16	195	6

ERROR NO. 9
LOCATION 11
VALUE 3.00

	H MEAN	H SIGMA	DH MEAN	DH SIGMA	THETA MEAN	THETA SIGMA	DTHETA MEAN	DTHETA SIGMA
APR=	.326730E 02	[illegible]	.193243E-01	.462129E-02	.211814E-01	.125937E-01	.487935E-04	.556466E-04
AUG=	.332686E 02	[illegible]	.171013E-01	.264906E-02	.199847E-01	.792227E-02	.393392E-04	.180326E-04
OCT=	.354715E 02	[illegible]	.222609E-01	.526729E-02	.386517E-01	.133703E-01	.772212E-04	.464584E-04
JAN=	.321949E 02	[illegible]	.229075E-01	.732911E-02	.574213E-01	.322172E-01	.996296E-04	.917976E-04
TOT=	.361445E 02	[illegible]	.233233E-01	.596884E-02	.343097E-01	.244184E-01	.662459E-04	.637777E-04

MAX H	MIN H	MAX DH	MIN DH	MAX THETA	MIN THETA	MAX DTHETA	MIN DTHETA
.406845E 02	[illegible]	.435043E-01	.120242E-01	.122154E 00	.232229E-02	.345434E-03	.444884E-05
SEQ. NO.	SEQ. NO.	SEQ. NO.	SEQ. NO.	SEQ. NO.	SEQ. NO.	SEQ. NO.	SEQ. NO.
56	[illegible]	360	134	360	6	360	349

TABLE G1. - RADIOMETRIC ERROR ANALYSIS RESULTS - Continued

ERROR NO. 6
LOCATOR L2
VALUE .15

	H MEAN	H SIGMA	DH MEAN	DH SIGMA	THETA MEAN	THETA SIGMA	DTHETA MEAN	DTHETA SIGMA
APR-	.518772E 02	.208186E 00	.293862E-01	.180207E-02	.326127E-02	.260670E-02	.231363E-04	.146636E-04
AUG-	.510848E 02	.441010E 00	.301373E-01	.339131E-02	.722342E-02	.502554E-02	.414812E-04	.177901E-04
OCT-	.510140E 02	.897577E 00	.332444E-01	.678660E-02	.117033E-01	.780919E-02	.905027E-04	.717769E-04
JAN-	.497641E 02	.148031E 01	.405354E-01	.943019E-02	.214872E-01	.141155E-01	.128870E-03	.767093E-04
TOT-	.509350E 02	.117706E 01	.345758E-01	.783171E-02	.109189E-01	.109188E-01	.709975E-04	.679326E-04

MAX H	MIN H	MAX DH	MIN DH	MAX THETA	MIN THETA	MAX DTHETA	MIN DTHETA
.526283E 02	.470455E 02	.605153E-01	.254206E-01	.452933E-01	.239731E-03	.300433E-03	.307006E-05
SEQ. NO.	SEQ. NO.	SEQ. NO.	SEQ. NO.	SEQ. NO.	SEQ. NO.	SEQ. NO.	SEQ. NO.
214	367	363	136	378	2	363	6

ERROR NO. 6
LOCATOR L2
VALUE .90

	H MEAN	H SIGMA	DH MEAN	DH SIGMA	THETA MEAN	THETA SIGMA	DTHETA MEAN	DTHETA SIGMA
APR-	.267736E 02	.216[illegible]E 01	.312623E-02	.183757E-02	.315450E-01	.129605E-01	.259825E-04	.166265E-04
AUG-	.269274E 02	.467251E 00	.329677E-02	.170827E-02	.653829E-02	.492253E-02	.198681E-04	.141880E-04
OCT-	.253806E 02	.225743E 01	.353677E-02	.155474E-02	.330988E-01	.151560E-01	.195113E-04	.147229E-04
JAN-	.240759E 02	.260193E 01	.359212E-02	.180824E-02	.380336E-01	.185907E-01	.230321E-04	.173022E-04
TOT-	.257894E 02	.235[illegible]E 01	.334707E-02	.174085E-02	.273071E-01	.184602E-01	.220985E-04	.159804E-04

MAX H	MIN H	MAX DH	MIN DH	MAX THETA	MIN THETA	MAX DTHETA	MIN DTHETA
.297376E 02	.192[illegible]E 02	.683216E-02	-.378448E-04	.792803E-01	.626171E-03	.595947E-04	.254912E-06
SEQ. NO.	SEQ. NO.	SEQ. NO.	SEQ. NO.	SEQ. NO.	SEQ. NO.	SEQ. NO.	SEQ. NO.
52	3[illegible]	363	115	378	125	36	115

TABLE G1. - RADIOMETRIC ERROR ANALYSIS RESULTS - Continued

ERROR NO. 6
LOCATION L3
VALUE 1.50

	H MEAN	H SIGMA	DH MEAN	DH SIGMA	THETA MEAN	THETA SIGMA	DTHETA MEAN	DTHETA SIGMA
APR=	.532137E 02	.299388E 00	.145227E 00	.860257E-02	.489194E-02	.246707E-02	.138116E-03	.808924E-04
AUG=	.526691E 02	.6[illegible]E 00	.253994E 00	.150170E-01	.101933E-01	.687959E-02	.199907E-03	.138880E-03
OCT=	.530257E 02	.1[illegible]E 01	.133455E 00	.139028E-01	.137752E-01	.795790E-02	.184621E-03	.104729E-03
JAN=	.506791E 02	.151720E 01	.195748E 00	.269903E-01	.214921E-01	.117497E-01	.391772E-03	.242035E-03
TOT=	.521469E 02	.136369E 01	.162106E 00	.230907E-01	.125835E-01	.100054E-01	.228604E-03	.182312E-03

MAX H	MIN H	MAX DH	MIN DH	MAX THETA	MIN THETA	MAX DTHETA	MIN DTHETA
.538287E 02	.47[illegible]E 02	.234991E 00	.127576E 00	.334639E-01	.782254E-04	.827833E-03	.735040E-05
SEQ. NO.	SEQ. NO.	SEQ. NO.	SEQ. NO.	SEQ. NO.	SEQ. NO.	SEQ. NO.	SEQ. NO.
56	[illegible]	360	122	372	27	342	27

ERROR NO. 6
LOCATION L3
VALUE 21.00

	H MEAN	H SIGMA	DH MEAN	DH SIGMA	THETA MEAN	THETA SIGMA	DTHETA MEAN	DTHETA SIGMA
APR=	.422306E 02	.5[illegible]E 00	.653377E-01	.399140E-02	.822029E-02	.402943E-02	.523961E-04	.360946E-04
AUG=	.415886E 02	.962229E 00	.675643E-01	.570574E-02	.145410E-01	.767314E-02	.846131E-04	.474497E-04
OCT=	.403657E 02	.155737E 01	.737861E-01	.907338E-02	.223580E-01	.897028E-02	.128815E-03	.585334E-04
JAN=	.382961E 02	.251[illegible]E 01	.539924E-01	.110143E-01	.365901E-01	.168984E-01	.152598E-03	.788644E-04
TOT=	.406203E 02	.217[illegible]E 01	.727951E-01	.106144E-01	.204297E-01	.149167E-01	.104605E-03	.693090E-04

MAX H	MIN H	MAX DH	MIN DH	MAX THETA	MIN THETA	MAX DTHETA	MIN DTHETA
.432132E 02	.32[illegible]E 02	.102263E 00	.588912E-01	.672366E-01	.154060E-02	.343244E-03	.122762E-05
SEQ. NO.	SEQ. NO.	SEQ. NO.	SEQ. NO.	SEQ. NO.	SEQ. NO.	SEQ. NO.	SEQ. NO.
139	[illegible]	363	52	378	158	378	114

TABLE G1. - RADIOMETRIC ERROR ANALYSIS RESULTS - Continued

ERROR NO. 5
LOCATOR L4
VALUE 2.50

	H MEAN	H SIGMA	DH MEAN	DH SIGMA	THETA MEAN	THETA SIGMA	DTHETA MEAN	DTHETA SIGMA
APR-	.449769E 02	.322792E 00	.728275E-01	.445919E-02	.474874E-02	.383744E-02	.616801E-04	.361579E-04
AUG-	.443552E 02	.435702E 00	.739715E-01	.739704E-02	.740174E-02	.501541E-02	.101198E-03	.453967E-04
OCT-	.442327E 02	.958988E 00	.857895E-01	.111538E-01	.127212E-01	.785244E-02	.160401E-03	.725334E-04
JAN-	.431793E 02	.137397E 01	.102177E 00	.203929E-01	.193314E-01	.128067E-01	.297054E-03	.116237E-03
TOT-	.441860E 02	.109218E 01	.836913E-01	.171281E-01	.110500E-01	.987348E-02	.155083E-03	.116138E-03

MAX H	MIN H	MAX DH	MIN DH	MAX THETA	MIN THETA	MAX DTHETA	MIN DTHETA
.457991E 02	.407876E 02	.153676E 00	.615598E-01	.390090E-01	.774525E-04	.543732E-03	.568381E-05
SEQ. NO.	SEQ. NO.	SEQ. NO.	SEQ. NO.	SEQ. NO.	SEQ. NO.	SEQ. NO.	SEQ. NO.
56	367	360	139	378	182	378	42

ERROR NO. 6
LOCATOR L4
VALUE 10.00

	H MEAN	H SIGMA	DH MEAN	DH SIGMA	THETA MEAN	THETA SIGMA	DTHETA MEAN	DTHETA SIGMA
APR-	.312962E 02	.950604E 00	.341308E-01	.262317E-02	.133276E-01	.106861E-01	.366083E-04	.242567E-04
AUG-	.307037E 02	.406784E 00	.342030E-01	.265346E-02	.584555E-02	.498791E-02	.380080E-04	.167982E-04
OCT-	.310279E 02	.130601E 01	.402173E-01	.467797E-02	.617572E-01	.101455E-01	.678237E-04	.327811E-04
JAN-	.285342E 02	.135[illegible]E 01	.458809E-01	.802354E-02	.266858E-01	.154192E-01	.102496E-03	.718297E-04
TOT-	.301230E 02	.134[illegible]E 01	.385905E-01	.601845E-02	.169040E-01	.135469E-01	.612340E-04	.499913E-04

MAX H	MIN H	MAX DH	MIN DH	MAX THETA	MIN THETA	MAX DTHETA	MIN DTHETA
.328644E 02	.234[illegible]E 02	.730612E-01	.297153E-01	.601975E-01	.176785E-03	.275935E-03	.410163E-07
SEQ. NO.	SEQ. NO.	SEQ. NO.	SEQ. NO.	SEQ. NO.	SEQ. NO.	SEQ. NO.	SEQ. NO.
56	367	360	136	378	128	360	114

TABLE G1. - RADIOMETRIC ERROR ANALYSIS RESULTS - Continued

ERROR NO. 7
LOCATION L1
VALUE 2.00

	H MEAN	H SIGMA	DH MEAN	DH SIGMA	THETA MEAN	THETA SIGMA	DTHETA MEAN	DTHETA SIGMA
APR=	.437778E 02	.976[illegible]E 00	.541039E-01	.567867E-02	.124324E-01	.859069E-02	.839681E-04	.572955E-04
AUG=	.430362E 02	.3[illegible]E 01	.546913E-01	.824662E-02	.231191E-01	.943093E-02	.107792E-03	.945376E-04
OCT=	.412142E 02	.2[illegible]E 01	.5[illegible]E-01	.123845E-01	.342892E-01	.139258E-01	.161033E-03	.124162E-03
JAN=	.382831E 02	.3[illegible]E 01	.672768E-01	.846686E-02	.511673E-01	.234247E-01	.101004E-03	.870146E-04
JUL=	.415778E 02	.31[illegible]E 01	.591720E-01	.104663E-01	.302521E-01	.207821E-01	.113449E-03	.981429E-04

MAX H	MIN H	MAX DH	MIN DH	MAX THETA	MIN THETA	MAX DTHETA	MIN DTHETA
.452288E 02	.31[illegible]E 02	.105147E 00	.450880E-01	.104233E 00	.266032E-03	.543791E-03	.528409E-05
SEQ. NO.	SEQ. NO.	SEQ. NO.	SEQ. NO.	SEQ. NO.	SEQ. NO.	SEQ. NO.	SEQ. NO.
139	[illegible]	195	48	378	16	195	6

ERROR NO. 7
LOCATION L1
VALUE 3.00

	H MEAN	H SIGMA	DH MEAN	DH SIGMA	THETA MEAN	THETA SIGMA	DTHETA MEAN	DTHETA SIGMA
APR=	.397320E 02	.13[illegible]E 01	.443423E-01	.115290E-01	.211243E-01	.125669E-01	.121024E-03	.139435E-03
AUG=	.382944E 02	.135[illegible]E 01	.433515E-01	.657877E-02	.200116E-01	.793942E-02	.966765E-04	.462532E-04
OCT=	.355148E 02	.2[illegible]E 01	.555256E-01	.127172E-01	.385963E-01	.139677E-01	.190514E-03	.108753E-03
JAN=	.321395E 02	.1[illegible]E 01	.575551E-01	.104890E-01	.573250E-01	.321156E-01	.248251E-03	.228811E-03
JUL=	.361752E 02	.3[illegible]E 01	.511686E-01	.146174E-01	.342641E-01	.243617E-01	.164116E-03	.158069E-03

MAX H	MIN H	MAX DH	MIN DH	MAX THETA	MIN THETA	MAX DTHETA	MIN DTHETA
.407067E 02	.3[illegible]E 02	.104046E 00	.304489E-01	.121615E 00	.230648E-02	.863603E-03	.106907E-04
SEQ. NO.	SEQ. NO.	SEQ. NO.	SEQ. NO.	SEQ. NO.	SEQ. NO.	SEQ. NO.	SEQ. NO.
56	[illegible]	360	134	360	6	360	349

TABLE G1. - RADIOMETRIC ERROR ANALYSIS RESULTS - Continued

ERROR NO. 7
LOCATOR L2
VALUE .15

	H MEAN	H SIGMA	DH MEAN	DH SIGMA	THETA MEAN	THETA SIGMA	DTHETA MEAN	DTHETA SIGMA
APR-	.519225E 02	.209126E 00	.746917E-01	.345978E-02	.327643E-02	.261176E-02	.530456E-04	.433362E-04
AUG-	.511303E 02	.839405E 00	.755457E-01	.721113E-02	.719078E-02	.500580E-02	.871100E-04	.494715E-04
OCT-	.510719E 02	.8917[illegible]5E 00	.961640E-01	.151541E-01	.116791E-01	.777588E-02	.190473E-03	.149904E-03
JAN-	.498256E 02	.147[illegible]9E 01	.101964E 00	.232357E-01	.213566E-01	.140711E-01	.291886E-03	.213165E-03
TOT-	.509876E 02	.116[illegible]3E 01	.871163E-01	.188531E-01	.108796E-01	.108646E-01	.155629E-03	.163733E-03

MAX H	MIN H	MAX DH	MIN DH	MAX THETA	MIN THETA	MAX DTHETA	MIN DTHETA
.526754E 02	.471169E 02	.153144E 00	.637259E-01	.450299E-01	.269221E-03	.731860E-03	.355995E-07
SEQ. NO.	SEQ. NO.	SEQ. NO.	SEQ. NO.	SEQ. NO.	SEQ. NO.	SEQ. NO.	SEQ. NO.
214	[illegible]	360	134	378	2	363	178

ERROR NO. 7
LOCATOR L2
VALUE .90

	H MEAN	H SIGMA	DH MEAN	DH SIGMA	THETA MEAN	THETA SIGMA	DTHETA MEAN	DTHETA SIGMA
APR-	.267785E 02	.216[illegible]1E 01	.795424E-02	.171210E-02	.315486E-01	.128595E-01	.192638E-04	.978493E-05
AUG-	.269317E 02	.467150E 00	.761113E-02	.174048E-02	.654059E-02	.492061E-02	.216950E-04	.144712E-04
OCT-	.253854E 02	.225[illegible]9E 01	.840120E-02	.201520E-02	.330957E-01	.151458E-01	.263393E-04	.219868E-04
JAN-	.240917E 02	.260[illegible]2E 01	.933844E-02	.196042E-02	.380353E-01	.185987E-01	.215690E-04	.190789E-04
TOT-	.257943E 02	.235[illegible]5E 01	.832875E-02	.195129E-02	.273052E-01	.184576E-01	.222168E-04	.171682E-04

MAX H	MIN H	MAX DH	MIN DH	MAX THETA	MIN THETA	MAX DTHETA	MIN DTHETA
.297426E 02	.19[illegible]E 02	.144570E-01	.329623E-02	.795043E-01	.632937E-03	.788901E-04	.329425E-06
SEQ. NO.	SEQ. NO.	SEQ. NO.	SEQ. NO.	SEQ. NO.	SEQ. NO.	SEQ. NO.	SEQ. NO.
52	[illegible]	339	169	378	125	210	382

TABLE G1. - RADIOMETRIC ERROR ANALYSIS RESULTS - Continued

ERROR NO. 7
LOCATOR 13
VALUE 0.50

	H MEAN	H SIGMA	DH MEAN	DH SIGMA	THETA MEAN	THETA SIGMA	DTHETA MEAN	DTHETA SIGMA
APR=	.534288E 02	.287[illegible]E 00	.360337E 00	.208395E-01	.069516E-02	.235338E-02	.336131E-03	.197465E-03
AUG=	.529032E 02	.64[illegible]E 00	.388131E 00	.389702E-01	.994193E-02	.671814E-02	.514032E-03	.415047E-03
OCT=	.522741E 02	.10[illegible]E 01	.411917E 00	.364031E-01	.135253E-01	.797243E-02	.474958E-03	.310948E-03
JAN=	.509617E 02	.147[illegible]E 01	.468323E 00	.668843E-01	.209391E-01	.114356E-01	.953579E-03	.554296E-03
TOT=	.523920E 02	.133[illegible]E 01	.407177E 00	.593094E-01	.122754E-01	.979056E-02	.569675E-03	.455297E-03

MAX H	MIN H	MAX DH	MIN DH	MAX THETA	MIN THETA	MAX DTHETA	MIN DTHETA
.540234E 02	.474573E 02	.605425E 00	.316670E 00	.323488E-01	.181517E-04	.187370E-02	.159745E-04
SEQ. NO.	SEQ. NO.	SEQ. NO.	SEQ. NO.	SEQ. NO.	SEQ. NO.	SEQ. NO.	SEQ. NO.
56	[illegible]	360	122	372	173	372	148

ERROR NO. 7
LOCATOR 13
VALUE 60.00

	H MEAN	H SIGMA	DH MEAN	DH SIGMA	THETA MEAN	THETA SIGMA	DTHETA MEAN	DTHETA SIGMA
APR=	.423297E 02	.493[illegible]E 00	.165001E 00	.994823E-02	.814909E-02	.397084E-02	.132391E-03	.951278E-04
AUG=	.416904E 02	.961620E 00	.169284E 00	.134549E-01	.144174E-01	.767278E-02	.209822E-03	.101916E-03
OCT=	.404774E 02	.154531E 01	.185516E 00	.220436E-01	.221669E-01	.893920E-02	.316900E-03	.133423E-03
JAN=	.384231E 02	.240[illegible]E 01	.210943E 00	.285271E-01	.363561E-01	.168177E-01	.395575E-03	.197924E-03
TOT=	.407301E 02	.216[illegible]E 01	.182686E 00	.268260E-01	.202731E-01	.148402E-01	.263672E-03	.170864E-03

MAX H	MIN H	MAX DH	MIN DH	MAX THETA	MIN THETA	MAX DTHETA	MIN DTHETA
.433082E 02	.331[illegible]E 02	.260745E 00	.146862E 00	.667255E-01	.137171E-02	.854339E-03	.415970E-05
SEQ. NO.	SEQ. NO.	SEQ. NO.	SEQ. NO.	SEQ. NO.	SEQ. NO.	SEQ. NO.	SEQ. NO.
139	360	360	52	378	158	378	42

TABLE G1. - RADIOMETRIC ERROR ANALYSIS RESULTS - Continued

ERROR NO. 7
LOCATION [illegible]
VALUE 0.50

	H MEAN	H SIGMA	DH MEAN	DH SIGMA	THETA MEAN	THETA SIGMA	DTHETA MEAN	DTHETA SIGMA
APR-	.450977E 02	.31[illegible]E 00	.183557E 00	.101517E-01	.268129E-02	.380006E-02	.139212E-03	.902371E-04
AUG-	.446662E 02	.3[illegible]E 00	.184936E 00	.184145E-01	.735193E-02	.495195E-02	.264131E-03	.109707E-03
OCT-	.443612E 02	.[illegible]E 00	.214272E 00	.278269E-01	.125569E-01	.773746E-02	.409599E-03	.174737E-03
JAN-	.443315E 02	.3[illegible]E 01	.254405E 00	.505363E-01	.189269E-01	.126761E-01	.734638E-03	.286984E-03
TOT-	.443116E 02	.107151E 01	.209303E 00	.421023E-01	.108785E-01	.972004E-02	.386895E-03	.287632E-03

MAX H	MIN H	MAX DH	MIN DH	MAX THETA	MIN THETA	MAX DTHETA	MIN DTHETA
.458084E 02	.409[illegible]E 02	.381726E 00	.153500E 00	.384869E-01	.892918E-04	.135197E-02	.860052E-05
SEQ. NO.	SEQ. NO.	SEQ. NO.	SEQ. NO.	SEQ. NO.	SEQ. NO.	SEQ. NO.	SEQ. NO.
56	3[illegible]	360	139	342	2	378	42

ERROR NO. 7
LOCATION [illegible]
VALUE 10.00

	H MEAN	H SIGMA	DH MEAN	DH SIGMA	THETA MEAN	THETA SIGMA	DTHETA MEAN	DTHETA SIGMA
APR-	.312773E 02	.[illegible]E 00	.152743E-01	.651014E-02	.132759E-01	.106676E-01	.905173E-04	.589698E-04
AUG-	.307550E 02	.[illegible]E 00	.156260E-01	.659989E-02	.592312E-02	.496526E-02	.950329E-04	.403712E-04
OCT-	.300882E 02	.150[illegible]E 01	.100533E 00	.117628E-01	.216590E-01	.101402E-01	.167999E-03	.918977E-04
JAN-	.296927E 02	.1[illegible]E 01	.141[illegible]E 00	.199503E-01	.265427E-01	.154037E-01	.255788E-03	.175353E-03
TOT-	.301408E 02	.1[illegible]E 01	.163943E-01	.172002E-01	.168252E-01	.135091E-01	.152334E-03	.123102E-03

MAX H	MIN H	MAX DH	MIN DH	MAX THETA	MIN THETA	MAX DTHETA	MIN DTHETA
.339100E 02	.2[illegible]E 02	.179494E 00	.743053E-01	.296667E-01	.229500E-03	.687386E-03	.398890E-05
SEQ. NO.	SEQ. NO.	SEQ. NO.	SEQ. NO.	SEQ. NO.	SEQ. NO.	SEQ. NO.	SEQ. NO.
56	367	360	136	378	128	360	46

TABLE G1. - RADIOMETRIC ERROR ANALYSIS RESULTS - Continued

ERROR NO. 8
LOCATION 1
VALUE 3.00

	H MEAN	H SIGMA	DH MEAN	DH SIGMA	THETA MEAN	THETA SIGMA	DTHETA MEAN	DTHETA SIGMA
APR=	.439416E 02	.361[illegible]E 00	.217362E 00	.238254E-01	.122221E-01	.846431E-02	.322101E-03	.240046E-03
AUG=	.432013E 02	.147[illegible]E 01	.219797E 00	.344319E-01	.230009E-01	.946982E-02	.434521E-03	.412509E-03
OCT=	.413081E 02	.232[illegible]E 01	.244535E 00	.503923E-01	.239512E-01	.136595E-01	.644541E-03	.492876E-03
JAN=	.324972E 02	.347[illegible]E 01	.271360E 00	.324366E-01	.510244E-01	.234214E-01	.417481E-03	.309874E-03
TOT=	.317571E 02	.3[illegible]E 01	.238385E 00	.425315E-01	.300247E-01	.207266E-01	.454661E-03	.394382E-03

MAX H	MIN H	MAX DH	MIN DH	MAX THETA	MIN THETA	MAX DTHETA	MIN DTHETA
.354189E 02	.313[illegible]E 02	.424613E 00	.1[illegible]E 00	.103935E 00	.329121E-03	.217685E-02	.223093E-04
SEQ. NO.	SEQ. NO.	SEQ. NO.	SEQ. NO.	SEQ. NO.	SEQ. NO.	SEQ. NO.	SEQ. NO.
133	3[illegible]	195	[illegible]	378	16	195	6

ERROR NO. 8
LOCATION 1
VALUE 3.00

	H MEAN	H SIGMA	DH MEAN	DH SIGMA	THETA MEAN	THETA SIGMA	DTHETA MEAN	DTHETA SIGMA
APR=	.398172E 02	.1[illegible]E 01	.193495E 00	.443251E-01	.208333E-01	.174227E-01	.451309E-03	.556613E-03
AUG=	.374234E 02	.136[illegible]E 01	.171841E 00	.262247E-01	.201511E-01	.810742E-02	.384179E-03	.185832E-03
OCT=	.356674E 02	.2[illegible]E 01	.218134E 00	.422081E-01	.384006E-01	.139202E-01	.656575E-03	.304766E-03
JAN=	.323720E 02	.315[illegible]E 01	.231120E 00	.773576E-01	.568395E-01	.316194E-01	.988091E-03	.915815E-03
TOT=	.363275E 02	.3[illegible]E 01	.283333E 00	.559496E-01	.340561E-01	.240820E-01	.620038E-03	.611729E-03

MAX H	MIN H	MAX DH	MIN DH	MAX THETA	MIN THETA	MAX DTHETA	MIN DTHETA
.3[illegible]179E 02	.1[illegible]E 00	.4[illegible]E 00	.121447E 00	.119365E 00	.212531E-02	.345445E-02	.120831E-03
SEQ. NO.	SEQ. NO.	SEQ. NO.	SEQ. NO.	SEQ. NO.	SEQ. NO.	SEQ. NO.	SEQ. NO.
56	3[illegible]	360	134	360	337	360	16

TABLE G1. - RADIOMETRIC ERROR ANALYSIS RESULTS - Continued

ERROR NO. 8
LOCATOR L2
VALUE .15

	H MEAN	H SIGMA	DH MEAN	DH SIGMA	THETA MEAN	THETA SIGMA	DTHETA MEAN	DTHETA SIGMA
APR=	.521504E 02	.214234E 00	.302545E 00	.135880E-01	.339391E-02	.268520E-02	.213818E-03	.165354E-03
AUG=	.513576E 02	.429312E 00	.302979E 00	.250337E-01	.710159E-02	.493762E-02	.287356E-03	.196294E-03
OCT=	.513634E 02	.381433E 00	.387679E 00	.585670E-01	.115145E-01	.770577E-02	.758397E-03	.591706E-03
JAN=	.501406E 02	.142133E 01	.416930E 00	.103315E 00	.206833E-01	.138896E-01	.130434E-02	.102970E-02
TOT=	.512530E 02	.112832E 01	.352545E 00	.794646E-01	.106483E-01	.105895E-01	.640902E-03	.747970E-03

MAX H	MIN H	MAX DH	MIN DH	MAX THETA	MIN THETA	MAX DTHETA	MIN DTHETA
.529105E 02	.374837E 02	.677669E 00	.258752E 00	.433153E-01	.159657E-03	.363835E-02	.817495E-06
SEQ. NO.	SEQ. NO.	SEQ. NO.	SEQ. NO.	SEQ. NO.	SEQ. NO.	SEQ. NO.	SEQ. NO.
214	347	360	136	379	2	363	42

ERROR NO. 8
LOCATOR L2
VALUE .90

	H MEAN	H SIGMA	DH MEAN	DH SIGMA	THETA MEAN	THETA SIGMA	DTHETA MEAN	DTHETA SIGMA
APR=	.268330E 02	.216[illegible]E 01	.325496E-01	.453331E-02	.315446E-01	.128279E-01	.721679E-04	.479555E-04
AUG=	.269543E 02	.162913E 00	.302845E-01	.355014E-02	.657158E-02	.495844E-02	.487049E-04	.357745E-04
OCT=	.254110E 02	.225436E 01	.339845E-01	.644452E-02	.330531E-01	.150950E-01	.958568E-04	.700652E-04
JAN=	.241085E 02	.259[illegible]E 01	.361787E-01	.650922E-02	.380968E-01	.185971E-01	.695085E-04	.517825E-04
TOT=	.258192E 02	.233[illegible]E 01	.332493E-01	.581045E-02	.272933E-01	.184247E-01	.715596E-04	.554242E-04

MAX H	MIN H	MAX DH	MIN DH	MAX THETA	MIN THETA	MAX DTHETA	MIN DTHETA
.297662E 02	.[illegible]E 02	.383556E-01	.218048E-01	.792423E-01	.627990E-03	.287670E-03	.171595E-05
SEQ. NO.	SEQ. NO.	SEQ. NO.	SEQ. NO.	SEQ. NO.	SEQ. NO.	SEQ. NO.	SEQ. NO.
52	36[illegible]	216	169	378	125	210	349

TABLE G1. - RADIOMETRIC ERROR ANALYSIS RESULTS - Continued

FRIJE NO. 8
LOCATION L3
VALUE [illegible].50

	H MEAN	H SIGMA	DH MEAN	DH SIGMA	THETA MEAN	THETA SIGMA	DTHETA MEAN	DTHETA SIGMA
APR-	.545951E 02	.299[illegible]E 00	.152666E 01	.183208E-01	.[illegible]641E-02	.238205E-02	.268444E-03	.154856E-03
AUG-	.541321E 02	.5[illegible]E 00	.161695E 01	.962942E-01	.905856E-02	.613366E-02	.140191E-02	.836797E-03
OCT-	.535363E 02	.9[illegible]E 00	.167408E 01	.119177E 00	.127709E-01	.715557E-02	.145747E-02	.115010E-02
JAN-	.524222E 02	.127[illegible]E 01	.192885E 01	.262617E 00	.189824E-01	.981577E-02	.393674E-02	.203854E-02
TOT-	.536714E 02	.11[illegible]E 01	.168663E 01	.215197E 00	.111871E-01	.844607E-02	.176614E-02	.182928E-02

MAX H	MIN H	MAX DH	MIN DH	MAX THETA	MIN THETA	MAX DTHETA	MIN DTHETA
.552019E 02	.493[illegible]E 02	.249633E 01	.146285E 01	.287706E-01	.115777E-03	.734912E-02	.323356E-05
SEQ. NO.	SEQ. NO.	SEQ. NO.	SEQ. NO.	SEQ. NO.	SEQ. NO.	SEQ. NO.	SEQ. NO.
56	[illegible]	360	214	372	27	378	182

FRIJE NO. 9
LOCATION L3
VALUE 20.00

	H MEAN	H SIGMA	DH MEAN	DH SIGMA	THETA MEAN	THETA SIGMA	DTHETA MEAN	DTHETA SIGMA
APR-	.428316E 02	.177[illegible]E 00	.066849E 00	.357266E-01	.773859E-02	.378703E-02	.499101E-03	.364460E-03
AUG-	.422046E 02	.924332E 00	.083536E 00	.531952E-01	.138002E-01	.763690E-02	.835425E-03	.391108E-03
OCT-	.410394E 02	.149116E 01	.747529E 00	.798683E-01	.213203E-01	.870433E-02	.116652E-02	.529117E-03
JAN-	.390620E 02	.241[illegible]E 01	.343875E 00	.114132E 00	.351064E-01	.163217E-01	.164628E-02	.817500E-03
TOT-	.412844E 02	.28[illegible]E 01	.736947E 00	.105050E 00	.195037E-01	.144162E-01	.103683E-02	.698576E-03

MAX H	MIN H	MAX DH	MIN DH	MAX THETA	MIN THETA	MAX DTHETA	MIN DTHETA
.437758E 02	.339[illegible]E 02	.106166E 01	.618248E 00	.640467E-01	.607438E-03	.353513E-02	.448313E-04
SEQ. NO.	SEQ. NO.	SEQ. NO.	SEQ. NO.	SEQ. NO.	SEQ. NO.	SEQ. NO.	SEQ. NO.
139	360	360	52	378	158	378	46

TABLE G1. - RADIOMETRIC ERROR ANALYSIS RESULTS - Continued

ERROR NO. 6
LOCATION LA
VALUE [illegible]

	H MEAN	H SIGMA	DH MEAN	DH SIGMA	THETA MEAN	THETA SIGMA	DTHETA MEAN	DTHETA SIGMA
APR-	.456430E 02	.201[illegible]E 00	.733918E 00	.459211E-01	.430555E-02	.356498E-02	.654583E-03	.419916E-03
MAY-	.45[illegible]303E 02	.[illegible]E 00	.749394E 00	.712725E-01	.725327E-02	.466412E-02	.109013E-02	.375370E-03
OCT-	.450150E 02	.[illegible]E 00	.363065E 00	.100924E 00	.117103E-01	.719093E-02	.158299E-02	.657826E-03
JAN-	.441074E 02	.127[illegible]E 01	.103028E 01	.211604E 00	.171103E-01	.116285E-01	.307087E-02	.120829E-02
TOT-	.459859E 02	.[illegible]E 00	.346590E 00	.172578E 00	.100903E-01	.887360E-02	.159964E-02	.117553E-02

MAX H	MIN H	MAX DH	MIN DH	MAX THETA	MIN THETA	MAX DTHETA	MIN DTHETA
.46[illegible]E 02	.[illegible]E 02	.153504E 01	.636805E 00	.361173E-01	.451967E-03	.526205E-02	.329621E-04
SEQ. NO.	SEQ. NO.	SEQ. NO.	SEQ. NO.	SEQ. NO.	SEQ. NO.	SEQ. NO.	SEQ. NO.
56	367	360	136	342	136	363	16

ERROR NO. 8
LOCATION LA
VALUE 10.00

	H MEAN	H SIGMA	DH MEAN	DH SIGMA	THETA MEAN	THETA SIGMA	DTHETA MEAN	DTHETA SIGMA
APR-	.335325E 02	.331[illegible]E 00	.342418E 00	.246406E-01	.133360E-01	.105648E-01	.347382E-03	.226312E-03
MAY-	.326111E 02	.327[illegible]E 00	.341727E 00	.258528E-01	.570978E-02	.485464E-02	.372097E-03	.158608E-03
OCT-	.303890E 02	.[illegible]E 01	.401284E 00	.474560E-01	.211485E-01	.101360E-01	.687695E-03	.302548E-03
JAN-	.285445E 02	.1[illegible]E 01	.355940E 00	.807740E-01	.259461E-01	.152344E-01	.105362E-02	.682193E-03
TOT-	.314693E 02	.1[illegible]E 01	.384844E 00	.693027E-01	.164333E-01	.132973E-01	.615199E-03	.490304E-03

MAX H	MIN H	MAX DH	MIN DH	MAX THETA	MIN THETA	MAX DTHETA	MIN DTHETA
.331398E 02	.2[illegible]E 02	.713046E 00	.300636E 00	.587281E-01	.342685E-03	.267931E-02	.255690E-04
SEQ. NO.	SEQ. NO.	SEQ. NO.	SEQ. NO.	SEQ. NO.	SEQ. NO.	SEQ. NO.	SEQ. NO.
56	367	360	136	378	360	360	114

TABLE G1. - RADIOMETRIC ERROR ANALYSIS RESULTS - Continued

FRAME NO. 9
LOCATION 11
VALUE 2.00

	H MEAN	H SIGMA	DH MEAN	DH SIGMA	THETA MEAN	THETA SIGMA	DTHETA MEAN	DTHETA SIGMA
APR-	.437188E 02	.377[illegible]E 00	-.[illegible]896515E-02	.396130E-01	.121[illegible]E-01	.883418E-02	.525137E-03	.334845E-03
AUG-	.[illegible]25671E 02	.1[illegible]E 01	-.[illegible]44406E-01	.428740E-01	.233952E-01	.942132E-02	.548269E-03	.341731E-03
OCT-	.[illegible]11590E 02	.2383[illegible]E 01	.[illegible]49372E-02	.587578E-01	.344852E-01	.138856E-01	.681838E-03	.577045E-03
JAN-	.382212E 02	.3434[illegible]E 01	.533167E-02	.473602E-01	.511812E-01	.231750E-01	.699403E-03	.335694E-03
TJT-	.[illegible]1516[illegible]E 02	.31[illegible]E 01	-.213008E-02	.461306E-01	.303066E-01	.207791E-01	.613662E-03	.417937E-03

MAX H	MIN H	MAX DH	MIN DH	MAX THETA	MIN THETA	MAX DTHETA	MIN DTHETA
.451516E 02	.31[illegible]E 02	.[illegible]449888E 00	-.112320E 00	.10[illegible]E 00	.108785E-03	.170934E-02	.114692E-04
SEQ. NO.	SEQ. NO.	SEQ. NO.	SEQ. NO.	SEQ. NO.	SEQ. NO.	SEQ. NO.	SEQ. NO.
139	3[illegible]	192	56	370	16	192	174

FRAME NO. 9
LOCATION 11
VALUE 3.00

	H MEAN	H SIGMA	DH MEAN	DH SIGMA	THETA MEAN	THETA SIGMA	DTHETA MEAN	DTHETA SIGMA
APR-	.[illegible]6[illegible]E 02	.[illegible]E 01	-.[illegible]98[illegible]E-02	.531716E-01	.20[illegible]E-01	.129493E-01	.688029E-03	.543169E-03
AUG-	.362250E 02	.1343[illegible]E 01	-.165735E-01	.406077E-01	.202194E-01	.759661E-02	.595723E-03	.423988E-03
OCT-	.354575E 02	.2623[illegible]E 01	.127193E-02	.717498E-01	.387[illegible]E-01	.140563E-01	.973835E-03	.855623E-03
JAN-	.32147[illegible]E 02	.3[illegible]E 01	.[illegible]3041E-02	.613709E-01	.574[illegible]E-01	.321257E-01	.898123E-03	.477654E-03
TJT-	.361225E 02	.3[illegible]E 01	-.162424E-02	.603893E-01	.343[illegible]E-01	.244317E-01	.788928E-03	.618196E-03

MAX H	MIN H	MAX DH	MIN DH	MAX THETA	MIN THETA	MAX DTHETA	MIN DTHETA
.[illegible]47[illegible]E 02	.3[illegible]E 02	.[illegible]01301E 00	-.131519E 00	.123545E 00	.115852E-02	.264902E-02	.462810E-05
SEQ. NO.	SEQ. NO.	SEQ. NO.	SEQ. NO.	SEQ. NO.	SEQ. NO.	SEQ. NO.	SEQ. NO.
56	3[illegible]	192	159	360	6	181	174

TABLE G1. - RADIOMETRIC ERROR ANALYSIS RESULTS - Continued

ERROR NO. 9
LOCATOR L2
VALUE .15

	H MEAN	H SIGMA	DH MEAN	DH SIGMA	THETA MEAN	THETA SIGMA	DTHETA MEAN	DTHETA SIGMA
APR-	.518478E 02	.207[illegible]E 00	-.585134E-05	.281053E-04	.324858E-02	.260235E-02	.403483E-06	.328035E-06
AUG-	.510546E 02	.443[illegible]E 00	-.771557E-05	.271165E-04	.724196E-02	.504764E-02	.419840E-06	.165133E-06
OCT-	.509757E 02	.89[illegible]E 00	.147099E-05	.276509E-04	.117297E-01	.783762E-02	.209948E-06	.161033E-06
JAN-	.497236E 02	.149[illegible]E 01	.384113E-05	.330951E-04	.215601E-01	.141664E-01	.383542E-06	.269528E-06
TOT-	.509904E 02	.118[illegible]E 01	-.206370E-05	.294903E-04	.109448E-01	.109614E-01	.354203E-06	.255861E-06

MAX H	MIN H	MAX DH	MIN DH	MAX THETA	MIN THETA	MAX DTHETA	MIN DTHETA
.525990E 02	.47[illegible]E 02	.483551E-04	-.499997E-04	.455519E-01	.233733E-03	.958104E-06	.328728E-08
SEQ. NO.	SEQ. NO.	SEQ. NO.	SEQ. NO.	SEQ. NO.	SEQ. NO.	SEQ. NO.	SEQ. NO.
214	367	342	346	374	337	1	346

ERROR NO. 9
LOCATOR L2
VALUE .90

	H MEAN	H SIGMA	DH MEAN	DH SIGMA	THETA MEAN	THETA SIGMA	DTHETA MEAN	DTHETA SIGMA
APR-	.267705E 02	.214[illegible]E 01	-.116173E-04	.269598E-04	.315550E-01	.128629E-01	.435460E-06	.264662E-06
AUG-	.269241E 02	.467[illegible]E 00	.473050E-05	.301541E-04	.653089E-02	.492592E-02	.414587E-06	.352380E-06
OCT-	.253770E 02	.225[illegible]E 01	.905358E-05	.267224E-04	.331035E-01	.151659E-01	.304591E-06	.183189E-06
JAN-	.240723E 02	.24[illegible]E 01	-.106163E-05	.238654E-04	.380512E-01	.185954E-01	.285334E-06	.207293E-06
TOT-	.257860E 02	.233[illegible]E 01	.473791E-06	.281096E-04	.273161E-01	.184678E-01	.359993E-06	.268359E-06

MAX H	MIN H	MAX DH	MIN DH	MAX THETA	MIN THETA	MAX DTHETA	MIN DTHETA
.297327E 02	.[illegible]E 02	.491567E-04	-.497715E-04	.793139E-01	.593267E-03	.103497E-05	.261934E-11
SEQ. NO.	SEQ. NO.	SEQ. NO.	SEQ. NO.	SEQ. NO.	SEQ. NO.	SEQ. NO.	SEQ. NO.
52	364	43	371	378	125	8	178

TABLE G1. - RADIOMETRIC ERROR ANALYSIS RESULTS - Continued

ERROR NO. 9
LOCATOR L3
VALUE 6.50

	H MEAN	H SIGMA	DH MEAN	DH SIGMA	THETA MEAN	THETA SIGMA	DTHETA MEAN	DTHETA SIGMA
APR=	.530658E 02	.504266E 00	-.263752E-02	.227721E-01	.492962E-02	.261364E-02	.301540E-03	.208735E-03
AUG=	.525072E 02	.[illegible]E 00	-.793879E-02	.242585E-01	.103012E-01	.701871E-02	.299988E-03	.203334E-03
OCT=	.518654E 02	.[illegible]E 01	.318643E-02	.266253E-01	.138631E-01	.811622E-02	.374116E-03	.298877E-03
JAN=	.504965E 02	.154036E 01	.314977E-02	.248737E-01	.217935E-01	.119808E-01	.363713E-03	.187340E-03
TOT=	.519837E 02	.138174E 01	-.106002E-02	.251009E-01	.127261E-01	.101941E-01	.334839E-03	.231321E-03

MAX H	MIN H	MAX DH	MIN DH	MAX THETA	MIN THETA	MAX DTHETA	MIN DTHETA
.536410E 02	.468[illegible]E 02	.659467E-01	-.601091E-01	.346061E-01	.231515E-03	.998901E-03	.663417E-05
SEQ. NO.	SEQ. NO.	SEQ. NO.	SEQ. NO.	SEQ. NO.	SEQ. NO.	SEQ. NO.	SEQ. NO.
56	3[illegible]	302	56	373	27	181	184

ERROR NO. 9
LOCATOR L3
VALUE 20.00

	H MEAN	H SIGMA	DH MEAN	DH SIGMA	THETA MEAN	THETA SIGMA	DTHETA MEAN	DTHETA SIGMA
APR=	.421605E 02	.5[illegible]E 00	-.425321E-02	.328782E-01	.800035E-02	.412826E-02	.432429E-03	.292716E-03
AUG=	.415098E 02	.971714E 00	-.112963E-01	.351382E-01	.148172E-01	.749035E-02	.440637E-03	.305709E-03
OCT=	.402966E 02	.154037E 01	.470697E-02	.379925E-01	.225370E-01	.896091E-02	.531100E-03	.415660E-03
JAN=	.382172E 02	.252159E 01	.524501E-02	.345046E-01	.367262E-01	.168101E-01	.511103E-03	.252121E-03
TOT=	.405460E 02	.213[illegible]E 01	-.144916E-02	.356280E-01	.206423E-01	.149138E-01	.478817E-03	.325140E-03

MAX H	MIN H	MAX DH	MIN DH	MAX THETA	MIN THETA	MAX DTHETA	MIN DTHETA
.431399E 02	.32[illegible]E 02	.946547E-01	-.951808E-01	.679187E-01	.238650E-02	.136732E-02	.251275E-04
SEQ. NO.	SEQ. NO.	SEQ. NO.	SEQ. NO.	SEQ. NO.	SEQ. NO.	SEQ. NO.	SEQ. NO.
139	36[illegible]	192	159	378	158	181	174

TABLE G1. - RADIOMETRIC ERROR ANALYSIS RESULTS - Continued

FREQ NO. 9
LOCATOR LA
VALUE 2.50

	H MEAN	H SIGMA	DH MEAN	DH SIGMA	THETA MEAN	THETA SIGMA	DTHETA MEAN	DTHETA SIGMA
APR=	.449041E 02	.324113E 00	-.144978E-04	.287174E-04	.978340E-02	.387008E-02	.361675E-06	.275984E-06
AUG=	.442812E 02	[illegible]	.424016E-06	.261728E-04	.742503E-02	.505140E-02	.321273E-06	.186738E-06
OCT=	.441469E 02	[illegible]	-.337455E-05	.297978E-04	.128383E-01	.791234E-02	.379516E-06	.294205E-06
JAN=	.430771E 02	.139227E 01	-.223637E-05	.270184E-04	.196072E-01	.128954E-01	.319482E-06	.193767E-06
TOT=	.441023E 02	.110711E 01	-.542117E-05	.277984E-04	.111633E-01	.997841E-02	.345486E-06	.243836E-06

MAX H	MIN H	MAX DH	MIN DH	MAX THETA	MIN THETA	MAX DTHETA	MIN DTHETA
.457329E 02	[illegible]	.494218E-04	-.490896E-04	.395527E-01	.783960E-04	.104952E-05	.778469E-06
SEQ. NO.	SEQ. NO.	SEQ. NO.	SEQ. NO.	SEQ. NO.	SEQ. NO.	SEQ. NO.	SEQ. NO.
56	[illegible]	376	5	378	182	2	184

FREQ NO. 9
LOCATOR LA
VALUE 10.00

	H MEAN	H SIGMA	DH MEAN	DH SIGMA	THETA MEAN	THETA SIGMA	DTHETA MEAN	DTHETA SIGMA
APR=	.311921E 02	[illegible]	.791273E-05	.324468E-04	.133603E-01	.104988E-01	.421894E-06	.285114E-06
AUG=	.306694E 02	[illegible]	.407756E-05	.266293E-04	.586182E-02	.500316E-02	.386802E-06	.285855E-06
OCT=	.299877E 02	.151[illegible]E 01	-.122926E-05	.294777E-04	.218236E-01	.101504E-01	.404585E-06	.247520E-06
JAN=	.284385E 02	[illegible]	.380552E-05	.284605E-04	.267800E-01	.153305E-01	.411488E-06	.294796E-06
TOT=	.300844E 02	[illegible]	.414154E-05	.285301E-04	.169573E-01	.135727E-01	.406192E-06	.279208E-06

MAX H	MIN H	MAX DH	MIN DH	MAX THETA	MIN THETA	MAX DTHETA	MIN DTHETA
.328338E 02	.2[illegible]E 02	.497270E-04	-.494143E-04	.603502E-01	.142127E-03	.104810E-05	.465981E-03
SEQ. NO.	SEQ. NO.	SEQ. NO.	SEQ. NO.	SEQ. NO.	SEQ. NO.	SEQ. NO.	SEQ. NO.
56	367	20	126	378	128	46	139

TABLE G1. - RADIOMETRIC ERROR ANALYSIS RESULTS - Continued

ERROR NO.10
LOCATOR L1
VALUE 2.00

	F MEAN	F SIGMA	DF MEAN	DF SIGMA	THETA MEAN	THETA SIGMA	DTHETA MEAN	DTHETA SIGMA
APR-	.437229E 02	.891130E 00	-.326074E-03	.123369E 00	.132093E-01	.823896E-02	.187949E-02	.113929E-02
AUG-	.429947E 02	.150455E 01	.131662E-01	.104660E 00	.238146E-01	.100311E-01	.157009E-02	.950966E-03
OCT-	.411111E 02	.240140E 01	-.424916E-01	.144493E 00	.344223E-01	.160300E-01	.203906E-02	.170988E-02
JAN-	.381767E 02	.351545E 01	-.316441E-01	.147661E 00	.517769E-01	.234841E-01	.198504E-02	.154745E-02
TOT-	.415013E 02	.314455E 01	-.173454E-01	.133364E 00	.350053E-01	.209595E-01	.186965E-02	.138479E-02

MAX F	MIN F	MAX DF	MIN DF	MAX THETA	MIN THETA	MAX DTHETA	MIN DTHETA
.451685E 02	.309351E 02	.341422E 00	-.368022E 00	.150069E 00	.205733E-02	.703361E-02	.112797E-03
SEQ. NO.	SEQ. NO.	SEQ. NO.	SEQ. NO.	SEQ. NO.	SEQ. NO.	SEQ. NO.	SEQ. NO.
139	360	205	360	378	46	195	181

ERROR NO.10
LOCATOR L1
VALUE 3.00

	F MEAN	F SIGMA	DF MEAN	DF SIGMA	THETA MEAN	THETA SIGMA	DTHETA MEAN	DTHETA SIGMA
APR-	.386514E 02	.134501E 01	-.230301E-02	.153201E 00	.213308E-01	.133476E-01	.235007E-02	.142536E-02
AUG-	.382672E 02	.136591E 01	.151127E-01	.129492E 00	.200192E-01	.827531E-02	.191197E-02	.121755E-02
OCT-	.354003E 02	.267080E 01	-.486995E-01	.200492E 00	.387722E-01	.157939E-01	.277915E-02	.244001E-02
JAN-	.320702E 02	.433081E 01	-.716883E-01	.221063E 00	.589645E-01	.345491E-01	.288613E-02	.267543E-02
TOT-	.360973E 02	.379321E 01	-.269419E-01	.183175E 00	.346617E-01	.257865E-01	.248183E-02	.207493E-02

MAX F	MIN F	MAX DF	MIN DF	MAX THETA	MIN THETA	MAX DTHETA	MIN DTHETA
.426153E 02	.183750E 02	.542632E 00	-.868200E 00	.134147E 00	.216499E-02	.116493E-01	.985009E-04
SEQ. NO.	SEQ. NO.	SEQ. NO.	SEQ. NO.	SEQ. NO.	SEQ. NO.	SEQ. NO.	SEQ. NO.
56	360	205	360	360	337	360	2

TABLE G1. - RADIOMETRIC ERROR ANALYSIS RESULTS - Continued

ERROR NO.10
LOCATOR L2
VALUE .15

	H MEAN	H SIGMA	DH MEAN	DH SIGMA	THETA MEAN	THETA SIGMA	DTHETA MEAN	DTHETA SIGMA
APR-	.518478E 02	.207861E 00	-.585134E-05	.281053E-04	.324858E-02	.260235E-02	.403483E-06	.328035E-06
AUG-	.510546E 02	.443123E 00	-.771557E-05	.271165E-04	.724196E-02	.504764E-02	.419840E-06	.165133E-06
OCT-	.509757E 02	.895655E 00	.147099E-05	.276509E-04	.117287E-01	.783762E-02	.209948E-06	.161033E-06
JAN-	.497236E 02	.149626E 01	.384113E-05	.330951E-04	.215601E-01	.141664E-01	.383542E-06	.269528E-06
TOT-	.509004E 02	.118242E 01	-.206370E-05	.294003E-04	.109448E-01	.109614E-01	.354203E-06	.255861E-06

MAX H	MIN H	MAX DH	MIN DH	MAX THETA	MIN THETA	MAX DTHETA	MIN DTHETA
.525990E 02	.470000E 02	.488551E-04	-.499997E-04	.455519E-01	.233733E-03	.958104E-06	.328728E-08
SEQ. NO.	SEQ. NO.	SEQ. NO.	SEQ. NO.	SEQ. NO.	SEQ. NO.	SEQ. NO.	SEQ. NO.
214	367	342	346	378	337	1	346

ERROR NO.10
LOCATOR L2
VALUE .90

	H MEAN	H SIGMA	DH MEAN	DH SIGMA	THETA MEAN	THETA SIGMA	DTHETA MEAN	DTHETA SIGMA
APR-	.267705E 02	.216363E 01	-.116173E-04	.269698E-04	.315550E-01	.128629E-01	.435460E-06	.264662E-06
AUG-	.269241E 02	.467035E 00	.473050E-05	.301541E-04	.653089E-02	.492532E-02	.414587E-06	.352380E-06
OCT-	.253770E 02	.225817E 01	.906358E-05	.267224E-04	.331035E-01	.151659E-01	.304591E-06	.193189E-06
JAN-	.240723E 02	.260249E 01	-.106163E-05	.238654E-04	.380512E-01	.185954E-01	.285334E-06	.207293E-06
TOT-	.257860E 02	.235265E 01	.278791E-06	.281096E-04	.273101E-01	.184678E-01	.359993E-06	.268359E-06

MAX H	MIN H	MAX DH	MIN DH	MAX THETA	MIN THETA	MAX DTHETA	MIN DTHETA
.297327E 02	.190415E 02	.490567E-04	-.497715E-04	.793130E-01	.593267E-03	.103497E-05	.261934E-11
SEQ. NO.	SEQ. NO.	SEQ. NO.	SEQ. NO.	SEQ. NO.	SEQ. NO.	SEQ. NO.	SEQ. NO.
52	360	43	371	376	125	9	178

TABLE G1. - RADIOMETRIC ERROR ANALYSIS RESULTS - Continued

ERROR NO.10
LOCATOR L3
VALUE 4.50

	H MEAN	H SIGMA	DH MEAN	DH SIGMA	THETA MEAN	THETA SIGMA	DTHETA MEAN	DTHETA SIGMA
APR-	.530688E 02	.309054E 00	.323915E-03	.662617E-01	.486591E-02	.262853E-02	.102051E-02	.620993E-03
AUG-	.525246E 02	.682442E 00	.944420E-02	.610943E-01	.104036E-01	.735771E-02	.917875E-03	.571980E-03
OCT-	.518437E 02	.103857E 01	-.184962E-01	.756373E-01	.139281E-01	.812566E-02	.102221E-02	.832102E-03
JAN-	.504749E 02	.155774E 01	-.185141E-01	.758017E-01	.222217E-01	.121192E-01	.106094E-02	.694721E-03
TOT-	.519780E 02	.139933E 01	-.681056E-02	.710258E-01	.128548E-01	.104004E-01	.100536E-02	.689034E-03

MAX H	MIN H	MAX DH	MIN DH	MAX THETA	MIN THETA	MAX DTHETA	MIN DTHETA
.536743E 02	.467069E 02	.214036E 00	-.155137E 00	.348755E-01	.224565E-03	.334916E-02	.730845E-04
SEQ. NO.	SEQ. NO.	SEQ. NO.	SEQ. NO.	SEQ. NO.	SEQ. NO.	SEQ. NO.	SEQ. NO.
56	360	205	174	372	173	195	337

ERROR NO.10
LOCATOR L3
VALUE 20.00

	H MEAN	H SIGMA	DH MEAN	DH SIGMA	THETA MEAN	THETA SIGMA	DTHETA MEAN	DTHETA SIGMA
APR-	.421651E 02	.516616E 00	.436923E-03	.958497E-01	.834367E-02	.436685E-02	.147643E-02	.890949E-03
AUG-	.415306E 02	.990941E 00	.950174E-02	.869140E-01	.152072E-01	.784504E-02	.129424E-02	.831615E-03
OCT-	.402625E 02	.158830E 01	-.294462E-01	.107952E 00	.223393E-01	.972141E-02	.147913E-02	.116064E-02
JAN-	.381862E 02	.254465E 01	-.259230E-01	.110192E 00	.371949E-01	.171488E-01	.146390E-02	.101396E-02
TOT-	.405361E 02	.220716E 01	-.113576E-01	.102042E 00	.207713E-01	.152217E-01	.142842E-02	.985484E-03

MAX H	MIN H	MAX DH	MIN DH	MAX THETA	MIN THETA	MAX DTHETA	MIN DTHETA
.431516E 02	.326464E 02	.269789E 00	-.246356E 00	.689262E-01	.352343E-03	.462215E-02	.554604E-04
SEQ. NO.	SEQ. NO.	SEQ. NO.	SEQ. NO.	SEQ. NO.	SEQ. NO.	SEQ. NO.	SEQ. NO.
139	360	205	174	378	16	195	337

TABLE G1. - RADIOMETRIC ERROR ANALYSIS RESULTS - Continued

ERROR NO.10
LOCATOR L4
VALUE 2.50

	H MEAN	H SIGMA	DH MEAN	DH SIGMA	THETA MEAN	THETA SIGMA	DTHETA MEAN	DTHETA SIGMA
APR-	.449041E 02	.326113E 00	-.144978E-04	.257174E-04	.478340E-02	.387008E-02	.361675E-06	.275984E-06
AUG-	.442812E 02	.438909E 00	.424016E-06	.261728E-04	.742503E-02	.506140E-02	.321273E-06	.186738E-06
OCT-	.441469E 02	.967722E 00	-.537455E-05	.297078E-04	.128385E-01	.791234E-02	.379516E-06	.294205E-06
JAN-	.430771E 02	.139227E 01	-.223637E-05	.270184E-04	.196072E-01	.128954E-01	.319492E-06	.193767E-06
OCT-	.441023E 02	.110701E 01	-.542117E-05	.277084E-04	.111635E-01	.997841E-02	.345486E-06	.243836E-06

MAX H	MIN H	MAX DH	MIN DH	MAX THETA	MIN THETA	MAX DTHETA	MIN DTHETA
.457329E 02	.406683E 02	.494218E-04	-.480996E-04	.395527E-01	.783960E-04	.104952E-05	.778469E-08
SEQ. NO.	SEQ. NO.	SEQ. NO.	SEQ. NO.	SEQ. NO.	SEQ. NO.	SEQ. NO.	SEQ. NO.
56	367	376	5	378	182	2	184

ERROR NO.10
LOCATOR L4
VALUE 10.00

	H MEAN	H SIGMA	DH MEAN	DH SIGMA	THETA MEAN	THETA SIGMA	DTHETA MEAN	DTHETA SIGMA
APR-	.311921E 02	.952755E 00	.791273E-05	.324468E-04	.133628E-01	.106988E-01	.421894E-06	.285114E-06
AUG-	.306694E 02	.408427E 00	.607756E-05	.266293E-04	.584102E-02	.500316E-02	.386802E-06	.285855E-06
OCT-	.299877E 02	.151099E 01	-.122926E-05	.294777E-04	.219236E-01	.101504E-01	.404595E-06	.247520E-06
JAN-	.284885E 02	.186514E 01	.380552E-05	.284665E-04	.267820E-01	.154305E-01	.411488E-06	.294796E-06
OCT-	.300944E 02	.165542E 01	.414164E-05	.295301E-04	.169573E-01	.135727E-01	.406192E-06	.279208E-06

MAX H	MIN H	MAX DH	MIN DH	MAX THETA	MIN THETA	MAX DTHETA	MIN DTHETA
.328338E 02	.253631E 02	.497270E-04	-.494143E-04	.603502E-01	.142127E-03	.104810E-05	.465981E-08
SEQ. NO.	SEQ. NO.	SEQ. NO.	SEQ. NO.	SEQ. NO.	SEQ. NO.	SEQ. NO.	SEQ. NO.
56	367	20	126	378	128	46	139

TABLE G1. - RADIOMETRIC ERROR ANALYSIS RESULTS - Continued

ERROR NO.11
LOCATOR L1
VALUE 2.00

	H MEAN	H SIGMA	DH MEAN	DH SIGMA	THETA MEAN	THETA SIGMA	DTHETA MEAN	DTHETA SIGMA
APR-	.437731E 02	.957121E 00	.493830E-01	.210911E 00	.137187E-01	.844440E-02	.320447E-02	.166096E-02
ALG-	.429663E 02	.142561E 01	-.152096E-01	.203902E 00	.224518E-01	.100328E-01	.325008E-02	.194140E-02
CCT-	.411403E 02	.235385E 01	-.132986E-01	.193494E 00	.343274E-01	.141126E-01	.306449E-02	.193102E-02
JAN-	.391989E 02	.360187E 01	-.269648E-01	.268223E 00	.518109E-01	.244991E-01	.244768E-02	.160339E-02
TCT-	.415171E 02	.315719E 01	-.152251E-02	.223029E 00	.305772E-01	.211335E-01	.299168E-02	.181940E-02

MAX H	MIN H	MAX DH	MIN DH	MAX THETA	MIN THETA	MAX DTHETA	MIN DTHETA
.452205E 02	.305361E 02	.470685E 00	-.766997E 01	.108105E 00	.265444E-03	.806224E-02	.207659E-03
SEQ. NO.	SEQ. NO.	SEQ. NO.	SEQ. NO.	SEQ. NO.	SEQ. NO.	SEQ. NO.	SEQ. NO.
122	360	350	360	378	337	120	339

ERROR NO.11
LOCATOR L1
VALUE 3.00

	H MEAN	H SIGMA	DH MEAN	DH SIGMA	THETA MEAN	THETA SIGMA	DTHETA MEAN	DTHETA SIGMA
APR-	.397092E 02	.143792E 01	.564957E-01	.305042E 00	.222769E-01	.130339E-01	.453020E-02	.237964E-02
ALG-	.382187E 02	.127976E 01	-.328573E-01	.252258E 00	.193016E-01	.913728E-02	.401076E-02	.203070E-02
CCT-	.354274E 02	.261459E 01	-.218742E-01	.248664E 00	.387592E-01	.142730E-01	.403775E-02	.241231E-02
JAN-	.320600E 02	.446174E 01	-.918711E-01	.437957E 00	.596327E-01	.342636E-01	.376697E-02	.370809E-02
TCT-	.361038E 02	.382488E 01	-.202767E-01	.324012E 00	.349926E-01	.257891E-01	.408642E-02	.272317E-02

MAX H	MIN H	MAX DH	MIN DH	MAX THETA	MIN THETA	MAX DTHETA	MIN DTHETA
.406555E 02	.174015E 02	.692416E 00	-.184167E 01	.138490E 00	.400078E-02	.159911E-01	.266421E-03
SEQ. NO.	SEQ. NO.	SEQ. NO.	SEQ. NO.	SEQ. NO.	SEQ. NO.	SEQ. NO.	SEQ. NO.
56	360	47	360	360	158	360	1

TABLE G1. - RADIOMETRIC ERROR ANALYSIS RESULTS - Continued

ERROR NO.11
LOCATOR L2
VALUE .15

	H MEAN	H SIGMA	DH MEAN	DH SIGMA	THETA MEAN	THETA SIGMA	DTHETA MEAN	DTHETA SIGMA
APR-	.519478E 02	.207861E 00	-.585134E-05	.281053E-04	.324858E-02	.260235E-02	.403483E-06	.328035E-06
AUG-	.510546E 02	.443123E 00	-.771557E-05	.271165E-04	.724196E-02	.504764E-02	.419840E-06	.165133E-06
OCT-	.509757E 02	.895655E 00	.147099E-05	.276509E-04	.117287E-01	.783762E-02	.209948E-06	.161033E-06
JAN-	.497236E 02	.149626E 01	.384113E-05	.330951E-04	.215601E-01	.141664E-01	.383542E-06	.269528E-06
TOT-	.509004E 02	.118242E 01	-.206370E-05	.294903E-04	.109448E-01	.109614E-01	.354203E-06	.255861E-06

MAX H	MIN H	MAX DH	MIN DH	MAX THETA	MIN THETA	MAX DTHETA	MIN DTHETA
.525990E 02	.470000E 02	.488551E-04	-.499997E-04	.455519E-01	.233733E-03	.958104E-06	.328728E-08
SEQ. NO.	SEQ. NO.	SEQ. NO.	SEQ. NO.	SEQ. NO.	SEQ. NO.	SEQ. NO.	SEQ. NO.
214	367	342	346	378	337	1	346

ERROR NO.11
LOCATOR L2
VALUE .90

	H MEAN	H SIGMA	DH MEAN	DH SIGMA	THETA MEAN	THETA SIGMA	DTHETA MEAN	DTHETA SIGMA
APR-	.267705E 02	.216363E 01	-.116173E-04	.269698E-04	.315550E-01	.128629E-01	.435460E-06	.264662E-06
AUG-	.269241E 02	.467035E 00	.473050E-05	.301541E-04	.653089E-02	.492592E-02	.414587E-06	.352380E-06
OCT-	.253770E 02	.225817E 01	.906358E-05	.267224E-04	.331035E-01	.151659E-01	.304591E-06	.183189E-06
JAN-	.240723E 02	.260249E 01	-.106163E-05	.238654E-04	.380512E-01	.185954E-01	.285334E-06	.207293E-06
TOT-	.257860E 02	.235265E 01	.278791E-06	.281096E-04	.273101E-01	.184678E-01	.359993E-06	.268359E-06

MAX H	MIN H	MAX DH	MIN DH	MAX THETA	MIN THETA	MAX DTHETA	MIN DTHETA
.297327E 02	.190415E 02	.490567E-04	-.497715E-04	.793130E-01	.593267E-03	.103497E-05	.261934E-11
SEQ. NO.	SEQ. NO.	SEQ. NO.	SEQ. NO.	SEQ. NO.	SEQ. NO.	SEQ. NO.	SEQ. NO.
52	360	43	371	378	125	8	178

TABLE G1. - RADIOMETRIC ERROR ANALYSIS RESULTS - Continued

ERROR NO.11
LOCATOR L3
VALUE 4.50

	H MEAN	H SIGMA	DH MEAN	DH SIGMA	THETA MEAN	THETA SIGMA	DTHETA MEAN	DTHETA SIGMA
APR-	.530972E 02	.341301E 00	.287710E-01	.124915E 00	.527937E-02	.268094E-02	.190170E-02	.896685E-03
AUG-	.526030E 02	.651501E 00	-.121573E-01	.123036E 00	.107588E-01	.634160E-02	.197832E-02	.104131E-02
OCT-	.518538E 02	.103239E 01	-.839955E-02	.997465E-01	.143151E-01	.772524E-02	.161199E-02	.884825E-03
JAN-	.504786E 02	.159295E 01	-.147550E-01	.136110E 00	.225317E-01	.117169E-01	.123645E-02	.768918E-03
TOT-	.519832E 02	.140855E 01	-.163522E-02	.122953E 00	.132212E-01	.100173E-01	.168211E-02	.948948E-03

MAX H	MIN H	MAX DH	MIN DH	MAX THETA	MIN THETA	MAX DTHETA	MIN DTHETA
.536941E 02	.465450E 02	.298181E 00	-.306900E 00	.330607E-01	.690935E-03	.406435E-02	.209513E-03
SEQ. NO. 56	SEQ. NO. 360	SEQ. NO. 47	SEQ. NO. 360	SEQ. NO. 378	SEQ. NO. 344	SEQ. NO. 120	SEQ. NO. 139

ERROR NO.11
LOCATOR L3
VALUE 20.00

	H MEAN	H SIGMA	DH MEAN	DH SIGMA	THETA MEAN	THETA SIGMA	DTHETA MEAN	DTHETA SIGMA
APR-	.422057E 02	.573293E 00	.410384E-01	.174595E 00	.882400E-02	.452639E-02	.265431E-02	.129686E-02
AUG-	.415070E 02	.938213E 00	-.141165E-01	.167331E 00	.145314E-01	.803752E-02	.269066E-02	.149860E-02
OCT-	.402921E 02	.156532E 01	-.979383E-02	.143634E 00	.225473E-01	.931237E-02	.232215E-02	.130514E-02
JAN-	.381984E 02	.259806E 01	-.237371E-01	.191644E 00	.372008E-01	.175473E-01	.173608E-02	.116496E-02
TOT-	.405458E 02	.222008E 01	-.164975E-02	.172027E 00	.207759E-01	.152846E-01	.235080E-02	.137609E-02

MAX H	MIN H	MAX DH	MIN DH	MAX THETA	MIN THETA	MAX DTHETA	MIN DTHETA
.432311E 02	.324209E 02	.398372E 00	-.448850E 00	.688612E-01	.106716E-02	.571017E-02	.270216E-03
SEQ. NO. 122	SEQ. NO. 360	SEQ. NO. 47	SEQ. NO. 356	SEQ. NO. 378	SEQ. NO. 337	SEQ. NO. 120	SEQ. NO. 1

TABLE G1. - RADIOMETRIC ERROR ANALYSIS RESULTS - Continued

ERROR NO.11
LOCATOR L4
VALUE 2.50

	F MEAN	F SIGMA	DH MEAN	DH SIGMA	THETA MEAN	THETA SIGMA	DTHETA MEAN	DTHETA SIGMA
APR-	.449041E 02	.326113E 00	-.144978E-04	.257174E-04	.478340E-02	.387008E-02	.361675E-06	.275984E-06
AUG-	.442812E 02	.438909E 00	.424016E-06	.261728E-04	.742503E-02	.506140E-02	.321273E-06	.196738E-06
OCT-	.441469E 02	.567722E 00	-.537495E-05	.297978E-04	.128385E-01	.791234E-02	.379516E-06	.294205E-06
JAN-	.430771E 02	.139227E 01	-.223637E-05	.270184E-04	.196072E-01	.128954E-01	.319482E-06	.193767E-06
TOT-	.441023E 02	.110701E 01	-.542117E-05	.277984E-04	.111635E-01	.997841E-02	.345486E-06	.243836E-06

MAX F	MIN F	MAX DH	MIN DH	MAX THETA	MIN THETA	MAX DTHETA	MIN DTHETA
.457329E 02	.406683E 02	.494218E-04	-.490996E-04	.395527E-01	.783960E-04	.104952E-05	.778469E-08
SEQ. NO.	SEQ. NO.	SEQ. NO.	SEQ. NO.	SEQ. NO.	SEQ. NO.	SEQ. NO.	SEQ. NO.
56	367	376	5	378	182	2	184

ERROR NO.11
LOCATOR L4
VALUE 10.00

	F MEAN	F SIGMA	DH MEAN	DH SIGMA	THETA MEAN	THETA SIGMA	DTHETA MEAN	DTHETA SIGMA
APR-	.311921E 02	.952755E 00	.791273E-05	.324468E-04	.133628E-01	.106988E-01	.421804E-06	.285114E-06
AUG-	.306694E 02	.408427E 00	.607756E-05	.266293E-04	.586102E-02	.500316E-02	.386802E-06	.285955E-06
OCT-	.299877E 02	.151098E 01	-.122926E-05	.294777E-04	.213236E-01	.101504E-01	.404585E-06	.247520E-06
JAN-	.294885E 02	.186514E 01	.380552E-05	.284665E-04	.267820E-01	.154305E-01	.411488E-06	.294796E-06
TOT-	.300944E 02	.165542E 01	.414164E-05	.295301E-04	.169573E-01	.135727E-01	.406192E-06	.279208E-06

MAX F	MIN F	MAX DH	MIN DH	MAX THETA	MIN THETA	MAX DTHETA	MIN DTHETA
.328338E 02	.253631E 02	.497270E-04	-.494143E-04	.603502E-01	.142127E-03	.104810E-05	.465981E-08
SEQ. NO.	SEQ. NO.	SEQ. NO.	SEQ. NO.	SEQ. NO.	SEQ. NO.	SEQ. NO.	SEQ. NO.
56	367	20	126	378	128	46	139

TABLE G1. - RADIOMETRIC ERROR ANALYSIS RESULTS - Continued

ERROR 10.12
LOCATION L1
VALUE 2.00

	R MEAN	R SIGMA	DR MEAN	DR SIGMA	THETA MEAN	THETA SIGMA	DTHETA MEAN	DTHETA SIGMA
APR-	.436550E 02	.931473E 00	-.287815E-01	.490[illegible]	.130559E-01	.729126E-02	.592391E-02	.349084E-02
ALG-	.429954E 02	.152495E 01	.140623E-01	.705[illegible]	.220683E-01	.153816E-01	.991917E-02	.669620E-02
CCT-	.414603E 02	.233268E 01	.306760E 00	.474[illegible]	.331072E-01	.162369E-01	.536906E-02	.519145E-02
JAN-	.383601E 02	.347475E 01	.144221E 00	.544[illegible]	.528935E-01	.229325E-01	.721967E-02	.548506E-02
TCT-	.416177E 02	.305285E 01	.390655E-01	.578[illegible]	.302812E-01	.221515E-01	.710795E-02	.562146E-02

MAX R	MIN R	MAX DR	MIN DR	MAX THETA	MIN THETA	MAX DTHETA	MIN DTHETA
.454317E 02	.319081E 02	.149376E 01	-.133[illegible]	.928505E-01	.760073E-03	.247570E-01	.111522E-03
SEC. NO.	SEC. NO.	SEC. NO.	SEC. NO.	SEC. NO.	SEC. NO.	SEC. NO.	SEC. NO.
130	360	184	5	378	117	148	342

ERROR 10.12
LOCATION L1
VALUE 3.00

	R MEAN	R SIGMA	DR MEAN	DR SIGMA	THETA MEAN	THETA SIGMA	DTHETA MEAN	DTHETA SIGMA
APR-	.385500E 02	.141571E 01	-.103683E 00	.206502E 00	.211728E-01	.115745E-01	.907699E-02	.691532E-02
ALG-	.382212E 02	.156101E 01	-.303064E-01	.573979E 00	.206773E-01	.145347E-01	.120962E-01	.349024E-02
CCT-	.358442E 02	.261856E 01	.394577E 00	.724723E 00	.382158E-01	.170935E-01	.775639E-02	.393239E-02
JAN-	.323244E 02	.414190E 01	.182534E 00	.636169E 00	.593773E-01	.313364E-01	.829922E-02	.635946E-02
TCT-	.362350E 02	.364701E 01	.110880E 00	.789851E 00	.348108E-01	.255877E-01	.930720E-02	.845958E-02

MAX R	MIN R	MAX DR	MIN DR	MAX THETA	MIN THETA	MAX DTHETA	MIN DTHETA
.411837E 02	.204028E 02	.316221E 01	-.299034E 01	.117291E 00	.703337E-03	.412835E-01	.972188E-04
SEC. NO.	SEC. NO.	SEC. NO.	SEC. NO.	SEC. NO.	SEC. NO.	SEC. NO.	SEC. NO.
130	360	184	5	363	115	184	350

TABLE G1. - RADIOMETRIC ERROR ANALYSIS RESULTS - Continued

ERROR NO.12
LOCATOR L2
VALUE .15

	H MEAN	H SIGMA	DH MEAN	DH SIGMA	THETA MEAN	THETA SIGMA	DTHETA MEAN	DTHETA SIGMA
APR-	.518478E 02	.207861E 00	-.585134E-05	.291053E-04	.324858E-02	.260235E-02	.403433E-06	.328035E-06
AUG-	.510546E 02	.443123E 00	-.771557E-05	.271165E-04	.724196E-02	.504764E-02	.419840E-06	.165133E-06
OCT-	.509757E 02	.805655E 00	.147099E-05	.276509E-04	.117287E-01	.783762E-02	.209948E-06	.161033E-06
JAN-	.497236E 02	.149626E 01	.384113E-05	.330951E-04	.215601E-01	.141664E-01	.383542E-06	.269528E-06
TOT-	.509004E 02	.118242E 01	-.206370E-05	.294903E-04	.109448E-01	.109614E-01	.354203E-06	.255861E-06

MAX H	MIN H	MAX DH	MIN DH	MAX THETA	MIN THETA	MAX DTHETA	MIN DTHETA
.525990E 02	.470000E 02	.488551E-04	-.499997E-04	.455519E-01	.233733E-03	.958104E-06	.328728E-08
SEQ. NO.	SEQ. NO.	SEQ. NO.	SEQ. NO.	SEQ. NO.	SEQ. NO.	SEQ. NO.	SEQ. NO.
214	367	342	346	378	337	1	346

ERROR NO.12
LOCATOR L2
VALUE .90

	H MEAN	H SIGMA	DH MEAN	DH SIGMA	THETA MEAN	THETA SIGMA	DTHETA MEAN	DTHETA SIGMA
APR-	.267705E 02	.216363E 01	-.116173E-04	.269698E-04	.315550E-01	.128629E-01	.435460E-06	.264662E-06
AUG-	.269241E 02	.467035E 00	.473050E-05	.301541E-04	.653089E-02	.492592E-02	.414597E-06	.352380E-06
OCT-	.253770E 02	.225817E 01	.906358E-05	.267224E-04	.331035E-01	.151659E-01	.304591E-06	.183189E-06
JAN-	.240723E 02	.260249E 01	-.106163E-05	.238654E-04	.380512E-01	.185954E-01	.285334E-06	.207293E-06
TOT-	.257860E 02	.235265E 01	.278791E-06	.281096E-04	.273101E-01	.184678E-01	.359903E-06	.268359E-06

MAX H	MIN H	MAX DH	MIN DH	MAX THETA	MIN THETA	MAX DTHETA	MIN DTHETA
.297327E 02	.190415E 02	.490567E-04	-.497715E-04	.793130E-01	.593267E-03	.103497E-05	.261934E-11
SEQ. NO.	SEQ. NO.	SEQ. NO.	SEQ. NO.	SEQ. NO.	SEQ. NO.	SEQ. NO.	SEQ. NO.
52	360	43	371	378	125	.	178

TABLE G1. - RADIOMETRIC ERROR ANALYSIS RESULTS - Continued

ERROR NO.12
LOCATOR L3
VALUE 4.50

	H MEAN	H SIGMA	DH MEAN	DH SIGMA	THETA MEAN	THETA SIGMA	DTHETA MEAN	DTHETA SIGMA
APR-	.530226E 02	.412004E 00	-.458349E-01	.284345E 00	.529849E-02	.368306E-02	.341041E-02	.184810E-02
AUG-	.525228E 02	.766604E 00	.771226E-02	.409955E 00	.115516E-01	.801020E-02	.570341E-02	.417092E-02
OCT-	.520173E 02	.105909E 01	.155093E 00	.260119E 00	.143607E-01	.891202E-02	.290688E-02	.308854E-02
JAN-	.505695E 02	.156917E 01	.761507E-01	.287571E 00	.234150E-01	.123175E-01	.381970E-02	.298335E-02
TOT-	.520331E 02	.138769E 01	.482802E-01	.324793E 00	.136565E-01	.109417E-01	.396010E-02	.330612E-02

MAX H	MIN H	MAX DH	MIN DH	MAX THETA	MIN THETA	MAX DTHETA	MIN DTHETA
.538884E 02	.470988E 02	.282760E 00	-.801061E 00	.390885E-01	.451910E-04	.156752E-01	.441131E-04
SEQ. NO. 130	SEQ. NO. 360	SEQ. NO. 184	SEQ. NO. 5	SEQ. NO. 352	SEQ. NO. 173	SEQ. NO. 148	SEQ. NO. 178

ERROR NO.12
LOCATOR L3
VALUE 20.00

	H MEAN	H SIGMA	DH MEAN	DH SIGMA	THETA MEAN	THETA SIGMA	DTHETA MEAN	DTHETA SIGMA
APR-	.421074E 02	.605269E 00	-.573373E-01	.403158E 00	.809011E-02	.541996E-02	.494468E-02	.277756E-02
AUG-	.415244E 02	.109655E 01	.328756E-02	.567076E 00	.157786E-01	.104157E-01	.793591E-02	.590282E-02
OCT-	.405214E 02	.158265E 01	.229463E 00	.391182E 00	.215439E-01	.119973E-01	.424048E-02	.449877E-02
JAN-	.383207E 02	.253394E 01	.108498E 00	.412961E 00	.380979E-01	.173326E-01	.552961E-02	.436277E-02
TOT-	.406184E 02	.216917E 01	.709776E-01	.460304E 00	.208776E-01	.163456E-01	.566272E-02	.473164E-02

MAX H	MIN H	MAX DH	MIN DH	MAX THETA	MIN THETA	MAX DTHETA	MIN DTHETA
.433424E 02	.331931E 02	.130117E 01	-.111078E 01	.644300E-01	.574771E-03	.225027E-01	.150520E-05
SEQ. NO. 130	SEQ. NO. 360	SEQ. NO. 184	SEQ. NO. 5	SEQ. NO. 378	SEQ. NO. 2	SEQ. NO. 148	SEQ. NO. 126

ERROR NO.12
LOCATOR L4
VALUE 2.50

	H MEAN	H SIGMA	DH MEAN	DH SIGMA	THETA MEAN	THETA SIGMA	DTHETA MEAN	DTHETA SIGMA
APR-	.449041E 02	.326113E 00	-.144978E-04	.257174E-04	.478340E-02	.387008E-02	.361675E-06	.275984E-06
AUG-	.442812E 02	.438909E 00	.424016E-06	.261728E-04	.742503E-02	.506140E-02	.321273E-06	.186738E-06
OCT-	.441469E 02	.967722E 00	-.537455E-05	.297978E-04	.128385E-01	.791234E-02	.379516E-06	.294205E-06
JAN-	.430771E 02	.139227E 01	-.223637E-05	.270184E-04	.196072E-01	.128954E-01	.319432E-06	.193767E-06
TOT-	.441023E 02	.110701E 01	-.542117E-05	.277964E-04	.111635E-01	.997841E-02	.345416E-06	.243836E-06

MAX H	MIN H	MAX DH	MIN DH	MAX THETA	MIN THETA	MAX DTHETA	MIN DTHETA
.457329E 02	.406683E 02	.494218E-04	-.480996E-04	.395527E-01	.783960E-04	.104952E-05	.778469E-08
SEQ. NO.	SEQ. NO.	SEQ. NO.	SEQ. NO.	SEQ. NO.	SEQ. NO.	SEQ. NO.	SEQ. NO.
56	367	376	5	378	182	2	184

ERROR NO.12
LOCATOR L4
VALUE 10.00

	H MEAN	H SIGMA	DH MEAN	DH SIGMA	THETA MEAN	THETA SIGMA	DTHETA MEAN	DTHETA SIGMA
APR-	.311921E 02	.952755E 00	.791273E-05	.324468E-04	.133628E-01	.106988E-01	.421894E-06	.285114E-06
AUG-	.306694E 02	.408427E 00	.607756E-05	.266294E-04	.586102E-02	.500316E-02	.386802E-06	.285855E-06
OCT-	.299877E 02	.151098E 01	-.122626E-05	.294777E-04	.218236E-01	.101504E-01	.404535E-06	.247520E-06
JAN-	.284885E 02	.196514E 01	.380552E-05	.284665E-04	.267820E-01	.154305E-01	.411488E-06	.294796E-06
TOT-	.300844E 02	.165542E 01	.414164E-05	.295301E-04	.169573E-01	.135727E-01	.406192E-06	.279208E-06

MAX H	MIN H	MAX DH	MIN DH	MAX THETA	MIN THETA	MAX DTHETA	MIN DTHETA
.328338E 02	.253631E 02	.497270E-04	-.494143E-04	.603502E-01	.142127E-03	.104810E-05	.465981E-08
SEQ. NO.	SEQ. NO.	SEQ. NO.	SEQ. NO.	SEQ. NO.	SEQ. NO.	SEQ. NO.	SEQ. NO.
56	367	20	126	378	128	46	139

TABLE G1. - RADIOMETRIC ERROR ANALYSIS RESULTS - Continued

ERROR NO.13
LOCATOR L1
VALUE 2.00

	H MEAN	H SIGMA	DH MEAN	DH SIGMA	THETA MEAN	THETA SIGMA	DTHETA MEAN	DTHETA SIGMA
APR-	.437239E 02	.880672E 00	.196443E-03	.588913E-02	.124872E-01	.862184E-02	.727851E-04	.470813E-04
ALG-	.429844E 02	.148282E 01	.285877E-02	.515479E-02	.231089E-01	.939565E-02	.801410E-04	.528318E-04
CCT-	.411549E 02	.236341E 01	.135934E-02	.503545E-02	.344252E-01	.140100E-01	.472786E-04	.367624E-04
JAN-	.382141E 02	.349104E 01	-.175949E-02	.691068E-02	.512603E-01	.233543E-01	.113270E-03	.745570E-04
TCT-	.415193E 02	.311494E 01	.663765E-03	.603654E-02	.303204E-01	.207947E-01	.783686E-04	.594497E-04

MAX H	MIN H	MAX DH	MIN DH	MAX THETA	MIN THETA	MAX DTHETA	MIN DTHETA
.451597E 02	.312892E 02	.126434E-01	-.138601E-01	.104184E 00	.110872E-03	.233705E-03	.492062E-06
SEQ. NO.	SEQ. NO.	SEQ. NO.	SEQ. NO.	SEQ. NO.	SEQ. NO.	SEQ. NO.	SEQ. NO.
139	360	168	360	378	16	363	195

ERROR NO.13
LOCATOR L1
VALUE 3.00

	H MEAN	H SIGMA	DH MEAN	DH SIGMA	THETA MEAN	THETA SIGMA	DTHETA MEAN	DTHETA SIGMA
APR-	.396537E 02	.132136E 01	.126652E-04	.523500E-02	.212064E-01	.125978E-01	.608207E-04	.417409E-04
ALG-	.382539E 02	.135161E 01	.223369E-02	.400104E-02	.199390E-01	.788235E-02	.587694E-04	.433632E-04
CCT-	.354504E 02	.261284E 01	.113424E-02	.479724E-02	.386811E-01	.139705E-01	.456878E-04	.332276E-04
JAN-	.321396E 02	.421606E 01	-.226817E-02	.701294E-02	.575537E-01	.322857E-01	.108924E-03	.832036E-04
TCT-	.361244E 02	.372287E 01	.279166E-03	.562636E-02	.343450E-01	.244744E-01	.685504E-04	.590714E-04

MAX H	MIN H	MAX DH	MIN DH	MAX THETA	MIN THETA	MAX DTHETA	MIN DTHETA
.406683E 02	.192258E 02	.116201E-01	-.189739E-01	.122700E 00	.248038E-02	.294320E-03	.870623E-06
SEQ. NO.	SEQ. NO.	SEQ. NO.	SEQ. NO.	SEQ. NO.	SEQ. NO.	SEQ. NO.	SEQ. NO.
56	360	47	363	360	6	363	192

TABLE G1. - RADIOMETRIC ERROR ANALYSIS RESULTS - Continued

ERROR NO.13
LOCATOR L2
VALUE .15

	H MEAN	H SIGMA	DH MEAN	DH SIGMA	THETA MEAN	THETA SIGMA	DTHETA MEAN	DTHETA SIGMA
APR-	.518474E 02	.206149E 00	-.405067E-03	.794988E-02	.320726E-02	.258736E-02	.108418E-03	.656745E-04
ALG-	.510590E 02	.442503E 00	.433877E-02	.727215E-02	.724752E-02	.497685E-02	.113835E-03	.729542E-04
OCT-	.509774E 02	.896868E 00	.167968E-02	.793107E-02	.117409E-01	.786057E-02	.731808E-04	.579181E-04
JAN-	.497208E 02	.149864E 01	-.274524E-02	.109853E-01	.215812E-01	.141673E-01	.169091E-03	.137435E-03
TCT-	.509012E 02	.118405E 01	.717036E-03	.905191E-02	.109442E-01	.109669E-01	.116131E-03	.956461E-04

MAX H	MIN H	MAX DH	MIN DH	MAX THETA	MIN THETA	MAX DTHETA	MIN DTHETA
.526110E 02	.469813E 02	.205000E-01	-.289824E-01	.453351E-01	.936300E-04	.408419E-03	.693314E-07
SEQ. NO.	SEQ. NO.	SEQ. NO.	SEQ. NO.	SEQ. NO.	SEQ. NO.	SEQ. NO.	SEQ. NO.
215	367	168	339	378	337	334	344

ERROR NO.13
LOCATOR L2
VALUE .90

	H MEAN	H SIGMA	DH MEAN	DH SIGMA	THETA MEAN	THETA SIGMA	DTHETA MEAN	DTHETA SIGMA
APR-	.267703E 02	.216383E 01	-.230138E-03	.123729E-02	.315506E-01	.128681E-01	.879607E-05	.178725E-04
ALG-	.269242E 02	.467480E 00	.141734E-03	.126458E-02	.653896E-02	.492845E-02	.908644E-05	.138320E-04
OCT-	.253767E 02	.225812E 01	-.298105E-03	.124983E-02	.331029E-01	.151642E-01	.123423E-04	.163150E-04
JAN-	.240721E 02	.260261E 01	-.266368E-03	.151802E-02	.380526E-01	.185914E-01	.178877E-04	.233442E-04
TCT-	.257858E 02	.235280E 01	-.163219E-03	.133443E-02	.273113E-01	.184652E-01	.120281E-04	.185433E-04

MAX H	MIN H	MAX DH	MIN DH	MAX THETA	MIN THETA	MAX DTHETA	MIN DTHETA
.297327E 02	.190375E 02	.484615E-02	-.615000E-02	.792841E-01	.593267E-03	.851317E-04	.261934E-11
SEQ. NO.	SEQ. NO.	SEQ. NO.	SEQ. NO.	SEQ. NO.	SEQ. NO.	SEQ. NO.	SEQ. NO.
52	360	134	19	378	125	372	178

TABLE G1. - RADIOMETRIC ERROR ANALYSIS RESULTS - Continued

ERROR NO.13
LOCATOR L3
VALUE 4.50

	H MEAN	H SIGMA	DH MEAN	DH SIGMA	THETA MEAN	THETA SIGMA	DTHETA MEAN	DTHETA SIGMA
APR-	.530692E 02	.315638E 00	.768910E-03	.407609E-01	.503491E-02	.252596E-02	.489912E-03	.324224E-03
ALG-	.525358E 02	.671610E 00	.207244E-01	.352790E-01	.101679E-01	.671998E-02	.544535E-03	.327452E-03
OCT-	.518719E 02	.102824E 01	.972057E-02	.355888E-01	.138156E-01	.799767E-02	.338295E-03	.273188E-03
JAN-	.504827E 02	.155712E 01	-.111999E-01	.496992E-01	.221395E-01	.120360E-01	.785636E-03	.567392E-03
TOT-	.519898E 02	.139489E 01	.500349E-02	.421104E-01	.127895E-01	.101962E-01	.539595E-03	.422037E-03

MAX H	MIN H	MAX DH	MIN DH	MAX THETA	MIN THETA	MAX DTHETA	MIN DTHETA
.536896E 02	.466698E 02	.973314E-01	-.971934E-01	.338419E-01	.344357E-03	.173211E-02	.214233E-04
SEQ. NO. 56	SEQ. NO. 360	SEQ. NO. 47	SEQ. NO. 339	SEQ. NO. 363	SEQ. NO. 173	SEQ. NO. 363	SEQ. NO. 204

ERROR NO.13
LOCATOR L3
VALUE 20.00

	H MEAN	H SIGMA	DH MEAN	DH SIGMA	THETA MEAN	THETA SIGMA	DTHETA MEAN	DTHETA SIGMA
APR-	.421652E 02	.508082E 00	.513299E-03	.180729E-01	.822749E-02	.402496E-02	.220450E-03	.144546E-03
ALG-	.415303E 02	.971929E 00	.922161E-02	.160307E-01	.144855E-01	.763388E-02	.252517E-03	.168118E-03
OCT-	.402958E 02	.156817E 01	.389800E-02	.161217E-01	.224356E-01	.903463E-02	.157651E-03	.129135E-03
JAN-	.382069E 02	.253030E 01	-.527340E-02	.215603E-01	.369615E-01	.167611E-01	.353125E-03	.247446E-03
TOT-	.405495E 02	.219026E 01	.208988E-02	.188362E-01	.205275E-01	.149879E-01	.245936E-03	.191728E-03

MAX H	MIN H	MAX DH	MIN DH	MAX THETA	MIN THETA	MAX DTHETA	MIN DTHETA
.431469E 02	.328120E 02	.436265E-01	-.429148E-01	.671406E-01	.120841E-02	.738753E-03	.804955E-05
SEQ. NO. 136	SEQ. NO. 360	SEQ. NO. 168	SEQ. NO. 339	SEQ. NO. 378	SEQ. NO. 154	SEQ. NO. 339	SEQ. NO. 352

TABLE G1. - RADIOMETRIC ERROR ANALYSIS RESULTS - Continued

ERRC NO.13
LOCATOR L4
VALUE 2.50

	H MEAN	H SIGMA	DH MEAN	DH SIGMA	THETA MEAN	THETA SIGMA	DTHETA MEAN	DTHETA SIGMA
APR-	.449046E 02	.323939E 00	.505856E-03	.195225E-01	.471423E-02	.381210E-02	.236294E-03	.156743E-03
AUG-	.442913E 02	.437240E 00	.100791E-01	.176415E-01	.747952E-02	.485315E-02	.276354E-03	.187774E-03
OCT-	.441513E 02	.969519E 00	.439281E-02	.187217E-01	.127615E-01	.799234E-02	.183362E-03	.149416E-03
JAN-	.430697E 02	.139866E 01	-.739942E-02	.273775E-01	.197958E-01	.127639E-01	.443673E-03	.319575E-03
OCT-	.441042E 02	.111134E 01	.189698E-02	.221065E-01	.111878E-01	.996366E-02	.284918E-03	.235710E-03

MAX H	MIN H	MAX DH	MIN DH	MAX THETA	MIN THETA	MAX DTHETA	MIN DTHETA
.457270E 02	.406230E 02	.505479E-01	-.604664E-01	.397077E-01	.427859E-04	.990639E-03	.308327E-05
SEG. NO.	SEG. NO.	SEG. NO.	SEG. NO.	SEG. NO.	SEG. NO.	SEG. NO.	SEG. NO.
56	367	168	339	342	182	363	352

ERROR NO.13
LOCATOR L4
VALUE 10.00

	H MEAN	H SIGMA	DH MEAN	DH SIGMA	THETA MEAN	THETA SIGMA	DTHETA MEAN	DTHETA SIGMA
APR-	.311923E 02	.951432E 00	.283502E-03	.914824E-02	.133014E-01	.107000E-01	.111410E-03	.723980E-04
AUG-	.306740E 02	.407817E 00	.461714E-02	.797056E-02	.582092E-02	.496005E-02	.125304E-03	.827619E-04
OCT-	.299899E 02	.151212E 01	.216682E-02	.876434E-02	.217980E-01	.101663E-01	.858091E-04	.666966E-04
JAN-	.284952E 02	.186762E 01	-.331938E-02	.122526E-01	.268617E-01	.153547E-01	.198034E-03	.141456E-03
OCT-	.300854E 02	.165737E 01	.937022E-03	.100965E-01	.169455E-01	.135750E-01	.130139E-03	.104281E-03

MAX H	MIN H	MAX DH	MIN DH	MAX THETA	MIN THETA	MAX DTHETA	MIN DTHETA
.328310E 02	.253434E 02	.211098E-01	-.259180E-01	.601061E-01	.235553E-03	.444486E-03	.206205E-05
SEG. NO.	SEG. NO.	SEG. NO.	SEG. NO.	SEG. NO.	SEG. NO.	SEG. NO.	SEG. NO.
56	367	168	360	378	123	363	352

TABLE G1. - RADIOMETRIC ERROR ANALYSIS RESULTS - Continued

ERROR NO.14
LOCATOR L1
VALUE 2.00

	F MEAN	F SIGMA	DF MEAN	DF SIGMA	THETA MEAN	THETA SIGMA	DTHETA MEAN	DTHETA SIGMA
APR-	.437151E 02	.880602E 00	-.865713E-02	.156462E-01	.124984E-01	.867733E-02	.243534E-03	.189453E-03
AUG-	.429848E 02	.148536E 01	.325084E-02	.251221E-01	.232402E-01	.944086E-02	.225085E-03	.225709E-03
OCT-	.411541E 02	.235787E 01	.507647E-03	.229854E-01	.343471E-01	.140378E-01	.321000E-03	.245695E-03
JAN-	.332074E 02	.348451E 01	-.342262E-02	.296100E-01	.511464E-01	.234545E-01	.479674E-03	.363468E-03
TOT-	.415153E 02	.311264E 01	-.333032E-02	.244641E-01	.303080E-01	.207934E-01	.317323E-03	.280545E-03

MAX F	MIN F	MAX DF	MIN DF	MAX THETA	MIN THETA	MAX DTHETA	MIN DTHETA
.451988E 02	.313011E 02	.599791E-01	-.795786E-01	.104264E 00	.938549E-04	.122045E-02	.207216E-07
SEQ. NO. 139	SEQ. NO. 360	SEQ. NO. 176	SEQ. NO. 392	SEQ. NO. 378	SEQ. NO. 16	SEQ. NO. 339	SEQ. NO. 125

ERROR NO.14
LOCATOR L1
VALUE 3.00

	F MEAN	F SIGMA	DF MEAN	DF SIGMA	THETA MEAN	THETA SIGMA	DTHETA MEAN	DTHETA SIGMA
APR-	.386458E 02	.132197E 01	-.792226E-02	.139561E-01	.212811E-01	.125364E-01	.215236E-03	.183846E-03
AUG-	.332549E 02	.135187E 01	.337411E-02	.195826E-01	.200393E-01	.786414E-02	.194274E-03	.149991E-03
OCT-	.354488E 02	.260781E 01	-.494992E-03	.208408E-01	.385950E-01	.140915E-01	.308674E-03	.223879E-03
JAN-	.321367E 02	.420911E 01	-.516149E-02	.244315E-01	.579355E-01	.322740E-01	.381388E-03	.309592E-03
TOT-	.361215E 02	.371977E 01	-.255116E-02	.205220E-01	.343377E-01	.244224E-01	.274906E-03	.237066E-03

MAX F	MIN F	MAX DF	MIN DF	MAX THETA	MIN THETA	MAX DTHETA	MIN DTHETA
.406716E 02	.192419E 02	.407890E-01	-.572985E-01	.122401E 00	.222749E-02	.111268E-02	.233748E-05
SEQ. NO. 56	SEQ. NO. 360	SEQ. NO. 339	SEQ. NO. 392	SEQ. NO. 360	SEQ. NO. 6	SEQ. NO. 339	SEQ. NO. 27

TABLE G1. - RADIOMETRIC ERROR ANALYSIS RESULTS - Continued

ERROR NO.14
LOCATOR L3
VALUE 4.50

	H MEAN	H SIGMA	DH MEAN	DH SIGMA	THETA MEAN	THETA SIGMA	DTHETA MEAN	DTHETA SIGMA
APR-	.530104E 02	.309745E 00	-.580311E-01	.101452E 00	.520563E-02	.296393E-02	.159753E-02	.126008E-02
AUG-	.525468E 02	.701783E 00	.316903E-01	.176962E 00	.105692E-01	.723574E-02	.161268E-02	.151411E-02
OCT-	.518619E 02	.102829E 01	-.307080E-03	.150747E 00	.140941E-01	.751359E-02	.211954E-02	.169879E-02
JAN-	.504458E 02	.152085E 01	-.475881E-01	.206923E 00	.216243E-01	.119759E-01	.334766E-02	.250216E-02
TOT-	.519662E 02	.138825E 01	-.185590E-01	.167637E 00	.128733E-01	.100438E-01	.216935E-02	.194002E-02

MAX H	MIN H	MAX DH	MIN DH	MAX THETA	MIN THETA	MAX DTHETA	MIN DTHETA
.537186E 02	.468428E 02	.399333E 00	-.504255E 00	.386885E-01	.105380E-03	.834926E-02	.241265E-04
SEQ. NO. 56	SEQ. NO. 360	SEQ. NO. 117	SEQ. NO. 350	SEQ. NO. 372	SEQ. NO. 27	SEQ. NO. 339	SEQ. NO. 378

ERROR NO.14
LOCATOR L3
VALUE 20.00

	H MEAN	H SIGMA	DH MEAN	DH SIGMA	THETA MEAN	THETA SIGMA	DTHETA MEAN	DTHETA SIGMA
APR-	.421387E 02	.504739E 00	-.260383E-01	.459229E-01	.843271E-02	.379953E-02	.725626E-03	.557789E-03
AUG-	.415325E 02	.979305E 00	.114771E-01	.783821E-01	.148941E-01	.754363E-02	.742792E-03	.619647E-03
OCT-	.402941E 02	.155589E 01	.217162E-02	.698702E-01	.222187E-01	.922377E-02	.945749E-03	.725682E-03
JAN-	.381892E 02	.251005E 01	-.229514E-01	.928387E-01	.366289E-01	.168932E-01	.150791E-02	.112896E-02
TOT-	.405386E 02	.218303E 01	-.983526E-02	.752392E-01	.205436E-01	.148487E-01	.980518E-03	.851042E-03

MAX H	MIN H	MAX DH	MIN DH	MAX THETA	MIN THETA	MAX DTHETA	MIN DTHETA
.432080E 02	.328445E 02	.182966E 00	-.218599E 00	.675268E-01	.239613E-02	.385889E-02	.144475E-04
SEQ. NO. 139	SEQ. NO. 360	SEQ. NO. 176	SEQ. NO. 350	SEQ. NO. 378	SEQ. NO. 153	SEQ. NO. 339	SEQ. NO. 178

TABLE G1. - RADIOMETRIC ERROR ANALYSIS RESULTS - Continued

ERROR NO.14
LOCATION L4
VALUE 2.50

	H MEAN	H SIGMA	DH MEAN	DH SIGMA	THETA MEAN	THETA SIGMA	DTHETA MEAN	DTHETA SIGMA
APR-	.448751E 02	.331733E 00	-.230556E-01	.508137E-01	.498251E-02	.394948E-02	.797994E-03	.614684E-03
ALC-	.442934E 02	.452633E 00	.122043E-01	.868095E-01	.727949E-02	.520738E-02	.826335E-03	.712002E-03
CCT-	.441492E 02	.562612E 00	.228463E-02	.803134E-01	.120942E-01	.736352E-02	.109601E-02	.859522E-03
JAN-	.430509E 02	.137802E 01	-.261800E-01	.112567E 00	.201236E-01	.110892E-01	.181900E-02	.139057E-02
TCT-	.440921E 02	.110469E 01	-.101942E-01	.873544E-01	.113449E-01	.971433E-02	.113483E-02	.102901E-02

MAX H	MIN H	MAX DH	MIN DH	MAX THETA	MIN THETA	MAX DTHETA	MIN DTHETA
.457420E 02	.407701E 02	.225230E 00	-.267132E 00	.396135E-01	.206577E-03	.490326E-02	.271813E-04
SEQ. NO.	SEQ. NO.	SEQ. NO.	SEQ. NO.	SEQ. NO.	SEQ. NO.	SEQ. NO.	SEQ. NO.
56	367	339	350	378	2	339	178

ERROR NO.14
LOCATION L4
VALUE 10.00

	H MEAN	H SIGMA	DH MEAN	DH SIGMA	THETA MEAN	THETA SIGMA	DTHETA MEAN	DTHETA SIGMA
APR-	.311785E 02	.955220E 00	-.135490E-01	.237739E-01	.133935E-01	.107747E-01	.372683E-03	.290249E-03
ALC-	.306753E 02	.412818E 00	.585948E-02	.400847E-01	.595064E-02	.499267E-02	.381451E-03	.332230E-03
CCT-	.299880E 02	.150421E 01	.329266E-03	.377182E-01	.216675E-01	.102356E-01	.524075E-03	.400259E-03
JAN-	.284766E 02	.185859E 01	-.119566E-01	.499002E-01	.270070E-01	.150482E-01	.806251E-03	.618179E-03
TCT-	.300796E 02	.165381E 01	-.482920E-02	.398791E-01	.170047E-01	.134978E-01	.521115E-03	.463633E-03

MAX H	MIN H	MAX DH	MIN DH	MAX THETA	MIN THETA	MAX DTHETA	MIN DTHETA
.328379E 02	.254074E 02	.270861E-01	-.114217E 00	.602921E-01	.244387E-03	.214075E-02	.201817E-04
SEQ. NO.	SEQ. NO.	SEQ. NO.	SEQ. NO.	SEQ. NO.	SEQ. NO.	SEQ. NO.	SEQ. NO.
56	367	176	350	378	16	339	178

TABLE G1. - RADIOMETRIC ERROR ANALYSIS RESULTS - Continued

ERROR NO.15
LOCATOR L1
VALUE 2.00

	H MEAN	H SIGMA	DH MEAN	DH SIGMA	THETA MEAN	THETA SIGMA	DTHETA MEAN	DTHETA SIGMA
APR-	.437309E 02	.885970E 00	.720836E-02	.457873E-01	.125893E-01	.896730E-02	.714280E-03	.540885E-03
AUG-	.429805E 02	.148445E 01	-.102480E-02	.461499E-01	.230733E-01	.944960E-02	.689104E-03	.554175E-03
OCT-	.411477E 02	.235592E 01	-.583528E-02	.612046E-01	.343592E-01	.138196E-01	.830948E-03	.561550E-03
JAN-	.381916E 02	.349559E 01	-.242253E-01	.754267E-01	.515050E-01	.233969E-01	.844563E-03	.494238E-03
TOT-	.415127E 02	.312233E 01	-.596999E-02	.595903E-01	.303817E-01	.208573E-01	.769746E-03	.540463E-03

MAX H	MIN H	MAX DH	MIN DH	MAX THETA	MIN THETA	MAX DTHETA	MIN DTHETA
.452446E 02	.312833E 02	.134814E 00	-.201030E 00	.105694E 00	.588288E-03	.197071E-02	.524133E-05
SEQ. NO.	SEQ. NO.	SEQ. NO.	SEQ. NO.	SEQ. NO.	SEQ. NO.	SEQ. NO.	SEQ. NO.
139	360	119	367	378	16	184	125

ERROR NO.15
LOCATOR L1
VALUE 3.00

	H MEAN	H SIGMA	DH MEAN	DH SIGMA	THETA MEAN	THETA SIGMA	DTHETA MEAN	DTHETA SIGMA
APR-	.386592E 02	.132459E 01	.549550E-02	.403894E-01	.213992E-01	.126441E-01	.623223E-03	.505773E-03
AUG-	.382521E 02	.136180E 01	.542178E-03	.321593E-01	.193716E-01	.788742E-02	.487922E-03	.391804E-03
OCT-	.354429E 02	.260829E 01	-.634366E-02	.576808E-01	.386010E-01	.139916E-01	.750807E-03	.528461E-03
JAN-	.321175E 02	.422554E 01	-.244303E-01	.642540E-01	.577879E-01	.327420E-01	.744220E-03	.521623E-03
TOT-	.361179E 02	.373203E 01	-.618467E-02	.515650E-01	.344149E-01	.246709E-01	.651540E-03	.501683E-03

MAX H	MIN H	MAX DH	MIN DH	MAX THETA	MIN THETA	MAX DTHETA	MIN DTHETA
.406924E 02	.192184E 02	.994472E-01	-.176005E 00	.123709E 00	.173721E-02	.200938E-02	.959359E-05
SEQ. NO.	SEQ. NO.	SEQ. NO.	SEQ. NO.	SEQ. NO.	SEQ. NO.	SEQ. NO.	SEQ. NO.
56	360	193	367	360	6	363	125

TABLE G1. - RADIOMETRIC ERROR ANALYSIS RESULTS - Continued

ERROR NO.15
LOCATOR L2
VALUE .15

	H MEAN	H SIGMA	DH MEAN	DH SIGMA	THETA MEAN	THETA SIGMA	DTHETA MEAN	DTHETA SIGMA
APR-	.518566E 02	.219136E 00	.874667E-02	.628905E-01	.346153E-02	.276850E-02	.983626E-03	.741964E-03
ALG-	.510543E 02	.434162E 00	-.317389E-03	.611864E-01	.689195E-02	.513401E-02	.893207E-03	.755839E-03
OCT-	.509675E 02	.899243E 00	-.819083E-02	.102093E 00	.119858E-01	.850710E-02	.138016E-02	.975225E-03
JAN-	.496825E 02	.152061E 01	-.410948E-01	.123674E 00	.219028E-01	.143934E-01	.136708E-02	.772253E-03
TCT-	.508902E 02	.120237E 01	-.102141E-01	.933172E-01	.110605E-01	.112594E-01	.115602E-02	.845994E-03

MAX H	MIN H	MAX DH	MIN DH	MAX THETA	MIN THETA	MAX DTHETA	MIN DTHETA
.526806E 02	.466296E 02	.183906E 00	-.370370E 00	.479483E-01	.280765E-04	.364628E-02	.385176E-04
SEQ. NO.	SEQ. NO.	SEQ. NO.	SEQ. NO.	SEQ. NO.	SEQ. NO.	SEQ. NO.	SEQ. NO.
214	367	371	367	378	2	184	125

ERROR NO.15
LOCATOR L2
VALUE .90

	H MEAN	H SIGMA	DH MEAN	DH SIGMA	THETA MEAN	THETA SIGMA	DTHETA MEAN	DTHETA SIGMA
APR-	.267707E 02	.216490E 01	.216108E-03	.737587E-02	.315970E-01	.128924E-01	.108014E-03	.943353E-04
ALG-	.269242E 02	.466691E 00	.951643E-04	.603841E-02	.652339E-02	.492984E-02	.868100E-04	.751303E-04
OCT-	.253758E 02	.225799E 01	-.117900E-02	.924775E-02	.330925E-01	.152191E-01	.129164E-03	.859017E-04
JAN-	.240686E 02	.260353E 01	-.377855E-02	.100853E-01	.380743E-01	.186258E-01	.106089E-03	.723443E-04
TCT-	.257948E 02	.235395E 01	-.116157E-02	.849155E-02	.273218E-01	.184988E-01	.107519E-03	.837499E-04

MAX H	MIN H	MAX DH	MIN DH	MAX THETA	MIN THETA	MAX DTHETA	MIN DTHETA
.297376E 02	.190375E 02	.189151E-01	-.278580E-01	.794952E-01	.593267E-03	.355262E-03	.733160E-06
SEQ. NO.	SEQ. NO.	SEQ. NO.	SEQ. NO.	SEQ. NO.	SEQ. NO.	SEQ. NO.	SEQ. NO.
52	360	8	367	378	125	184	125

TABLE G1. - RADIOMETRIC ERROR ANALYSIS RESULTS - Continued

ERROR NO.15
LOCATOR L3
VALUE 4.50

	H MEAN	H SIGMA	DH MEAN	DH SIGMA	THETA MEAN	THETA SIGMA	DTHETA MEAN	DTHETA SIGMA
APR-	.531136E 02	.429621E 00	.451775E-01	.315323E 00	.698408E-02	.446312E-02	.496153E-02	.378422E-02
AUG-	.525144E 02	.703769E 00	-.740697E-03	.314845E 00	.935350E-02	.792558E-02	.455055E-02	.373125E-02
OCT-	.518333E 02	.109392E 01	-.288984E-01	.404066E 00	.155476E-01	.943950E-02	.553615E-02	.361658E-02
JAN-	.503250E 02	.168732E 01	-.168400E 00	.553743E 00	.237264E-01	.150836E-01	.625548E-02	.366657E-02
TOT-	.519466E 02	.150420E 01	-.382153E-01	.418121E 00	.139029E-01	.119088E-01	.532593E-02	.375527E-02

MAX H	MIN H	MAX DH	MIN DH	MAX THETA	MIN THETA	MAX DTHETA	MIN DTHETA
.539531E 02	.467372E 02	.100892E 01	-.166059E 01	.435986E-01	.212305E-03	.137519E-01	.574090E-04
SEQ. NO. 139	SEQ. NO. 360	SEQ. NO. 118	SEQ. NO. 367	SEQ. NO. 378	SEQ. NO. 148	SEQ. NO. 118	SEQ. NO. 125

ERROR NO.15
LOCATOR L3
VALUE 20.00

	H MEAN	H SIGMA	DH MEAN	DH SIGMA	THETA MEAN	THETA SIGMA	DTHETA MEAN	DTHETA SIGMA
APR-	.421863E 02	.533072E 00	.215776E-01	.138522E 00	.885407E-02	.480984E-02	.218955E-02	.162892E-02
AUG-	.415190E 02	.973665E 00	-.206047E-02	.135171E 00	.143082E-01	.762831E-02	.199423E-02	.158420E-02
OCT-	.402809E 02	.155934E 01	-.110027E-01	.187031E 00	.222038E-01	.981812E-02	.254149E-02	.168142E-02
JAN-	.381313E 02	.256183E 01	-.808317E-01	.255897E 00	.377857E-01	.174351E-01	.276762E-02	.164231E-02
TOT-	.405294E 02	.222282E 01	-.180793E-01	.189566E 00	.207880E-01	.154680E-01	.237322E-02	.166197E-02

MAX H	MIN H	MAX DH	MIN DH	MAX THETA	MIN THETA	MAX DTHETA	MIN DTHETA
.433476E 02	.327975E 02	.418215E 00	-.765800E 00	.725534E-01	.255126E-02	.612828E-02	.720300E-04
SEQ. NO. 139	SEQ. NO. 360	SEQ. NO. 355	SEQ. NO. 367	SEQ. NO. 378	SEQ. NO. 16	SEQ. NO. 184	SEQ. NO. 125

TABLE G1. - RADIOMETRIC ERROR ANALYSIS RESULTS - Continued

ERROR NO.15
LOCATOR L4
VALUE 2.50

	H MEAN	H SIGMA	DH MEAN	DH SIGMA	THETA MEAN	THETA SIGMA	DTHETA MEAN	DTHETA SIGMA
APR-	.449283E 02	.374185E 00	.242135E-01	.164406E 00	.583771E-02	.455273E-02	.243024E-02	.184150E-02
AUG-	.442805E 02	.423607E 00	-.695953E-03	.148880E 00	.701500E-02	.479923E-02	.216096E-02	.175666E-02
OCT-	.441332E 02	.970958E 00	-.137496E-01	.218242E 00	.131800E-01	.856162E-02	.294443E-02	.193923E-02
JAN-	.429803E 02	.147318E 01	-.367336E-01	.313976E 00	.206900E-01	.130356E-01	.347975E-02	.208474E-02
TOT-	.440806E 02	.116237E 01	-.217414E-01	.223864E 00	.116807E-01	.103237E-01	.275384E-02	.197505E-02

MAX H	MIN H	MAX DH	MIN DH	MAX THETA	MIN THETA	MAX DTHETA	MIN DTHETA
.458351E 02	.397219E 02	.515221E 00	-.944423E 00	.455547E-01	.395221E-03	.716663E-02	.871264E-04
SEQ. NO.	SEQ. NO.	SEQ. NO.	SEQ. NO.	SEQ. NO.	SEQ. NO.	SEQ. NO.	SEQ. NO.
56	367	355	367	378	16	184	125

ERROR NO.15
LOCATOR L4
VALUE 10.00

	H MEAN	H SIGMA	DH MEAN	DH SIGMA	THETA MEAN	THETA SIGMA	DTHETA MEAN	DTHETA SIGMA
APR-	.312026E 02	.963909E 00	.105693E-01	.718009E-01	.138571E-01	.108015E-01	.112144E-02	.852422E-03
AUG-	.306687E 02	.402501E 00	-.747939E-03	.683594E-01	.588993E-02	.460286E-02	.100644E-02	.812382E-03
OCT-	.299790E 02	.150029E 01	-.367614E-02	.102249E 00	.216703E-01	.104245E-01	.137272E-02	.925431E-03
JAN-	.284436E 02	.189101E 01	-.449664E-01	.136254E 00	.271879E-01	.154772E-01	.153006E-02	.924372E-03
TOT-	.300735E 02	.167427E 01	-.109553E-01	.100720E 00	.171513E-01	.136472E-01	.125767E-02	.903685E-03

MAX H	MIN H	MAX DH	MIN DH	MAX THETA	MIN THETA	MAX DTHETA	MIN DTHETA
.328809E 02	.249514E 02	.208255E 00	-.411726E 00	.629074E-01	.545187E-04	.347466E-02	.316899E-04
SEQ. NO.	SEQ. NO.	SEQ. NO.	SEQ. NO.	SEQ. NO.	SEQ. NO.	SEQ. NO.	SEQ. NO.
56	367	371	367	378	117	184	125

TABLE G1. - RADIOMETRIC ERROR ANALYSIS RESULTS - Continued

ERROR NO.16
LOCATION L2
VALUE .15

	F MEAN	F SIGMA	DF MEAN	DF SIGMA	THETA MEAN	THETA SIGMA	DTHETA MEAN	DTHETA SIGMA
APR-	.519078E 02	.320746E 00	-.399993E-01	.284558E 00	.389296E-02	.338549E-02	.358415E-02	.309763E-02
AUG-	.510582E 02	.573491E 00	.357544E-02	.296368E 00	.824844E-02	.660732E-02	.395509E-02	.282115E-02
OCT-	.510417E 02	.962057E 00	.659865E-01	.330227E 00	.137282E-01	.653786E-02	.553693E-02	.330318E-02
JAN-	.497132E 02	.158832E 01	-.103613E-01	.435756E 00	.220488E-01	.166409E-01	.657846E-02	.517020E-02
TOT-	.509052E 02	.124073E 01	.480036E-02	.344137E 00	.119796E-01	.118168E-01	.491366E-02	.390649E-02

MAX F	MIN F	MAX DF	MIN DF	MAX THETA	MIN THETA	MAX DTHETA	MIN DTHETA
.531640E 02	.466894E 02	.103777E 01	-.120462E 01	.506536E-01	.235248E-03	.186173E-01	.924021E-04
SEQ. NO.	SEQ. NO.	SEQ. NO.	SEQ. NO.	SEQ. NO.	SEQ. NO.	SEQ. NO.	SEQ. NO.
215	367	363	392	378	8	346	113

ERROR NO.16
LOCATION L2
VALUE .90

	F MEAN	F SIGMA	DF MEAN	DF SIGMA	THETA MEAN	THETA SIGMA	DTHETA MEAN	DTHETA SIGMA
APR-	.267654E 02	.215974E 01	-.504400E-02	.347724E-01	.313378E-01	.129518E-01	.432126E-03	.413841E-03
AUG-	.269248E 02	.463799E 00	.790648E-03	.287277E-01	.658648E-02	.492612E-02	.384704E-03	.293925E-03
OCT-	.253844E 02	.225314E 01	.742316E-02	.313390E-01	.330444E-01	.150218E-01	.507491E-03	.291970E-03
JAN-	.240688E 02	.260266E 01	-.356491E-02	.404762E-01	.377717E-01	.190081E-01	.600859E-03	.484751E-03
TOT-	.257859E 02	.235034E 01	-.987733E-04	.344554E-01	.271851E-01	.184860E-01	.481317E-03	.388779E-03

MAX F	MIN F	MAX DF	MIN DF	MAX THETA	MIN THETA	MAX DTHETA	MIN DTHETA
.297327E 02	.190795E 02	.772714E-01	-.114387E 00	.798324E-01	.154485E-03	.162228E-02	.348106E-06
SEQ. NO.	SEQ. NO.	SEQ. NO.	SEQ. NO.	SEQ. NO.	SEQ. NO.	SEQ. NO.	SEQ. NO.
52	360	363	392	378	339	24	350

TABLE G1. - RADIOMETRIC ERROR ANALYSIS RESULTS - Continued

ERROR NO.16
LOCATOR L3
VALUE 4.50

	H MEAN	H SIGMA	DH MEAN	DH SIGMA	THETA MEAN	THETA SIGMA	DTHETA MEAN	DTHETA SIGMA
APR-	.529165E 02	.144126E 01	-.152011E 00	.136325E 01	.170906E-01	.169538E-01	.173385E-01	.151487E-01
ALG-	.526106E 02	.171394E 01	.955366E-01	.146620E 01	.247788E-01	.145136E-01	.192926E-01	.141608E-01
CCT-	.521897E 02	.173207E 01	.327504E 00	.139726E 01	.236604E-01	.182694E-01	.234031E-01	.124243E-01
JAN-	.504055E 02	.236623E 01	-.879664E-01	.181149E 01	.386488E-01	.159223E-01	.279980E-01	.203848E-01
TCT-	.520306E 02	.208575E 01	.457908E-01	.153141E 01	.260447E-01	.182462E-01	.220080E-01	.163319E-01

MAX H	MIN H	MAX DH	MIN DH	MAX THETA	MIN THETA	MAX DTHETA	MIN DTHETA
.561602E 02	.458051E 02	.384585E 01	-.456315E 01	.680528E-01	.467945E-03	.697165E-01	.577025E-03
SEQ. NO. 215	SEQ. NO. 392	SEQ. NO. 363	SEQ. NO. 392	SEQ. NO. 192	SEQ. NO. 36	SEQ. NO. 346	SEQ. NO. 113

ERROR NO.16
LOCATOR L3
VALUE 20.00

	H MEAN	H SIGMA	DH MEAN	DH SIGMA	THETA MEAN	THETA SIGMA	DTHETA MEAN	DTHETA SIGMA
APR-	.420855E 02	.819609E 00	-.792379E-01	.618443E 00	.921873E-02	.952137E-02	.777837E-02	.703647E-02
ALG-	.415411E 02	.126584E 01	.199829E-01	.648162E 00	.174887E-01	.114668E-01	.858762E-02	.641808E-02
CCT-	.404223E 02	.167626E 01	.130383E 00	.623330E 00	.225271E-01	.129878E-01	.104540E-01	.564341E-02
JAN-	.381398E 02	.267746E 01	-.723465E-01	.847860E 00	.357141E-01	.227585E-01	.129421E-01	.947515E-02
TCT-	.405472E 02	.231398E 01	-.304557E-03	.696223E 00	.212372E-01	.178782E-01	.994052E-02	.755163E-02

MAX H	MIN H	MAX DH	MIN DH	MAX THETA	MIN THETA	MAX DTHETA	MIN DTHETA
.440274E 02	.336536E 02	.158670E 01	-.224684E 01	.790993E-01	.246803E-03	.332183E-01	.173350E-03
SEQ. NO. 215	SEQ. NO. 360	SEQ. NO. 363	SEQ. NO. 392	SEQ. NO. 378	SEQ. NO. 346	SEQ. NO. 346	SEQ. NO. 350

TABLE G1. - RADIOMETRIC ERROR ANALYSIS RESULTS - Continued

ERROR NO.16
LOCATION L4
VALUE 2.50

	R MEAN	R SIGMA	DR MEAN	DR SIGMA	THETA MEAN	THETA SIGMA	DTHETA MEAN	DTHETA SIGMA
APR-	.448119E 02	.695793E 00	-.022976E-01	.680094E 00	.718295E-02	.800830E-02	.855739E-02	.778072E-02
ALC-	.442969E 02	.891139E 00	.157068E-01	.715684E 00	.140336E-01	.752899E-02	.947386E-02	.711101E-02
CCT-	.443021E 02	.122369E 01	.155232E 00	.719724E 00	.164736E-01	.120169E-01	.121528E-01	.649887E-02
JAN-	.430098E 02	.184765E 01	-.472742E-01	.104604E 01	.297647E-01	.122869E-01	.158616E-01	.120046E-01
TCT-	.441052E 02	.141105E 01	.284183E-02	.810171E 00	.168637E-01	.130815E-01	.115114E-01	.907835E-02

MAX R	MIN R	MAX DR	MIN DR	MAX THETA	MIN THETA	MAX DTHETA	MIN DTHETA
.469194E 02	.352890E 02	.226099E 01	-.265487E 01	.525996E-01	.481132E-03	.405748E-01	.148401E-03
SEQ. NO. 215	SEQ. NO. 354	SEQ. NO. 363	SEQ. NO. 302	SEQ. NO. 378	SEQ. NO. 14	SEQ. NO. 346	SEQ. NO. 154

ERROR NO.16
LOCATION L4
VALUE 10.00

	R MEAN	R SIGMA	DR MEAN	DR SIGMA	THETA MEAN	THETA SIGMA	DTHETA MEAN	DTHETA SIGMA
APR-	.311442E 02	.561333E 00	-.478637E-01	.322867E 00	.115866E-01	.109220E-01	.402954E-02	.370274E-02
ALC-	.306749E 02	.579148E 00	.543254E-02	.331664E 00	.861352E-02	.563925E-02	.439709E-02	.326600E-02
CCT-	.300577E 02	.154523E 01	.709266E-01	.341223E 00	.216211E-01	.119495E-01	.572633E-02	.313292E-02
JAN-	.284579E 02	.198107E 01	-.306881E-01	.478165E 00	.265273E-01	.190394E-01	.720292E-02	.553606E-02
TCT-	.300937E 02	.170954E 01	-.773177E-03	.376683E 00	.170871E-01	.147319E-01	.533897E-02	.421504E-02

MAX R	MIN R	MAX DR	MIN DR	MAX THETA	MIN THETA	MAX DTHETA	MIN DTHETA
.330964E 02	.250178E 02	.100861E 01	-.132386E 01	.665986E-01	.120617E-04	.194485E-01	.349752E-04
SEQ. NO. 215	SEQ. NO. 367	SEQ. NO. 363	SEQ. NO. 302	SEQ. NO. 378	SEQ. NO. 36	SEQ. NO. 346	SEQ. NO. 154

TABLE G1. - RADIOMETRIC ERROR ANALYSIS RESULTS - Continued

ERROR NO.17
LOCATOR L1
VALUE 2.00

	F MEAN	F SIGMA	DH MEAN	DH SIGMA	THETA MEAN	THETA SIGMA	DTHETA MEAN	DTHETA SIGMA
APR-	.437288E 02	.866625E 00	.510639E-02	.396655E-01	.123431E-01	.845365E-02	.618066E-03	.467241E-03
AUG-	.429747E 02	.147552E 01	-.681203E-02	.367208E-01	.230506E-01	.930870E-02	.383386E-03	.268783E-03
OCT-	.411413E 02	.236966E 01	-.122893E-01	.485999E-01	.345917E-01	.143967E-01	.593107E-03	.493232E-03
JAN-	.382261E 02	.349350E 01	.102641E-01	.469338E-01	.513506E-01	.231603E-01	.681533E-03	.520543E-03
TOT-	.415177E 02	.311193E 01	-.032721E-03	.439675E-01	.303340E-01	.208466E-01	.569046E-03	.462307E-03

MAX F	MIN F	MAX DH	MIN DH	MAX THETA	MIN THETA	MAX DTHETA	MIN DTHETA
.451947E 02	.313097E 02	.110029E 00	-.138150E 00	.102987E 00	.877976E-03	.176750E-02	.594049E-05
SEQ. NO.	SEQ. NO.	SEQ. NO.	SEQ. NO.	SEQ. NO.	SEQ. NO.	SEQ. NO.	SEQ. NO.
139	360	392	176	378	16	27	339

ERROR NO.17
LOCATOR L1
VALUE 3.00

	F MEAN	F SIGMA	DH MEAN	DH SIGMA	THETA MEAN	THETA SIGMA	DTHETA MEAN	DTHETA SIGMA
APR-	.386586E 02	.132942E 01	.493384E-02	.425372E-01	.212545E-01	.127821E-01	.667351E-03	.388083E-03
AUG-	.332351E 02	.133589E 01	-.164697E-01	.407172E-01	.195582E-01	.805111E-02	.708008E-03	.335860E-03
OCT-	.354413E 02	.262489E 01	-.792467E-02	.500344E-01	.390225E-01	.142886E-01	.710135E-03	.464745E-03
JAN-	.321463E 02	.419650E 01	.441015E-02	.564777E-01	.579556E-01	.323459E-01	.676909E-03	.461271E-03
TOT-	.361203E 02	.371556E 01	-.376259E-02	.496870E-01	.343227E-01	.246202E-01	.690616E-03	.416409E-03

MAX F	MIN F	MAX DH	MIN DH	MAX THETA	MIN THETA	MAX DTHETA	MIN DTHETA
.407171E 02	.193967E 02	.153533E 00	-.126971E 00	.121383E 00	.248096E-02	.145929E-02	.368610E-05
SEQ. NO.	SEQ. NO.	SEQ. NO.	SEQ. NO.	SEQ. NO.	SEQ. NO.	SEQ. NO.	SEQ. NO.
56	360	360	192	360	337	176	10

TABLE G1. - RADIOMETRIC ERROR ANALYSIS RESULTS - Continued

ERROR NO.17
LOCATOR L2
VALUE .15

	H MEAN	H SIGMA	DH MEAN	DH SIGMA	THETA MEAN	THETA SIGMA	DTHETA MEAN	DTHETA SIGMA
APR-	.518152E 02	.211046E 00	-.326439E-01	.348532E-01	.323268E-02	.267317E-02	.356881E-03	.328285E-03
AUG-	.510198E 02	.443433E 00	-.347750E-01	.298233E-01	.737533E-02	.496944E-02	.385581E-03	.363057E-03
OCT-	.509384E 02	.509675E 00	-.373633E-01	.395250E-01	.119241E-01	.794738E-02	.577738E-03	.438387E-03
JAN-	.496861E 02	.150094E 01	-.375266E-01	.346596E-01	.215814E-01	.139797E-01	.421554E-03	.357921E-03
TOT-	.508649E 02	.118781E 01	-.355772E-01	.349426E-01	.110284E-01	.109170E-01	.435439E-03	.383723E-03

MAX H	MIN H	MAX DH	MIN DH	MAX THETA	MIN THETA	MAX DTHETA	MIN DTHETA
.525913E 02	.469931E 02	.310663E-01	-.153551E 00	.451166E-01	.224334E-03	.199119E-02	.922531E-06
SEQ. NO. 215	SEQ. NO. 367	SEQ. NO. 48	SEQ. NO. 195	SEQ. NO. 378	SEQ. NO. 2	SEQ. NO. 195	SEQ. NO. 14

ERROR NO.17
LOCATOR L2
VALUE .90

	H MEAN	H SIGMA	DH MEAN	DH SIGMA	THETA MEAN	THETA SIGMA	DTHETA MEAN	DTHETA SIGMA
APR-	.266182E 02	.226549E 01	-.152337E 00	.267169E 00	.334573E-01	.119239E-01	.400814E-02	.223400E-02
AUG-	.267645E 02	.521217E 00	-.159557E 00	.195685E 00	.774366E-02	.572308E-02	.283979E-02	.209343E-02
OCT-	.251974E 02	.231493E 01	-.179612E 00	.177314E 00	.336769E-01	.171190E-01	.258536E-02	.157237E-02
JAN-	.239210E 02	.262091E 01	-.151362E 00	.148849E 00	.374671E-01	.196834E-01	.205772E-02	.144089E-02
TOT-	.256253E 02	.239810E 01	-.160717E 00	.202358E 00	.280863E-01	.188239E-01	.287275E-02	.199742E-02

MAX H	MIN H	MAX DH	MIN DH	MAX THETA	MIN THETA	MAX DTHETA	MIN DTHETA
.238723E 02	.191523E 02	.477637E 00	-.597123E 00	.798121E-01	.302023E-03	.761612E-02	.156550E-03
SEQ. NO. 43	SEQ. NO. 360	SEQ. NO. 48	SEQ. NO. 197	SEQ. NO. 378	SEQ. NO. 115	SEQ. NO. 42	SEQ. NO. 148

TABLE G1. - RADIOMETRIC ERROR ANALYSIS RESULTS - Continued

ERROR NO.17
LOCATOR L3
VALUE 4.50

	H MEAN	H SIGMA	DH MEAN	DH SIGMA	THETA MEAN	THETA SIGMA	DTHETA MEAN	DTHETA SIGMA
APR-	.530687E 02	.306816E 00	.191728E-03	.101268E-01	.498636E-02	.253469E-02	.123489E-03	.800732E-04
AUG-	.525174E 02	.674626E 00	.224097E-02	.106400E-01	.103551E-01	.699841E-02	.130692E-03	.898409E-04
OCT-	.518650E 02	.102998E 01	.275665E-02	.932988E-02	.139828E-01	.798028E-02	.954989E-04	.904426E-04
JAN-	.504967E 02	.154059E 01	.336707E-02	.100708E-01	.218731E-01	.118592E-01	.127095E-03	.119028E-03
TOT-	.519869E 02	.138488E 01	.213910E-02	.101230E-01	.127993E-01	.101301E-01	.119194E-03	.969602E-04

MAX H	MIN H	MAX DH	MIN DH	MAX THETA	MIN THETA	MAX DTHETA	MIN DTHETA
.537111E 02	.468560E 02	.273837E-01	-.296473E-01	.342721E-01	.472213E-04	.417383E-03	.261542E-05
SEQ. NO.	SEQ. NO.	SEQ. NO.	SEQ. NO.	SEQ. NO.	SEQ. NO.	SEQ. NO.	SEQ. NO.
56	360	384	18	372	27	350	192

ERROR NO.17
LOCATOR L3
VALUE 20.00

	H MEAN	H SIGMA	DH MEAN	DH SIGMA	THETA MEAN	THETA SIGMA	DTHETA MEAN	DTHETA SIGMA
APR-	.421641E 02	.505547E 00	-.623657E-03	.690303E-02	.818448E-02	.407099E-02	.976199E-04	.743564E-04
AUG-	.415214E 02	.971763E 00	.332208E-03	.816206E-02	.146361E-01	.764546E-02	.853542E-04	.694013E-04
OCT-	.402931E 02	.156593E 01	.119035E-02	.102675E-01	.225109E-01	.903389E-02	.138979E-03	.625940E-04
JAN-	.382149E 02	.252310E 01	.273603E-02	.832851E-02	.367181E-01	.169184E-01	.120230E-03	.793802E-04
TOT-	.405484E 02	.218435E 01	.008731E-03	.859004E-02	.205124E-01	.149666E-01	.110546E-03	.746133E-04

MAX H	MIN H	MAX DH	MIN DH	MAX THETA	MIN THETA	MAX DTHETA	MIN DTHETA
.431447E 02	.328542E 02	.208493E-01	-.262657E-01	.672453E-01	.157859E-02	.334614E-03	.387553E-05
SEQ. NO.	SEQ. NO.	SEQ. NO.	SEQ. NO.	SEQ. NO.	SEQ. NO.	SEQ. NO.	SEQ. NO.
139	360	143	216	378	158	373	341

TABLE G1. - RADIOMETRIC ERROR ANALYSIS RESULTS - Continued

ERROR NO.17
LOCATOR L4
VALUE 2.50

	H MEAN	H SIGMA	DH MEAN	DH SIGMA	THETA MEAN	THETA SIGMA	DTHETA MEAN	DTHETA SIGMA
APR-	.448701E 02	.333617E 00	-.333830E-01	.234230E-01	.471465E-02	.405117E-02	.257975E-03	.238447E-03
ALG-	.442470E 02	.434225E 00	-.342454E-01	.229137E-01	.744468E-02	.491265E-02	.284426E-03	.252739E-03
CCT-	.441113E 02	.979744E 00	-.356534E-01	.264550E-01	.130349E-01	.801219E-02	.348774E-03	.317428E-03
JAN-	.430366E 02	.139923E 01	-.424733E-01	.265422E-01	.195743E-01	.132256E-01	.371636E-03	.249128E-03
TCT-	.440662E 02	.111309E 01	-.360888E-01	.250264E-01	.111921E-01	.109527E-01	.315703E-03	.270228E-03

MAX H	MIN H	MAX DH	MIN DH	MAX THETA	MIN THETA	MAX DTHETA	MIN DTHETA
.457081E 02	.406471E 02	.221035E-01	-.121365E 00	.394403E-01	.914426E-04	.123209E-02	.413690E-05
SEQ. NO.	SEQ. NO.	SEQ. NO.	SEQ. NO.	SEQ. NO.	SEQ. NO.	SEQ. NO.	SEQ. NO.
56	367	120	195	342	182	195	114

ERROR NO.17
LOCATOR L4
VALUE 10.00

	H MEAN	H SIGMA	DH MEAN	DH SIGMA	THETA MEAN	THETA SIGMA	DTHETA MEAN	DTHETA SIGMA
APR-	.311428E 02	.964362E 00	-.452478E-01	.373591E-01	.132212E-01	.109991E-01	.495257E-03	.303292E-03
ALG-	.306127E 02	.402018E 00	-.367036E-01	.371409E-01	.584065E-02	.480456E-02	.450943E-03	.370756E-03
CCT-	.299271E 02	.152820E 01	-.406112E-01	.399307E-01	.220197E-01	.103961E-01	.442023E-03	.451749E-03
JAN-	.284313E 02	.187193E 01	-.571913E-01	.305071E-01	.267643E-01	.155619E-01	.406330E-03	.265737E-03
TCT-	.300285E 02	.166398E 01	-.559385E-01	.363683E-01	.169665E-01	.137224E-01	.448613E-03	.356423E-03

MAX H	MIN H	MAX DH	MIN DH	MAX THETA	MIN THETA	MAX DTHETA	MIN DTHETA
.327935E 02	.253226E 02	.306809E-01	-.187732E 00	.596270E-01	.390024E-04	.181613E-02	.645790E-05
SEQ. NO.	SEQ. NO.	SEQ. NO.	SEQ. NO.	SEQ. NO.	SEQ. NO.	SEQ. NO.	SEQ. NO.
56	367	120	195	378	117	195	14

TABLE G1. - RADIOMETRIC ERROR ANALYSIS RESULTS - Continued

ERROR NO.18
LOCATION L1
VALUE 2.00

	H MEAN	H SIGMA	DH MEAN	DH SIGMA	THETA MEAN	THETA SIGMA	DTHETA MEAN	DTHETA SIGMA
APR-	.437111E 02	.693635E 00	-.126611E-01	.833660E-01	.123519E-01	.849941E-02	.107072E-02	.865349E-03
AUG-	.429934E 02	.145654E 01	.185232E-02	.748386E-01	.227174E-01	.931516E-02	.958005E-03	.800827E-03
OCT-	.411839E 02	.233855E 01	.303559E-01	.109658E 00	.341935E-01	.136942E-01	.144961E-02	.753995E-03
JAN-	.392140E 02	.343835E 01	-.125013E-02	.115671E 00	.506409E-01	.231962E-01	.130437E-02	.878260E-03
TOT-	.415231E 02	.309015E 01	.442426E-02	.986975E-01	.299759E-01	.205714E-01	.119568E-02	.848292E-03

MAX H	MIN H	MAX DH	MIN DH	MAX THETA	MIN THETA	MAX DTHETA	MIN DTHETA
.449982E 02	.312937E 02	.316830E 00	-.365644E 00	.101942E 00	.721468E-03	.336832E-02	.248977E-04
SEQ. NO.	SEQ. NO.	SEQ. NO.	SEQ. NO.	SEQ. NO.	SEQ. NO.	SEQ. NO.	SEQ. NO.
139	360	195	376	378	36	195	1

ERROR NO.18
LOCATION L1
VALUE 3.00

	H MEAN	H SIGMA	DH MEAN	DH SIGMA	THETA MEAN	THETA SIGMA	DTHETA MEAN	DTHETA SIGMA
APR-	.396321E 02	.134146E 01	-.218864E-01	.113569E 00	.214535E-01	.125679E-01	.125624E-02	.116425E-02
AUG-	.382691E 02	.194492E 01	.171108E-01	.122728E 00	.192735E-01	.796377E-02	.160337E-02	.129198E-02
OCT-	.354542E 02	.264974E 01	.495056E-02	.131979E 00	.309962E-01	.134522E-01	.191301E-02	.132541E-02
JAN-	.321231E 02	.421604E 01	-.187860E-01	.157679E 00	.575997E-01	.321905E-01	.235734E-02	.120736E-02
TOT-	.361196E 02	.373314E 01	-.447849E-02	.133504E 00	.345807E-01	.245175E-01	.178249E-02	.131298E-02

MAX H	MIN H	MAX DH	MIN DH	MAX THETA	MIN THETA	MAX DTHETA	MIN DTHETA
.406182E 02	.194800E 02	.356353E 00	-.429140E 00	.120098E 00	.170773E-02	.560007E-02	.279772E-04
SEQ. NO.	SEQ. NO.	SEQ. NO.	SEQ. NO.	SEQ. NO.	SEQ. NO.	SEQ. NO.	SEQ. NO.
56	360	131	192	360	[illegible]	192	8

TABLE G1. - RADIOMETRIC ERROR ANALYSIS RESULTS - Continued

ERROR NO.18
LOCATOR L2
VALUE .15

	H MEAN	H SIGMA	DH MEAN	DH SIGMA	THETA MEAN	THETA SIGMA	DTHETA MEAN	DTHETA SIGMA
APR-	.517370E 02	.208662E 00	-.110843E 00	.700599E-01	.345009E-02	.241201E-02	.971927E-03	.652886E-03
AUG-	.509528E 02	.450571E 00	-.101818E 00	.639724E-01	.749758E-02	.518519E-02	.853402E-03	.570830E-03
OCT-	.508589E 02	.917234E 00	-.116791E 00	.109997E 00	.126427E-01	.770649E-02	.132571E-02	.870447E-03
JAN-	.495906E 02	.152254E 01	-.133040E 00	.754352E-01	.220515E-01	.142730E-01	.119334E-02	.673748E-03
TOT-	.507848E 02	.120131E 01	-.115623E 00	.843224E-01	.114105E-01	.110613E-01	.108622E-02	.724556E-03

MAX H	MIN H	MAX DH	MIN DH	MAX THETA	MIN THETA	MAX DTHETA	MIN DTHETA
.526533E 02	.468552E 02	.114892E 00	-.315720E 00	.472181E-01	.289713E-03	.299705E-02	.521692E-04
SEQ. NO. 214	SEQ. NO. 367	SEQ. NO. 52	SEQ. NO. 186	SEQ. NO. 378	SEQ. NO. 113	SEQ. NO. 194	SEQ. NO. 338

ERROR NO.18
LOCATOR L2
VALUE .30

	H MEAN	H SIGMA	DH MEAN	DH SIGMA	THETA MEAN	THETA SIGMA	DTHETA MEAN	DTHETA SIGMA
APR-	.261720E 02	.216985E 01	-.598477E 00	.475617E 00	.315014E-01	.159097E-01	.763531E-02	.497729E-02
AUG-	.262968E 02	.815103E 00	-.427292E 00	.508710E 00	.105714E-01	.865430E-02	.674654E-02	.493558E-02
OCT-	.246204E 02	.250302E 01	-.756584E 00	.540024E 00	.380034E-01	.196951E-01	.898251E-02	.635339E-02
JAN-	.235534E 02	.266815E 01	-.518976E 00	.352470E 00	.382164E-01	.199336E-01	.537235E-02	.336080E-02
TOT-	.251606E 02	.244671E 01	-.625332E 00	.482214E 00	.295732E-01	.201466E-01	.718418E-02	.518906E-02

MAX H	MIN H	MAX DH	MIN DH	MAX THETA	MIN THETA	MAX DTHETA	MIN DTHETA
.294369E 02	.190244E 02	.481346E 00	-.214609E 01	.885081E-01	.170588E-02	.214968E-01	.973151E-04
SEQ. NO. 214	SEQ. NO. 360	SEQ. NO. 382	SEQ. NO. 143	SEQ. NO. 378	SEQ. NO. 182	SEQ. NO. 114	SEQ. NO. 346

TABLE G1. - RADIOMETRIC ERROR ANALYSIS RESULTS - Continued

ERROR NO.18
LOCATION L3
VALUE 4.50

	H MEAN	H SIGMA	DH MEAN	DH SIGMA	THETA MEAN	THETA SIGMA	DTHETA MEAN	DTHETA SIGMA
APR-	.530728E 02	.309947E 00	.433770E-02	.219134E-01	.509772E-02	.257022E-02	.256765E-03	.229016E-03
AUG-	.525164E 02	.664535E 00	.126211E-02	.308157E-01	.101510E-01	.682844E-02	.399968E-03	.256166E-03
OCT-	.518656E 02	.102521E 01	.342351E-02	.252618E-01	.139243E-01	.782648E-02	.339127E-03	.246276E-03
JAN-	.505001E 02	.154356E 01	.676045E-02	.265588E-01	.220450E-01	.117222E-01	.400968E-03	.269256E-03
TOT-	.519987E 02	.138348E 01	.394594E-02	.264049E-01	.128045E-01	.100620E-01	.349182E-03	.257446E-03

MAX H	MIN H	MAX DH	MIN DH	MAX THETA	MIN THETA	MAX DTHETA	MIN DTHETA
.536892E 02	.468485E 02	.924445E-01	-.614250E-01	.339612E-01	.999667E-04	.132416E-02	.566984E-05
SEQ. NO. 56	SEQ. NO. 360	SEQ. NO. 376	SEQ. NO. 168	SEQ. NO. 372	SEQ. NO. 173	SEQ. NO. 344	SEQ. NO. 128

ERROR NO.18
LOCATION L3
VALUE 20.00

	H MEAN	H SIGMA	DH MEAN	DH SIGMA	THETA MEAN	THETA SIGMA	DTHETA MEAN	DTHETA SIGMA
APR-	.421439E 02	.507789E 00	-.753420E-03	.151870E-01	.832113E-02	.404040E-02	.214594E-03	.138508E-03
AUG-	.415132E 02	.974586E 00	-.783045E-02	.227148E-01	.146648E-01	.762121E-02	.379393E-03	.212438E-03
OCT-	.403002E 02	.156957E 01	.829625E-02	.244902E-01	.225037E-01	.906318E-02	.395060E-03	.246022E-03
JAN-	.382115E 02	.252396E 01	-.634189E-03	.246897E-01	.368787E-01	.168088E-01	.270054E-03	.239035E-03
TOT-	.405472E 02	.218546E 01	-.230453E-03	.233924E-01	.205921E-01	.149474E-01	.314775E-03	.226184E-03

MAX H	MIN H	MAX DH	MIN DH	MAX THETA	MIN THETA	MAX DTHETA	MIN DTHETA
.431348E 02	.328102E 02	.624235E-01	-.467281E-01	.675953E-01	.248668E-02	.832932E-03	.332743E-05
SEQ. NO. 139	SEQ. NO. 360	SEQ. NO. 176	SEQ. NO. 156	SEQ. NO. 378	SEQ. NO. 159	SEQ. NO. 154	SEQ. NO. 346

TABLE G1. - RADIOMETRIC ERROR ANALYSIS RESULTS - Continued

ERROR NO.18
LOCATION L4
VALUE 2.50

	R MEAN	R SIGMA	DR MEAN	DR SIGMA	THETA MEAN	THETA SIGMA	DTHETA MEAN	DTHETA SIGMA
APR-	.447856E 02	.335096E 00	-.119620E 00	.561209E-01	.526304E-02	.399627E-02	.928366E-03	.520618E-03
ALC-	.441621E 02	.437839E 00	-.119132E 00	.501555E-01	.724381E-02	.518995E-02	.652188E-03	.393613E-03
CCT-	.440313E 02	.396687E 00	-.115648E 00	.456546E-01	.135830E-01	.760213E-02	.877036E-03	.555004E-03
JAN-	.429370E 02	.141193E 01	-.140123E 00	.525867E-01	.201297E-01	.124130E-01	.770932E-03	.515963E-03
TCT-	.439790E 02	.112535E 01	-.123356E 00	.572014E-01	.115549E-01	.109397E-01	.807143E-03	.511156E-03

MAX R	MIN R	MAX DR	MIN DR	MAX THETA	MIN THETA	MAX DTHETA	MIN DTHETA
.456789E 02	.404909E 02	.499996E-01	-.275255E 00	.411310E-01	.673042E-04	.209313E-02	.105857E-04
SEQ. NO.	SEQ. NO.	SEQ. NO.	SEQ. NO.	SEQ. NO.	SEQ. NO.	SEQ. NO.	SEQ. NO.
214	367	214	346	342	42	179	339

ERROR NO.18
LOCATION L4
VALUE 10.00

	R MEAN	R SIGMA	DR MEAN	DR SIGMA	THETA MEAN	THETA SIGMA	DTHETA MEAN	DTHETA SIGMA
APR-	.309999E 02	.964805E 00	-.192723E 00	.760463E-01	.139649E-01	.107341E-01	.124938E-02	.623756E-03
ALC-	.304889E 02	.395453E 00	-.120557E 00	.813559E-01	.544963E-02	.491188E-02	.934813E-03	.698992E-03
CCT-	.297999E 02	.154750E 01	-.177747E 00	.664412E-01	.223567E-01	.102099E-01	.118359E-02	.571912E-03
JAN-	.282721E 02	.187375E 01	-.216488E 00	.704239E-01	.270938E-01	.151767E-01	.840021E-03	.485078E-03
TCT-	.298900E 02	.167392E 01	-.164384E 00	.827534E-01	.172163E-01	.136649E-01	.105195E-02	.623496E-03

MAX R	MIN R	MAX DR	MIN DR	MAX THETA	MIN THETA	MAX DTHETA	MIN DTHETA
.325515E 02	.251775E 02	.344617E-01	-.420816E 00	.594316E-01	.556555E-03	.267131E-02	.325993E-06
SEQ. NO.	SEQ. NO.	SEQ. NO.	SEQ. NO.	SEQ. NO.	SEQ. NO.	SEQ. NO.	SEQ. NO.
214	367	214	220	378	126	13	339

TABLE G1. - RADIOMETRIC ERROR ANALYSIS RESULTS - Continued

ERROR NO.19
LOCATOR L1
VALUE 2.00

	F MEAN	F SIGMA	DF MEAN	DF SIGMA	THETA MEAN	THETA SIGMA	DTHETA MEAN	DTHETA SIGMA
APR-	.437091E 02	.522348E 00	-.146829E-01	.133408E 00	.131779E-01	.874994E-02	.178994E-02	.109007E-02
AUG-	.429720E 02	.160453E 01	-.949766E-02	.203805E 00	.252530E-01	.105481E-01	.262607E-02	.226082E-02
OCT-	.411016E 02	.238570E 01	-.519320E-01	.211331E 00	.350179E-01	.133054E-01	.317027E-02	.191667E-02
JAN-	.382224E 02	.349443E 01	.651947E-02	.233671E 00	.516183E-01	.242100E-01	.251211E-02	.222651E-02
TOT-	.415013E 02	.313354E 01	-.173983E-01	.200269E 00	.312668E-01	.208723E-01	.252460E-02	.199359E-02

MAX F	MIN F	MAX DF	MIN DF	MAX THETA	MIN THETA	MAX DTHETA	MIN DTHETA
.452663E 02	.315272E 02	.458309E 00	-.684940E 00	.105983E 00	.132516E-03	.988509E-02	.542531E-04
SEQ. NO.	SEQ. NO.	SEQ. NO.	SEQ. NO.	SEQ. NO.	SEQ. NO.	SEQ. NO.	SEQ. NO.
139	360	143	144	378	16	352	6

ERROR NO.19
LOCATOR L1
VALUE 3.00

	F MEAN	F SIGMA	DF MEAN	DF SIGMA	THETA MEAN	THETA SIGMA	DTHETA MEAN	DTHETA SIGMA
APR-	.386912E 02	.134885E 01	.274772E-01	.207243E 00	.212309E-01	.139004E-01	.249741E-02	.179855E-02
AUG-	.392971E 02	.143474E 01	.455565E-01	.203558E 00	.208474E-01	.924498E-02	.151595E-02	.134119E-02
OCT-	.354758E 02	.261790E 01	.265504E-01	.238449E 00	.336825E-01	.151627E-01	.300436E-02	.257195E-02
JAN-	.322216E 02	.406479E 01	.796527E-01	.296120E 00	.548386E-01	.309750E-01	.358321E-02	.243623E-02
TOT-	.361689E 02	.367955E 01	.448092E-01	.240198E 00	.339499E-01	.239390E-01	.265024E-02	.222988E-02

MAX F	MIN F	MAX DF	MIN DF	MAX THETA	MIN THETA	MAX DTHETA	MIN DTHETA
.406763E 02	.201676E 02	.924398E 00	-.647034E 00	.116070E 00	.138489E-02	.967957E-02	.891210E-06
SEQ. NO.	SEQ. NO.	SEQ. NO.	SEQ. NO.	SEQ. NO.	SEQ. NO.	SEQ. NO.	SEQ. NO.
56	360	360	338	360	337	352	27

TABLE G1. - RADIOMETRIC ERROR ANALYSIS RESULTS - Continued

ERROR NO.19
LOCATOR L2
VALUE .15

	H MEAN	H SIGMA	DH MEAN	DH SIGMA	THETA MEAN	THETA SIGMA	DTHETA MEAN	DTHETA SIGMA
APR-	.516454E 02	.300536E 00	-.202447E 00	.134638E 00	.442066E-02	.370458E-02	.183973E-02	.124683E-02
AUG-	.507996E 02	.429565E 00	-.255056E 00	.149298E 00	.698380E-02	.458396E-02	.188053E-02	.102267E-02
OCT-	.506782E 02	.909412E 00	-.297506E 00	.109596E 00	.118988E-01	.844934E-02	.160048E-02	.137674E-02
JAN-	.494408E 02	.158124E 01	-.242821E 00	.180979E 00	.223240E-01	.151140E-01	.234215E-02	.203168E-02
TOT-	.506410E 02	.123269E 01	-.259457E 00	.150370E 00	.115568E-01	.115729E-01	.191572E-02	.149263E-02

MAX H	MIN H	MAX DH	MIN DH	MAX THETA	MIN THETA	MAX DTHETA	MIN DTHETA
.526364E 02	.467614E 02	.103297E 00	-.783838E 00	.506428E-01	.576158E-03	.754691E-02	.790777E-04
SEQ. NO.	SEQ. NO.	SEQ. NO.	SEQ. NO.	SEQ. NO.	SEQ. NO.	SEQ. NO.	SEQ. NO.
56	367	52	386	378	16	382	176

ERROR NO.19
LOCATOR L2
VALUE .30

	H MEAN	H SIGMA	DH MEAN	DH SIGMA	THETA MEAN	THETA SIGMA	DTHETA MEAN	DTHETA SIGMA
APR-	.257282E 02	.230027E 01	-.104234E 01	.876456E 00	.402708E-01	.157292E-01	.969277E-02	.104968E-01
AUG-	.254832E 02	.997023E 00	-.144023E 01	.714970E 00	.126907E-01	.883652E-02	.848193E-02	.697782E-02
OCT-	.238576E 02	.285281E 01	-.151940E 01	.990069E 00	.371066E-01	.287692E-01	.147115E-01	.101438E-01
JAN-	.224589E 02	.275872E 01	-.161341E 01	.943311E 00	.349543E-01	.223160E-01	.129005E-01	.729774E-02
TOT-	.243820E 02	.269408E 01	-.140399E 01	.913613E 00	.312556E-01	.230489E-01	.114467E-01	.919618E-02

MAX H	MIN H	MAX DH	MIN DH	MAX THETA	MIN THETA	MAX DTHETA	MIN DTHETA
.300532E 02	.170407E 02	.396156E 00	-.375349E 01	.108096E 00	.901060E-03	.420502E-01	.357276E-03
SEQ. NO.	SEQ. NO.	SEQ. NO.	SEQ. NO.	SEQ. NO.	SEQ. NO.	SEQ. NO.	SEQ. NO.
47	360	47	216	210	337	210	126

TABLE G1. - RADIOMETRIC ERROR ANALYSIS RESULTS - Continued

ERROR NO.19
LOCATOR L3
VALUE 4.50

	H MEAN	H SIGMA	DH MEAN	DH SIGMA	THETA MEAN	THETA SIGMA	DTHETA MEAN	DTHETA SIGMA
APR-	.530612E 02	.317708E 00	-.723749E-02	.569715E-01	.520042E-02	.251242E-02	.690517E-03	.454750E-03
AUG-	.525227E 02	.683981E 00	.759870E-02	.482135E-01	.105388E-01	.713882E-02	.539798E-03	.468909E-03
OCT-	.518517E 02	.101813E 01	-.105540E-01	.515701E-01	.136308E-01	.799842E-02	.699960E-03	.516154E-03
JAN-	.505076E 02	.154634E 01	.142244E-01	.519531E-01	.216561E-01	.118707E-01	.794012E-03	.492602E-03
TOT-	.519858E 02	.138243E 01	.100790E-02	.532651E-01	.127565E-01	.100517E-01	.681072E-03	.492165E-03

MAX H	MIN H	MAX DH	MIN DH	MAX THETA	MIN THETA	MAX DTHETA	MIN DTHETA
.537247E 02	.467643E 02	.115317E 00	-.125138E 00	.338309E-01	.996602E-04	.209701E-02	.208122E-04
SEQ. NO.	SEQ. NO.	SEQ. NO.	SEQ. NO.	SEQ. NO.	SEQ. NO.	SEQ. NO.	SEQ. NO.
56	360	126	16	372	173	170	24

ERROR NO.19
LOCATOR L3
VALUE 20.00

	H MEAN	H SIGMA	DH MEAN	DH SIGMA	THETA MEAN	THETA SIGMA	DTHETA MEAN	DTHETA SIGMA
APR-	.421653E 02	.517887E 00	.606717E-03	.421719E-01	.840682E-02	.408622E-02	.497131E-03	.400243E-03
AUG-	.415264E 02	.984920E 00	.530863E-02	.443330E-01	.147357E-01	.793179E-02	.508476E-03	.418016E-03
OCT-	.402761E 02	.155087E 01	-.158275E-01	.605140E-01	.220545E-01	.914210E-02	.848057E-03	.647724E-03
JAN-	.382132E 02	.252564E 01	.106634E-02	.470857E-01	.364801E-01	.166743E-01	.676952E-03	.458004E-03
TOT-	.405452E 02	.218634E 01	-.221145E-02	.497080E-01	.204193E-01	.148193E-01	.632654E-03	.511467E-03

MAX H	MIN H	MAX DH	MIN DH	MAX THETA	MIN THETA	MAX DTHETA	MIN DTHETA
.431761E 02	.327900E 02	.108582E 00	-.121750E 00	.673635E-01	.918876E-03	.230701E-02	.454815E-05
SEQ. NO.	SEQ. NO.	SEQ. NO.	SEQ. NO.	SEQ. NO.	SEQ. NO.	SEQ. NO.	SEQ. NO.
56	360	48	216	378	153	210	182

TABLE G1. - RADIOMETRIC ERROR ANALYSIS RESULTS - Continued

ERROR NO.19
LOCATION L4
VALUE 2.50

	H MEAN	H SIGMA	DH MEAN	DH SIGMA	THETA MEAN	THETA SIGMA	DTHETA MEAN	DTHETA SIGMA
APR-	.446509E 02	.372248E 00	-.263208E 00	.104650E 00	.554717E-02	.432730E-02	.140971E-02	.124740E-02
ALC-	.440219E 02	.440189E 00	-.256327E 00	.953375E-01	.760578E-02	.470396E-02	.111663E-02	.803895E-03
CCT-	.438479E 02	.101283E 01	-.298970E 00	.994215E-01	.132402E-01	.831958E-02	.139715E-02	.102686E-02
JAN-	.427779E 02	.144531E 01	-.269210E 00	.808034E-01	.203091E-01	.131115E-01	.110102E-02	.776917E-03
TCT-	.439247E 02	.114728E 01	-.277679E 00	.995755E-01	.116756E-01	.101623E-01	.125613E-02	.993391E-03

MAX H	MIN H	MAX DH	MIN DH	MAX THETA	MIN THETA	MAX DTHETA	MIN DTHETA
.455612E 02	.403549E 02	-.553048E-01	-.536647E 00	.417031E-01	.577878E-04	.429307E-02	.227760E-05
SEQ. NO.	SEQ. NO.	SEQ. NO.	SEQ. NO.	SEQ. NO.	SEQ. NO.	SEQ. NO.	SEQ. NO.
56	367	210	186	378	360	3	16

ERROR NO.19
LOCATION L4
VALUE 10.00

	H MEAN	H SIGMA	DH MEAN	DH SIGMA	THETA MEAN	THETA SIGMA	DTHETA MEAN	DTHETA SIGMA
APR-	.308090E 02	.101552E 01	-.383100E 00	.154926E 00	.149748E-01	.110638E-01	.199516E-02	.177311E-02
ALC-	.302575E 02	.423114E 00	-.411882E 00	.138000E 00	.575316E-02	.489516E-02	.190464E-02	.975348E-03
CCT-	.295296E 02	.158555E 01	-.458120E 00	.148226E 00	.226919E-01	.108099E-01	.224319E-02	.159417E-02
JAN-	.280369E 02	.161862E 01	-.451648E 00	.116324E 00	.274652E-01	.156732E-01	.108324E-02	.101631E-02
TCT-	.296582E 02	.171275E 01	-.426187E 00	.143420E 00	.177213E-01	.139538E-01	.180656E-02	.145158E-02

MAX H	MIN H	MAX DH	MIN DH	MAX THETA	MIN THETA	MAX DTHETA	MIN DTHETA
.324594E 02	.250165E 02	-.111348E 00	-.786649E 00	.627329E-01	.838836E-04	.598155E-02	.967536E-05
SEQ. NO.	SEQ. NO.	SEQ. NO.	SEQ. NO.	SEQ. NO.	SEQ. NO.	SEQ. NO.	SEQ. NO.
56	367	184	3	378	140	3	181

TABLE G1. - RADIOMETRIC ERROR ANALYSIS RESULTS - Continued

ERROR NO.20
LOCATOR L1
VALUE 2.00

	F MEAN	F SIGMA	DH MEAN	DH SIGMA	THETA MEAN	THETA SIGMA	DTHETA MEAN	DTHETA SIGMA
APR-	.438193E 02	.860629E 00	.955278E-01	.473037E 00	.136884E-01	.747762E-02	.652668E-02	.503982E-02
AUG-	.430564E 02	.146011E 01	.748302E-01	.479695E 00	.215516E-01	.977508E-02	.676282E-02	.546682E-02
OCT-	.413458E 02	.243608E 01	.192221E 00	.382650E 00	.332574E-01	.168203E-01	.412297E-02	.234838E-02
JAN-	.330075E 02	.359499E 01	-.118345E 00	.372940E 00	.530926E-01	.231740E-01	.440978E-02	.292426E-02
TOT-	.415797E 02	.320576E 01	.610595E-01	.444464E 00	.303975E-01	.215181E-01	.545556E-02	.433237E-02

MAX F	MIN F	MAX DH	MIN DH	MAX THETA	MIN THETA	MAX DTHETA	MIN DTHETA
.457543E 02	.305833E 02	.144341E 01	-.750802E 00	.105605E 00	.321854E-03	.190814E-01	.316655E-03
SEQ. NO.	SEQ. NO.	SEQ. NO.	SEQ. NO.	SEQ. NO.	SEQ. NO.	SEQ. NO.	SEQ. NO.
136	360	132	373	378	36	117	114

ERROR NO.20
LOCATOR L1
VALUE 3.00

	F MEAN	F SIGMA	DH MEAN	DH SIGMA	THETA MEAN	THETA SIGMA	DTHETA MEAN	DTHETA SIGMA
APR-	.387193E 02	.136598E 01	.655909E-01	.477399E 00	.226722E-01	.140090E-01	.675895E-02	.419313E-02
AUG-	.382480E 02	.165599E 01	-.368109E-02	.448959E 00	.225749E-01	.105075E-01	.453929E-02	.323481E-02
OCT-	.353367E 02	.276541E 01	-.112561E 00	.638354E 00	.405709E-01	.182637E-01	.765123E-02	.508562E-02
JAN-	.321375E 02	.427105E 01	-.439357E-02	.612850E 00	.583312E-01	.350787E-01	.777888E-02	.463875E-02
TOT-	.361104E 02	.382443E 01	-.137362E-01	.554257E 00	.360373E-01	.262115E-01	.668209E-02	.453232E-02

MAX F	MIN F	MAX DH	MIN DH	MAX THETA	MIN THETA	MAX DTHETA	MIN DTHETA
.411921E 02	.179888E 02	.184245E 01	-.158418E 01	.134679E 00	.127990E-02	.166321E-01	.337709E-03
SEQ. NO.	SEQ. NO.	SEQ. NO.	SEQ. NO.	SEQ. NO.	SEQ. NO.	SEQ. NO.	SEQ. NO.
130	360	363	216	360	337	363	46

TABLE G1. - RADIOMETRIC ERROR ANALYSIS RESULTS - Continued

ERRCR NC.20
LCCATCR L2
VALLE .15

	H MEAN	H SIGMA	DH MEAN	DH SIGMA	THETA MEAN	THETA SIGMA	DTHETA MEAN	DTHETA SIGMA
APR-	.513192E 02	.526107E 00	-.528625E 00	.435964E 00	.794340E-02	.681364E-02	.651771E-02	.516071E-02
ALG-	.503750E 02	.598832E 00	-.679657E 00	.348669E 00	.908668E-02	.629028E-02	.397921E-02	.279454E-02
CCT-	.500972E 02	.118222E 01	-.878535E 00	.533565E 00	.140312E-01	.102442E-01	.583562E-02	.547591E-02
JAN-	.489666E 02	.160814E 01	-.757028E 00	.402216E 00	.237878E-01	.155245E-01	.509472E-02	.340403E-02
TCT-	.501895E 02	.136326E 01	-.710961E 00	.453468E 00	.137123E-01	.121268E-01	.535682E-02	.445979E-02

MAX H	MIN H	MAX DH	MIN DH	MAX THETA	MIN THETA	MAX DTHETA	MIN DTHETA
.525367E 02	.464393E 02	.457016E 00	-.210914E 01	.558385E-01	.179372E-04	.199431E-01	.338779E-05
SEQ. NO.	SEQ. NO.	SEQ. NO.	SEQ. NO.	SEQ. NO.	SEQ. NO.	SEQ. NO.	SEQ. NO.
215	354	36	174	378	176	8	169

ERRCR NC.20
LCCATCR L2
VALLE .90

	H MEAN	H SIGMA	DH MEAN	DH SIGMA	THETA MEAN	THETA SIGMA	DTHETA MEAN	DTHETA SIGMA
APR-	.236049E 02	.312947E 01	-.316556E 01	.229529E 01	.419507E-01	.341828E-01	.365899E-01	.212282E-01
ALG-	.239044E 02	.202021E 01	-.311968E 01	.194946E 01	.262687E-01	.194778E-01	.237602E-01	.192767E-01
CCT-	.214709E 02	.411845E 01	-.390613E 01	.274972E 01	.510383E-01	.307447E-01	.312602E-01	.282015E-01
JAN-	.204637E 02	.471712E 01	-.360869E 01	.331698E 01	.675482E-01	.542454E-01	.402020E-01	.441015E-01
TCT-	.223360E 02	.390858E 01	-.345002E 01	.263037E 01	.467015E-01	.397779E-01	.329553E-01	.304777E-01

MAX H	MIN H	MAX DH	MIN DH	MAX THETA	MIN THETA	MAX DTHETA	MIN DTHETA
.291175E 02	.590658E 01	.953062E 00	-.147263E 02	.170212E 00	.107111E-03	.144847E 00	.145039E-03
SEQ. NO.	SEQ. NO.	SEQ. NO.	SEQ. NO.	SEQ. NO.	SEQ. NO.	SEQ. NO.	SEQ. NO.
16	367	352	367	336	346	33	339

TABLE G1. - RADIOMETRIC ERROR ANALYSIS RESULTS - Continued

ERROR NO.20
LOCATOR L3
VALUE 4.50

	H MEAN	H SIGMA	DH MEAN	DH SIGMA	THETA MEAN	THETA SIGMA	DTHETA MEAN	DTHETA SIGMA
APR-	.530996E 02	.334595E 00	.311334E-01	.127839E 00	.560095E-02	.229935E-02	.169415E-02	.646188E-03
AUG-	.525199E 02	.694336E 00	.477771E-02	.109194E 00	.108231E-01	.762831E-02	.146600E-02	.858197E-03
OCT-	.518576E 02	.106328E 01	-.462902E-02	.134313E 00	.133947E-01	.801498E-02	.144958E-02	.912312E-03
JAN-	.504700E 02	.154724E 01	-.233868E-01	.124640E 00	.221839E-01	.116010E-01	.169675E-02	.141898E-02
TOT-	.519869E 02	.141055E 01	.197382E-02	.125883E 00	.130007E-01	.100783E-01	.157662E-02	.100704E-02

MAX H	MIN H	MAX DH	MIN DH	MAX THETA	MIN THETA	MAX DTHETA	MIN DTHETA
.536702E 02	.468352E 02	.320022E 00	-.266058E 00	.353682E-01	.566682E-04	.583739E-02	.483351E-04
SEQ. NO.	SEQ. NO.	SEQ. NO.	SEQ. NO.	SEQ. NO.	SEQ. NO.	SEQ. NO.	SEQ. NO.
122	360	354	171	372	173	342	341

ERROR NO.20
LOCATOR L3
VALUE 20.00

	H MEAN	H SIGMA	DH MEAN	DH SIGMA	THETA MEAN	THETA SIGMA	DTHETA MEAN	DTHETA SIGMA
APR-	.421775E 02	.504665E 00	.128002E-01	.121141E 00	.921524E-02	.408611E-02	.172523E-02	.131166E-02
AUG-	.415274E 02	.968428E 00	.633390E-02	.123686E 00	.142789E-01	.809468E-02	.145021E-02	.182380E-02
OCT-	.403090E 02	.159534E 01	.170997E-01	.103455E 00	.224048E-01	.969847E-02	.115412E-02	.114121E-02
JAN-	.382085E 02	.251955E 01	-.364410E-02	.118999E 00	.369161E-01	.169329E-01	.144098E-02	.970007E-03
TOT-	.405556E 02	.219262E 01	.814743E-02	.118683E 00	.204538E-01	.152129E-01	.144264E-02	.136502E-02

MAX H	MIN H	MAX DH	MIN DH	MAX THETA	MIN THETA	MAX DTHETA	MIN DTHETA
.431993E 02	.326778E 02	.366054E 00	-.286053E 00	.667473E-01	.117172E-03	.733621E-02	.372322E-05
SEQ. NO.	SEQ. NO.	SEQ. NO.	SEQ. NO.	SEQ. NO.	SEQ. NO.	SEQ. NO.	SEQ. NO.
136	360	154	160	378	158	154	148

TABLE G1. - RADIOMETRIC ERROR ANALYSIS RESULTS - Continued

ERROR NO.20
LOCATION L4
VALUE 2.50

	R MEAN	R SIGMA	DR MEAN	DR SIGMA	THETA MEAN	THETA SIGMA	DTHETA MEAN	DTHETA SIGMA
APR-	.442914E 02	.424534E 00	-.622725E 00	.214227E 00	.581162E-02	.503913E-02	.288654E-02	.257171E-02
ALC-	.436043E 02	.492238E 00	-.676882E 00	.180971E 00	.792414E-02	.576309E-02	.231143E-02	.206356E-02
CCT-	.433679E 02	.110770E 01	-.779094E 00	.275302E 00	.146414E-01	.861035E-02	.371679E-02	.287003E-02
JAN-	.423483E 02	.146402E 01	-.728745E 00	.254709E 00	.215622E-01	.142750E-01	.332635E-02	.346031E-02
TCT-	.434005E 02	.119567E 01	-.701861E 00	.241291E 00	.124848E-01	.110557E-01	.306028E-02	.283618E-02

MAX R	MIN R	MAX DR	MIN DR	MAX THETA	MIN THETA	MAX DTHETA	MIN DTHETA
.453137E 02	.397934E 02	-.328791E 00	-.156234E 01	.442401E-01	.922555E-04	.140415E-01	.432321E-04
SEQ. NO. 214	SEQ. NO. 367	SEQ. NO. 147	SEQ. NO. 349	SEQ. NO. 378	SEQ. NO. 6	SEQ. NO. 349	SEQ. NO. 115

ERROR NO.20
LOCATION L4
VALUE 10.00

	R MEAN	R SIGMA	DR MEAN	DR SIGMA	THETA MEAN	THETA SIGMA	DTHETA MEAN	DTHETA SIGMA
APR-	.302114E 02	.108390E 01	-.980657E 00	.322248E 00	.147314E-01	.121385E-01	.375162E-02	.418412E-02
ALC-	.295451E 02	.468092E 00	-.112428E 01	.251033E 00	.655942E-02	.491712E-02	.336390E-02	.208709E-02
CCT-	.237262E 02	.170059E 01	-.126145E 01	.383334E 00	.249838E-01	.106877E-01	.494996E-02	.411542E-02
JAN-	.273481E 02	.197031E 01	-.114046E 01	.382285E 00	.293746E-01	.192484E-01	.524653E-02	.507159E-02
TCT-	.289577E 02	.178491E 01	-.112671E 01	.352967E 00	.189123E-01	.152901E-01	.432800E-02	.409307E-02

MAX R	MIN R	MAX DR	MIN DR	MAX THETA	MIN THETA	MAX DTHETA	MIN DTHETA
.320088E 02	.238381E 02	-.511560E 00	-.233446E 01	.678074E-01	.818575E-03	.197280E-01	.122119E-03
SEQ. NO. 56	SEQ. NO. 367	SEQ. NO. 147	SEQ. NO. 349	SEQ. NO. 378	SEQ. NO. 149	SEQ. NO. 349	SEQ. NO. 36

TABLE G1. - RADIOMETRIC ERROR ANALYSIS RESULTS - Continued

ERROR NO. 21
LOCATION 11
VALUE 2.00

	R MEAN	R SIGMA	DR MEAN	DR SIGMA	THETA MEAN	THETA SIGMA	DTHETA MEAN	DTHETA SIGMA
APR-	.437235E 02	.877852E 00	-.231605E-03	.391210E-02	.124799E-01	.963228E-02	.504692E-04	.423850E-04
AUG-	.429817E 02	.146213E 01	.160998E-03	.577944E-02	.231550E-01	.941918E-02	.796862E-04	.422752E-04
OCT-	.411529E 02	.235297E 01	-.622468E-03	.629019E-02	.344425E-01	.140526E-01	.929289E-04	.655826E-04
JAN-	.382172E 02	.344121E 01	.135618E-02	.498779E-02	.512309E-01	.234370E-01	.591576E-04	.419302E-04
JUL-	.415188E 02	.211361E 01	.171769E-03	.532815E-02	.303271E-01	.208169E-01	.705602E-04	.518658E-04

MAX R	MIN R	MAX DR	MIN DR	MAX THETA	MIN THETA	MAX DTHETA	MIN DTHETA
.451697E 02	.313039E 02	.162210E-01	-.142264E-01	.104359E 00	.122924E-03	.239179E-03	.883335E-06
SEQ. NO.	SEQ. NO.	SEQ. NO.	SEQ. NO.	SEQ. NO.	SEQ. NO.	SEQ. NO.	SEQ. NO.
139	360	124	105	378	16	174	6

ERROR NO. 21
LOCATION 11
VALUE 3.00

	R MEAN	R SIGMA	DR MEAN	DR SIGMA	THETA MEAN	THETA SIGMA	DTHETA MEAN	DTHETA SIGMA
APR-	.396531E 02	.132272E 01	-.577406E-03	.392533E-02	.212364E-01	.126117E-01	.481169E-04	.307718E-04
AUG-	.392513E 02	.135178E 01	-.259134E-03	.256065E-02	.139652E-01	.785616E-02	.376101E-04	.261919E-04
OCT-	.354488E 02	.261164E 01	-.413463E-03	.435876E-02	.397291E-01	.137569E-01	.489131E-04	.270608E-04
JAN-	.321431E 02	.421193E 01	.120131E-02	.446904E-02	.574656E-01	.322734E-01	.679083E-04	.335141E-04
JUL-	.361241E 02	.372037E 01	-.119383E-04	.401764E-02	.343491E-01	.244454E-01	.506371E-04	.314870E-04

MAX R	MIN R	MAX DR	MIN DR	MAX THETA	MIN THETA	MAX DTHETA	MIN DTHETA
.406660E 02	.162445E 02	.956674E-02	-.149250E-01	.122495E 00	.237728E-02	.144992E-03	.218055E-05
SEQ. NO.	SEQ. NO.	SEQ. NO.	SEQ. NO.	SEQ. NO.	SEQ. NO.	SEQ. NO.	SEQ. NO.
54	360	34	203	360	6	352	3

TABLE G1. - RADIOMETRIC ERROR ANALYSIS RESULTS - Continued

ERROR NO. 21
LOCATION L2
VALUE .15

	H MEAN	H SIGMA	DH MEAN	DH SIGMA	THETA MEAN	THETA SIGMA	DTHETA MEAN	DTHETA SIGMA
APR-	.518463E 02	.207799E 00	-.150592E-02	.818021E-02	.322753E-02	.262920E-02	.947137E-04	.819461E-04
AUG-	.510543E 02	.441748E 00	-.327252E-03	.661436E-02	.719142E-02	.504818E-02	.106512E-03	.576336E-04
OCT-	.509738E 02	.894042E 00	-.197537E-02	.120111E-01	.116604E-01	.780465E-02	.173816E-03	.812321E-04
JAN-	.437218E 02	.149611E 01	-.183850E-02	.765030E-02	.215527E-01	.141947E-01	.955492E-04	.830335E-04
TOT-	.508990E 02	.118205E 01	-.141176E-02	.887191E-02	.109080E-01	.103713E-01	.117648E-03	.834016E-04

MAX H	MIN H	MAX DH	MIN DH	MAX THETA	MIN THETA	MAX DTHETA	MIN DTHETA
.525916E 02	.470000E 02	.228865E-01	-.295050E-01	.455473E-01	.300665E-03	.368535E-03	.833214E-07
SEQ. NO.	SEQ. NO.	SEQ. NO.	SEQ. NO.	SEQ. NO.	SEQ. NO.	SEQ. NO.	SEQ. NO.
214	367	181	184	378	337	195	27

ERROR NO. 21
LOCATION L2
VALUE .30

	H MEAN	H SIGMA	DH MEAN	DH SIGMA	THETA MEAN	THETA SIGMA	DTHETA MEAN	DTHETA SIGMA
APR-	.267696E 02	.216413E 01	-.910867E-03	.926054E-02	.315272E-01	.129063E-01	.141573E-03	.842422E-04
AUG-	.249224E 02	.466533E 00	-.170574E-02	.743784E-02	.647360E-02	.491260E-02	.907409E-04	.666133E-04
OCT-	.253744E 02	.225694E 01	-.258933E-02	.106366E-01	.331193E-01	.151064E-01	.153627E-03	.112228E-03
JAN-	.240684E 02	.260434E 01	-.397941E-02	.978210E-02	.380468E-01	.185597E-01	.122037E-03	.776820E-04
TOT-	.257937E 02	.235350E 01	-.229633E-02	.942416E-02	.272917E-01	.184685E-01	.126994E-03	.900340E-04

MAX H	MIN H	MAX DH	MIN DH	MAX THETA	MIN THETA	MAX DTHETA	MIN DTHETA
.297728E 02	.190363E 02	.295682E-01	-.322052E-01	.791141E-01	.635294E-03	.400558E-03	.310645E-05
SEQ. NO.	SEQ. NO.	SEQ. NO.	SEQ. NO.	SEQ. NO.	SEQ. NO.	SEQ. NO.	SEQ. NO.
52	360	216	336	378	115	210	128

TABLE G1. - RADIOMETRIC ERROR ANALYSIS RESULTS - Continued

ERROR NO. 21
LOCATION L3
VALUE 4.50

	H MEAN	H SIGMA	DH MEAN	DH SIGMA	THETA MEAN	THETA SIGMA	DTHETA MEAN	DTHETA SIGMA
APR-	.530703E 02	.306154E 00	.179976E-02	.136695E-01	.499180E-02	.258179E-02	.143914E-03	.170102E-03
AUG-	.525177E 02	.672694E 00	.263074E-02	.148758E-01	.102596E-01	.701693E-02	.185807E-03	.160954E-03
OCT-	.518661E 02	.102486E 01	.386657E-02	.163074E-01	.139403E-01	.781036E-02	.237154E-03	.195747E-03
JAN-	.504952E 02	.153979E 01	.187638E-02	.131304E-01	.218132E-01	.119389E-01	.192596E-03	.114745E-03
TOT-	.516873E 02	.134409E 01	.254094E-02	.145710E-01	.127512E-01	.101167E-01	.189868E-03	.166355E-03

MAX H	MIN H	MAX DH	MIN DH	MAX THETA	MIN THETA	MAX DTHETA	MIN DTHETA
.536986E 02	.468388E 02	.402939E-01	-.367763E-01	.338898E-01	.355400E-03	.656619E-03	.826227E-05
SEQ. NO.	SEQ. NO.	SEQ. NO.	SEQ. NO.	SEQ. NO.	SEQ. NO.	SEQ. NO.	SEQ. NO.
56	360	199	171	372	27	5	169

ERROR NO. 21
LOCATION L3
VALUE 20.00

	H MEAN	H SIGMA	DH MEAN	DH SIGMA	THETA MEAN	THETA SIGMA	DTHETA MEAN	DTHETA SIGMA
APR-	.421657E 02	.506392E 00	.464078E-03	.454572E-02	.824490E-02	.404645E-02	.470151E-04	.544633E-04
AUG-	.415221E 02	.972509E 00	.989751E-03	.507788E-02	.146261E-01	.767265E-02	.685356E-04	.596667E-04
OCT-	.402933E 02	.156460E 01	.143250E-02	.573300E-02	.224589E-01	.899825E-02	.770017E-04	.643311E-04
JAN-	.382133E 02	.252365E 01	.109190E-02	.479472E-02	.367462E-01	.169296E-01	.705894E-04	.450386E-04
TOT-	.405485E 02	.218511E 01	.994556E-03	.506921E-02	.205190E-01	.149607E-01	.657854E-04	.571921E-04

MAX H	MIN H	MAX DH	MIN DH	MAX THETA	MIN THETA	MAX DTHETA	MIN DTHETA
.431472E 02	.328431E 02	.138183E-01	-.131447E-01	.676939E-01	.178831E-02	.250162E-03	.118609E-06
SEQ. NO.	SEQ. NO.	SEQ. NO.	SEQ. NO.	SEQ. NO.	SEQ. NO.	SEQ. NO.	SEQ. NO.
139	360	199	171	378	158	125	154

TABLE G1. - RADIOMETRIC ERROR ANALYSIS RESULTS - Continued

ERROR NO. 21
LOCATOR L4
VALUE 2.50

	F MEAN	F SIGMA	DF MEAN	DF SIGMA	THETA MEAN	THETA SIGMA	DTHETA MEAN	DTHETA SIGMA
APR-	.416043E 02	.325745E 00	.217405E-03	.597297E-02	.674115E-02	.388215E-02	.569989E-04	.740239E-04
ALG-	.442818E 02	.437493E 00	.585359E-03	.650894E-02	.748557E-02	.503495E-02	.845004E-04	.755450E-04
CCT-	.441483E 02	.566603E 00	.135[illegible]6E-02	.798087E-02	.123186E-01	.792637E-02	.109648E-03	.876254E-04
JAN-	.437772E 02	.139164E 01	.134929E-03	.645686E-02	.196129E-01	.178531E-01	.101888E-03	.400394E-04
TCT-	.441029E 02	.110645E 01	.571034E-03	.678854E-02	.111446E-01	.997433E-02	.182590E-04	.756715E-04

MAX F	MIN F	MAX DF	MIN DF	MAX THETA	MIN THETA	MAX DTHETA	MIN DTHETA
.452208E 02	.406846E 02	.367[illegible]E-01	-.196651E-01	.3[illegible]5E-01	.280825E-04	.307577E-03	.114204E-05
SEQ. NO.	SEQ. NO.	SEQ. NO.	SEQ. NO.	SEQ. NO.	SEQ. NO.	SEQ. NO.	SEQ. NO.
56	367	199	171	379	182	125	36

ERROR NO. 21
LOCATOR L4
VALUE 10.00

	F MEAN	F SIGMA	DF MEAN	DF SIGMA	THETA MEAN	THETA SIGMA	DTHETA MEAN	DTHETA SIGMA
APR-	.311620E 02	.953026E 00	-.889719E-04	.322052E-02	.133496E-01	.107044E-01	.359797E-04	.328033E-04
ALG-	.324492E 02	.408621E 00	-.[illegible]E-03	.295764E-02	.[illegible]E-02	.500036E-02	.350318E-04	.322829E-04
CCT-	.236876E 02	.151041E 01	-.749618E-04	.417158E-02	.215150E-01	.101668E-01	.552063E-04	.437811E-04
JAN-	.284975E 02	.196527E 01	-.105428E-02	.332436E-02	.267826E-01	.154153E-01	.394838E-04	.356906E-04
TCT-	.300941E 02	.165556E 01	-.350925E-03	.347410E-02	.169493E-01	.135748E-01	.414254E-04	.373265E-04

MAX F	MIN F	MAX DF	MIN DF	MAX THETA	MIN THETA	MAX DTHETA	MIN DTHETA
.328326E 02	.253705E 02	.100856E-01	-.115149E-01	.603675E-01	.119325E-03	.128533E-03	.155982E-07
SEQ. NO.	SEQ. NO.	SEQ. NO.	SEQ. NO.	SEQ. NO.	SEQ. NO.	SEQ. NO.	SEQ. NO.
56	367	199	171	376	123	6	117

TABLE G1. - RADIOMETRIC ERROR ANALYSIS RESULTS - Continued

ERROR NO.* 22
LOCATION L1
VALUE 2.00

	H MEAN	H SIGMA	DH MEAN	DH SIGMA	THETA MEAN	THETA SIGMA	DTHETA MEAN	DTHETA SIGMA
APR-	.437229E 02	.882795E 00	-.838442E-03	.159530E-01	.125141E-01	.872921E-02	.203091E-03	.190476E-03
AUG-	.429944E 02	.148747E 01	.282746E-02	.205809E-01	.232357E-01	.953014E-02	.315674E-03	.193329E-03
OCT-	.411467E 02	.236614E 01	-.686157E-02	.172191E-01	.344891E-01	.141148E-01	.196595E-03	.206557E-03
JAN-	.392163E 02	.348982E 01	.433315E-03	.204012E-01	.510902E-01	.233297E-01	.303537E-03	.165995E-03
TOT-	.415176E 02	.311530E 01	-.110951E-02	.189856E-01	.303323E-01	.207759E-01	.254722E-03	.194152E-03

MAX H	MIN H	MAX DH	MIN DH	MAX THETA	MIN THETA	MAX DTHETA	MIN DTHETA
.451726E 02	.313394E 02	.410472E-01	-.455548E-01	.103858E 00	.225957E-03	.708099E-03	.589502E-05
SEQ. NO.	SEQ. NO.	SEQ. NO.	SEQ. NO.	SEQ. NO.	SEQ. NO.	SEQ. NO.	SEQ. NO.
139	360	372	178	378	16	115	181

ERROR NO.* 23
LOCATION L1
VALUE 3.00

	H MEAN	H SIGMA	DH MEAN	DH SIGMA	THETA MEAN	THETA SIGMA	DTHETA MEAN	DTHETA SIGMA
APR-	.336539E 02	.132158E 01	.235985E-03	.183190E-01	.212086E-01	.126516E-01	.216864E-03	.204733E-03
AUG-	.382537E 02	.134720E 01	.211277E-02	.176777E-01	.199293E-01	.802755E-02	.187398E-03	.166370E-03
OCT-	.354489E 02	.260961E 01	-.334831E-03	.162160E-01	.386086E-01	.140253E-01	.219603E-03	.131470E-03
JAN-	.321439E 02	.420219E 01	.201621E-02	.214581E-01	.573767E-01	.321293E-01	.277210E-03	.246775E-03
TOT-	.361251E 02	.371694E 01	.100754E-02	.185483E-01	.342798E-01	.244054E-01	.225246E-03	.194948E-03

MAX H	MIN H	MAX DH	MIN DH	MAX THETA	MIN THETA	MAX DTHETA	MIN DTHETA
.406933E 02	.192637E 02	.515992E-01	-.424566E-01	.122632E 00	.233013E-02	.774492E-03	.536879E-05
SEQ. NO.	SEQ. NO.	SEQ. NO.	SEQ. NO.	SEQ. NO.	SEQ. NO.	SEQ. NO.	SEQ. NO.
56	360	354	143	360	6	342	6

TABLE G1. - RADIOMETRIC ERROR ANALYSIS RESULTS - Continued

ERROR NO.*
LOCATOR L2
VALUE .15

	H MEAN	H SIGMA	DH MEAN	DH SIGMA	THETA MEAN	THETA SIGMA	DTHETA MEAN	DTHETA SIGMA
APR-	.518379E 02	.207776E 00	-.999954E-02	.250672E-01	.328897E-02	.268411E-02	.246455E-03	.118824E-03
AUG-	.510471E 02	.444142E 00	-.754311E-02	.320845E-01	.728607E-02	.484543E-02	.458839E-03	.403967E-03
OCT-	.509851E 02	.911737E 00	.939602E-02	.359336E-01	.120445E-01	.799106E-02	.461704E-03	.321079E-03
JAN-	.497188E 02	.149291E 01	-.483235E-02	.404164E-01	.215920E-01	.141810E-01	.410534E-03	.440654E-03
TOT-	.508972E 02	.113366E 01	-.324475E-02	.346731E-01	.110529E-01	.109791E-01	.394436E-03	.355464E-03

MAX H	MIN H	MAX DH	MIN DH	MAX THETA	MIN THETA	MAX DTHETA	MIN DTHETA
.526425E 02	.469474E 02	.100465E 00	-.944621E-01	.456325E-01	.113796E-05	.176826E-02	.626405E-05
SEQ. NO. 214	SEQ. NO. 367	SEQ. NO. 338	SEQ. NO. 356	SEQ. NO. 378	SEQ. NO. 2	SEQ. NO. 12[illegible]	SEQ. NO. 363

ERROR NO.*
LOCATOR L2
VALUE .90

	H MEAN	H SIGMA	DH MEAN	DH SIGMA	THETA MEAN	THETA SIGMA	DTHETA MEAN	DTHETA SIGMA
APR-	.267594E 02	.217490E 01	-.110936E-01	.444672E-01	.313287E-01	.131043E-01	.440005E-03	.352440E-03
AUG-	.269127E 02	.445032E 00	-.113484E-01	.360710E-01	.648701E-02	.491339E-02	.478802E-03	.395508E-03
OCT-	.253555E 02	.227114E 01	-.215248E-01	.391772E-01	.333535E-01	.152570E-01	.561905E-03	.426053E-03
JAN-	.240582E 02	.260689E 01	-.141931E-01	.404177E-01	.381683E-01	.197630E-01	.459828E-03	.352037E-03
TOT-	.257714E 02	.236047E 01	-.145400E-01	.401457E-01	.273344E-01	.186059E-01	.485133E-03	.395584E-03

MAX H	MIN H	MAX DH	MIN DH	MAX THETA	MIN THETA	MAX DTHETA	MIN DTHETA
.296884E 02	.190410E 02	.683675E-01	-.978294E-01	.796866E-01	.346730E-03	.163515E-02	.174057E-04
SEQ. NO. 47	SEQ. NO. 360	SEQ. NO. 210	SEQ. NO. 14	SEQ. NO. 378	SEQ. NO. 115	SEQ. NO. 124	SEQ. NO. 154

TABLE G1. - RADIOMETRIC ERROR ANALYSIS RESULTS - Continued

ERROR NO.*
LOCATOR L3
VALUE 4.50

	H MEAN	H SIGMA	DH MEAN	DH SIGMA	THETA MEAN	THETA SIGMA	DTHETA MEAN	DTHETA SIGMA
APR-	.530716E 02	.304719E 00	.317723E-02	.510468E-01	.499609E-02	.283496E-02	.754089E-03	.506167E-03
AUG-	.525210E 02	.680109E 00	.583945E-02	.536240E-01	.105443E-01	.711872E-02	.723835E-03	.471681E-03
OCT-	.518539E 02	.102368E 01	-.829234E-02	.522984E-01	.140369E-01	.791718E-02	.737948E-03	.620267E-03
JAN-	.504947E 02	.155182E 01	.134835E-02	.567254E-01	.221902E-01	.120277E-01	.744012E-03	.497817E-03
TOT-	.519953E 02	.138904E 01	.518171E-03	.537329E-01	.129419E-01	.102674E-01	.739971E-03	.527191E-03

MAX H	MIN H	MAX DH	MIN DH	MAX THETA	MIN THETA	MAX DTHETA	MIN DTHETA
.536769E 02	.468074E 02	.125182E 00	-.146228E 00	.363694E-01	.643558E-04	.214692E-02	.422554E-04
SEQ. NO.	SEQ. NO.	SEQ. NO.	SEQ. NO.	SEQ. NO.	SEQ. NO.	SEQ. NO.	SEQ. NO.
122	360	18	220	372	27	372	114

ERROR NO.*
LOCATOR L3
VALUE 20.00

	H MEAN	H SIGMA	DH MEAN	DH SIGMA	THETA MEAN	THETA SIGMA	DTHETA MEAN	DTHETA SIGMA
APR-	.421657E 02	.501345E 00	.100164E-02	.184707E-01	.827228E-02	.386803E-02	.258177E-03	.167039E-03
AUG-	.415218E 02	.975265E 00	.779466E-03	.191986E-01	.146674E-01	.775621E-02	.276072E-03	.159670E-03
OCT-	.402900E 02	.156512E 01	-.193049E-02	.166440E-01	.224934E-01	.904305E-02	.239446E-03	.177273E-03
JAN-	.382121E 02	.252689E 01	-.847244E-04	.186680E-01	.367562E-01	.171036E-01	.257364E-03	.178357E-03
TOT-	.405474E 02	.218665E 01	-.585261E-04	.183071E-01	.205474E-01	.150100E-01	.257765E-03	.171249E-03

MAX H	MIN H	MAX DH	MIN DH	MAX THETA	MIN THETA	MAX DTHETA	MIN DTHETA
.431719E 02	.328452E 02	.425917E-01	-.424843E-01	.678713E-01	.189596E-02	.656610E-03	.740463E-05
SEQ. NO.	SEQ. NO.	SEQ. NO.	SEQ. NO.	SEQ. NO.	SEQ. NO.	SEQ. NO.	SEQ. NO.
139	360	18	132	378	15[illegible]	8	349

TABLE G1. - RADIOMETRIC ERROR ANALYSIS RESULTS - Continued

ERROR NO.*
LOCATION L4
VALUE 2.50

	R MEAN	R SIGMA	DR MEAN	DR SIGMA	THETA MEAN	THETA SIGMA	DTHETA MEAN	DTHETA SIGMA
APR-	.446023E 02	.324148E 00	-.134220E-02	.231356E-01	.447659E-02	.388246E-02	.321291E-03	.232198E-03
ALG-	.442791E 02	.443356E 00	-.216696E-02	.255713E-01	.737502E-02	.526327E-02	.364894E-03	.253976E-03
CCT-	.441395E 02	.569051E 00	-.744437E-02	.239117E-01	.129330E-01	.790225E-02	.348557E-03	.282885E-03
JAN-	.430727E 02	.134926E 01	-.434269E-02	.207654E-01	.196466E-01	.130113E-01	.391287E-03	.294764E-03
TCT-	.440984E 02	.110985E 01	-.354905E-02	.253211E-01	.111578E-01	.100749E-01	.356507E-03	.268288E-03

MAX R	MIN R	MAX DR	MIN DR	MAX THETA	MIN THETA	MAX DTHETA	MIN DTHETA
.457018E 02	.406356E 02	.535188E-01	-.668224E-01	.400317E-01	.522635E-04	.998059E-03	.377200E-05
SEQ. NO. 56	SEQ. NO. 367	SEQ. NO. 373	SEQ. NO. 199	SEQ. NO. 378	SEQ. NO. 2	SEQ. NO. 178	SEQ. NO. 192

ERROR NO.*
LOCATION L4
VALUE 10.00

	R MEAN	R SIGMA	DR MEAN	DR SIGMA	THETA MEAN	THETA SIGMA	DTHETA MEAN	DTHETA SIGMA
APR-	.311981E 02	.953776E 00	-.389141E-02	.123649E-01	.132696E-01	.107510E-01	.160779E-03	.116606E-03
ALG-	.306650E 02	.412612E 00	-.442284E-02	.154231E-01	.889973E-02	.507148E-02	.230378E-03	.173431E-03
CCT-	.298779E 02	.151364E 01	-.276744E-02	.127172E-01	.219036E-01	.101609E-01	.193331E-03	.165475E-03
JAN-	.284827E 02	.186847E 01	-.589376E-02	.124562E-01	.268010E-01	.154724E-01	.166466E-03	.154130E-03
TCT-	.300784E 02	.165788E 01	-.601386E-02	.134925E-01	.169685E-01	.136123E-01	.187739E-03	.146802E-03

MAX R	MIN R	MAX DR	MIN DR	MAX THETA	MIN THETA	MAX DTHETA	MIN DTHETA
.328155E 02	.253414E 02	.288617E-01	-.392784E-01	.605396E-01	.261479E-03	.542655E-03	.300692E-05
SEQ. NO. 56	SEQ. NO. 367	SEQ. NO. 35	SEQ. NO. 199	SEQ. NO. 378	SEQ. NO. 124	SEQ. NO. 148	SEQ. NO. 174

TABLE G1. - RADIOMETRIC ERROR ANALYSIS RESULTS - Continued

ERROR NO.*
LOCATOR L1
VALUE 2.00

	H MEAN	H SIGMA	DH MEAN	DH SIGMA	THETA MEAN	THETA SIGMA	DTHETA MEAN	DTHETA SIGMA
APO-	.437149E 02	.891037E 00	-.879631E-02	.451432E-01	.126919E-01	.887244E-02	.490867E-03	.487261E-03
ALC-	.429727E 02	.148181E 01	-.884807E-02	.437501E-01	.227590E-01	.967389E-02	.680932E-03	.476014E-03
CCT-	.411458E 02	.234371E 01	-.778359E-02	.542619E-01	.341912E-01	.141251E-01	.664843E-03	.407581E-03
JAK-	.381978E 02	.348332E 01	-.160913E-01	.597677E-01	.512933E-01	.229208E-01	.104677E-02	.490239E-03
TCT-	.415079E 02	.311131E 01	-.108798E-01	.510394E-01	.304339E-01	.207361E-01	.720852E-03	.506115E-03

MAX H	MIN H	MAX DH	MIN DH	MAX THETA	MIN THETA	MAX DTHETA	MIN DTHETA
.451707E 02	.312968E 02	.117103E 00	-.133514E 00	.102966E 00	.505363E-03	.170770E-02	.218895E-05
SEQ. NO.	SEQ. NO.	SEQ. NO.	SEQ. NO.	SEQ. NO.	SEQ. NO.	SEQ. NO.	SEQ. NO.
139	360	205	13	378	16	334	14

ERROR NO.*
LOCATOR L1
VALUE 3.00

	H MEAN	H SIGMA	DH MEAN	DH SIGMA	THETA MEAN	THETA SIGMA	DTHETA MEAN	DTHETA SIGMA
APO-	.396347E 02	.133719E 01	-.180431E-01	.452361E-01	.215161E-01	.125724E-01	.615905E-03	.451398E-03
ALC-	.382533E 02	.134367E 01	.173359E-02	.416014E-01	.199556E-01	.778025E-02	.647987E-03	.349239E-03
CCT-	.354552E 02	.261874E 01	.567573E-02	.449130E-01	.388009E-01	.142356E-01	.536191E-03	.461433E-03
JAK-	.321220E 02	.423851E 01	-.199327E-01	.616695E-01	.577847E-01	.328730E-01	.670530E-03	.958647E-03
TCT-	.361163E 02	.373221E 01	-.779163E-02	.504133E-01	.345143E-01	.247117E-01	.617653E-03	.605807E-03

MAX H	MIN H	MAX DH	MIN DH	MAX THETA	MIN THETA	MAX DTHETA	MIN DTHETA
.405910E 02	.189539E 02	.992303E-01	-.289288E 00	.126543E 00	.205556E-02	.404438E-02	.210583E-05
SEQ. NO.	SEQ. NO.	SEQ. NO.	SEQ. NO.	SEQ. NO.	SEQ. NO.	SEQ. NO.	SEQ. NO.
56	360	143	360	360	337	360	192

TABLE G1. - RADIOMETRIC ERROR ANALYSIS RESULTS - Continued

ERROR NO.*
LOCATOR L2
VALUE .15

	H MEAN	H SIGMA	DH MEAN	DH SIGMA	THETA MEAN	THETA SIGMA	DTHETA MEAN	DTHETA SIGMA
APR-	.518398E 02	.230382E 00	-.904546E-02	.705227E-01	.338248E-02	.287075E-02	.979397E-03	.669218E-03
AUG-	.510179E 02	.441733E 00	-.367081E-01	.602253E-01	.722315E-02	.481427E-02	.917695E-03	.526677E-03
OCT-	.509176E 02	.935302E 00	-.581475E-01	.893948E-01	.122349E-01	.830226E-02	.142776E-02	.906859E-03
JAN-	.497117E 02	.150551E 01	-.119042E-01	.102598E 00	.219506E-01	.138897E-01	.110760E-02	.768268E-03
TOT-	.508717E 02	.119330E 01	-.787013E-01	.847886E-01	.111978E-01	.110323E-01	.110811E-02	.757112E-03

MAX H	MIN H	MAX DH	MIN DH	MAX THETA	MIN THETA	MAX DTHETA	MIN DTHETA
.526563E 02	.468284E 02	.174463E 00	-.325277E 00	.441822E-01	.865025E-04	.336568E-02	.443174E-04
SEQ. NO.	SEQ. NO.	SEQ. NO.	SEQ. NO.	SEQ. NO.	SEQ. NO.	SEQ. NO.	SEQ. NO.
214	367	354	372	378	[illegible]	171	13

ERROR NO.* 23
LOCATOR L2
VALUE .90

	H MEAN	H SIGMA	DH MEAN	DH SIGMA	THETA MEAN	THETA SIGMA	DTHETA MEAN	DTHETA SIGMA
APR-	.266962E 02	.217157E 01	-.743225E-01	.865698E-01	.317045E-01	.129959E-01	.129831E-02	.561157E-03
AUG-	.268517E 02	.500569E 00	-.723386E-01	.938397E-01	.689058E-02	.524519E-02	.126895E-02	.785064E-03
OCT-	.253062E 02	.229933E 01	-.708052E-01	.948830E-01	.341115E-01	.159976E-01	.147714E-02	.990207E-03
JAN-	.239806E 02	.264117E 01	-.917807E-01	.112319E 00	.386102E-01	.189015E-01	.140552E-02	.120143E-02
TOT-	.257087E 02	.238007E 01	-.773117E-01	.977268E-01	.278292E-01	.182331E-01	.136248E-02	.916970E-03

MAX H	MIN H	MAX DH	MIN DH	MAX THETA	MIN THETA	MAX DTHETA	MIN DTHETA
.297650E 02	.185704E 02	.115776E 00	-.471103E 00	.795750E-01	.315416E-03	.414364E-02	.186459E-03
SEQ. NO.	SEQ. NO.	SEQ. NO.	SEQ. NO.	SEQ. NO.	SEQ. NO.	SEQ. NO.	SEQ. NO.
52	360	56	360	378	115	360	372

TABLE G1. - RADIOMETRIC ERROR ANALYSIS RESULTS - Continued

ERROR NO.*
LOCATOR L3
VALUE 4.50

	H MEAN	H SIGMA	DH MEAN	DH SIGMA	THETA MEAN	THETA SIGMA	DTHETA MEAN	DTHETA SIGMA
APR-	.530790E 02	.363853E 00	.105429E-01	.158984E 00	.609126E-02	.393416E-02	.207549E-02	.151635E-02
AUG-	.525146E 02	.656980E 00	-.531800E-03	.175421E 00	.985641E-02	.575414E-02	.299415E-02	.205151E-02
OCT-	.518622E 02	.102016E 01	-.579287E-04	.146076E 00	.140424E-01	.812651E-02	.179565E-02	.888057E-03
JAN-	.504589E 02	.154260E 01	-.344032E-01	.126360E 00	.219571E-01	.115810E-01	.122507E-02	.976694E-03
TOT-	.519787E 02	.139691E 01	-.611251E-02	.153704E 00	.129868E-01	.984474E-02	.202259E-02	.157201E-02

MAX H	MIN H	MAX DH	MIN DH	MAX THETA	MIN THETA	MAX DTHETA	MIN DTHETA
.536724E 02	.467374E 02	.483637E 00	-.312094E 00	.344774E-01	.225904E-04	.845965E-02	.104521E-04
SEQ. NO.	SEQ. NO.	SEQ. NO.	SEQ. NO.	SEQ. NO.	SEQ. NO.	SEQ. NO.	SEQ. NO.
49	360	131	19	372	113	136	27

ERROR NO.*
LOCATOR L3
VALUE 20.00

	H MEAN	H SIGMA	DH MEAN	DH SIGMA	THETA MEAN	THETA SIGMA	DTHETA MEAN	DTHETA SIGMA
APR-	.421716E 02	.518279E 00	.691260E-02	.537344E-01	.850293E-02	.440975E-02	.698348E-03	.509554E-03
AUG-	.415146E 02	.965529E 00	-.445880E-02	.589751E-01	.140800E-01	.761616E-02	.995853E-03	.654438E-03
OCT-	.402911E 02	.156001E 01	-.750521E-03	.491961E-01	.225113E-01	.907452E-02	.687244E-03	.340218E-03
JAN-	.382007E 02	.251914E 01	-.114752E-01	.460638E-01	.365550E-01	.170905E-01	.476559E-03	.471678E-03
TOT-	.405445E 02	.218671E 01	-.294298E-02	.526656E-01	.204123E-01	.149901E-01	.714501E-03	.539199E-03

MAX H	MIN H	MAX DH	MIN DH	MAX THETA	MIN THETA	MAX DTHETA	MIN DTHETA
.431492E 02	.328255E 02	.155389E 00	-.135851E 00	.675522E-01	.974251E-03	.296788E-02	.111140E-04
SEQ. NO.	SEQ. NO.	SEQ. NO.	SEQ. NO.	SEQ. NO.	SEQ. NO.	SEQ. NO.	SEQ. NO.
139	360	131	356	378	158	136	13

TABLE G1. - RADIOMETRIC ERROR ANALYSIS RESULTS - Continued

ERROR NO.*
LOCATOR L4
VALUE 2.50

	H MEAN	H SIGMA	DH MEAN	DH SIGMA	THETA MEAN	THETA SIGMA	DTHETA MEAN	DTHETA SIGMA
APO-	.448995E 02	.337676E 00	-.465105E-02	.697625E-01	.490209E-02	.407836E-02	.906132E-03	.747677E-03
ALG-	.442594E 02	.424128E 00	-.218724E-01	.716927E-01	.709730E-02	.464547E-02	.125568E-02	.694105E-03
CCT-	.441289E 02	.966023E 00	-.181536E-01	.666971E-01	.129256E-01	.782547E-02	.947652E-03	.562975E-03
JAN-	.430411E 02	.139449E 01	-.359718E-01	.699843E-01	.195904E-01	.127070E-01	.665309E-03	.576961E-03
TCT-	.440822E 02	.111322E 01	-.201637E-01	.695694E-01	.111288E-01	.988397E-02	.943692E-03	.683170E-03

MAX H	MIN H	MAX DH	MIN DH	MAX THETA	MIN THETA	MAX DTHETA	MIN DTHETA
.457216E 02	.406862E 02	.161370E 00	-.197581E 00	.398085E-01	.173167E-03	.322482E-02	.108895E-04
SEQ. NO. 56	SEQ. NO. 367	SEQ. NO. 131	SEQ. NO. 356	SEQ. NO. 378	SEQ. NO. 16	SEQ. NO. 136	SEQ. NO. 42

ERROR NO.*
LOCATOR L4
VALUE 10.00

	H MEAN	H SIGMA	DH MEAN	DH SIGMA	THETA MEAN	THETA SIGMA	DTHETA MEAN	DTHETA SIGMA
APO-	.311727E 02	.956286E 00	-.193555E-01	.376802E-01	.133953E-01	.107108E-01	.524516E-03	.447556E-03
ALG-	.306447E 02	.407697E 00	-.246803E-01	.368633E-01	.596954E-02	.461057E-02	.604220E-03	.345360E-03
CCT-	.299643E 02	.151151E 01	-.233964E-01	.284400E-01	.219976E-01	.101118E-01	.474630E-03	.288974E-03
JAN-	.284489E 02	.187074E 01	-.396120E-01	.300014E-01	.269274E-01	.154150E-01	.364804E-03	.345152E-03
TCT-	.300577E 02	.166205E 01	-.267610E-01	.343630E-01	.170725E-01	.135473E-01	.492065E-03	.368603E-03

MAX H	MIN H	MAX DH	MIN DH	MAX THETA	MIN THETA	MAX DTHETA	MIN DTHETA
.328101E 02	.253640E 02	.529181E-01	-.115702E 00	.601674E-01	.531707E-03	.188600E-02	.107362E-04
SEQ. NO. 56	SEQ. NO. 367	SEQ. NO. 36	SEQ. NO. 6	SEQ. NO. 378	SEQ. NO. 117	SEQ. NO. 6	SEQ. NO. 158

TABLE G1. - RADIOMETRIC ERROR ANALYSIS RESULTS - Continued

ERROR NO.*
LOCATOR L1
VALUE 2.00

	H MEAN	H SIGMA	DH MEAN	DH SIGMA	THETA MEAN	THETA SIGMA	DTHETA MEAN	DTHETA SIGMA
APR-	.436949E 02	.871514E 00	-.268331E-01	.187169E 00	.132818E-01	.839473E-02	.181619E-02	.152009E-02
AUG-	.429969E 02	.153752E 01	.153963E-01	.169012E 00	.233767E-01	.980650E-02	.142109E-02	.117805E-02
OCT-	.411823E 02	.231853E 01	.287867E-01	.220802E 00	.337776E-01	.136379E-01	.299460E-02	.199266E-02
JAN-	.381657E 02	.354183E 01	-.501600E-01	.249450E 00	.517063E-01	.235023E-01	.303332E-02	.207515E-02
OCT-	.415100E 02	.313529E 01	-.870378E-02	.211357E 00	.305356E-01	.206920E-01	.231630E-02	.187090E-02

MAX H	MIN H	MAX DH	MIN DH	MAX THETA	MIN THETA	MAX DTHETA	MIN DTHETA
.454626E 02	.307855E 02	.472632E 00	-.718551E 00	.100271E 00	.209617E-02	.788145E-02	.166549E-04
SEQ. NO.	SEQ. NO.	SEQ. NO.	SEQ. NO.	SEQ. NO.	SEQ. NO.	SEQ. NO.	SEQ. NO.
139	360	344	349	378	16	349	346

ERROR NO.* 24
LOCATOR L1
VALUE 3.00

	H MEAN	H SIGMA	DH MEAN	DH SIGMA	THETA MEAN	THETA SIGMA	DTHETA MEAN	DTHETA SIGMA
APR-	.386249E 02	.130022E 01	-.287555E-01	.201369E 00	.211069E-01	.131845E-01	.215830E-02	.178522E-02
AUG-	.392788E 02	.136794E 01	.272921E-01	.111539E 00	.206796E-01	.834539E-02	.163460E-02	.867054E-03
OCT-	.354451E 02	.267455E 01	-.413684E-02	.174128E 00	.305071E-01	.140253E-01	.236756E-02	.198140E-02
JAN-	.321756E 02	.421243E 01	.336545E-01	.149674E 00	.576295E-01	.331974E-01	.220258E-02	.155420E-02
OCT-	.361311E 02	.372184E 01	.701392E-02	.164498E 00	.347308E-01	.248620E-01	.209076E-02	.159654E-02

MAX H	MIN H	MAX DH	MIN DH	MAX THETA	MIN THETA	MAX DTHETA	MIN DTHETA
.406101E 02	.194744E 02	.543932E 00	-.500013E 00	.129611E 00	.566059E-03	.814936E-02	.204537E-03
SEQ. NO.	SEQ. NO.	SEQ. NO.	SEQ. NO.	SEQ. NO.	SEQ. NO.	SEQ. NO.	SEQ. NO.
49	360	2	192	360	337	192	372

TABLE G1. - RADIOMETRIC ERROR ANALYSIS RESULTS - Continued

ERROR NO.*
LOCATION L2
VALUE .15

	H MEAN	H SIGMA	DH MEAN	DH SIGMA	THETA MEAN	THETA SIGMA	DTHETA MEAN	DTHETA SIGMA
APR-	.517955E 02	.338085E 00	-.523565E-01	.238705E 00	.427157E-02	.278082E-02	.268749E-02	.124959E-02
AUG-	.510632E 02	.613452E 00	.963277E-02	.326367E 00	.937839E-02	.601982E-02	.434301E-02	.320690E-02
OCT-	.508209E 02	.109897E 01	-.154972E 00	.370415E 00	.150250E-01	.977930E-02	.507850E-02	.359744E-02
JAN-	.497109E 02	.154413E 01	-.126919E-01	.273952E 00	.232487E-01	.136306E-01	.386917E-02	.238829E-02
TOT-	.508476E 02	.125703E 01	-.528470E-01	.312884E 00	.129809E-01	.114437E-01	.399454E-02	.289447E-02

MAX H	MIN H	MAX DH	MIN DH	MAX THETA	MIN THETA	MAX DTHETA	MIN DTHETA
.526785E 02	.470037E 02	.735900E 00	-.874888E 00	.522834E-01	.237645E-03	.135663E-01	.157181E-03
SEQ. NO. 214	SEQ. NO. 367	SEQ. NO. 155	SEQ. NO. 173	SEQ. NO. 378	SEQ. NO. 170	SEQ. NO. 143	SEQ. NO. 382

ERROR NO.*
LOCATION L2
VALUE .90

	H MEAN	H SIGMA	DH MEAN	DH SIGMA	THETA MEAN	THETA SIGMA	DTHETA MEAN	DTHETA SIGMA
APR-	.263710E 02	.215114E 01	-.399475E 00	.282010E 00	.296172E-01	.127093E-01	.383828E-02	.196009E-02
AUG-	.264941E 02	.550355E 00	-.429966E 00	.366922E 00	.851145E-02	.675049E-02	.519793E-02	.340179E-02
OCT-	.249838E 02	.237876E 01	-.393193E 00	.305504E 00	.351754E-01	.167219E-01	.442808E-02	.282864E-02
JAN-	.234921E 02	.274738E 01	-.580257E 00	.451245E 00	.409508E-01	.212905E-01	.514027E-02	.380299E-02
TOT-	.253353E 02	.245555E 01	-.450723E 00	.365466E 00	.285637E-01	.196237E-01	.465112E-02	.312756E-02

MAX H	MIN H	MAX DH	MIN DH	MAX THETA	MIN THETA	MAX DTHETA	MIN DTHETA
.293407E 02	.176367E 02	.360860E 00	-.140480E 01	.822434E-01	.257056E-03	.124668E-01	.455888E-03
SEQ. NO. 52	SEQ. NO. 360	SEQ. NO. 356	SEQ. NO. 360	SEQ. NO. 378	SEQ. NO. 149	SEQ. NO. 350	SEQ. NO. 16

TABLE G1. - RADIOMETRIC ERROR ANALYSIS RESULTS - Continued

ERROR NO.*
LOCATOR L3
VALUE 4.50

	H MEAN	H SIGMA	DH MEAN	DH SIGMA	THETA MEAN	THETA SIGMA	DTHETA MEAN	DTHETA SIGMA
APR-	.531471E 02	.542079E 00	.796569E-01	.463239E 00	.572500E-02	.486454E-02	.482676E-02	.350385E-02
ALG-	.527485E 02	.915389E 00	.233357E 00	.596146E 00	.135400E-01	.108443E-01	.846741E-02	.650587E-02
OCT-	.519281E 02	.124175E 01	.658460E-01	.532018E 00	.157290E-01	.944824E-02	.592818E-02	.461140E-02
JAN-	.503916E 02	.152203E 01	-.101776E 00	.528821E 00	.232057E-01	.146039E-01	.594071E-02	.419099E-02
OCT-	.520538E 02	.153680E 01	.690211E-01	.545416E 00	.145500E-01	.122374E-01	.629077E-02	.501417E-02

MAX H	MIN H	MAX DH	MIN DH	MAX THETA	MIN THETA	MAX DTHETA	MIN DTHETA
.549681E 02	.468898E 02	.137342E 01	-.154205E 01	.461898E-01	.345928E-05	.226021E-01	.175271E-04
SEQ. NO.	SEQ. NO.	SEQ. NO.	SEQ. NO.	SEQ. NO.	SEQ. NO.	SEQ. NO.	SEQ. NO.
122	363	122	341	363	5	120	360

ERROR NO.*
LOCATOR L3
VALUE 20.00

	H MEAN	H SIGMA	DH MEAN	DH SIGMA	THETA MEAN	THETA SIGMA	DTHETA MEAN	DTHETA SIGMA
APR-	.421818E 02	.501964E 00	.171339E-01	.163234E 00	.750855E-02	.435841E-02	.187288E-02	.140320E-02
ALG-	.415929E 02	.100517E 01	.718530E-01	.190265E 00	.145267E-01	.924414E-02	.257638E-02	.213183E-02
OCT-	.403956E 02	.160420E 01	.176897E-01	.199766E 00	.234089E-01	.772813E-02	.200204E-02	.208347E-02
JAN-	.381825E 02	.250959E 01	-.296949E-01	.193680E 00	.377073E-01	.171999E-01	.206364E-02	.114854E-02
OCT-	.405667E 02	.221056E 01	.192454E-01	.188169E 00	.207879E-01	.155619E-01	.212806E-02	.176491E-02

MAX H	MIN H	MAX DH	MIN DH	MAX THETA	MIN THETA	MAX DTHETA	MIN DTHETA
.435279E 02	.328427E 02	.450329E 00	-.521704E 00	.667965E-01	.420782E-03	.744946E-02	.149857E-04
SEQ. NO.	SEQ. NO.	SEQ. NO.	SEQ. NO.	SEQ. NO.	SEQ. NO.	SEQ. NO.	SEQ. NO.
122	360	181	341	378	152	170	136

TABLE G1. - RADIOMETRIC ERROR ANALYSIS RESULTS - Continued

ERROR NO.*
LOCATION L4
VALUE 2.50

	H MEAN	H SIGMA	DH MEAN	DH SIGMA	THETA MEAN	THETA SIGMA	DTHETA MEAN	DTHETA SIGMA
APR-	.449529E 02	.358701E 00	-.512338E-01	.205144E 00	.530340E-02	.259156E-02	.238497E-02	.186741E-02
AUG-	.443009E 02	.543122E 00	.197121E-01	.233696E 00	.834793E-02	.717484E-02	.327074E-02	.236020E-02
OCT-	.440814E 02	.107255E 01	-.655150E-01	.282437E 00	.146647E-01	.714220E-02	.304719E-02	.306999E-02
JAN-	.429144E 02	.140792E 01	-.162670E 00	.284401E 00	.218136E-01	.132391E-01	.333887E-02	.241747E-02
TOT-	.440374E 02	.117832E 01	-.643266E-01	.262040E 00	.125324E-01	.105524E-01	.301044E-02	.249474E-02

MAX H	MIN H	MAX DH	MIN DH	MAX THETA	MIN THETA	MAX DTHETA	MIN DTHETA
.457726E 02	.405438E 02	.466912E 00	-.971456E 00	.423220E-01	.549615E-03	.112915E-01	.204518E-03
SEQ. NO. 211	SEQ. NO. 367	SEQ. NO. 13	SEQ. NO. 341	SEQ. NO. 342	SEQ. NO. 117	SEQ. NO. 170	SEQ. NO. 378

ERROR NO.*
LOCATION L4
VALUE 10.00

	H MEAN	H SIGMA	DH MEAN	DH SIGMA	THETA MEAN	THETA SIGMA	DTHETA MEAN	DTHETA SIGMA
APR-	.310829E 02	.946712E 00	-.109181E 00	.104224E 00	.135540E-01	.101816E-01	.125470E-02	.946407E-03
AUG-	.305938E 02	.455718E 00	-.756415E-01	.110274E 00	.632605E-02	.599920E-02	.151430E-02	.114949E-02
OCT-	.298592E 02	.157895E 01	-.129440E 00	.133189E 00	.232306E-01	.913396E-02	.165664E-02	.132544E-02
JAN-	.282942E 02	.189067E 01	-.194331E 00	.136873E 00	.282203E-01	.156133E-01	.180591E-02	.144926E-02
TOT-	.299575E 02	.170434E 01	-.126898E 00	.130714E 00	.176327E-01	.137351E-01	.155789E-02	.124893E-02

MAX H	MIN H	MAX DH	MIN DH	MAX THETA	MIN THETA	MAX DTHETA	MIN DTHETA
.327483E 02	.251345E 02	.212438E 00	-.533070E 00	.606338E-01	.143824E-02	.578255E-02	.330170E-04
SEQ. NO. 56	SEQ. NO. 367	SEQ. NO. 13	SEQ. NO. 363	SEQ. NO. 378	SEQ. NO. 117	SEQ. NO. 363	SEQ. NO. 46

REFERENCES

1. Duncan, J.; Wolfe, W.; Oppel, G.; and Burn, J.: Infrared Horizon Sensors. IRIA State-of-the-Art Report (NAVSO P-2841), Institute of Science and Technology, University of Michigan and Lockheed Missiles and Space Co., April 1965.

2. Thomas, J. R.: Derivation and Statistical Comparison of Various Analytical Techniques Which Define the Location of Reference Horizons in the Earth's Horizon Radiance Profile. NASA CR-726, October 1966.

3. Vogelzang, W. F.; and Ohring, G.: The 15μ Infrared Horizon Radiance Profile Temporal, Spatial, and Statistical Sampling Requirements for a Global Measurement Program. NASA CR-66190, October 1966.

4. Peterson, R. E.; Schuetz, J.; Shenk, W. E.; and Tang, W.: Derivation of a Meteorological Body of Data Covering the Northern Hemisphere in the Longitude Region Between 60°W and 160°W from March 1964 Through February 1965. NASA CR-723, October 1966.

5. Ballard, H. N.: The Measurement of Temperature in the Stratosphere and Mesosphere. Journal of Applied Meteorology, vol. 6, no. 1, February 1967, pp. 150-163.

6. Robert, W. O.: The Global Atmospheric Research Program. Bulletin of the Am. Meteorol. Soc., vol. 48, no. 2, 1967, pp. 85-93.

7. Leovy, C.: Radiative Equilibrium of the Mesosphere. Journal of Atm. Sci., vol. 21, no. 3, 1964, pp. 238-248.

8. Thiele, O.: Observed Diurnal Oscillations of Pressure and Density in the Upper Stratosphere and Lower Mesosphere. Journal of Atm. Sci., vol. 23, no. 4, 1966, pp. 424-430.

9. Gregory, J. B.: The Influence of Atmospheric Circulation on Mesospheric Electron Densities in Winter. Journal of Atm. Sci., vol. 21, no. 3, 1965, pp. 18-23.

10. Schilling, G. F.: Latitudinal Variation of Mesopause Height Inferred from Eclipse Observations. Journal of Atm. Sci., vol. 22, no. 2, 1965, pp. 110-115.

11. Lettau, B.: Persistance of Small-Scale Features in the Mesospheric Wind Field. AFCRL Environmental Research Paper No. 198, AFCRL, Bedford, Mass., 1966.

12. Smagorinsky, J.: The Role of Numerical Modeling. Bulletin of the Am. Meteorol. Soc., vol. 48, no. 2, 1967, pp. 94-101.

13. Wagner, N.K.: Theoretical Accuracy of a Meteorological Rocketsonde Thermistor. Journal of Applied Meteorology, vol. 3, no. 4, August 1964, pp. 461-469.

14. Johnson, F.S.: High-Altitude Diurnal Temperature Changes Due to Ozone Absorption. AMS Bulletin, vol. 34, 1953, pp. 106-110.

15. Pressman, J.: Diurnal Temperature Variations in the Middle Atmosphere. AMS Bulletin, vol. 36, 1955, pp. 220-223.

16. Leovy, C.: Radiative Equilibrium of the Mesosphere. J. Atmos. Sci., vol. 21, 1964, pp. 238-248.

17. Beyers, N.J.; and Miers, B.T.: Diurnal Temperature Change in the Atmosphere Between 30 and 60 KM Over White Sands Missile Range. J. Atmos. Sci., vol. 22, 1965, pp. 262-265.

18. Beyers, N.J.; Miers, B.T.; and Reed, R.J.: Diurnal Tidal Motions Near the Stratopause During 48 Hours at White Sands Missile Range. J. Atmos. Sci., vol. 23, 1966. pp. 325-333.

19. Webb, W.L. et al.: Meteorological Rocket Network Probing of the Stratosphere and Lower Mesosphere. AMS Bulletin, vol. 47, 1966, pp. 788-799.

20. Finger, F.: and Woolf, H.M.: An Experiment Designed to Determine the Diurnal Temperature and Wind Variation and to Detect Possible Errors in Rocketsonde Temperature Measurements in the Upper Stratosphere. NASA TM X-1298, November 1966, p. 19.

21. Finger, F.: Personal Communication, December 1966.

22. U.S. Navy Weather Research Facility, Norfolk, Va., "The Daynighter". NWRF-00-0460-037, September 1960.

23. Burns, Y.: Introduction to the Theory of Error. Addison-Wesley Publishing Co., 1953.

24. Anon.: Compilation of Atmospheric Profiles and Synthesized 15μ Infrared Horizon Radiance Profiles Covering the Northern Hemisphere in the Longitude Region Between 60°W and 160°W from March 1964 through February 1965 - Part I, NASA CR-66184, October 1966.

25. Anon.: Compilation of Atmospheric Profiles and Synthesized 15μ Infrared Horizon Radiance Profiles Covering the Northern Hemisphere in the Longitude Region NASA CR-66185, October 1966.